THE ANALYSIS OF COMPLETE STRUCTURES CONSISTING OF BARE FRAMES, SHEAR WALLS AND PLATE COMPONENTS

by

PETER CHARLES LESTER CROXTON

A Thesis submitted for the degree

of

DOCTOR OF PHILOSOPHY

May 1974

SYNOPSIS

This thesis describes two methods for the elastic analysis of structures consisting of arbitrary parallel systems of shear walls and plane frames, subject to the effects of static wind forces and imposed vertical loads. Bending of the floors in their own planes is taken into account by treating the structure as a grillage of walls and floors. This is braced laterally by an assemblage of plane frames. An existing compact elimination technique for the solution of equations is modified for use in these analyses.

The first method of analysis uses a matrix force approach in which the conditions of compatibility at the frame-floor junctions are expressed in terms of influence coefficients, derived separately for the frames and the grillage. In the computer program for this method the regularity of the structure is exploited in order to simplify the preparation and checking of the data.

The second method employs a matrix displacement approach in which the stiffness matrices of the frames are condensed to form an assemblage of lateral stiffnesses, which is superimposed on the stiffness matrix of the grillage. The computer program in this case is designed to make use of backing storage, in order that fairly large structures can be analysed with only a moderate core store.

Analyses of three structures are discussed, with particular reference to the influence of in-plane bending of the floor slabs, the effects of eccentric vertical imposed loading, and the effects of axial deformations in the columns of the frames.

Verification of the methods of analysis is obtained by comparison with the results of previous analyses. Comparisons with experimental results and a finite element analysis are also made for a two storey model.

ACKNOWLEDGEMENTS

The author wishes to thank Professor K. I. Majid for his help and advice during the supervision of this project. Grateful thanks are also due to Professor M. Holmes, Head of the Department of Civil Engineering for his support, to Miss Carol Cunningham for preparing the typescript, to Miss Patricia Sage for tracing the diagrams, and to the technical staff of the department for help with the experimental work.

CONTENTS

CHAPTER 1

INTRODUCTION AND REVIEW OF PUBLSHED WORK

1.1 Introduction

From the point of view of the structural engineer, a tall building is one in which the vertical components of the structure must be designed to resist lateral forces, representative of wind and seismic action, in addition to the vertical dead and imposed loads. Rigidly jointed plane frames with rectangular panels are a convenient structural form architecturally and can be used to provide the whole of the lateral bracing in low-rise buildings. In taller buildings however their susceptibility to sway renders them uneconomic, especially if the partitions are light and non-structural. More efficient bracing can be provided by reinforced concrete shear walls and core structures, often in conjunction with frames.

The necessity for means of determining accurately the distribution of lateral forces carried by the bracing components has been well established. Only in very simple cases are rule-of-thumb methods, based on the relative stiffness of the components, sufficiently accurate. In general it is necessary to consider the complete interaction of a number of components, not only of different relative stiffness, but with different deflection characteristics. The problem has been the object of considerable research during the last decade and a number of reviews have been published [2,3,4]. In this chapter the basic techniques used in the analysis of complete structures are discussed with reference to work published before and during the period covering the work of this thesis. Consideration is first given to methods of analysis of bracing structures per se, followed by the analysis of complete structures.

1.2 Shear wall systems

A plane frame with rectangular panels relies entirely on the stiffness of its joints for lateral stability. Consequently, in order to provide adequate bracing against lateral forces economically, the stiffness of the frame is often increased by replacing one or more of its columns by a shear wall. An alternative arrangement is for one or more frames to be replaced entirely by shear walls, usually coupled at each storey by the floor slabs or by the lintel beams of door and window openings. Other methods of increasing the lateral stiffness, such as diagonal bracing in steel frames[5] and the use of infill panels are also common.

1.2.1 The wide-column frame analogy

Representation of a shear wall by an analogours wide column was probably first used by Clough, King and Wilson[6] in a modified form of the matrix displacement method of analysis which is now well established. On bending, the rotation of the cross section of the wall confers a vertical translation as well as a rotation to the end of a beam framing into its edge. In the wide column analogy, the finite width of the wall is simulated by connecting the joints on the column axis to the ends of the beams by rigid arms which rotate with the joints. The only modification necessary in the analysis is the introduction of additional non-zero terms, corresponding to the beam translations, into the displacement transformation matrix. This modification is described fully in Chapter 2 in the notation of this thesis.

1.2.2 Finite element methods

In the wide column analogy, the assumption of rigid bars between the centre line of a wall and the ends of the connecting beams precludes the determination of stresses in these regions. If complete details of local stresses and deformations are required, an analysis using the finite

element technique is necessary. The method is well established and consists briefly of dividing the structure into a mesh of small elements connected by nodes at their corners. A simplified displacement function is usually chosen to describe the elastic behaviour of the element in relation to the displacements of the nodes and to satisfy compatibility along its boundaries. This function forms the basis from which the stiffness matrix of the element is obtained. The stiffness matrix of the complete structure is constructed by combining the stiffness of individual elements as in the matrix displacement method.

Solution of the load-displacement equations gives nodal displacements which constitute a lower bound to the actual displacements. The degree of accuracy of the results depends upon the fineness of the mesh and the suitability of the chosen function to represent the behaviour of the structure. It is usual to vary the size of the mesh in accordance with the stress gradient and a number of elements with different characteristics may be used simultaneously to represent different parts of the structure.

In the analysis of coupled shear walls, Macleod[7] showed that, unless the connecting beams were relatively deep, their rotations could not adequately be represented by plane stress elements having translational degrees of freedom only at the nodes. In a later paper[8] he described a method using line elements for the beams. The end rotations of the beams were transmitted to the walls through rectangular plane elements having an additional rotational degree of freedom at the nodes. A unique rotation was achieved by using pairs of elements in which complementary rotations of a single edge were considered. In a more general approach, Majid and Williamson[9] dealt with in-plane rotations by connecting opposite nodes in a rectangular element by an imaginary prismatic member.

1.2.3 The continuum method

Both the wide column and the finite element methods conclude with the solution of a large system of simultaneous linear equations, for which a digital computer is necessary. A direct solution can however be obtained for shear walls, with sensibly uniform cross section and containing a single vertical band of openings, by the use of the continuum method. In this approach, the connecting beams are replaced by a continuous elastic medium. The lateral applied loads and displacements are also represented as continuous functions with respect to the distance from the top or bottom of the wall. From a consideration of the equilibrium of the system and by assuming continuous compatibility of lateral displacement of the walls, a second order differential equation is written in terms of a single statically indeterminate function. In order to derive an expression for the stiffness of the connecting medium it is usually assumed that a point of contraflexure occurs at the mid-span point in the beams. This assumption breaks down and leads to an over-estimate of the lateral stiffness of the wall when the wall sections are appreciably different in size, especially when the stiffnesses of the connecting beams and of the less stiff wall are comparable.

A number of different approaches using the continuum method have been proposed. These approaches yield similar results and their chief difference lies in the choice of the redundant function. Rosman[10] used the integral shear force in the connecting medium. The major developments, which are reviewed in references 2, 3 and 4, have been directed towards increasing the applications of the method to include multiple bands of openings and walls with varying stiffness. A recent approach by Coull et al.[11] uses a matrix progression formulation for the analysis of any number of coupled walls. The differential equations are performed in a stepwise manner, thus allowing discontinuities at any levels to be taken into account.

1.3 Secondary effects

The accuracy of the wide column frame method and the continuum method can usually be improved by the inclusion of one or more secondary effects.

1.3.1 Axial deformations

Neglect of axial deformation in the columns of a plane frame leads to an over-estimate of the lateral stiffness of the frame and to errors in bending moments, especially in the top storeys where the maximum axial deformations occur. Macleod[7] showed that axial deformation in the piers of coupled shear walls could also be important. Using the wide column analogy to analyse a number of shear walls with a height-to-width ratio of 3.15, he found that neglect of axial deformation in the columns resulted in a gross over-estimate of the lateral stiffness of the walls, especially when the connecting beams were relatively deep.

1.3.2 Shear distortion

The deflections produced by the action of shear stresses in a beam are frequently neglected. Their significance may be assessed by considering the deflections due to flexure and shear at the top of a vertical cantilever of height H, subject to a horizontal point load Q at the top. These are respectively $\frac{QH^3}{3EI}$ and $\frac{\alpha QH}{AG}$ where A and I are the area and second moment of area respectively of the section; E and G are the respective elastic and shear moduli, and α is the shape factor. For a rectangular section, a value of 1.2 is usually accepted for α. This value was obtained by Timoshenko[12] using a strain energy approach with elementary beam theory. A similar value was obtained by Cowper[13] using a rigorous elastic analysis and considering the mean rotation of the warped section. The alternative value of 1.5 obtained by Timoshenko is unrealistic as it is based on the rotation of a single point in the warped section at the neutral axis.

Using the above expressions for flexural and shear deflections it can be shown that the proportion of the deflection due to shear distortion

at the top of a plane shear wall with a height to width ratio of 3 would be approximately 8%. In similar walls containing openings the effect would be expected to be less and would be related to the stiffness of the connecting beams. Using the wide wolumn analogy, Macleod found that, for the walls described in section 1.3.1., the proportion of the deflection attributable to shear distortion was slightly higher than the above figure. He also concluded that shear distortion was more important in the columns than in the beams of the analogous frame except when the beams were slender.

In a wall-frame structure, Khan and Sbarounis[14] found that shear distortion in the wall made little difference except in the bottom two storeys where its inclusion increased the shear force carried by the frame by 10%.

1.3.3 Local bending

Local bending at the built-in end of a cantilever beam, connected to a wide column, was studied analytically and experimentally by O'Donnell[15] and later analytically by Michael[16]. Both writers reported similar results and concluded that local bending contributed significantly to the deflection at the free end of the cantilever. Michael showed that for beams whose depth was less than one sixth of the column width the effect of local bending could be simulated by increasing the cantilever span by half the depth of the section. These findings were corroborated experimentally by Puri and also by Macleod who showed that, for relatively deep beams, Michaels correction over-estimated the effect of local bending. Local bending can also occur in a wall at a sudden change in cross-section. Using a finite element analysis with a fine mesh near the discontinuity, Choudhury[17] examined the extreme case of the cantilever shown in Fig.1.1. Here it was found that local bending increased the deflection at the free end of the cantilever by only 2.8%.

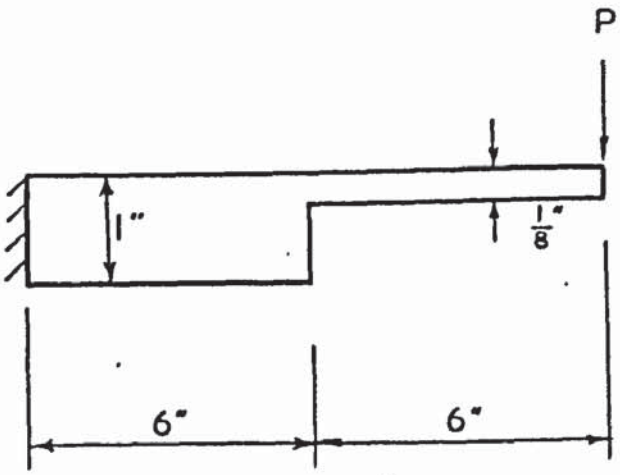

Fig. 1.1. Choudhury's cantilever

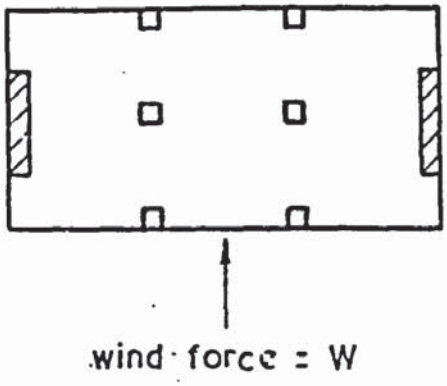

(a) floor plan

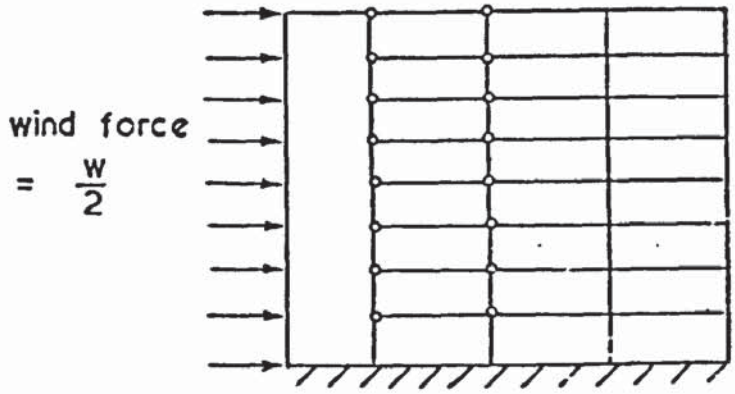

(b) idealised system

Fig. 1.2. Symmetrical structure

1.4 Analysis of complete structures

In a complete structure the lateral displacements of the bracing components are constrained at each floor level by the action of the floor slabs. Most methods of analysis derive simplified expressions for the compatibility of these displacements by assuming that the floor slabs translate and rotate in horizontal planes as rigid diaphragms but have no stiffness with respect to bending or torsion normal to that plane. When these assumptions are made, the methods of analysis can be classified by the number of degrees of freedom necessary to define the displacements of all the bracing structures at any floor level.

1.4.1 One degree systems

If all the bracing components form a symmetrical arrangement and the loading is also symmetrical, no rotation of the floor slabs takes place. The horizontal displacements of all the bracing components at a particular floor level are therefore equal and can be defined by a single degree of freedom. A typical structure of this type is shown diagramatically in plan in Fig.1.2a. The assumption of infinite out-of-plane flexibility of the floor slabs implies that the inter-action between the bracing components is one of the translation only. One degree systems can therefore be idealised as in-line systems of bracing components connected together by axially stiff pin-ended links as shown in Fig.1.2b.

An early hand method of analysis for this idealised system was presented by Khan and Sbarounis[14] who applied the total external load in the first place to the wall alone, computing the deflections at floor levels by simple beam theory. The forces in the connecting links necessary to produce the same deflections in the frame were next calculated, using a moment distribution or slope-deflection approach. Equal and opposite forces were then applied to the wall, modifying the initial deflections. The process was repeated until the deflections converged. Convergence was achieved after about 7 iterations but the rate could be improved by the

use of design charts to select initial distributions for the forces in the connecting links. A number of secondary effects such as the inclusion of axial deformation in the columns, elastic rotation of the wall foundations and moment connections between the walls and the frames could also be included.

Clough et al.[6] used the wide column frame analogy for similar structures consisting of skeletal frames and wall-frame systems. The frames were analysed separately, reducing each stiffness matrix to a condensed form relative to the lateral displacements only. The overall lateral stiffness matrix for the structure was then obtained by direct superposition of the contributions of the individual frames. The load vector consisted of the applied wind forces together with a set of lateral forces equivalent to the applied vertical and rotational loads. Vertical and rotational joint displacements in individual frames were obtained by back substitution of the common lateral displacements in the original load-displacement equations.

An analysis of a 20 storey structure showed that neglecting axial deformations in the frame columns resulted in errors of approximately 20% in the axial forces at the bases of some of the columns and a reduction of 14% in the lateral deflection at the top of the building. Shear distortion effects were not discussed.

The deflection characteristics of a wall and a frame are markedly different. Under a uniformly distributed lateral load the deflection of the wall is chiefly flexural as shown in Fig.1.3a, while the frame, on the other hand, deforms mainly by shearing as shown in Fig.1.3b. Coupling the two structures at each floor level results in the double curvature illustrated by Fig.1.3c. These characteristic deflected shapes were used as the basis for approximate methods of analysis by Rosman[19] and by Heidebrecht and Stafford Smith[20]. In both methods the flexural stiffness of the wall, ignoring shear distortion was considered to be the sum of the

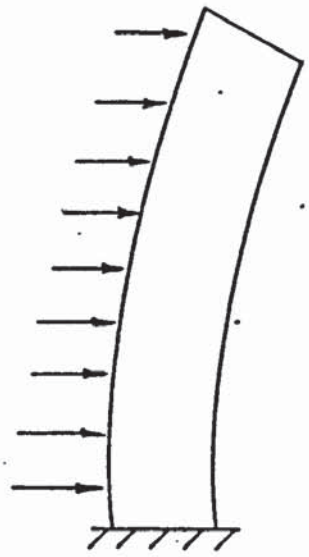

(a) deformation by flexure

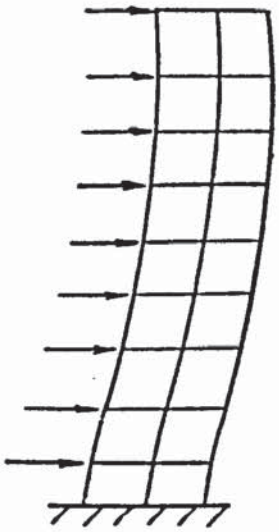

(b) deformation by shearing

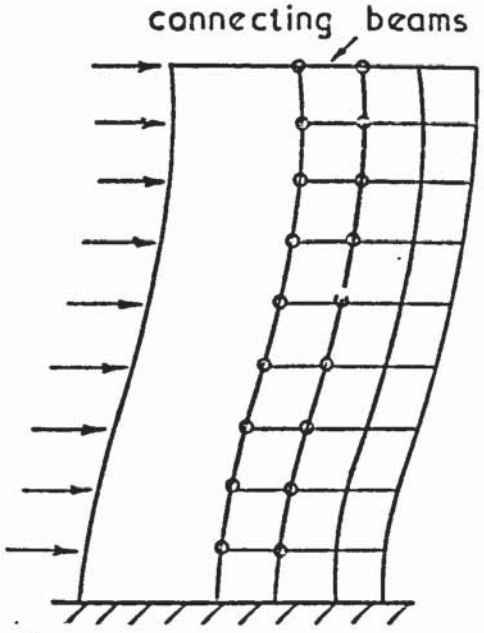

(c) deflection of coupled wall– frame system

Fig. 1.3 Deflection of coupled shear wall.

stiffness of all the individual walls parallel to the wind direction. Heidebrecht also included the bending stiffness of the frames normal to the wind direction. Similarly, the shear stiffness of the frames was obtained from the combined stiffnesses of all the frames parallel to the wind direction using the Portal method of analysis.[18] The forces in the connecting links were replaced by equal and opposite distributed horizontal forces acting on the two structures.

From a consideration of the equilibrium of horizontal shear forces and using the principle of stationary complementary energy, Rosman produced a second-order differential equation in terms of the bending moment in the wall. Direct solutions were obtained for uniformly and triangularly distributed loads. The forces in the connecting links were obtained by statics and distributed to the frame columns in proportion to their stiffnesses. Application of the method was restricted to the class of proportioned frames capable of analysis by the Portal method.

By assuming continuous compatibility of deflections and considering the equilibrium of the distributed forces applied to the wall and the frame, Heidebrecht obtained a fourth order differential equation in terms of the common deflection. A transfer matrix approach was proposed to deal with structures of non-uniform section. Shear walls with openings were considered as frames, using the modified beam method of Stafford Smith[21] to take account of wide column effects.

The results for a ten storey framed tube structure of uniform section were found to compare well with a more accurate computer solution. No results however, were quoted for analyses of more irregular structures where significant errors would have been expected to result from the use of the Portal method of frame analysis. Also, as the differential equation was formulated by assuming a shear cantilever analogy for the frame, comparative results would have been interesting for structures containing perforated shear walls which have deflection characteristics intermediate between those of a frame and a wall.

An alternative method for dealing with changes in structural stiffness was developed by Gluck[22] for structures consisting entirely of monolithic shear walls. The solution was obtained in two parts. Firstly the applied forces were distributed to the walls in proportion to their stiffness in a basic solution, assuming that the walls had a common deflection line maintained by imaginary torsion bars at the change points. In the second, or complementary solution, the bending moments in the walls were modified iteratively by the redistribution resulting from the removal of the torsion bars and the equalisation of deflections at floor levels only.

1.4.2 Two degree systems

Typical of this class of structure are buildings with a rectangular plan of fairly high aspect ratio, in which rotation of the floor slabs occurs as a result of asymmetrical loading or an asymmetrical arrangement of parallel walls and frames. The torsional stiffness of such a structure is derived mainly from the lateral, in-plane displacement of the bracing components. The secondary torsional stiffness of the components with respect to twisting about their own vertical axes has been shown, in the case of walls and frames, to be relatively unimportant[11, 23]. The movement of the walls and frames at each floor level can therefore be defined by their positions in relation to some fixed point in the floor slab and by two displacements which effectively give the rotation of the floor slab and its translation in the direction of the plane of the walls or frames.

Webster[24] used a wide column frame analogy in which the stiffness matrices of the analogous frames were partitioned as in Clough's method. Their lateral stiffness was then obtained by a method of condensation similar to that described in chapter 5 of this thesis. A consideration of the equilibrium of the external wind loads and the forces carried by the frames at each floor level yielded a set of equations in terms of the lateral storey displacements of the first and last frames, deriving compatibility relationships for the intermediate frames by simple proportion.

Axial strains and shear distortion were ignored.

For a structure consisting of an asymmetrical arrangement of core walls and parallel shear walls coupled by floor slabs, Coull and Irwin[25] proposed a method in which the continuum method was used to obtain influence coefficients for the shear walls, taking account of the effects of axial deformations in the piers of the walls, but ignoring shear distortion. Torsional stiffnesses of the core walls about their own vertical axes were included, using elementary methods. Two sets of equilibrium equations were formed for the lateral forces and the torques respectively. Solution of these equations yielded the respective storey translations and rotations. A feature of the method was that the equilibrium equations could be solved separately for the lateral forces and torques so that the total number of equations to be solved at one time was equal to the number of storeys.

Gluck[26] extended his earlier method of dealing with walls of varying stiffness to include the effects of torsion. In the basic solution, lateral forces were dealt with as before. Torques were distributed in proportion to the sectorial stiffnesses of the walls with respect to the shear centre. Colinearity of the deflected forms of the walls during the basic solution was maintained by the introduction of imaginary, torsionally rigid planes at the changes in section. Bending moments and bimoments in the walls were re-distributed on removal of these planes in the complementary solution. The method was applicable only to structures consisting of monolithic shear walls.

1.4.3 Three degree systems

In a general structure, where the walls and frames are not necessarily arranged symmetrically or in parallel planes, two orthogonal translations and a rotation are necessary at each floor level to define the displacements of the bracing components

Probably the earliest analysis of this class of structure was made

by Weaver and Nelson[23] who extended the work of Clough to take torsional effects into account. The complete structure was analysed as a space frame in which the degrees of freedom of the joints were reduced, by the diaphragm action of the slabs, to three per joint with two additional translations and a rotation at each floor level. The method of condensation of the stiffness matrix was very similar to that of Clough, resulting in a set of equations in terms of the rigid body displacements of the floor slabs. The analysis of an L shaped building, subject to a uniform wind load on the long face and a uniformly distributed vertical load on each floor, showed that neglect of axial deformation in the columns resulted in a 20% reduction in floor translations and a significant reduction in floor rotations, especially in the top storeys.

Winokur and Gluck[27] used a matrix displacement approach in which the lateral stiffness matrices of the individual bracing components were obtained separately by standard methods of analysis or by the use of models, assuming unit translations applied at each floor level in turn, in the directions of the component axes, while zero displacements were maintained at the other levels by imaginary reactive forces. The overall stiffness matrix of the complete structure, in terms of the storey displacements was formed in a similar way by considering unit translations and a rotation in the plane of each floor in turn.

The results of an analysis of a ten storey structure showed that the concept of a shear centre, based on the relative lateral stiffnesses of the bracing components at each floor is invalid. In fact it was shown in later work by Gluck[26] that such a concept is only valid when the deflected forms of the components are colinear.

In a similar approach by Stamato and Stafford Smith[28], account was taken of the interaction of vertical forces where frames or walls intersect at an angle. The effect of these forces was shown to be particularly significant in the framed tube type of structure where the frames normal to the wind direction behave like the flanges of a box girder. The

characteristic "shear lag" distribution of axial forces in the columns of such frames is described and illustrated in reference 4.

A later method by Heidebrecht and Swift[29] also used the matrix displacement method. A modified form of the wide column analogy using rigid body transformation matrices was employed to take account of the finite size of beam to column joints and non-coincidence of the shear centre and centroid in wall piers. The warping of non-planar piers was included by developing a special member stiffness matrix which included the bimoment and the rate of change of longitudinal displacement as additional force and displacement components.

Simulation of the bending action of the floor slabs by a system of connecting beams was proposed, but the method of selecting suitable beam sizes was not reported.

The continuum method has also been extended to deal with three degree systems and two methods were published at about the same time by Rosman[30] and Gluck[31]. Rosman used the shear forces along bands of openings in wall assemblies as the unknown functions in a set of simultaneous second order differential equations. The number of equations was generally equal to the number of opening bands in the system. Gluck formulated a system of three third order differential equations with constant coefficients in terms of continuous functions representing the lateral translation and the rotation of the floor slabs.

1.4.4 The effects of bending in floor slabs

The effects of out-of-plane bending of the floor slabs has been ignored in nearly all the methods of analysis of complete structures except where the slab provides the coupling medium between shear walls. When the walls are in the same vertical plane, the effect of the slab can be simulated by an equivalent beam of the same depth. The choice of an effective width for the equivalent beam has been the subject of some research, notably by Khan and Sbarounis[14] who investigated a single column

in a slab with idealised boundary forces.

Graphs of effective width were produced for a number of aspect ratios and thicknesses of slab.

Barnard and Schwaighofer[32] studied the case of a single pair of walls connected by slabs with unrestrained edges. The extreme fibre stresses in the walls, obtained by Rosman's continuum method, were found to be in fairly close agreement with experiments on a plastic model when the full width of the slab was considered to be effective. In subsequent discussion however Quadeer demonstrated that the continuum method is not suffieiently sensitive to variations in slab width for accurate judgements to be made.

Quadeer and Stafford Smith[33], in a more comprehensive theoretical study, assuming a number of identical pairs of coupled walls, concluded that, in general, the effective width is considerably less than the full width of the slab. Design graphs were presented for direct estimations to be made.

When the walls are not in the same vertical plane, the interaction is more complex and can only be studied effectively with the aid of finite element techniques. Further research is necessary into the significance of out-of-plane bending of the slabs in certain classes of structure. For example, the "shear lag" effect noticed by Stomato and Stafford Smith in a framed tube structure is likely to be reduced if the vertical forces transmitted to the inner columns of the frames by the floor slabs are considered.

In buildings of the so called "slab type" which have a high aspect ratio in plan, the distribution of lateral forces among the bracing components may be significantly affected by the bending of the floor slabs in their own planes.

Goldberg[34] proposed a method in which the floor slabs were assumed to behave as deep beams subject to shear distortion as well as flexure. Out-of-plane bending was once again ignored. The analysis was restricted to

structures containing parallel arrangements of monolithic shear walls or skeletal frames with rectangular panels. Axial deformations in the beams and columns of the frames were neglected and no provision was made for the inclusion of wide column effects. Equilibrium of lateral forces at junctions of walls or frames with the floor slabs was assumed, but moment equilibrium between the vertical bracing components and the slabs was ignored. This latter assumption is reasonable as it has been shown that the torsional stiffness of walls and frames about their own axes is relatively unimportant. The method of solution was a matrix displacement approach in which equilibrium equations were formed in terms of the lateral displacements of the floor slabs at each wall or column line. Elimination of the equations was carried out storey by storey by the method now generally known as the "method of substructures".

Analyses were carried out on two symmetrical structures, one of ten and one of twenty storeys having two end walls and seven intermediate frames. The variations in deflections resulting from the bending of the floor slabs were shown to be insignificant in both structures. A comparison of the lateral forces carried by the centre and outer frames however, showed that the shear in the bottom storey was approximately 50% greater in the centre frame while at the top, the shear in the centre frame was reduced in approximately the same proportion. At other levels the differences between the frames were slight. The effect of neglecting shear distortion in the walls and slabs was shown to be significant.

1.5 Conclusions from published literature

In the methods of analysis of complete structures described in this review, a variety of simplifying assumptions are made, the effect of which is to restrict the range of structural configurations to which particular methods can be applied. Completely general methods of analysis, based on finite elements are available. For example, in a recent program developed by Bray[35], library subroutines for several different types of

element are accessible. In the case of multi-storey building structures, however, the volume of data required, and the core storage necessary for such a program would be prohibitive. The alternative of a number of simpler methods, each capable of analysing a range of structural configurations, is more acceptable.

The methods having the most general application are those based on the matrix displacement method in which analogous frames are used. With these methods a wide variety of structural forms for the bracing components can be handled with little or no increase in data preparation or computation time.

Computational advantages can be obtained by the use of the continuum method for the analysis of simple structures with sensibly uniform sectional and material properties. For more complex structures however the advantages are less evident and even with the most recent developments, the method is not capable of such general application as the wide column frame analogy.

1.6 The scope of this thesis

Apart from the work of Goldberg, the bending of the floor slabs in their own planes has largely been ignored. Similarly, although facilities for dealing with the effect of imposed vertical loading on the frames have been included in some earlier analyses, no reports of its effects on the overall behaviour of the structure have been found. In this thesis two new computer methods, incorporating the above effects, are proposed for the elastic analysis of complete structures of the type shown in Fig. 1.4. The structures consist of parallel walls and frames arranged arbitrarily and interconnected by continuous floor slabs. Static loads due to wind and the imposed vertical loads carried by the floor slabs are considered.

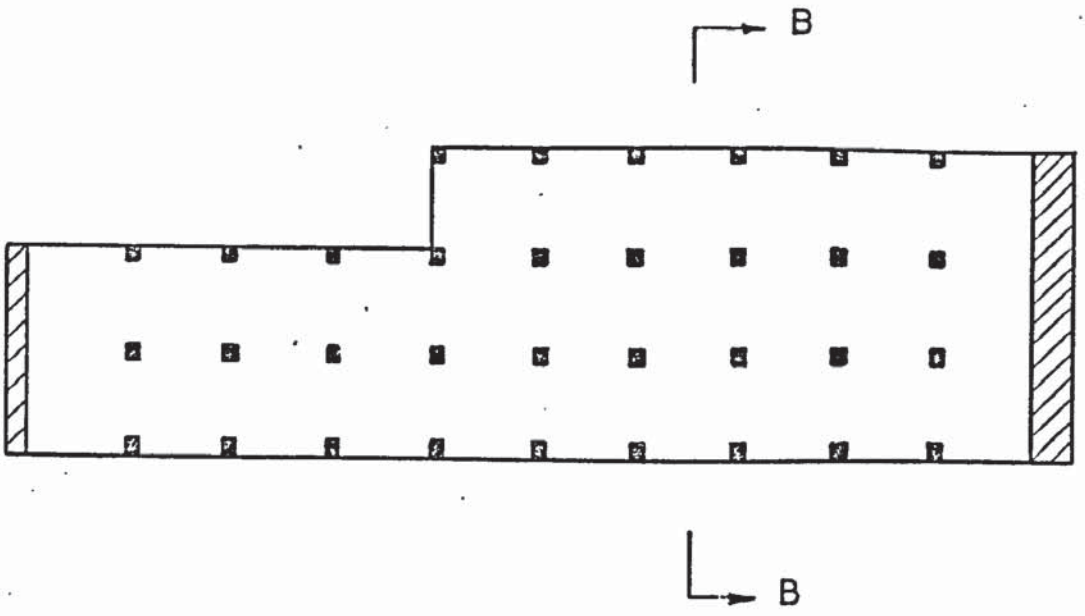

section A-A

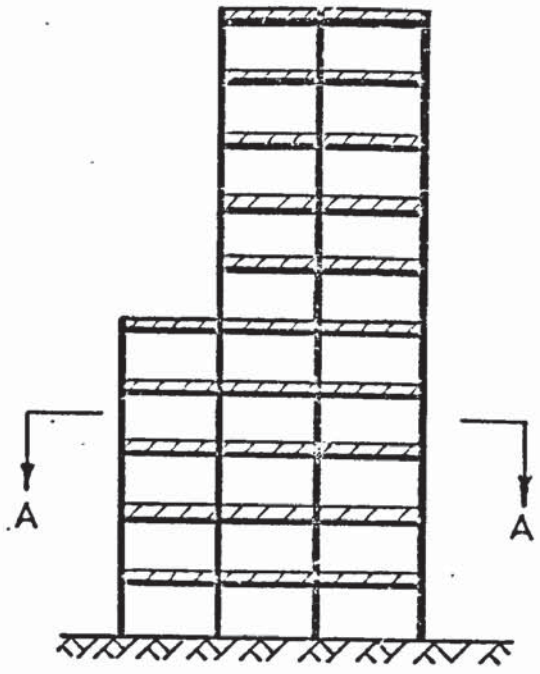

section B - B

Fig. 1.4 Typical parallel arrangement of walls and frames

In these methods, the complete structure is treated as a grillage of walls and floors which act as deep beams, bending in their own planes, and braced against lateral displacement by the frames. Part of the analysis consists of the separate analysis, using the matrix displacement method, of these two basic types of structure. Chapter 2 describes the notation and sign conventions used in the matrix displacement analysis and gives the derivation of the basic matrices.

A special subroutine has been written for the compact storage and solution of equations. This subroutine, which is described in Chapter 3, is based on two original methods due to Jenning's et al and combines a compact form of Gaussian elimination with the use of direct access disc backing storage.

Chapters 4 and 5 describe the proposed methods of analysis. The first of these takes advantage of the regular natures of the grillage and the frames so that very little data preparation is necessary. The second is more general and incorporates the wide column frame analogy, thus permitting a greater range of structures to be analysed. The second method also makes use of backing storage so that fairly large structures may be analysed with a moderate core store.

Computer programs for both methods are described in Chapter 6. For the first approach, the computer program is described in outline only, with special reference to the method of presentation and interpretation of the data. The program for the second method is described in more detail. It is considerably more complex, owing to the use of backing storage and to the special partitioned form required for the stiffness matrices of the frames.

Chapter 7 contains an account of experimental work carried out on a two storey model structure consisting of Perspex walls and floors, braced by steel frames. The results are compared with analytical solutions obtained by the proposed methods and by a general finite element analysis.

The final section of the work, namely an investigation into the behaviour of three larger practical structures, follows in Chapter 8. These structures are chosen to illustrate the effects of wind and eccentric vertical loading and to examine the influence of in-plane bending of the floor slabs, axial deformations in the columns of the frames, and the effect of local irregularities or discontinuities in the properties of the structural members.

CHAPTER 2

BASIC MATRICES

2.1 Notation

$\underline{A}$	displacement transformation matrix.
a,b,d,e,f,q	member stiffness coefficients.
A	cross sectional area.
A_1, B_1, C_1, etc.	stiffness coefficients for a general frame.
E	Young's modulus.
G	modulus of rigidity.
h	depth of section.
i	joint number at end 1 of a member.
j	joint number at end 2 of a member.
I	second moment of area.
$\underline{k}$	assemblage of member stiffnesses.
$\underline{K}$	stiffness matrix.
$\underline{K}_{ij}$ etc.	contributions of a member to the stiffness matrix.
$\underline{L}$	matrix of applied loads.
ℓ	flexural length of a member.
ℓ_p, ℓ_q, m_p, m_q	direction cosines.
M_1, M_2	moments at ends 1 and 2 of a member.
$\underline{P}$	matrix of member forces.
P	axial force.
Q	shear force.
r	radius of gyration.
s_1, s_2	rigid extensions of a beam connected to a wide column.
t	thickness of a plate member.
T	torque.
u	axial deformation of a member.

v	sway of a member.
$\underline{X}$	matrix of displacements at joints.
x,y,z	coordinates of joint displacements.
$\underline{Z}$	matrix of member displacements equivalent to $\underline{P}$.
α	shape factor of a section.
β	constant relating shear and flexural deflections.
ν	Poisson's ratio.
θ	rotation.
θ_T	angle of twist.
$\theta^x,\theta^y,\theta^z$	rotations about the x, y and z axes.
θ_i,θ_j	rotations at joints i and j.
θ_1,θ_2	rotations at ends 1 and 2 of a member.

2.2 Introduction

In this thesis two basic structural forms, namely the grillage and the plane frame, are analysed using the matrix displacement method. Briefly summarising, the relationship between the external loads $\underline{L}$ and the vectorially equivalent joint displacements $\underline{X}$, in terms of the system coordinates, is expressed by the equation

$$\underline{L} = \underline{K}\,\underline{X} \qquad \ldots\ldots \quad (2.1)$$

where $\underline{K}$ is the stiffness matrix of the structure. The corresponding relationship in terms of the local member coordinates is given by

$$\underline{P} = \underline{k}\,\underline{Z} \qquad \ldots\ldots \quad (2.2)$$

where $\underline{P}$ and $\underline{Z}$ are equivalent vectors of the respective member forces and displacements, and $\underline{k}$ is a diagonal assemblage of member stiffnesses. Transformation from system to local coordinates is effected by the equation

$$\underline{Z} = \underline{A}\,\underline{X} \qquad \ldots\ldots \quad (2.3)$$

where $\underline{A}$ is the displacement transformation matrix. The stiffness matrix is constructed directly from the stiffnesses of individual members by using the relationship

$$\underline{K} = \underline{A}'\,\underline{k}\,\underline{A} \qquad \ldots\ldots \quad (2.4)$$

where the prime denotes the transpose of the matrix. For a single member, this operation results in the submatrices

$$\left[\begin{array}{c|c} \underline{K}_{ii} & \underline{K}_{ij} \\ \hline \underline{K}_{ji} & \underline{K}_{jj} \end{array}\right]$$

These are the contributions of the member to the overall stiffness matrix of the structure. The subscripts i and j refer to the joints at ends 1 and 2 respectively of the member.

2.3 Grillage analysis

The floor slab elements and solid wall panels of the complete structure are assumed to act as the members of a grillage loaded by the wind forces. It is assumed that the members are rigidly connected deep beams bending in their own planes and subject to torsion about their longitudinal axes. Walls are assumed to be encastré at their bases. The positive sign convention adopted for forces and displacements is in accordance with the right hand screw rule and is shown diagrammatically for a horizontal and a vertical member in Fig. 2.1. The axes of the members lie in the x y plane and the joints have degrees of freedom in the z, θ^x and θ^y directions.

The conventional form of the slope-deflection equations must be modified for a deep beam to take account of shear distortion. Thus, for a member of length l, using the sign convention and notation of Fig. 2.1,

$$M_1 = \frac{2EI}{l}\left(\frac{2+\beta}{1+2\beta}\right)\theta_1 + \frac{2EI}{l}\left(\frac{1-\beta}{1+2\beta}\right)\theta_2 - \frac{6EI}{l^2}\left(\frac{1}{1+2\beta}\right)v$$

$$M_2 = \frac{2EI}{l}\left(\frac{1-\beta}{1+2\beta}\right)\theta_1 + \frac{2EI}{l}\left(\frac{2+\beta}{1+2\beta}\right)\theta_2 - \frac{6EI}{l^2}\left(\frac{1}{1+2\beta}\right)v \qquad \ldots\ldots \quad (2.5a)$$

Taking moments about one end of the member and substituting for the end moments,

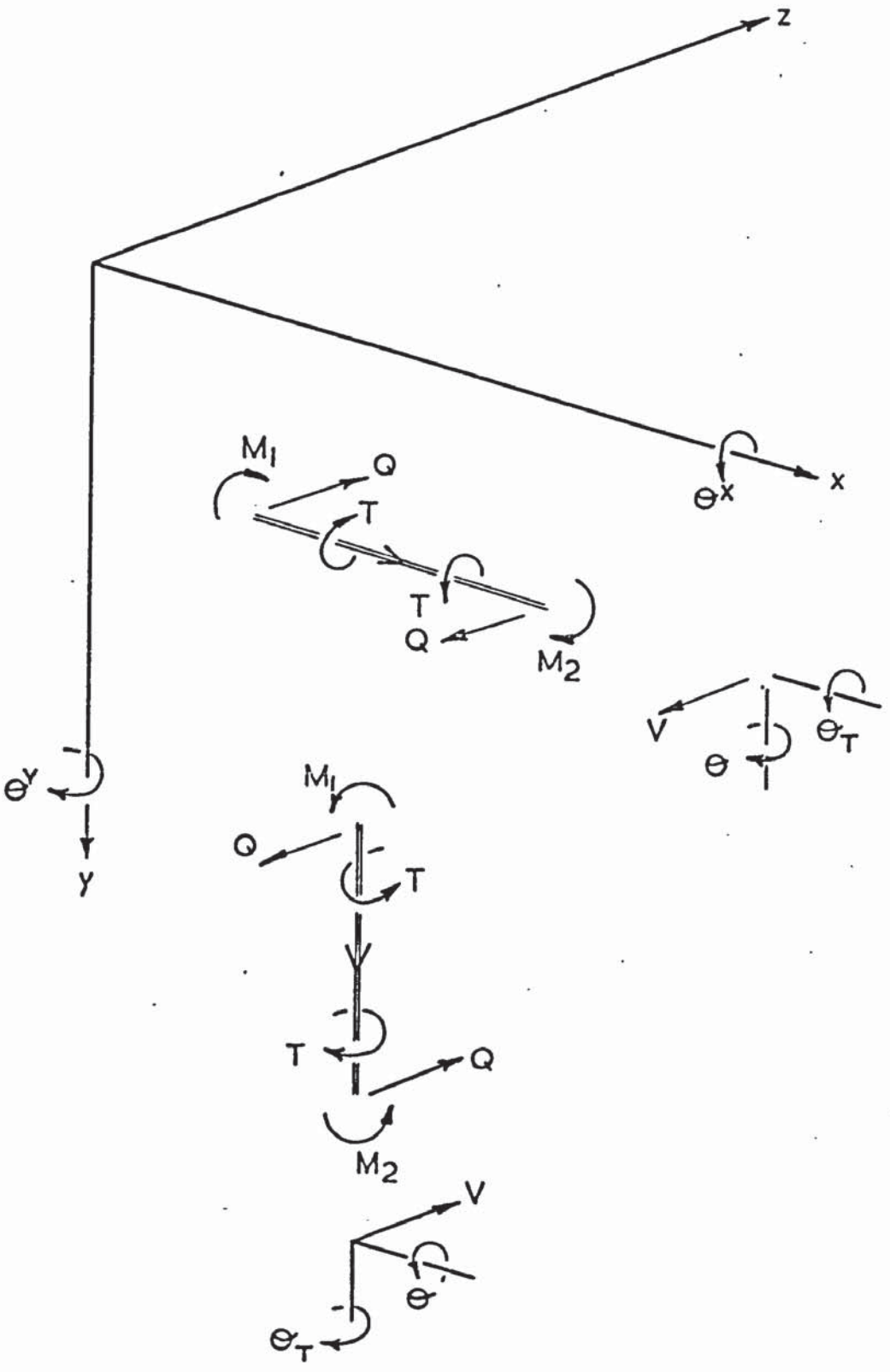

Fig. 2.1. Sign convention for grillage

$$Q = -\frac{6EI}{\ell^2}\left(\frac{1}{1+2\beta}\right)\theta_1 - \frac{6EI}{\ell^2}\left(\frac{1}{1+2\beta}\right)\theta_2 + \frac{12EI}{\ell^3}\left(\frac{1}{1+2\beta}\right)v \quad \ldots\ldots \quad (2.5b)$$

where E is Young's modulus and I is the second moment of area of the section. β is a constant relating the deflections of a member due to shear distortion and flexure. Its value is dependent on the geometrical proportions of the member and may be expressed in terms of the slenderness ratio, thus

$$\beta = \frac{12\alpha(1+\nu)}{\left(\frac{\ell}{r}\right)^2} \quad \ldots\ldots \quad (2.6)$$

where α is the shape factor of the section, ν is Poisson's ratio and r is the radius of gyration in the plane of bending. Equation (2.6) shows that for slender members β tends to zero and the slope deflection equations then assume the standard form for a prismatic member.

When the restraint on the warping of the cross sections is slight, the wall and slab panels may be assumed to behave in torsion as long rectangular strips in which the torque T and the angle of twist θ_T are related by the equation

$$T = \frac{G\,h\,t^3}{3\ell}\,\theta_T \quad \ldots\ldots \quad (2.7)$$

where h is the depth and t the thickness of the section. From equations (2.5) and (2.7) the force-displacement equations for a grillage member may now be written in the form of equation (2.2), thus

$$\begin{bmatrix} Q \\ M_1 \\ M_2 \\ T \end{bmatrix} = \begin{bmatrix} b & d & d & 0 \\ d & e & f & 0 \\ d & f & e & 0 \\ 0 & 0 & 0 & q \end{bmatrix} \begin{bmatrix} v \\ \theta_1 \\ \theta_2 \\ \theta_T \end{bmatrix} \quad \ldots\ldots \quad (2.8)$$

where $b = \frac{12EI}{\ell^3}\left(\frac{1}{1+2\beta}\right)$

$d = -\frac{6EI}{\ell^2}\left(\frac{1}{1+2\beta}\right)$

$e = \frac{2EI}{\ell}\left(\frac{2+\beta}{1+2\beta}\right)$

$f = \frac{2EI}{\ell}\left(\frac{1-\beta}{1+2\beta}\right)$

$q = \frac{G\,h\,t^3}{3\ell}$

Since the grillage members represent the floor slabs and walls of a building they may be assumed to be either horizontal or vertical. It is convenient therefore to construct two sets of displacement and transformation equations, using the sign convention and notation of Fig. 2.1. For a horizontal member, with joint i at end 1 and joint j at end 2, the displacement transformation equations may be written in the form of equation (2.3), thus

$$\begin{matrix} & & \text{joint i} & & & \text{joint j} & & \\ \begin{bmatrix} v \\ \theta_{y_1} \\ \theta_{y_2} \\ \theta_{x_2} \end{bmatrix} & = & \left[\begin{array}{ccc:ccc} 1 & 0 & 0 & -1 & 0 & 0 \\ 0 & 0 & 1 & 0 & 0 & 0 \\ 0 & 0 & 0 & 0 & 0 & 1 \\ 0 & -1 & 0 & 0 & 1 & 0 \end{array}\right] & \begin{bmatrix} z \\ \theta^x \\ \theta^y \\ — \\ z \\ \theta^x \\ \theta^y \end{bmatrix} & \begin{matrix} \\ \\ \\ \\ \\ \\ \\ \end{matrix} & \begin{matrix} \\ \text{joint i} \\ \\ \\ \\ \text{joint j} \\ \\ \end{matrix} \end{matrix} \qquad \ldots\ldots \quad (2.9a)$$

while for a vertical member

$$\begin{bmatrix} v \\ \theta_{1} \\ \theta_{2} \\ \theta_{T} \end{bmatrix} = \left[\begin{array}{ccc|ccc} -1 & 0 & 0 & -1 & 0 & 0 \\ 0 & 1 & 0 & 0 & 0 & 0 \\ 0 & 0 & 0 & 0 & 1 & 0 \\ 0 & 0 & -1 & 0 & 0 & 1 \end{array}\right] \begin{bmatrix} z \\ \theta^{x} \\ \theta^{y} \\ \hline z \\ \theta^{x} \\ \theta^{y} \end{bmatrix} \begin{matrix} \\ \\ \\ \\ \text{joint i} \\ \\ \\ \text{joint j} \end{matrix} \qquad \ldots\ldots \quad (2.9b)$$

The operation described by equation (2.4) produces the contributions of the member to the overall stiffness matrix. Thus for a horizontal member,

$$\left[\begin{array}{c|c} \underline{K}_{ii} & \underline{K}_{ij} \\ \hline \underline{K}_{ji} & \underline{K}_{jj} \end{array}\right] = \left[\begin{array}{ccc|ccc} b & 0 & d & -b & 0 & d \\ 0 & q & 0 & 0 & -q & 0 \\ d & 0 & e & -d & 0 & f \\ \hline -b & 0 & -d & b & 0 & d \\ 0 & -q & 0 & 0 & q & 0 \\ d & 0 & f & -d & 0 & e \end{array}\right] \qquad \ldots\ldots \quad (2.10a)$$

while for a vertical member,

$$\left[\begin{array}{c|c} \underline{K}_{ii} & \underline{K}_{ij} \\ \hline \underline{K}_{ji} & \underline{K}_{jj} \end{array}\right] = \left[\begin{array}{ccc|ccc} b & -d & 0 & -b & -d & 0 \\ -d & e & 0 & d & f & 0 \\ 0 & 0 & q & 0 & 0 & q \\ \hline -b & d & 0 & b & d & 0 \\ -d & f & 0 & d & e & 0 \\ 0 & 0 & -q & 0 & 0 & q \end{array}\right] \qquad \ldots\ldots \quad (2.10b)$$

General expressions for the determination of member forces from the joint displacements may be obtained by combining equations (2.8) and (2.9). Hence, for a horizontal member,

$$\begin{bmatrix} Q \\ M_1 \\ M_2 \\ T \end{bmatrix} = \left[\begin{array}{ccc|ccc} b & 0 & d & -b & 0 & d \\ d & 0 & e & -d & 0 & f \\ d & 0 & f & -d & 0 & e \\ 0 & -q & 0 & 0 & q & 0 \end{array}\right] \begin{bmatrix} z \\ \theta^x \\ \theta^y \\ \hline z \\ \theta^x \\ \theta^y \end{bmatrix} \begin{matrix} \\ \text{joint i} \\ \\ \\ \\ \text{joint j} \\ \\ \end{matrix} \quad \ldots\ldots \quad (2.11a)$$

and for a vertical member,

$$\begin{bmatrix} Q \\ M_1 \\ M_2 \\ T \end{bmatrix} = \left[\begin{array}{ccc|ccc} -b & d & 0 & b & d & 0 \\ -d & e & 0 & d & f & 0 \\ -d & f & 0 & d & e & 0 \\ 0 & 0 & -q & 0 & 0 & q \end{array}\right] \begin{bmatrix} z \\ \theta^x \\ \theta^y \\ \hline z \\ \theta^x \\ \theta^y \end{bmatrix} \begin{matrix} \\ \text{joint i} \\ \\ \\ \\ \text{joint j} \\ \\ \end{matrix} \quad \ldots\ldots \quad (2.11b)$$

2.4 Frame analysis

The term "frame" is used here in a general sense to denote either a skeletal frame consisting of prismatic members, or a wide-column analogous frame representing a shear wall system. Since the analysis of the frames is made separately from that of the grillage, axes may be chosen arbitrarily to define the plane of the frame. The x and y axes

are used in this thesis as shown in Fig. 2.2 which also shows the positive sign convention for forces and displacements. Joints may be allocated from zero to three degrees of freedom in the x, y and θ directions.

The force-displacement equations for a single member of length ℓ and cross sectional area A may be obtained directly from the slope deflection equations (2.5) and the axial stiffness of the member, thus

$$\begin{bmatrix} P \\ Q \\ M_1 \\ M_2 \end{bmatrix} = \begin{bmatrix} a & 0 & 0 & 0 \\ 0 & b & d & d \\ 0 & d & e & f \\ 0 & d & f & e \end{bmatrix} \begin{bmatrix} u \\ v \\ \theta_1 \\ \theta_2 \end{bmatrix} \qquad \ldots\ldots \quad (2.12)$$

where $a = \frac{AE}{\ell}$, the axial stiffness. The other coefficients have already been defined.

For a prismatic member with joint i at end 1 and joint j at end 2, the displacement transformation equations may be written in the form

$$\begin{bmatrix} u \\ v \\ \theta_1 \\ \theta_2 \end{bmatrix} = \begin{bmatrix} -\ell_p & -m_p & 0 & \ell_p & m_p & 0 \\ -\ell_q & -m_q & 0 & \ell_q & m_q & 0 \\ 0 & 0 & 1 & 0 & 0 & 0 \\ 0 & 0 & 0 & 0 & 0 & 1 \end{bmatrix} \begin{bmatrix} x \\ y \\ \theta \\ - \\ x \\ y \\ \theta \end{bmatrix} \begin{matrix} \\ \\ \\ \\ \text{joint i} \\ \\ \text{joint j} \end{matrix} \qquad \ldots\ldots \quad (2.13)$$

where ℓ_p, m_p, ℓ_q, m_q are direction cosines.

The effect of a wide-column is shown diagrammatically in Fig. 2.3a. Here the shaded areas are assumed to rotate as rigid arms of length s_1 and s_2 at ends 1 and 2 respectively of the beam. The arms are measured

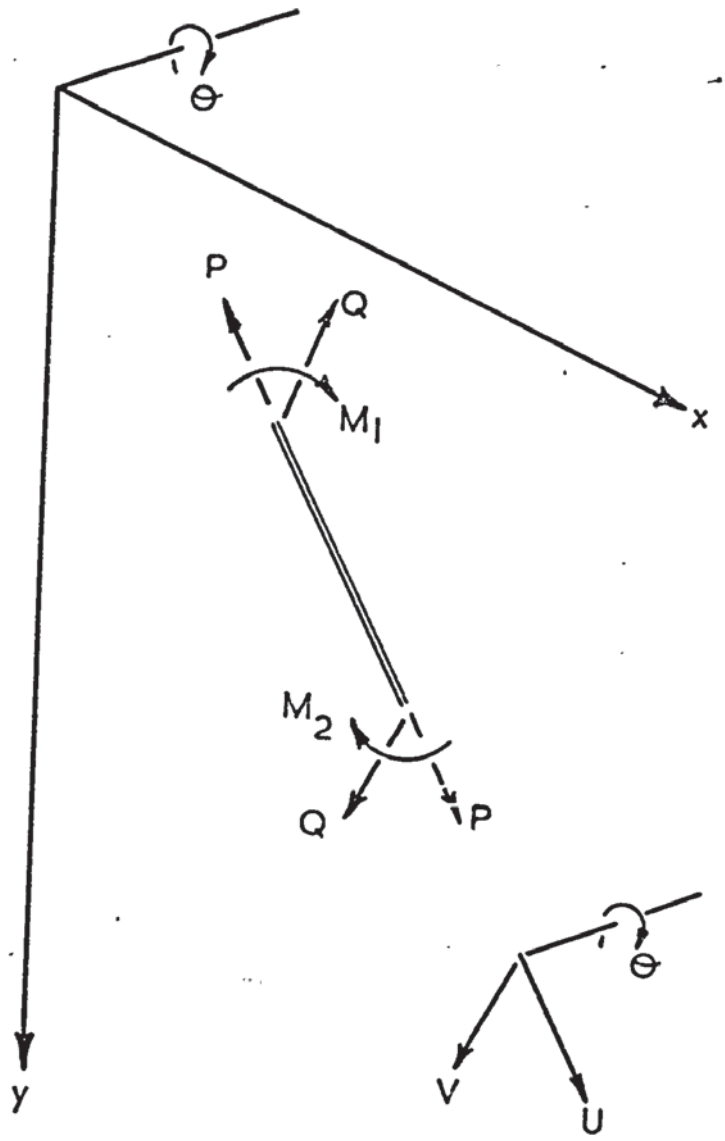

Fig. 2.2 Sign convention for plane frame

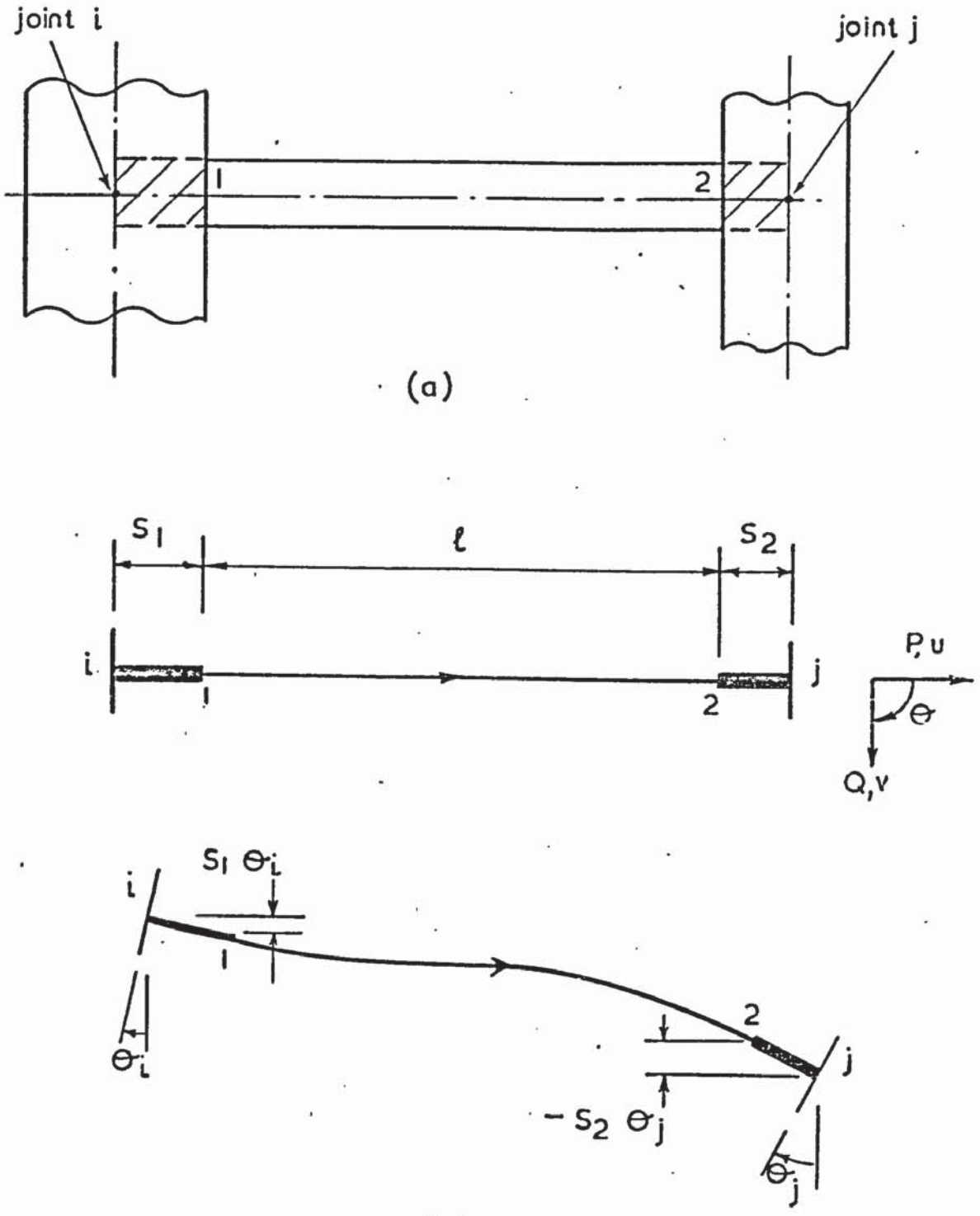

Fig 2.3 Wide column effect

positively from the joint to the end of the beam in the positive direction of the P axis. In the figure therefore, s_2 is negative. Rotation of the joints in a positive direction causes a reduction in the relative lateral displacement of the ends of the flexible span of the beam as shown in Fig. 2.3b. Equation 2.13 is consequently altered to

$$\begin{bmatrix} u \\ v \\ \theta_1 \\ \theta_2 \end{bmatrix} = \left[\begin{array}{ccc|ccc} -\ell_p & -m_p & 0 & \ell_p & m_p & 0 \\ -\ell_q & -m_q & -s_1 & \ell_q & m_q & s_2 \\ 0 & 0 & 1 & 0 & 0 & 0 \\ 0 & 0 & 0 & 0 & 0 & 1 \end{array}\right] \left[\begin{array}{c} x \\ y \\ \theta \\ \hline x \\ y \\ \theta \end{array}\right] \begin{array}{l} \\ \\ \text{joint i} \\ \\ \\ \text{joint j} \end{array} \quad \ldots\ldots \quad (2.14)$$

The application of equation (2.4) to the member stiffness matrix of equation (2.12) and the displacement transformation matrix of equation (2.14) yields the contributions of the member to the overall stiffness matrix of the frame, thus

$$\left[\begin{array}{c|c} \underline{K}_{ii} & \underline{K}_{ij} \\ \hline \underline{K}_{ji} & \underline{K}_{jj} \end{array}\right] = \left[\begin{array}{ccc|ccc} A_1 & B_1 & -C_1 & -A_1 & -B_1 & -C_2 \\ B_1 & F_1 & -T_1 & -B_1 & -F_1 & -T_2 \\ -C_1 & -T_1 & E_1 & C_1 & T_1 & F_2 \\ \hline -A_1 & -B_1 & C_1 & A_1 & B_1 & C_2 \\ -B_1 & -F_1 & T_1 & B_1 & F_1 & T_2 \\ -C_2 & -T_2 & F_2 & C_2 & T_2 & E_2 \end{array}\right] \quad \ldots\ldots \quad (2.15)$$

where:

$$A_1 = \ell_p^2 a + \ell_q^2 b \qquad C_2 = \ell_q (d + s_2 b)$$

$$B_1 = \ell_p m_p a + \ell_q m_q b \qquad E_2 = s_2^2 b + 2 s_2 d + e$$

$$C_1 = \ell_q (d - s_1 b) \qquad F_2 = d (s_2 - s_1) - s_1 s_2 b + f$$

$$E_1 = s_1^2 b - 2 s_1 d + e \qquad T_2 = m_q (d + s_2 b)$$

$$F_1 = m_p^2 a + m_q^2 b$$

$$T_1 = m_q (d - s_1 b)$$

Member forces for each individual member are determined from the joint displacements by combining equations (2.12) and (2.14), thus

$$\begin{bmatrix} P \\ Q \\ M_1 \\ M_2 \end{bmatrix} = \left[\begin{array}{ccc|ccc} -a\ell_p & -am_q & 0 & a\ell_p & am_p & 0 \\ -b\ell_q & -bm_q & (d-s_1 b) & b\ell_q & bm_q & (d+s_2 b) \\ -d\ell_q & -dm_q & (e-s_1 d) & d\ell_q & dm_q & (f+s_2 d) \\ -d\ell_q & -dm_q & (f-s_1 d) & d\ell_q & dm_q & (e+s_2 d) \end{array}\right] \begin{bmatrix} x \\ y \\ \theta \\ -- \\ x \\ y \\ \theta \end{bmatrix} \begin{array}{l} \\ \\ \text{joint i} \\ \\ \\ \\ \text{joint j} \end{array} \qquad (2.16)$$

For regular skeletal frames it is convenient to construct separate matrices for the beams and columns, assuming that the direction of the P axis for the beams is from left to right, while for the columns it is vertically downwards. The terms involving s_1 or s_2 are eliminated. Thus for a beam equation (2.15) is simplified to become

$$\left[\begin{array}{c|c} \underline{K}_{ii} & \underline{K}_{ij} \\ \hline \underline{K}_{ji} & \underline{K}_{jj} \end{array}\right] = \left[\begin{array}{ccc|ccc} a & 0 & 0 & -a & 0 & 0 \\ 0 & b & -d & 0 & -b & -d \\ 0 & -d & e & 0 & d & f \\ \hline -a & 0 & 0 & a & 0 & 0 \\ 0 & -b & d & 0 & b & d \\ 0 & -d & f & 0 & d & e \end{array}\right] \quad \ldots\ldots \quad (2.17a)$$

Similarly, for a column

$$\left[\begin{array}{c|c} \underline{K}_{ii} & \underline{K}_{ij} \\ \hline \underline{K}_{ji} & \underline{K}_{jj} \end{array}\right] = \left[\begin{array}{ccc|ccc} b & 0 & d & -b & 0 & d \\ 0 & a & 0 & 0 & -a & 0 \\ d & 0 & e & -d & 0 & f \\ \hline -b & 0 & -d & b & 0 & -d \\ 0 & -a & 0 & 0 & a & 0 \\ d & 0 & f & -d & 0 & e \end{array}\right] \quad \ldots\ldots \quad (2.17b)$$

In a similar manner simplified forms of equation (2.16) may also be derived for the determination of member forces.

CHAPTER 3

COMPACT STORAGE AND SOLUTION OF EQUATIONS

3.1 Notation

$\underline{A}$	coefficient matrix.
a_{ij}	typical element of $\underline{A}$.
$\underline{B}$	right hand side matrix.
b_{iq}	typical element of $\underline{B}$.
$\underline{C}$	matrix of temporary reduction factors.
c_j, c_{ij}	elements of $\underline{C}$.
i, j, k	row and column subscripts.
m	number of right hand side columns.
n	number of equations.
q	column subscript for matrix $\underline{B}$.
r_i	column number of first non-zero element in row i of $\underline{A}$.
$\underline{X}$	matrix of unknown variables in equation $\underline{A}\,\underline{X} = \underline{B}$.

3.2 Introduction

In the methods of analysis used in this thesis the load-displacement equations give rise to stiffness matrices that are large, sparse, positive definite and symmetrical, but in which the elements do not necessarily form a well defined band. A solution sub-routine has been written based on the compact methods of storage and elimination due to Jennings et al[36,37] which take advantage of the non-uniform band width and of the symmetry of the matrix to reduce storage requirements.

3.3 Jennings' method using Gaussian elimination

Jennings' original method may be described by considering the solution of the set of n equations

$$\underline{A}\,\underline{X} = \underline{B} \qquad \ldots\ldots \quad (3.1)$$

where $\underline{A}$ is a symmetrical, positive definite coefficient matrix of order n x n. $\underline{B}$ and $\underline{X}$ are matrices containing respectively m columns of right hand elements and the corresponding m vectors of unknown variables. The matrix $\underline{A}$ is stored as a continuous sequence row by row, starting from the first non-zero element in each row and finishing with the pivotal element on the leading diagonal. In order to locate the position of each individual row in this sequence, the addresses of the leading diagonal elements are stored as a separate sequence. The right hand side matrix $\underline{B}$ is stored in full matrix form and is overwritten by the solution matrix $\underline{X}$ after a process of reduction and back-substitution based on Gaussian elimination. Both matrices $\underline{A}$ and $\underline{B}$ are wholly stored in core.

In the reduction of a typical row i of $\underline{A}$, a set of temporary reduction factors c_j are determined for each column j starting from the first non-zero element and finishing at the leading diagonal. The number of temporary factors for row i is therefore equal to the number of stored elements a_{ij}, from which the factors are obtained, thus:

$$c_j = a_{ij} - \sum_{k=r_i}^{j-1} c_k \, a_{jk} \qquad \ldots\ldots \quad (3.2)$$

where r_i is the column number of the first non-zero element in row i. In the summation, since k never exceeds j-1, all the values of c_k will already have been determined. The elements a_{ij} are then replaced by $c_j \, a_{jj}$ for values of j from r_i to i-1. The pivotal element a_{ii} is replaced by $1/c_i$. A new set of quantities c_j is formed during the reduction of each row and is stored in the temporary sequence C.

Reduction of the m right hand side columns takes place row by row. For a typical row i the process consists of replacing each right hand side element b_{iq} by the quantity

$$\frac{1}{c_i} \left(b_{iq} - \sum_{j=r_i}^{i-1} c_j \, b_{jq} \right) \qquad \ldots\ldots \quad (3.3)$$

where q = 1, 2, ... m. Once again, since j is always less than i, all the elements b_{jq} in the summation will already have been reduced.

The back-substitution process is carried out for a typical row i of A by subtracting the product $a_{ik} \, b_{iq}$ from each b_{kq}, where q = 1, 2, ... m, for each value of k from r_i to i-1. Successive applications of this operation for i = n, n-1, ... 2 converts the right hand side matrix B into the solution matrix.

3.4 Jennings' method using backing storage

Jennings' later method employs the same system of computer storage for the coefficient matrix but makes use of backing store facilities to enable larger systems of equations to be solved with less core storage. The method of solution is based on Choleski factorisation. The coefficient matrix is partitioned into a number of segments, each of which consists of an integral number of rows. These segments are stored on a

direct access disc file in fixed length blocks such that each block is wholly or partially filled by one complete segment. The right hand side matrix is stored entirely in the core.

Reduction of the coefficient matrix takes place in a working area of core store which, at any stage of the process, contains an active and a passive block. The active block contains the elements currently being reduced while the passive block contains those elements which are required during the reduction of the active block. Active blocks are divided into sections to avoid unnecessary transfer of passive blocks between core and disc. Reduction then takes place row by row within the sections. Reduction of the right hand sides, which are stored entirely in the core, takes place either during or after reduction of the coefficient matrix.

3.5 Modified method of solution

In the method of solution which follows, Jennings' original approach using Gaussian elimination is modified to make use of the backing store facilities just described. The right hand side matrix is also stored in fixed length blocks on a direct access disc file in order to accommodate the large number of right hand side columns arising in the analysis of the frames. The matrices are partitioned so that corresponding segments of $\underline{A}$ and $\underline{B}$ contain equal numbers of rows. Gaussian elimination rather than Choleski factorisation was chosen so that the subroutine would be of the most general use in future research projects. Choleski factorisation is prone to give difficulties with negative square roots in problems where the coefficient matrix has weak diagonal elements. Previous work[38,39] has shown however that load-deflection curves can successfully be obtained, using Gaussian elimination, for structures with up to 2000 degrees of freedom even when the structure is approaching

instability. The additional storage required for the temporary reduction factors is only equal to one disc block (a maximum of 512 real numbers) and does not constitute a significant disadvantage.

The solution process may be described by considering the coefficient matrix and right hand side columns of the set of equations illustrated diagrammatically in Fig. 3.1. It is assumed that reduction of the coefficient matrix has reached the stage where block 3 is about to be reduced. Block 3 is therefore brought into the core as the active block. The block is divided into sections as shown. It can be seen from the diagram that reduction of the elements in section 1 requires only the elements of block 1 and so-on. The reduction process therefore takes place by reducing all the elements in section 1 with block 1 also in core as a passive block. Reduction then proceeds to section 2, replacing block 1 by block 2 as the passive block and so-on. Since each section generally contains several rows of elements it follows that the number of temporary c factors required will be the same as the total number of elements in the active block and that the elements of $\underline{C}$ will have a one to one correspondence with the elements of $\underline{A}$ as shown. Equation (3.2) therefore becomes

$$c_{ij} = a_{ij} - \sum_{k=r_j}^{j-1} c_{ik}\, a_{jk} \qquad \ldots\ldots \qquad (3.4)$$

Elements a_{ij} are replaced by $c_{ij}\, a_{jj}$ and a_{ii} is replaced by $1/c_{ii}$. During the reduction it is necessary to include tests to ensure that operations are not carried out on zero elements of $\underline{A}$ which occur before the first non-zero element in a row and are consequently not stored in the compact sequence. The possibility of this occuring in the summation

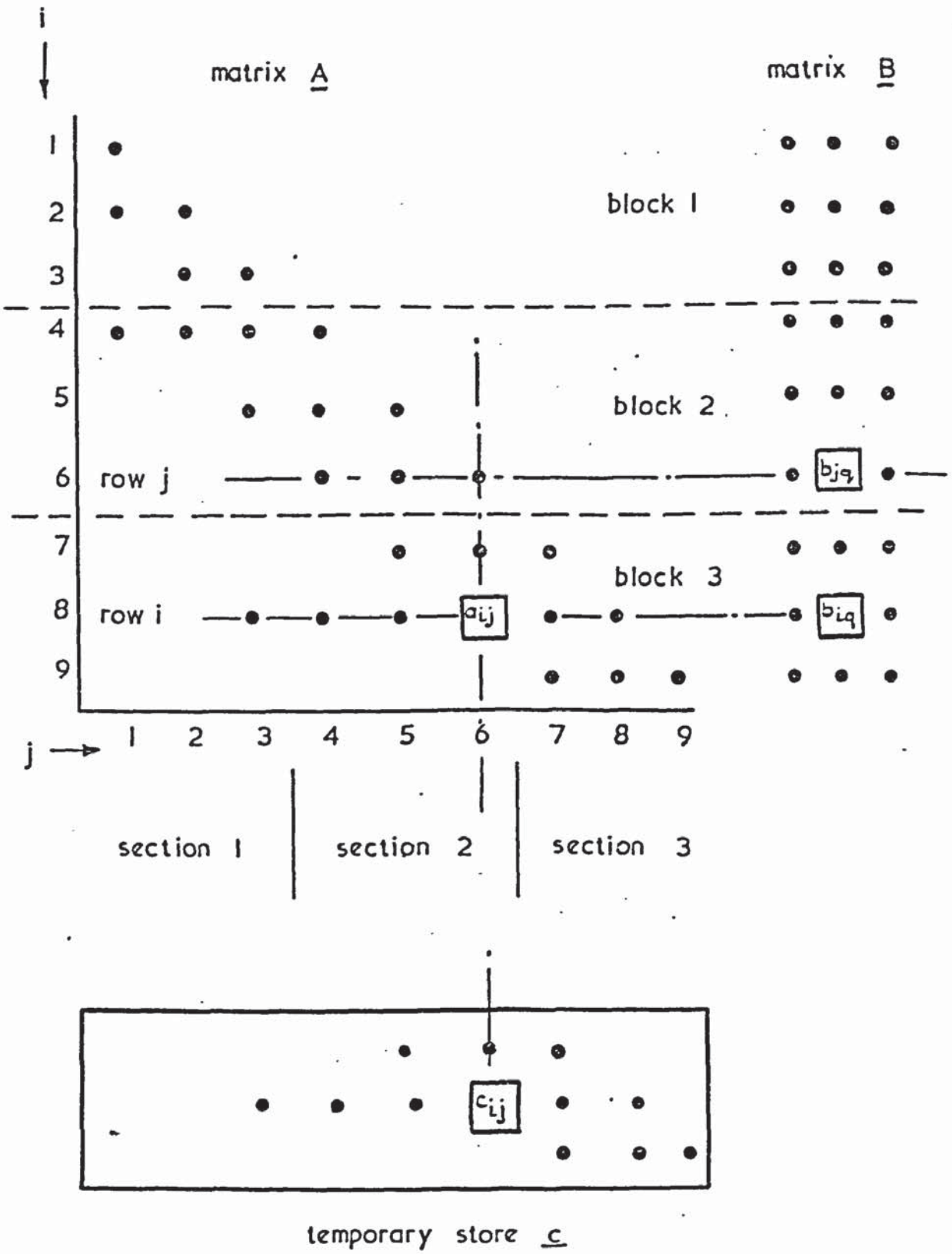

Fig. 3.1 Structure of matrices

part of equation (3.4) is excluded if reduction of the active block takes place column by column, starting the summation with k set to r_j as shown, where r_j is the column number of the first non-zero element in row j. For example, if j = 6 and i = 8 as in Fig. 3.1, then k is set to 4 and

$$c_{86} = a_{86} - c_{84}\, a_{64} - c_{85}\, a_{65}$$

Reduction of the right hand sides may be carried out in parallel with the reduction of the coefficient matrix. Alternatively, as in the present version of the program, the temporary stores may be written tc disc as they are formed and called back into core later for the reduction of the right hand sides, when the reduction of the coefficient matrix has been completed. In this case the expression (3.3) becomes

$$\frac{1}{c_{ii}} \left(b_{iq} - \sum_{j=r_i}^{i-1} c_{ij}\, b_{jq} \right) \qquad \ldots\ldots \qquad (3.5)$$

In order to obtain all the terms b_{jq} to complete the summation it is usually necessary to have recourse to several passive blocks. Accordingly, to economise on block transfers, all the elements b_{jq} required from a particular passive block are used before the next passive block is brought into store. For example b_{8q} in active block 3 is reduced by successively subtracting the following quantities from it.

Passive block 1 $\quad c_{83}\, b_{3q}$

Passive block 2 $\quad \sum_{j=4}^{6} c_{8j}\, b_{jq}$

Passive block 3 $\quad c_{87}\, b_{7q}$

In each case q takes the values 1, 2, 3.

After the reduction process has been completed the coefficient matrix is an upper triangular matrix with its diagonal elements equal to unity. This matrix is stored in transposed form in the locations vacated by the original elements of $\underline{A}$. Solution of the reduced set of equations proceeds by back substitution starting with row n-1 of $\underline{B}$. The process consists of subtracting from each element b_{iq}, the quantity

$$\sum_{k=i+1}^{n} a_{ki}\, b_{kq} \qquad \ldots\ldots \qquad (3.6)$$

where q = 1, 2 ..... m.

Suffix i refers to the rows of the current active block of $\underline{B}$ while suffix k denotes the rows of the passive blocks of $\underline{A}$ and $\underline{B}$. To minimise block transfers, all possible summations are carried out with any pair of passive blocks before bringing the next pair into core. For example, the operations on active block 2 with passive blocks 3 in core as follows:

$$b_{6q} \text{ is replaced by } b_{6q} - \sum_{k=7}^{8} a_{k6}\, b_{kq} \qquad \ldots\ldots \qquad (3.7)$$

$$b_{5q} \text{ is replaced by } b_{5q} - \sum_{k=7}^{8} a_{k5}\, b_{kq} \qquad \ldots\ldots \qquad (3.8)$$

$$b_{4q} \text{ is replaced by } b_{4q} - a_{84}\, b_{8q} \qquad \ldots\ldots \qquad (3.9)$$

where q takes the values 1, 2, 3 in each case.

It should be explained that elements $\underline{A}$ which are called for by the general expression (3.6) do not appear in the summations if they are zero elements not stored in the compact sequence. In the examples quoted above a_{96}, a_{95}, a_{94} and a_{74} are all omitted for this reason.

In operation (3.7) the subscript k starts at its correct initial value of 7. Its final value of 9 is disallowed for the reasons stated above. All possible operations called for by the general expression (3.6) have thus been carried out on the element b_{6q}, which therefore becomes a solution. The operations on the elements b_{5q} and b_{4q} in operations (3.8) and (3.9) on the other hand are seen to be incomplete. Further operations with lower values of k are required to be carried out when the subsequent passive block 2 is brought into store.

A computer program was written for the method, in the form of the Fortran subroutine CDM, by J. S. Sidhu, under the supervision of the author. An outline flow diagram for this subroutine is given in Fig. 3.2. When the subroutine is called, the matrices $\underline{A}$ and $\underline{B}$ are stored in the correct form on direct access disc files. On exit from the subroutine the matrix $\underline{A}$ contains reduced elements and $\underline{B}$ contains the solution vectors. The function of the subroutine in the context of a program for the analysis of complete structures is described in Chapter 6.

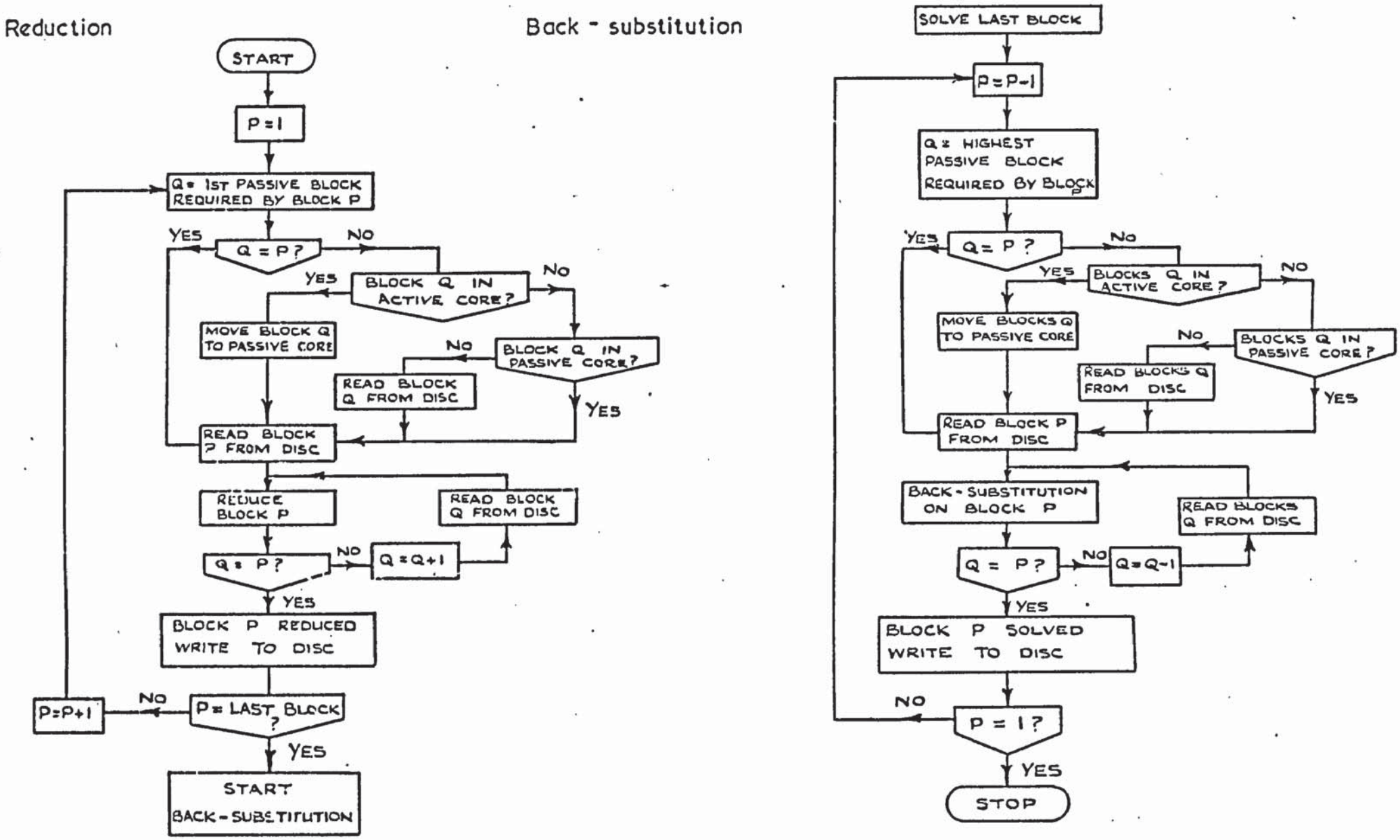

Fig. 3.2 Flow diagram for subroutine CDM

CHAPTER 4

ANALYSIS BY INFLUENCE COEFFICIENTS

4.1 Notations

$\underline{a}$	horizontal deflection vector at all the frame junctions due to $\underline{w}$.
a_{ij}	horizontal deflection of the grillage at junction ij due to $\underline{w}$.
$\underline{b}$	horizontal deflection vector of the frames due to eccentric imposed loading.
b_{ij}	deflection of a frame horizontally at junction ij due to imposed loading.
$\underline{c}$	horizontal deflection vector of the frames due to $\underline{f}$.
c_{ij}	horizontal deflection of a frame at junction ij due to $\underline{f}$.
$\underline{d}$	horizontal deflection vector at all the frame junctions due to $\underline{g}$ and $\underline{w}$.
d_{ij}	total deflection of the grillage at junction ij.
E	Young's modulus.
$\underline{f}$	vector of loads transmitted to the frames.
f_{ij}	horizontal force transmitted to a frame at junction ij.
$\underline{F}$	influence coefficient matrix for the frames.
$F_{ij',\ i\ell}$	horizontal deflection of frame i at junction ij due to unit horizontal force acting on the frame at junction $i\ell$.
$\underline{g}$	vector of loads transmitted to the grillage.
g_{ij}	horizontal force transmitted to the grillage at frame junction ij.
$\underline{G}$	influence ccefficient matrix for the grillage.
$G_{ij'k\ell}$	horizontal displacement of the grillage at junction ij due to unit horizontal force acting at junction $k\ell$.
$\underline{K}$	stiffness matrix of a frame or grillage.
$\underline{L}$	load matrix for determination of influence coefficients.
m	total number of storeys.

n	total number of frames.
$\underline{p}$	external wind load vector.
p_{ij}	wind force at junction of frame i with floor j.
$\underline{w}$	actual wind load vector acting at the wall junctions.
w_{ij}	wind force at the junction of wall i with floor j.
x, y, z	co-ordinates of joint displacements.
x_r	displacement in the direction of the rth degree of freedom of the grillage.
$\underline{X}$	displacement matrix resulting from the solution of $\underline{X}=\underline{K}^{-1}\underline{L}$.
X_{rj}	element in row r, column j of $\underline{X}$.
ν	Poisson's ratio.
θ	rotation of a joint in a plane frame.
θ^x	rotation of a joint in the grillage about the x axis.

4.2 Introduction

The basic assumptions made in the analysis of the complete structure have been described in Chapter 1. Briefly recapitulating, the structure is assumed to consist of a grillage of solid walls and floor slabs which is stiffened against horizontal displacements by the action of a number of plane frames.

In this method the grillage and the frames are analysed separately under the action of a system of unit horizontal forces in order to determine their influence coefficients. The sub-structures are then re-assembled so that the horizontal equilibrium and compatibility conditions are satisfied at the junctions of the floors with the frames. The method is basically a force method which leads to a set of compatibility equations in terms of the horizontal forces carried by the frames at each floor level. The number of these equations is therefore equal to the number of frame-floor junctions in the complete structure.

Determination of the influence coefficients is carried out by the matrix displacement method, using the basic matrices developed in Chapter 2. Computer programming and data preparation are simplified in this approach by using the particular form of these matrices developed for horizontal and vertical members.

4.3 Analysis for wind loading

It is assumed in this analysis, and also in the alternative approach described in the next chapter, that the statical equivalent of the wind load can be expressed as a system of concentrated loads acting at the junctions of the floors with the walls (wall junctions), and with the frames (frame junctions). Each of these junctions constitutes a joint in the grillage and is defined, as shown in Fig.4.1, by two reference numbers. The first number indicates the position in the structure of

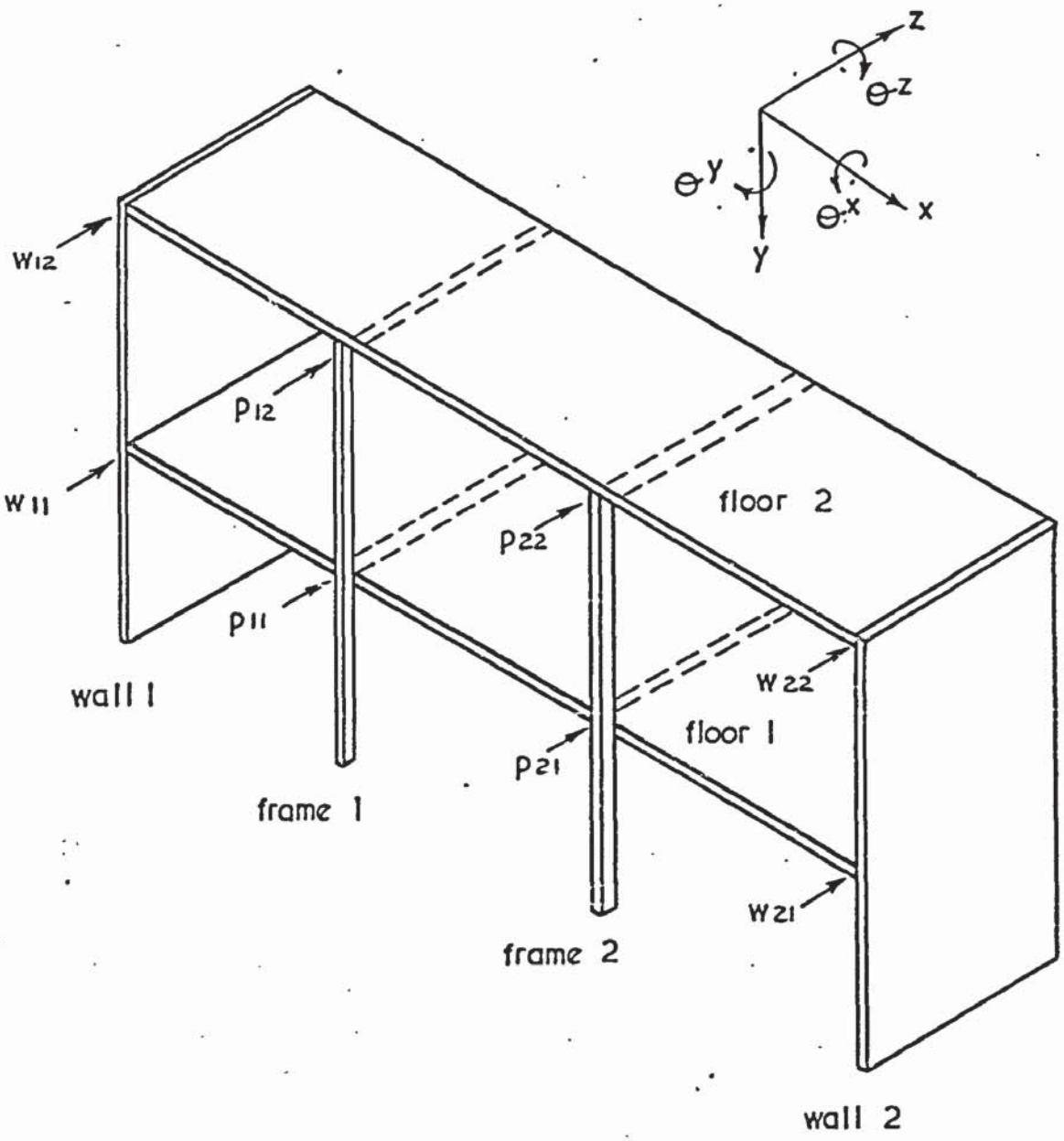

Fig. 4.1. Numbering of wall and frame junctions

the wall or frame, numbering from left to right. The second refers to the level of the junction. For instance, p_{12} and w_{12} are the wind forces acting at the junctions of frame 1 and wall 1 respectively with floor 2.

Consider first the wind force p_{ij} acting at a typical frame junction ij. A portion of this force f_{ij} is carried by the bare frame while the remainder g_{ij} is transmitted to the grillage. Thus, for equilibrium

$$p_{ij} = f_{ij} + g_{ij} \qquad \ldots\ldots \quad (4.1)$$

The horizontal equilibrium at all the frame junctions may be expressed in matrix form by the set of equations

$$\underline{p} = \underline{f} + \underline{g} \qquad \ldots\ldots \quad (4.2)$$

Equation (4.2) implies that the only interactive forces relative to the frames and the slabs are the lateral forces, an assumption made by most workers with regard to structures of the type considered in this thesis. The stiffness of the slabs with respect to bending normal to their planes is ignored except when part of the slab may be considered as a beam spanning between the columns of the frames. Approximate methods for establishing the width of the beam in such cases were discussed in Chapter 1. The resistance of the frames to twisting about their vertical axes has been shown to be negligible[23] and is ignored. The restraint provided by the frames to the twisting of the slabs about their longitudinal axes is also ignored in this analysis. Its effect, however, on the behaviour of a complete structure, is tested in Chapter 8.

The deflections of the grillage at the frame junctions, resulting from the unknown forces $\underline{g}$, may now be considered. Influence coefficients can be defined such that a typical coefficient $G_{ij,k\ell}$ is the horizontal

displacement of the grillage at frame junction ij resulting from a unit horizontal force applied at another frame junction $k\ell$. The deflection of junction ij due to the force $g_{k\ell}$ is therefore $G_{ij,k\ell}\ g_{k\ell}$. For example, in the structure of Fig.4.1, the total deflections at the frame junctions would be given by

$$\begin{aligned} d_{11} &= G_{11,11}\ g_{11} + G_{11,21}\ g_{21} + G_{11,12}\ g_{12} + G_{11,22}\ g_{22} \\ d_{21} &= G_{21,11}\ g_{11} + G_{21,21}\ g_{21} + G_{21,12}\ g_{12} + G_{21,22}\ g_{22} \\ d_{12} &= G_{12,11}\ g_{11} + G_{12,21}\ g_{21} + G_{12,12}\ g_{12} + G_{12,22}\ g_{22} \\ d_{22} &= G_{22,11}\ g_{11} + G_{22,21}\ g_{21} + G_{22,12}\ g_{12} + G_{22,22}\ g_{22} \end{aligned} \quad \ldots\ldots \quad (4.3)$$

It follows that the total deflection d_{ij} at frame junction ij due to all the loads $\underline{g}$ is given by

$$d_{ij} = \sum_{\ell=1}^{m} \sum_{k=1}^{n} G_{ij,k\ell}\ g_{k\ell} \quad \ldots\ldots \quad (4.4)$$

where m is the total number of storeys and n is the total number of frames.

To the above deflection has to be added an amount a_{ij} which is the horizontal deflection of the grillage at frame junction ij due to the action of all the wind forces $\underline{w}$ acting on the shear walls. This additional deflection is directly calculable because the whole of any wind force applied to a shear wall is transmitted to the grillage. The final deflections $\underline{d}$ at all the frame junctions in the grillage are therefore given by

$$\underline{d} = \underline{G}\ \underline{g} + \underline{a} \quad \ldots\ldots \quad (4.5)$$

where $\underline{G}$ is the influence coefficient matrix for the grillage and $\underline{a}$ is

the vector of horizontal deflections at all the frame junctions resulting from the wind force vector $\underline{w}$.

A second expression for the deflection at the frame junctions may be obtained by considering the independent action of the frames resulting from the unknown horizontal force vector $\underline{f}$. Ignoring axial strains in the beams, it may be assumed that the horizontal deflections of all the columns at any floor level in a frame are equal. A set of influence coefficients may therefore be defined such that a typical coefficient $F_{ij,i\ell}$ is the horizontal deflection of the frame at junction ij due to a unit horizontal force acting at junction $i\ell$. The first subscripts in each pair are always identical because it is the behaviour of individual frames that is being considered at this stage. The total deflection c_{ij} of frame i at junction ij resulting from all the forces $f_{i\ell}$ transmitted to the frame is given by

$$c_{ij} = \sum_{\ell=1}^{m} F_{ij,i\ell}\, f_{i\ell} \qquad \ldots\ldots \quad (4.6)$$

Hence, the deflections $\underline{c}$ at all the frame junctions due to the vector $\underline{f}$ are given by

$$\underline{c} = \underline{F}\,\underline{f} \qquad \ldots\ldots \quad (4.7)$$

where $\underline{F}$ is the influence coefficient matrix for all the frames. In order to satisfy the conditions of compatibility at the frame junctions, the deflections given by equations (4.5) and (4.7) must be equal and hence,

$$\underline{G}\,\underline{g} + \underline{a} = \underline{F}\,\underline{f} \qquad \ldots\ldots \quad (4.8)$$

Substituting for $\underline{g}$ from equation (4.2) into (4.8) and re-arranging,

$$(\underline{G} + \underline{F})\,\underline{f} = \underline{G}\,\underline{p} + \underline{a} \qquad \ldots\ldots \quad (4.9)$$

Solution of this equation yields the unknown horizontal forces $\underline{f}$ carried by the frames, thus

$$\underline{f} = (\underline{G} + \underline{F})^{-1}\,(\underline{G}\,\underline{p} + \underline{a}) \qquad \ldots\ldots \quad (4.10)$$

The portion $\underline{g}$ of the wind loads carried by the grillage may then be obtained from the equilibrium equation (4.2).

4.4 Influence coefficient matrices

The influence coefficient matrices $\underline{G}$ and $\underline{F}$ are square matrices whose order is mn, the total number of frame junctions. For example, matrix $\underline{G}$ for the structure of Fig.4.1 may be obtained directly from equation (4.3), thus

$$\underline{G} = \left[\begin{array}{cc|cc} G_{11,11} & G_{11,21} & G_{11,12} & G_{11,22} \\ G_{21,11} & G_{21,21} & G_{21,12} & G_{21,22} \\ \hline G_{12,11} & G_{12,21} & G_{12,12} & G_{12,22} \\ G_{22,11} & G_{22,21} & G_{22,12} & G_{22,22} \end{array}\right] \begin{array}{l} \\ \\ \text{Floor 1} \\ \\ \\ \\ \text{Floor 2} \end{array} \qquad \ldots\ldots \quad (4.11)$$

Here it can be seen that in a row, the initial pairs of subscripts are identical, indicating that the elements of a row are the deflections at a given frame junction resulting from the application of a unit load at each frame junction in turn. Similarly, in a column, the second pair of subscripts are identical, denoting that a column contains the deflections at all the frame junctions due to a unit load applied at a single junction. The matrix is symmetrical in accordance with Maxwell's reciprocal theorem.

The influence coefficient matrix $\underline{F}$ for the frames is constructed in a similar way except that each column refers to a single independent frame. Elements corresponding to deflections in other frames are therefore zero. For the structure of Fig.4.1, for example

$$\underline{F} = \left[\begin{array}{cc|cc} F_{11,11} & 0 & F_{11,12} & 0 \\ 0 & F_{21,21} & 0 & F_{21,22} \\ \hline F_{12,11} & 0 & F_{12,12} & 0 \\ 0 & F_{22,21} & 0 & F_{22,22} \end{array}\right] \begin{array}{l} \text{Floor 1} \\ \\ \\ \text{Floor 2} \end{array} \quad \ldots\ldots \quad (4.12)$$

The elements of the influence coefficient matrices are obtained by carrying out separate analyses of the frames and the grillage, using the matrix displacement method as described in Chapter 2. For each frame the load matrix $\underline{L}$ of equation (2.1) consists of m columns, each containing a single unit horizontal load. The influence coefficients are given by the rows of the displacement matrix $\underline{X}$ corresponding to the unit loads in $\underline{L}$.

It is assumed that each joint has three degrees of freedom in the x, y and θ directions, implying that the horizontal displacements of all the joints are independent. It is necessary therefore to suppress axial deformations in the beams in order to ensure that column displacements at a given level are equal. This can be accomplished by the insertion of large fictitious cross sectional areas for the beams into the analysis. In practice however, it was found that if the correct cross sectional areas were used, the effect on the results was negligible. The inclusion of unnecessary degrees of freedom is however wasteful of computer time and storage, and in the later method of analysis, described in Chapter 5, a single horizontal displacement is assumed at each floor level.

As an example, the load and displacement matrices for frame 1 of Fig.4.1 are shown in Fig.4.2a. Displacements not required in the construction of the influence coefficient matrices are omitted from matrix $\underline{X}$ in the figure. The numbering of the joints is given by the encircled numbers in Fig.4.2b, which also illustrates the physical meaning of the influence coefficients. In the diagrams load-case 1 corresponds with column 1 of $\underline{L}$ and the resulting displacements are given in column 1 of $\underline{X}$. Similarly, load-case 2 corresponds with column 2 of the matrices.

When skew symmetry exists, computer time and storage can be saved by analysing only half of the frame. In this case the displacements of joints on the line of symmetry are suppressed in the y direction and the unit loads of $\underline{L}$ are divided by 2.

Influence coefficients for the grillage are determined by a similar analysis, but with the load matrix in this case consisting of mn columns. The elements of the displacement vector $\underline{a}$ are also determined at this stage by including the wind load vector $\underline{w}$ as an additional column in the load matrix. The corresponding horizontal deflections at the frame junctions are the required elements of $\underline{a}$. The construction of the load and displacement matrices for the grillage of Fig.4.1 is illustrated in Fig.4.3. Displacements not required at this stage of the analysis are again omitted from matrix $\underline{X}$ in the figure.

4.5 The effect of imposed loading

Equations (4.5) and (4.7) imply that the sidesways produced in the frames and the grillage are the result of lateral wind forces only. It is well known however that sidesways also result from the action of imposed vertical loads unless they are symmetrically applied and the configuration of the frame or wall is also symmetrical. The effects of these loads was included in some earlier analyses[6,23], which were concerned

(a)

$$\underline{L} = \begin{bmatrix} 1 & 0 \\ 0 & 0 \\ 0 & 0 \\ \hline 0 & 0 \\ 0 & 0 \\ 0 & 0 \\ \hline 0 & 1 \\ 0 & 0 \\ 0 & 0 \\ \hline 0 & 0 \\ 0 & 0 \\ 0 & 0 \end{bmatrix} \quad \begin{matrix} \\ \text{Joint 1} \\ \\ \\ \\ \text{Joint 2} \\ \\ \\ \\ \text{Joint 3} \\ \\ \\ \\ \text{Joint 4} \\ \\ \end{matrix} \qquad \underline{X} = \begin{bmatrix} F_{11,11} & F_{11,12} \\ \\ \\ \\ \\ \\ F_{12,11} & F_{12,12} \\ \\ \\ \\ \\ \\ \\ \end{bmatrix}$$

(b)

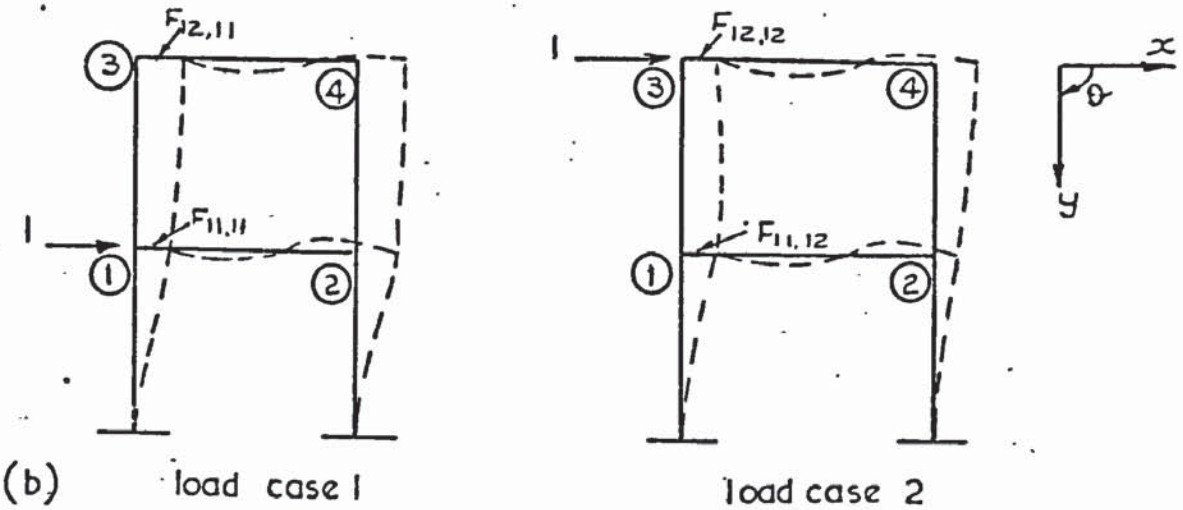

Fig. 4.2. Frame load and displacement matrices

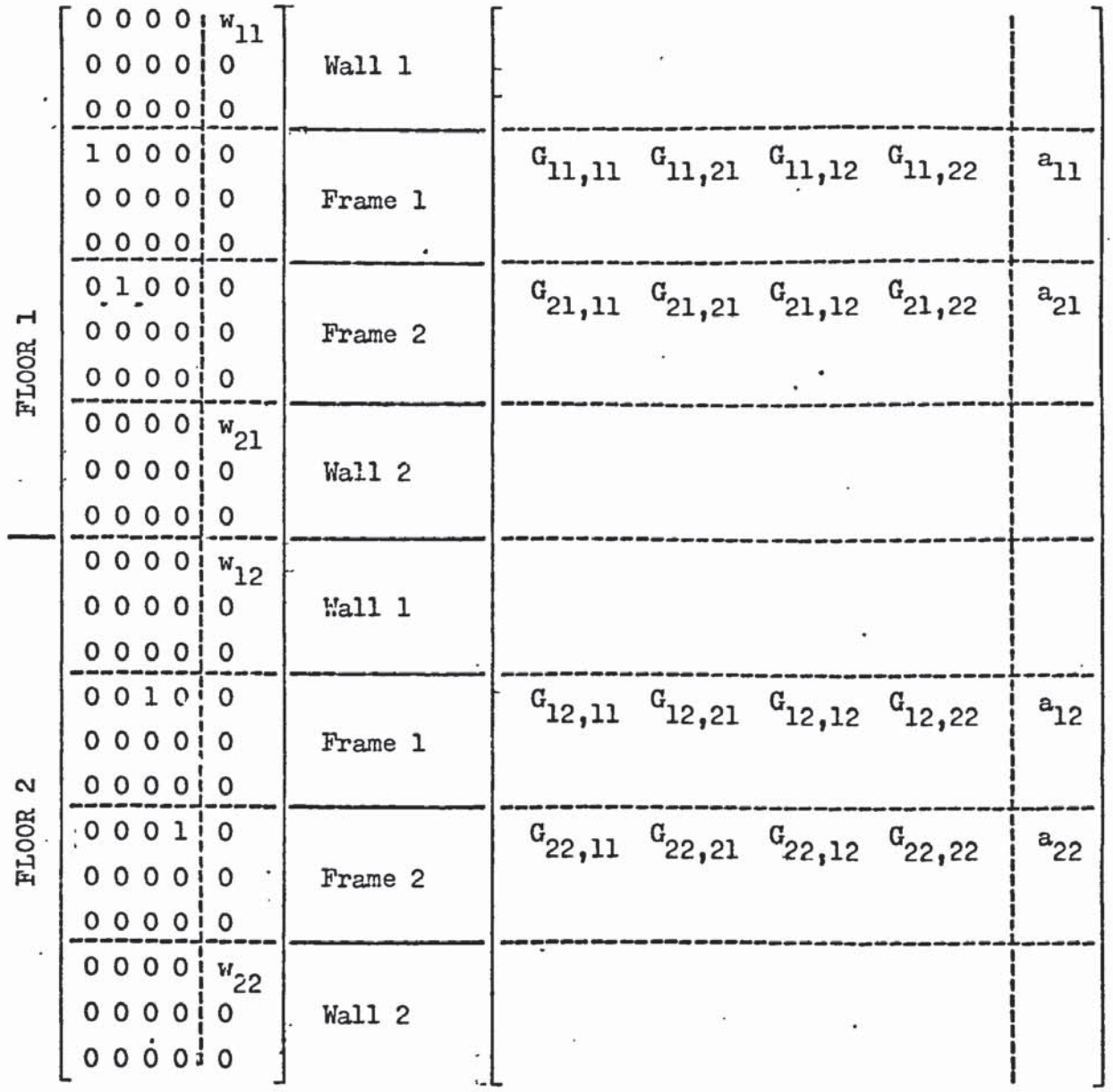

Fig. 4.3 Grillage load and displacement matrices

with structures consisting of frames and slabs only. Very few other instances have been found in the published literature where provision has been made for this type of loading. In particular, analyses in which axial deformations of the columns are neglected, automatically exclude their consideration. Similarly it would be difficult to include their effects into analyses based on the continuum approach unless a considerable degree of uniformity of the imposed loading was assumed.

Usually an eccentric wall consists of two or more uniform elements whose centre lines do not coincide. In such cases uniform loads from the floor slabs in the upper elements produce an overturning moment about the base of the wall. This effect can be reproduced by replacing the eccentrically applied loading by a resultant vertical load acting through the centre-line of the base of the wall, together with an overturning moment applied at the base of each element. Since the vertical forces cause no sway it is only necessary to consider the effect of the overturning moments. As an example, the derivation of these moments is given for the tapered wall in Fig.4.4.

Consider first the narrowest part of the wall containing m_1 floors each carrying a total uniformly distributed load L_1. The resultant load from these floors is $m_1 L_1$ acting at an eccentricity of $\frac{e_1}{2}$ from the neutral axis of the segment below. The overturning moment at the junction ab is therefore given by

$$M_1 = m_1 L_1 \frac{e_1}{2}$$

Similarly, the overturning moment at junction cd is given by

$$M_2 = (m_1 L_1 + m_2 L_2) \frac{e_2}{2}$$

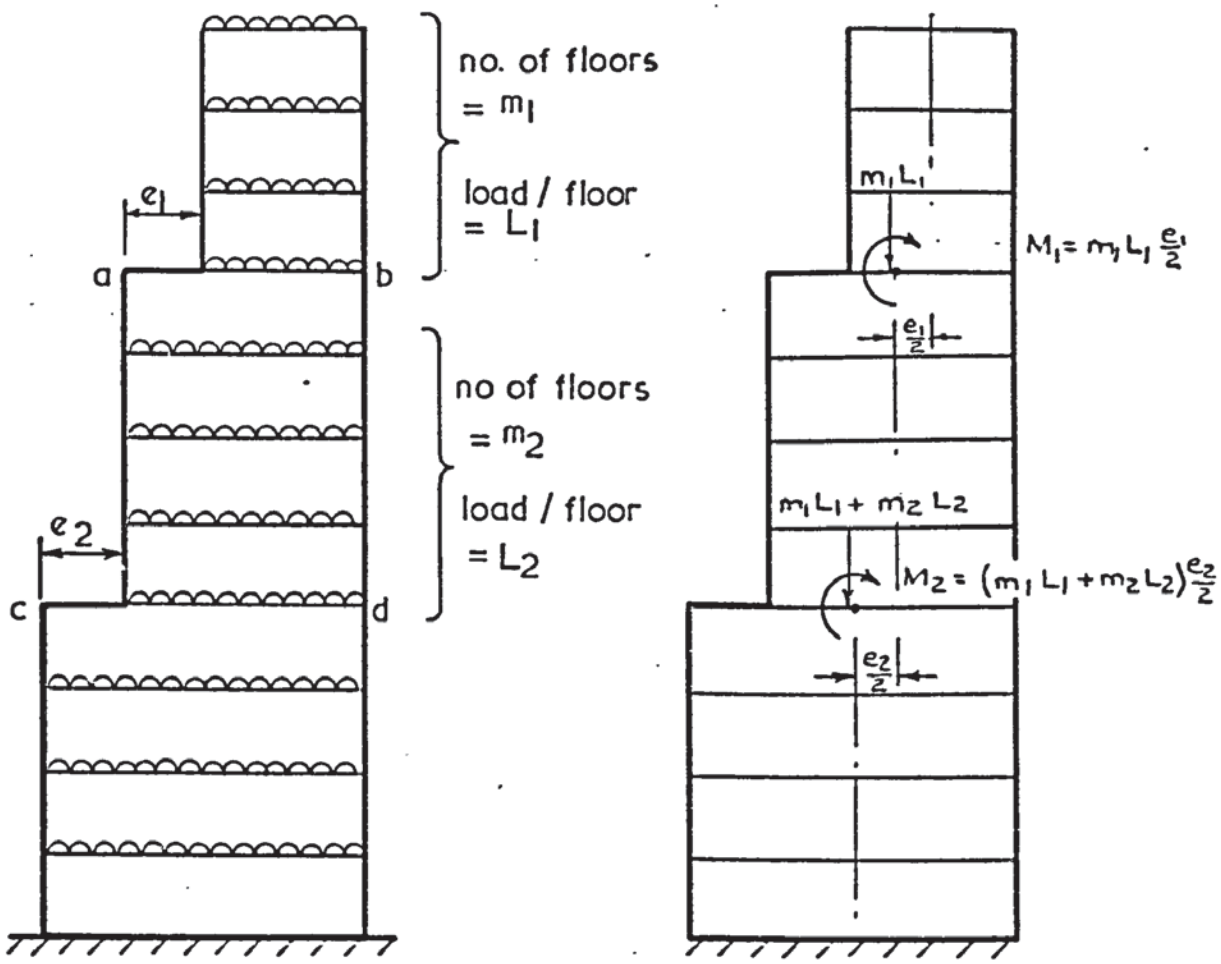

(a) actual floor loading (b) loads causing side sway

Fig. 4.4. Eccentric wall loading

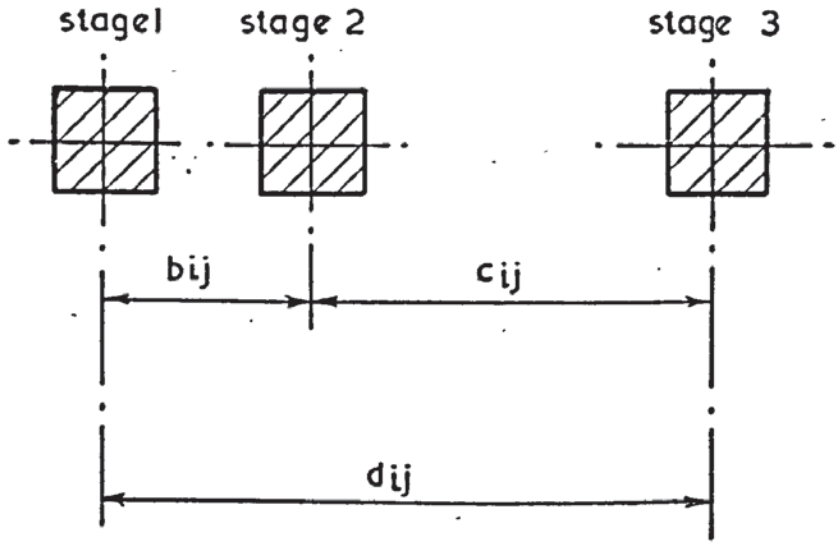

Fig. 4.5 Effect of differential side sway of frames

where the subscript 2 refers to the segment of wall between junctions ab and cd. Since M_1 and M_2 act directly on the grillage, their effect on the value of the displacements $\underline{a}$ can be determined by including them in the load vector $\underline{w}$.

The effect of eccentric loading on the frames on the other hand, is to produce sidesways which alter the compatibility equations at the frame junctions. In Fig.4.5 the deflections of the frame and the grillage at a typical frame junction ij are shown diagrammatically. Stage 1 represents the initial unloaded state of the frame and the grillage. The eccentric vertical loads cause the frame to move horizontally a distance b_{ij} to stage 2. The wind loads, which are shared between the frame and the grillage, cause the frame to deflect by a further amount c_{ij} while the grillage deflects by d_{ij} to stage 3. The total deflections of the frame and the grillage must be equal as shown and hence

$$d_{ij} = c_{ij} + b_{ij} \qquad \ldots\ldots \qquad (4.13)$$

The conditions of compatibility at all the frame junctions are therefore given in matrix form by

$$\underline{d} = \underline{c} + \underline{b} \qquad \ldots\ldots \qquad (4.14)$$

Substitution for $\underline{d}$ and $\underline{c}$ from equations (4.5) and (4.7) yields

$$\underline{G}\,\underline{g} + \underline{a} = \underline{F}\,\underline{f} + \underline{b} \qquad \ldots\ldots \qquad (4.15)$$

and equation (4.10) is therefore modified to become

$$\underline{f} = (\underline{G} + \underline{F})^{-1} \; (\underline{G}\,\underline{p} + \underline{a} - \underline{b}) \qquad \ldots\ldots \qquad (4.16)$$

The elements of vector $\underline{b}$, which are the sway deflections at the frame junctions due to the action of eccentric vertical loads on the separate frames, may be determined by including an additional column of vertical forces in the load matrix during the calculation of the frame influence coefficients. Alternatively the sidesways may be obtained from a preliminary analysis of the frames subjected to vertical loads only.

4.6 Displacements and member forces

The horizontal forces $\underline{g}$ and $\underline{f}$ are now used to determine the displacements and member forces in the grillage and the individual frames. In the case of the grillage, it can be seen by referring back to Fig.4.3 that in addition to the horizontal influence coefficients required in the construction of matrix $\underline{G}$, the displacement matrix $\underline{X}$ contains influence coefficients for all the other displacements in the grillage. It also contains, in the last column, the actual displacements resulting from the load vector $\underline{w}$. The actual displacements at the grillage joints, resulting from all the forces acting on the grillage, are therefore obtained by multiplying all the elements except the last in each row of $\underline{X}$ by $\underline{g}$ and then adding the last element. For example, the typical displacement x_r, obtained from the rth row of $\underline{X}$, is given by

$$x_r = \sum_{j=1}^{s} (X_{rj}\, g_j) + X_{r,s+1} \qquad \ldots\ldots \qquad (4.17)$$

where $s = mn$, the number of frame junctions.

The displacements at the joints in the frames are determined by analysing each frame separately, using the appropriate horizontal loads extracted from the vector $\underline{f}$. As in the grillage these displacements may be obtained directly from the influence coefficients of the frames. A

more convenient approach however, involving less computer storage, is simply to re-analyse each frame completely using the member stiffnesses and other relevant data retained from the analyses of the frames earlier in the computer program.

Member forces in the grillage and the frames are obtained by the application of equations (2.11) and (2.16) respectively to each member in turn.

4.7 Verification of the analysis

Experimental verification of the analysis, using a two storey model structure, was carried out at this stage. However, as the experimental work forms the subject of Chapter 7, details of the results will not be repeated here.

Further verification was obtained by comparison with the results reported by Goldberg for the analysis of a 10 storey structure of a type commonly encountered in practice. This structure, which is illustrated in Fig.4.6, consists of reinforced concrete walls and slabs for which Young's modulus is 3×10^6 lb/in^2 and Poisson's ratio is 0.1. The frames are of steel sections with Young's modulus equal to 30×10^6 lb/in^2 and having the section properties tabulated in the figure. Cross sectional areas were not quoted by Goldberg, who did not include the effects of axial deformations in the columns. The figures given in the table are those of the nearest equivalent British sections. At the roof level the structure is subjected to wind loads of 1800 lb on the wall junctions and 3600 lb on the frame junctions. At all other levels these values are doubled.

Typical deflections and frame shears are given in Table 4.1. A comparison of the results from the method of influence coefficients with those of Goldberg shows that the two are in good agreement. It can also be seen

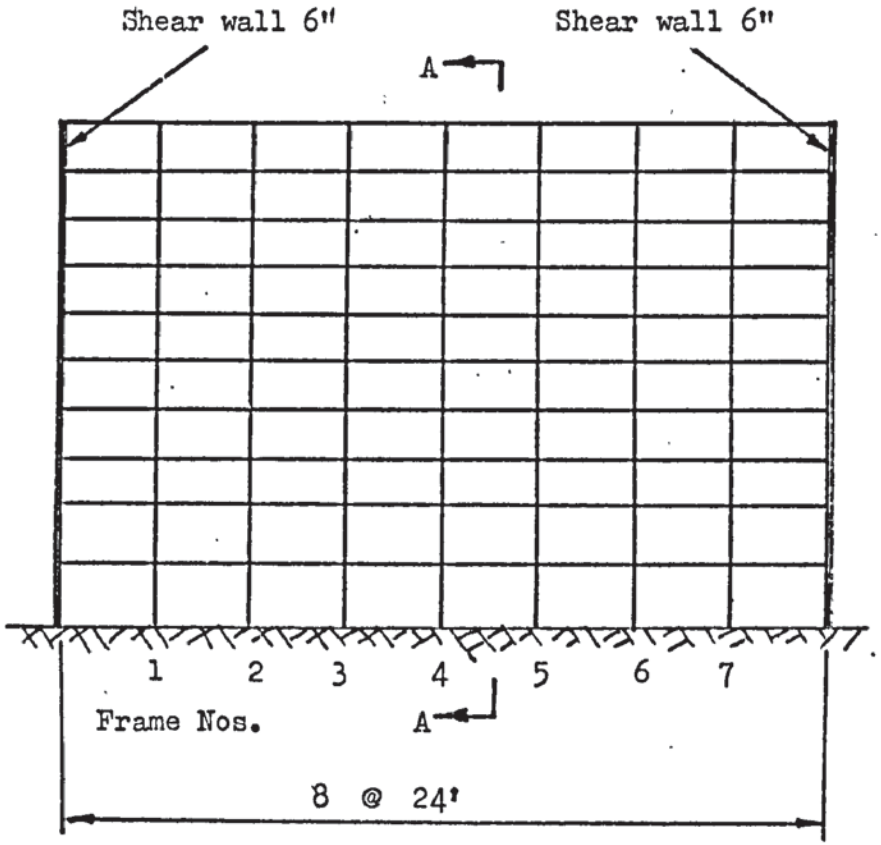

ELEVATION

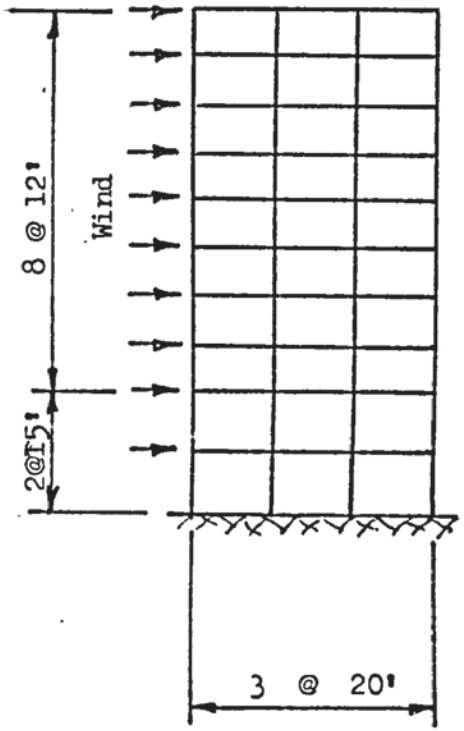

SECTION A-A

Fig. 4.6 Goldberg's 10 storey structure

Storey	I (in^4)	A (in^2)
10	254	13
9	443	23
8	739	25
7	927	25
6	1152	30
5	1414	35
4	1708	45
3	2168	55
2	2477	60
1	2627	65
Beams	1380	19

SECTIONAL PROPERTIES OF FRAME MEMBERS

Roof and slabs 3" thick

	Goldberg		Method of Influence Coefficients			
	Axial Strains ignored		Axial Strains ignored		Axial Strains included	
Storey	Wall	Frame 4	Wall	Frame 4	Wall	Frame 4
10	0.2434	0.2570	0.2446	0.2584	0.2460	0.2604
5	0.1100	0.1481	0.1105	0.1486	0.1100	0.1489
1	0.0142	0.0319	0.0143	0.0330	0.1440	0.0339

i. Deflections (in.)

	Goldberg		Method of Influence Coefficients			
	Axial Strains ignored		Axial Strains ignored		Axial Strains included	
Storey	Frame 1	Frame 4	Frame 1	Frame 4	Frame 1	Frame 4
10	1718	813	1662	774	1508	690
5	5415	5262	5274	5126	5073	4940
1	7156	10950	6727	10497	6539	10294

ii. Frame shears (lb.)

Table 4.1 Comparative results for Goldberg's structure

that the inclusion of axial deformations in the columns of the frames has little effect in this case. More detailed results of the analyses carried out on Goldberg's structure are discussed later in Chapter 8.

4.8 Discussion

A feature of this method of analysis is that the three dimensional structure is divided into plane structural elements which are then analysed quite separately. Consequently the number of degrees of freedom at any joint is limited to three and also the number of equations to be solved at any stage of the analysis is relatively small. For example, in Goldberg's 10 storey structure, displacements corresponding to 1110 degrees of freedom are determined. The largest number of simultaneous equations, however is the set of 270 load-displacement equations for the grillage. A further result of the separation of the grillage and the frames is that it is only necessary to prepare data once for each set of identical frames. Additional economies in data preparation and program running time arising from a consideration of the regularity of the structure are described in Chapter 6.

A limitation inherent in the method is that in order to be able to carry out independent analyses on the frames and the grillage it is necessary to ensure that on separation neither structure degenerates into a mechanism. This implies that the grillage must always contain sufficient monolithic shear walls to provide adequate bracing without the action of the frames. This limitation places a severe restriction on the range of structures that can be analysed by this method.

A further difficulty arises from the form of equations (4.10). Although the number of unknowns is relatively small (one for each frame junction), the equations are not sparse and could create a storage problem in the analysis of large structures. Evidence of ill-conditioning was

found in these equations during the analysis of Goldberg's 10 storey structure when the number of frames was increased from seven to ten, with a proportionate increase in the length of the structure. In this case an accurate solution was not possible using the standard library subroutine for the solution of the equations.

The method of analysis by influence coefficients was used by the writer to carry out a preliminary investigation into the elastic behaviour of complete structures, using Goldberg's 10 storey structure as an example[40]. The method was also used by Majid and Onen[41,42] as the basis for research into the elastic-plastic behaviour of structures loaded to collapse. However, in order to extend the range of structures that can be analysed, and having regard to the limitations described above, an alternative method of analysis was developed. This is described in the next Chapter.

CHAPTER 5

THE RESTRAINED GRILLAGE METHOD

5.1 Notation

$\underline{b}$	vector containing the horizontal deflections at all the frame junctions due to the imposed loading.
$\underline{b}^r$	vector of horizontal deflections in frame r due to the imposed load vector $\underline{\ell}$.
$\underline{c}$	vector containing the horizontal deflections of all the frames due to $\underline{f}$.
$\underline{c}^r$	horizontal deflection vector of frame r due to $\underline{f}^r$.
$\underline{d}$	complete displacement vector for the grillage.
$\underline{d}^r$	vector of horizontal deflections of the grillage at the junction with frame r.
$\underline{f}$	vector containing the horizontal loads transmitted to the frames.
$\underline{f}^r$	vector of loads transmitted to frame r.
$\underline{g}$	vector containing the loads transmitted to the grillage at the frame junctions.
$\underline{h}$	vector containing horizontal forces equivalent to the imposed loading on the frames.
$\underline{h}^r$	horizontal force vector equivalent to the imposed loading on frame r.
$\underline{H}$	stiffness matrix containing the horizontal stiffnesses of all the frames.
$\underline{H}^r$	horizontal stiffness matrix of frame r.
H^r_{ij}	horizontal force at floor level i in frame r when unit displacement is applied at floor level j.
$\underline{J}$	stiffness matrix of the grillage without the frames.
$\underline{K}_{11}, \underline{K}_{12}, \underline{K}_{21}, \underline{K}_{22}$	segments of the stiffness matrix of a typical frame.
$\underline{\ell}$	vector of imposed loads on a typical frame.
$\underline{p}$	complete external load vector for the equivalent grillage.

$\underline{x}$ vector of unknown displacements due to all the loads on a typical frame.

$\underline{X}$ matrix of unknown displacements in a typical frame.

$\underline{\emptyset}$ vector of vertical and rotational displacements due to $\underline{\ell}$.

5.2 Introduction

In this approach the complete structure is again considered as a grillage consisting of monolithic floor slabs and shear walls, restrained laterally by the frames. The matrix displacement method is used to determine the lateral stiffnesses of the individual frames by partitioning and condensation of their overall stiffness matrices. The stiffness matrix of the complete structure is formed by superimposing these lateral frame stiffnesses on to the stiffness matrix formed by the wall and floor slab panels of the grillage. Solution of the load displacement equations for this restrained grillage yields the displacements at all the wall and frame junctions in the complete structure. The analysis of the frames is completed by back-substitution of the horizontal displacements, extracted from the displacement vector for the complete structure, into the load displacement equations of each individual frame in turn.

The assumptions described in Chapter 1 concerning the configuration of the complete structure are unchanged. However, by the use of the wide column-frame analogy with arbitrary numbering of the joints, the meaning of the term "frame" has been extended to include a wider range of structures. Examples are shear walls with openings, wall-frame structures, and frames braced by diagonal trussing. The term "wall" on the other hand has been retained for the monolithic shear walls, which may form, with the floor slabs, an integral part of the unrestrained grillage. The assumptions made in the last Chapter with regard to the conditions of equilibrium and compatibility at the frame junctions are also retained.

5.3 Analysis for wind loading

The aim in this analysis is to produce a stiffness matrix for the grillage which contains additional terms representing the lateral

stiffness of the plane frames. It is not necessary therefore to employ a system of joint numbering that distinguishes between frame and wall junctions. The joints in this restrained grillage are located in vertical lines at the junctions of the floor slabs with the vertical components of the structure. Unsupported points in the floor slabs, such as on a vertical line of symmetry or at the free ends of cantilvered slabs, are also considered as joints.

The position of each joint is indicated by two subscripts, the first indicating its position relative to the left hand side of the structure, and the second denoting the level of the floor containing the joint. For example, in Fig.5.1 the horizontal wind load p_{12} acts at the joint formed by the junction of a wall in position 1 with the floor slab at level 2. Joints may have up to three degrees of freedom in the z, θ^x and θ^y directions as shown in the figure. It is assumed however that all the joints in any particular vertical line have the same degrees of freedom.

The equilibrium of all the applied forces acting at the joints is expressed by the equation

$$\underline{p} = \underline{g} + \underline{f} \qquad \ldots\ldots \quad (5.1)$$

This equation has the same form as that of equation (4.2) in the previous Chapter, but is not restricted to the frame junctions in this case. $\underline{p}$ is the vector of all the external forces acting on the restrained grillage and vector $\underline{g}$ is the portion of these forces carried by the walls and floor alone. $\underline{p}$ and $\underline{g}$ have an order equal to the total assumed degrees of freedom of the grillage and are necessarily identical except at the frame junctions, where it is assumed that a portion of the horizontal applied forces is transmitted to the frames. This portion forms the appropriate elements of vector $\underline{f}$. Since horizontal equilibrium only is considered at

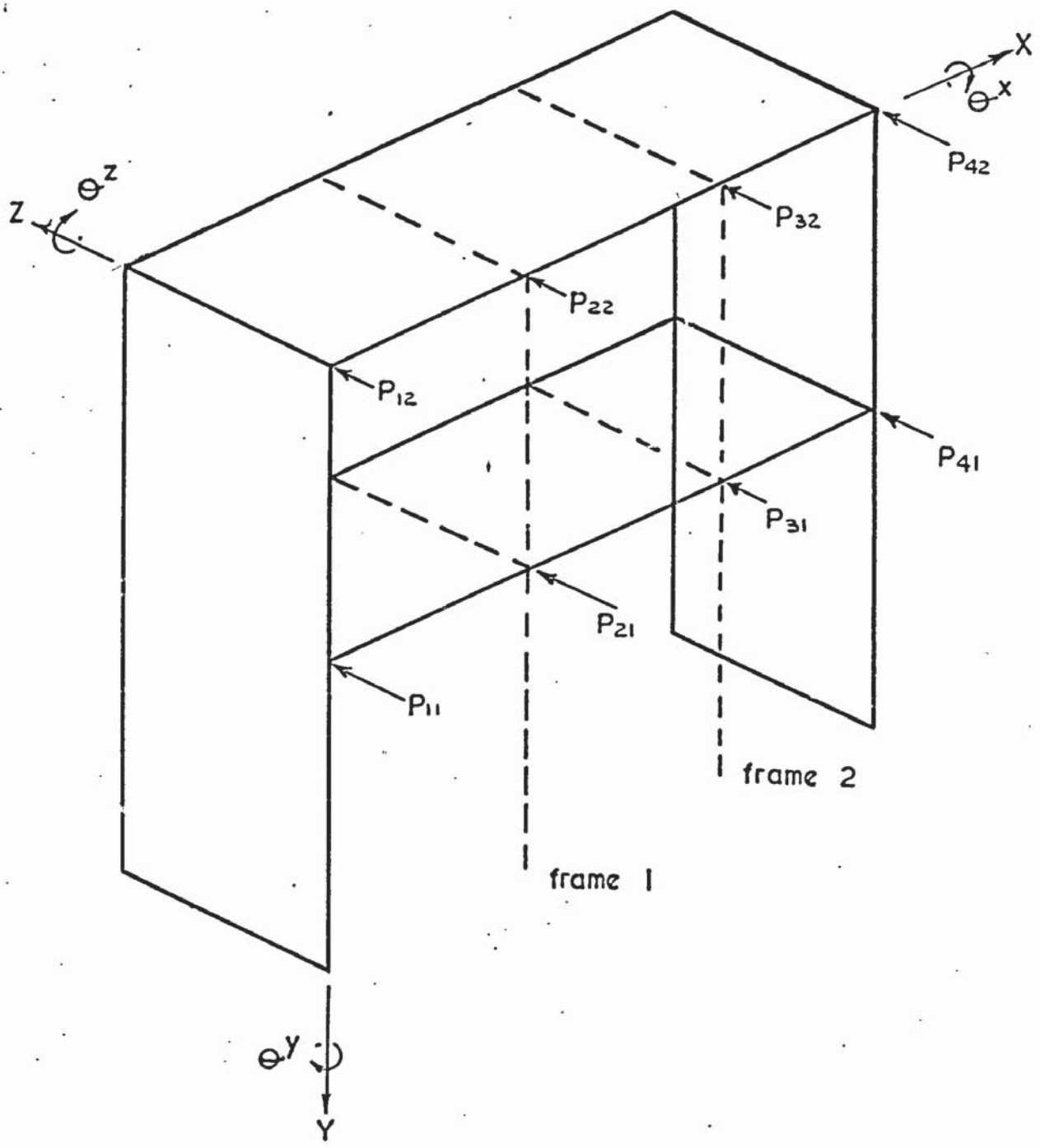

Fig. 5.1 Numbering of joints

the frame junctions, the remaining elements of $\underline{f}$ are zero. As an example the complete applied force vectors for the structure of Fig.5.1 are given in Fig.5.2.

The effect of the vector $\underline{g}$ acting on the unrestrained grillage would be to produce an equivalent set of displacements $\underline{d}$, thus

$$\underline{g} = \underline{J}\,\underline{d} \qquad \ldots\ldots \quad (5.2)$$

where $\underline{J}$ is the stiffness matrix of the unrestrained grillage. In some structures, for example one consisting entirely of floors and frames, the unrestrained grillage consists of a system of unconnected slabs and equation (5.2) has no meaning. In such a case it could be assumed that the floor slabs were connected by a system of flexible members providing a sufficient number of constraints to yield a non-singular stiffness matrix. It will be seen later that when the lateral restraints of the frames are applied, the stiffness coefficients contributed by these members can be removed without invalidating the overall load-displacement equations of the structure.

For the frames, the horizontal forces in $\underline{f}$ can be related to an equivalent set of displacements $\underline{c}$ by the equation

$$\underline{f} = \underline{H}\,\underline{c} \qquad \ldots\ldots \quad (5.3)$$

where $\underline{H}$ is a square matrix of the same order as $\underline{J}$, representing the lateral stiffness of all the frames. A typical coefficient H^{r}_{ij} may be defined as the horizontal force which must be applied to a frame of type r at floor level i when a unit horizontal displacement is produced at floor j, while the horizontal displacements at all other floor levels are held at zero. This definition is illustrated in Fig.5.3a for the frame of type 1 in Fig.5.1. As the compatibility condition at the frame junction is assumed to be in a horizontal direction only, the vertical and rotational displace-

	$\underline{p}$	=	$\underline{g}$	+	$\underline{f}$
Wall in position 1	p_{11}		g_{11}		0
	0		0		0
	0		0		0
	p_{12}		g_{12}		0
	0		0		0
	0		0		0
Frame in position 2	p_{21}		g_{21}		f_{21}
	0		0		0
	0		0		0
	p_{22}		g_{22}		f_{22}
	0		0		0
	0		0		0
Frame in position 3	p_{31}		g_{31}		f_{31}
	0		0		0
	0		0		0
	p_{32}		g_{32}		f_{32}
	0		0		0
	0		0		0
Wall in position 4	p_{41}		g_{41}		0
	0		0		0
	0		0		0
	p_{42}		g_{42}		0
	0		0		0
	0		0		0

Fig. 5.2 Applied force vectors for the complete structure of Fig. 5.1

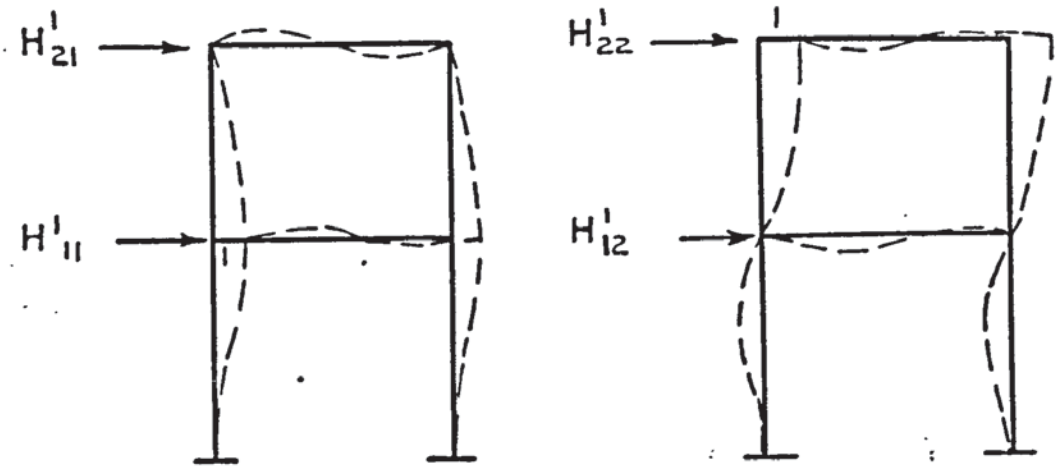

(a)

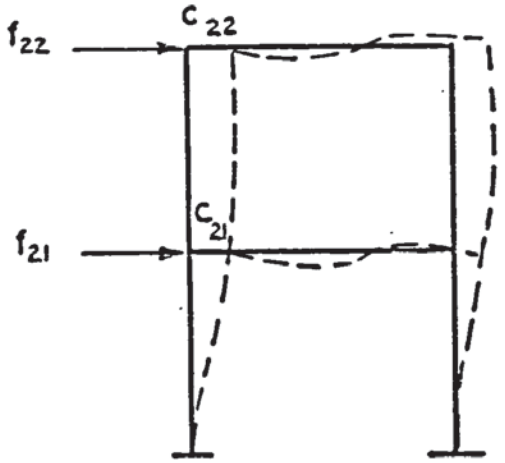

(b)

Fig . 5.3. Horizontal stiffness of a frame.

ments of the joints are not restrained. A further assumption, implicit in the above definition is that axial deformations in the beams are negligible, resulting in equal horizontal displacements of all the columns at any particular floor level.

For the same frame, Fig.5.3b shows the horizontal forces and displacements related by equation (5.3). Here the subscripts refer to the positions of the frame junctions in the complete structure. It can be seen from the diagrams that the relationship between these displacements may be expressed in terms of the lateral stiffness coefficients as follows:-

$$\begin{bmatrix} f_{21} \\ f_{22} \end{bmatrix} = \begin{bmatrix} H^1_{11} & H^1_{12} \\ H^1_{21} & H^1_{22} \end{bmatrix} \begin{bmatrix} c_{21} \\ c_{22} \end{bmatrix} \qquad \ldots\ldots \quad (5.4)$$

This equation has the same form as equation (5.3) and hence for a frame of type r

$$\underline{f}^r = \underline{H}^r \underline{c}^r \qquad \ldots\ldots \quad (5.5)$$

where $\underline{f}^r$, $\underline{H}^r$ and $\underline{c}^r$ are the contribution of any frame of type r to the corresponding terms of equation (5.3). Fig.5.4 shows the construction of equation (5.3) for the complete structure of Fig.5.1. Combining equations (5.1), (5.2) and (5.3)

$$\underline{p} = \underline{J}\,\underline{d} + \underline{H}\,\underline{c} \qquad \ldots\ldots \quad (5.6)$$

For compatibility at the frame junctions, the corresponding horizontal displacements in $\underline{c}$ and $\underline{d}$ must be equal. Also, since $\underline{H}$ contains rows and columns of zeros corresponding to all the remaining elements of $\underline{d}$, it follows that $\underline{c}$ can be replaced by $\underline{d}$ in equation (5.6), and hence

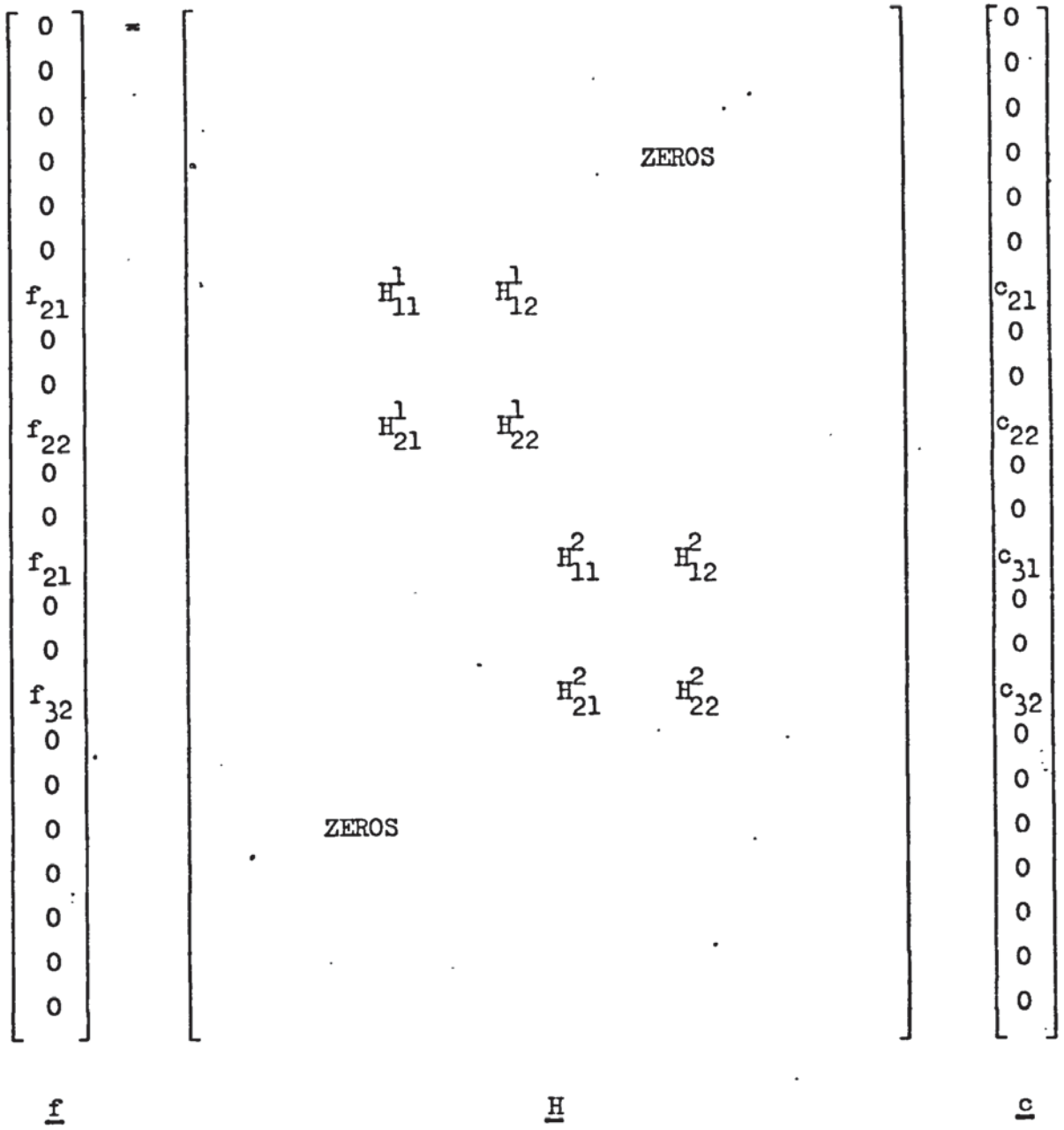

Fig. 5.4. Horizontal force-displacement equations for the frames of Fig. 5.1

$$\underline{p} = (\underline{J} + \underline{H})\,\underline{d} \qquad \ldots\ldots \qquad (5.7)$$

where the combined matrix $(\underline{J} + \underline{H})$ is the stiffness matrix of the restrained grillage. Solution of equation (5.7) gives $\underline{d}$, the complete displacement vector for the grillage joints resulting from the wind loads.

5.4 The effect of imposed loading

The overturning effect of eccentric vertical imposed loads acting on the walls and frames was described in section 4.5 of the previous Chapter. The same considerations again apply and in the case of the walls the overturning couples may be incorporated directly into the load vector $\underline{p}$ of equation (5.7).

The change in the compatibility conditions at the frame junctions produced by eccentric loading of the frames was expressed in equation (4.14) which is still valid in the notation of the present analysis provided that the vector $\underline{b}$ is correctly defined.

Re-arranging equation (4.14)

$$\underline{c} = \underline{d} - \underline{b} \qquad \ldots\ldots \qquad (5.8)$$

where $\underline{d}$ and $\underline{c}$ are now the displacements of equations (5.2) and (5.3) respectively and $\underline{b}$ is a vector containing the sidesways produced at all the frame junctions by eccentric imposed loads on the frames. The elements of $\underline{b}$ corresponding to the other degrees of freedom of the grillage are merely dummy values satisfying equation (5.8).

Combining equations (5.6) and (5.8)

$$\underline{p} = \underline{J}\,\underline{d} + \underline{H}\,(\underline{d} - \underline{b}) \qquad \ldots\ldots \qquad (5.9)$$

Re-arranging

$$\underline{P} + \underline{H}\,\underline{b} = (\underline{J} + \underline{H})\,\underline{d}$$

or

$$\underline{p} + \underline{h} = (\underline{J} + \underline{H})\,\underline{d} \qquad \ldots\ldots \quad (5.10)$$

where $\underline{h} = \underline{H}\,\underline{b}$ $\qquad \ldots\ldots \quad (5.11)$

It follows from the form of equation (5.11) that $\underline{h}$ is a vector whose non-zero elements are horizontal forces producing exactly the same sidesways in the frames as those produced by the eccentric imposed loading. Equation (5.10) shows that the effect of the imposed loads on the displacements of the complete structure can be obtained by adding these horizontal forces to the wind loads at the frame junctions.

5.5 Analysis of the frames

The contributions of a typical frame of type r to the lateral stiffness matrix $\underline{H}$ may be obtained by considering each column of $\underline{H}^r$ as a load vector producing a unit horizontal displacement at the corresponding floor level and zero horizontal displacements at all the other floors. The stiffness matrix of the frame is constructed directly, using the sub-matrices of equation (2.15). However, as the columns are assumed to have equal horizontal displacements at the floor levels, all the rows and columns of the stiffness matrix corresponding to these displacements are combined and grouped together at the bottom and right hand side of the matrix. The method of construction is illustrated in Fig.5.5 which shows the complete set of load-displacement equations for a two storey frame. The subscripts of the stiffness coefficients refer to the numbers allocated to the members of the frame as shown in the diagram.

$$
\begin{bmatrix} 0 & 0 \\ 0 & 0 \\ 0 & 0 \\ 0 & 0 \\ 0 & 0 \\ 0 & 0 \\ 0 & 0 \\ 0 & 0 \\ \hline H^r_{11} & H^r_{12} \\ H^r_{21} & H^r_{22} \end{bmatrix} =
\left[\begin{array}{cccccccc|cc}
a_1+b_2+a_4 & -d_2 & -b_2 & -d_2 & -a_4 & 0 & 0 & 0 & 0 & 0 \\
-d_2 & e_1+e_2+e_4 & d_2 & f_2 & 0 & f_4 & 0 & 0 & d_1-d_4 & d_4 \\
-b_2 & d_2 & b_2+a_3+a_6 & d_2 & 0 & 0 & -a_6 & 0 & 0 & 0 \\
-d_2 & f_2 & d_2 & e_2+e_3+e_6 & 0 & 0 & 0 & f_6 & d_3-d_6 & d_6 \\
-a_4 & 0 & 0 & 0 & a_4+b_5 & -d_5 & -b_5 & -d_5 & 0 & 0 \\
0 & f_4 & 0 & 0 & -d_5 & e_4+e_5 & d_5 & f_5 & -d_4 & d_4 \\
0 & 0 & -a_6 & 0 & -b_5 & d_5 & a_6+b_5 & d_5 & 0 & 0 \\
0 & 0 & 0 & f_6 & -d_5 & f_5 & d_5 & e_6+e_5 & -d_6 & d_6 \\
\hline
0 & d_1-d_4 & 0 & d_3-d_6 & 0 & -d_4 & 0 & -d_6 & b_1+b_4+b_3+b_6 & -b_4-b_6 \\
0 & d_4 & 0 & d_6 & 0 & d_4 & 0 & d_6 & -b_4-b_6 & b_4+b_6
\end{array}\right]
\begin{bmatrix} Y_{11} & Y_{12} \\ \Theta_{11} & \Theta_{12} \\ Y_{21} & Y_{22} \\ \Theta_{21} & \Theta_{22} \\ Y_{31} & Y_{32} \\ \Theta_{31} & \Theta_{32} \\ Y_{41} & Y_{42} \\ \Theta_{41} & \Theta_{42} \\ \hline 1 & 0 \\ 0 & 1 \end{bmatrix}
$$

unknown vertical and rotational displacements

unit horizontal displacements

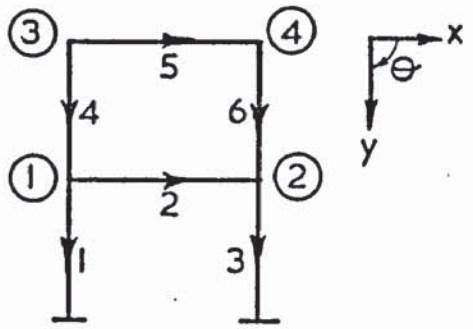

Fig. 5.5 Partitioned load - displacement equations

The only loads considered to be acting on the frame at this stage are the elements of $\underline{H}^r$. The displacement matrix consists of a unit matrix corresponding to $\underline{H}^r$, surmounted by a matrix of unknown vertical and rotational displacements. These displacements are not determined in the analysis, but have been included in the figure for the purpose of identification of the rows of the stiffness matrix. The subscripts refer respectively to the joint numbers in the frame and the columns of the displacement matrix.

For a general frame, the load-displacement equations of Fig.5.5 may be written as

$$\begin{bmatrix} \underline{o} \\ \hline \underline{H}^r \end{bmatrix} = \begin{bmatrix} \underline{K}_{11} & \underline{K}_{12} \\ \hline \underline{K}_{21} & \underline{K}_{22} \end{bmatrix} \begin{bmatrix} \underline{X} \\ \hline \underline{I} \end{bmatrix} \quad \ldots\ldots \quad (5.12)$$

from which

$$\underline{o} = \underline{K}_{11}\,\underline{X} + \underline{K}_{12} \quad \ldots\ldots \quad (5.13)$$

$$\underline{H}^r = \underline{K}_{21}\,\underline{X} + \underline{K}_{22} \quad \ldots\ldots \quad (5.14)$$

From equation (5.13)

$$\underline{X} = -\underline{K}_{11}^{-1}\,\underline{K}_{12} \quad \ldots\ldots \quad (5.15)$$

Substituting for $\underline{X}$ in equation (5.14)

$$\underline{H}^r = \underline{K}_{22} - \underline{K}_{21}\,\underline{K}_{11}^{-1}\,\underline{K}_{12} \quad \ldots\ldots \quad (5.16)$$

If sidesways are produced by the imposed loading, the frames contribute horizontal forces to the load vector $\underline{h}$. For frame r these horizontal forces $\underline{h}^r$ are related to the sidesways $\underline{b}^r$ by an equation of the same form as equation (5.11), thus

$$\underline{h}^r = \underline{H}^r \underline{b}^r \qquad \ldots\ldots \qquad (5.17)$$

Using this relationship, $\underline{h}^r$ may be determined by partitioning the load-displacement equations as follows

$$\begin{bmatrix} \underline{\ell} \\ \hline \underline{o} \end{bmatrix} = \begin{bmatrix} \underline{K}_{11} & \underline{K}_{12} \\ \hline \underline{K}_{21} & \underline{K}_{22} \end{bmatrix} \begin{bmatrix} \underline{\phi} \\ \hline \underline{b}^r \end{bmatrix} \qquad \ldots\ldots \qquad (5.18)$$

where $\underline{\ell}$ is the vector of imposed loads and $\underline{\phi}$ is the equivalent displacement vector. The horizontal forces at the floor levels in this loading case are assumed to be zero.

In expanded form, equations (5.18) may be written as

$$\underline{\ell} = \underline{K}_{11} \underline{\phi} + \underline{K}_{12} \underline{b}^r \qquad \ldots\ldots \qquad (5.19)$$

$$\underline{o} = \underline{K}_{21} \underline{\phi} + \underline{K}_{22} \underline{b}^r \qquad \ldots\ldots \qquad (5.20)$$

and from equation (5.19) we obtain

$$\underline{\phi} = \underline{K}_{11}^{-1} \underline{\ell} - \underline{K}_{11}^{-1} \underline{K}_{12} \underline{b}^r \qquad \ldots\ldots \qquad (5.21)$$

Substituting for $\underline{\phi}$ in equation (5.20)

$$\underline{o} = \underline{K}_{21} \underline{K}_{11}^{-1} \underline{\ell} + (\underline{K}_{22} - \underline{K}_{21} \underline{K}_{11}^{-1} \underline{K}_{12}) \underline{b}^r \qquad \ldots\ldots \qquad (5.22)$$

Using equation (5.16)

$$\underline{o} = \underline{K}_{21} \underline{K}_{11}^{-1} \underline{\ell} + \underline{H}^r \underline{b}^r \qquad \ldots\ldots \qquad (5.23)$$

and hence, using equation (5.17)

$$\underline{h}^r = -\underline{K}_{21} \underline{K}_{11}^{-1} \underline{\ell} \qquad \ldots\ldots \qquad (5.24)$$

Since the overall stiffness matrix of the frame is symmetrical, $\underline{K}_{21} = \underline{K}_{12}'$ where the prime denotes the transpose of the matrix. Equations (5.16) and (5.24) may therefore be re-written, thus

$$\underline{H}^r = \underline{K}_{22} - \underline{K}_{12}' \underline{K}_{11}^{-1} \underline{K}_{12} \quad \ldots\ldots \quad (5.25)$$

and $$\underline{h}^r = -\underline{K}_{12}' \underline{K}_{11}^{-1} \underline{\ell} \quad \ldots\ldots \quad (5.26)$$

Both those equations contain $\underline{K}_{12}' \underline{K}_{11}^{-1}$ and can conveniently be solved in one operation by compounding them as follows

$$[\underline{H}^r \mid \underline{h}^r] = [\underline{K}_{22} \mid \underline{o}] - \underline{K}_{12}' \underline{K}_{11}^{-1} [\underline{K}_{12} \mid \underline{\ell}] \ldots\ldots \quad (5.27)$$

Solution of this equation for each frame completes the preparation necessary for the construction of equation (5.10). It should be noted that identical frames, which are subjected to the same conditions of imposed loading, provide identical coefficients in $\underline{H}$ and $\underline{h}$. Repeated analyses of such frames are therefore unnecessary.

5.6 Determination of member forces

For the grillage, the displacements $\underline{d}$ at all the joints are obtained directly from the solution of equation (5.10). The end-moments, shears and torques in the grillage members may then be determined from these displacements by applying equations (2.11) to each member in turn.

For the frames, only the horizontal displacements at each floor level are known. These are equal to the deflections of the grillage at the frame junctions and may be extracted from the vector $\underline{d}$. The remaining displacements at all the joints in the frames can be obtained from the partitioned form of the load-displacement equations by back-substitution. Thus, for a typical frame r,

$$\begin{bmatrix} \underline{\ell} \\ \hline \underline{f}^r \end{bmatrix} = \left[\begin{array}{c|c} \underline{K}_{11} & \underline{K}_{12} \\ \hline \underline{K}_{21} & \underline{K}_{22} \end{array}\right] \begin{bmatrix} \underline{x} \\ \hline \underline{d}^r \end{bmatrix} \quad \ldots\ldots \quad (5.28)$$

where $\underline{d}^r$ is the vector of horizontal displacements extracted from $\underline{d}$ and $\underline{x}$ is the vector of unknown joint displacements. The load vector consists of the imposed loads $\underline{\ell}$ and an unknown vector $\underline{f}^r$ consisting of the horizontal forces carried by the frame.

Carrying out the multiplication for the upper segments

$$\underline{\ell} = \underline{K}_{11}\,\underline{x} + \underline{K}_{12}\,\underline{d}^r \quad \ldots\ldots \quad (5.29)$$

or $$\underline{x} = \underline{K}_{11}^{-1}\,\underline{\ell} - \underline{K}_{11}^{-1}\,\underline{K}_{12}\,\underline{d}^r \quad \ldots\ldots \quad (5.30)$$

Since $\underline{K}_{11}^{-1}\,[\underline{K}_{12} \mid \underline{\ell}]$ has already been determined in the solution of equation (5.27), $\underline{x}$ may be obtained directly from a single operation of multiplication by arranging equation (5.30) as follows

$$\underline{x} = \underline{K}_{11}^{-1}\,[\underline{K}_{12} \mid \underline{\ell}] \begin{bmatrix} -\underline{d}^r \\ \hline 1 \end{bmatrix} \quad \ldots\ldots \quad (5.31)$$

The combined displacements $\underline{x}$ and $\underline{d}^r$ can now be used with equation (2.16) to calculate the forces in the frame members. The unknown horizontal forces $\underline{f}^r$ may also be obtained if required, as follows.

From the lower segments of equation (5.28)

$$\underline{f}^r = \underline{K}_{21}\,\underline{x} + \underline{K}_{22}\,\underline{d}^r \quad \ldots\ldots \quad (5.32)$$

Substituting for $\underline{x}$ from equation (5.30)

$$\underline{f}^r = \underline{K}_{21}\,\underline{K}_{11}^{-1}\,\underline{\ell} + (\underline{K}_{22} - \underline{K}_{21}\,\underline{K}_{11}^{-1}\,\underline{K}_{12})\,\underline{d}^r \qquad \ldots\ldots \quad (5.33)$$

and hence, using equations (5.16) and (5.24)

$$\underline{f}^r = \underline{H}^r\,\underline{d}^r - \underline{h}^r \qquad \ldots\ldots \quad (5.34)$$

This result could also have been obtained by combining equations (5.5), (5.8) and (5.17).

5.7 Discussion

The advantages of the method of influence coefficients arising from the separation of the frames and grillage are preserved in the restrained grillage approach which also has some additional features. In particular, a stiffness approach is adopted throughout the analysis, with the result that the only equations to be solved are the load-displacement equations of the frames and the restrained grillage. These equations, which are sparse and of variable band width, are well suited to solution by Jennings' compact elimination technique.

In the determination of the lateral frame stiffnesses the amount of computation is probably similar to that required for the calculation of influence coefficients, although the actual number of equations to be solved is reduced by the compatibility of column displacements at the floor levels and by the fact that the horizontal displacements are known. The analysis is also neater in that no unwanted displacements are computed.

In the analysis of the grillage the need for the very large load matrix, previously required for the calculation of influence coefficients, is avoided. Furthermore, it is not necessary in this analysis for the wall and floor panels to make up a stiff structure. For example, in structures consisting of floor slabs braced only by frames, if the degrees of freedom in the θ^x direction are suppressed at the grillage joints, the addition of the lateral stiffness coefficients of the frames ensures that the stiffness matrix of the restrained grillage is non-singular.

CHAPTER 6

COMPUTER PROGRAMMING

6.1 Introduction

In the analysis of a multi-storey, multi-bay building by computer, a large proportion of the cost of the analysis arises from the preparation and checking of data. Even after careful checking some errors often remain, resulting in abortive runs and further expenditure of time. The number of such errors probably depends both upon the volume of data and upon the degree of difficulty with which information is transferred from a drawing or line diagram of the structure to a format acceptable to the program. In writing the program for analysis by influence coefficients the regular nature of buildings has been used to reduce the volume of data. Furthermore, a format has been adopted which facilitates rapid transferrence of data from line diagrams of the frames and the grillage. The program is written in Atlas autocode and was designed to operate within the core store of the Chilton Atlas computer without access to backing store.

The writing of the second program, for the restrained grillage approach, coincided with the installation of an I.C.L. 1905 computer at the University of Aston. The program is written in Fortran and was designed to make use of direct access disc storage so that fairly large structures could be analysed with the moderate core store available on this computer. Improvements in generality, together with the use of backing store, necessarily resulted in a more complicated program for this approach. In particular the special compact serial form in which the stiffness matrices are stored leads to fairly complicated programming especially when variable degrees of freedom and random numbering of the joints are introduced. In the analysis of the frames, additional difficulties arise because of the partitioned form of the stiffness matrices.

Both computer programs are of major size. However, as similar techniques are used in a number of instances, a full description of each

program would involve undue repetition. Description of the first program, which is the more straightforward, is therefore limited almost entirely to a discussion of the format and treatment of the data for the frames. The second, more complex program is discussed in greater detail.

6.2 Analysis by influence coefficients

A flow diagram of the program for the method of analysis by influence coefficients is given in Fig. 6.1. The diagram, which uses the notation of Chapter 4, is self explanatory and will not be discussed in detail. The advantages arising from the simplified data format, which is a feature of this program, may be described by taking the analysis of the frames as an example. When the beams and columns of a frame are known to form a regular pattern of rectangles, it is not necessary to number the individual members or joints. The necessity for setting up tables of member-joint incidence is thereby avoided. Also, since regular building frames usually contain a large number of identical members, the length and section properties of each type of member need only to be specified once.

The format of the data for a simple frame is shown diagrammatically in Fig. 6.2. Section (a) of the figure shows a line diagram of the frame in which all members with identical lengths and section properties are allocated a type number. General data for the frame consist of the three items shown in section (b) of the figure. The skew symmetry code is set to 2 when wind loading only is considered and only half the frame is to be analysed. In section (c) the properties of each type of member are specified. As it is tacitly assumed in section (b) that Young's modulus is constant for all the frames, variations can be made in section (c) for individual members by making proportional changes in the second moments of area of the sections.

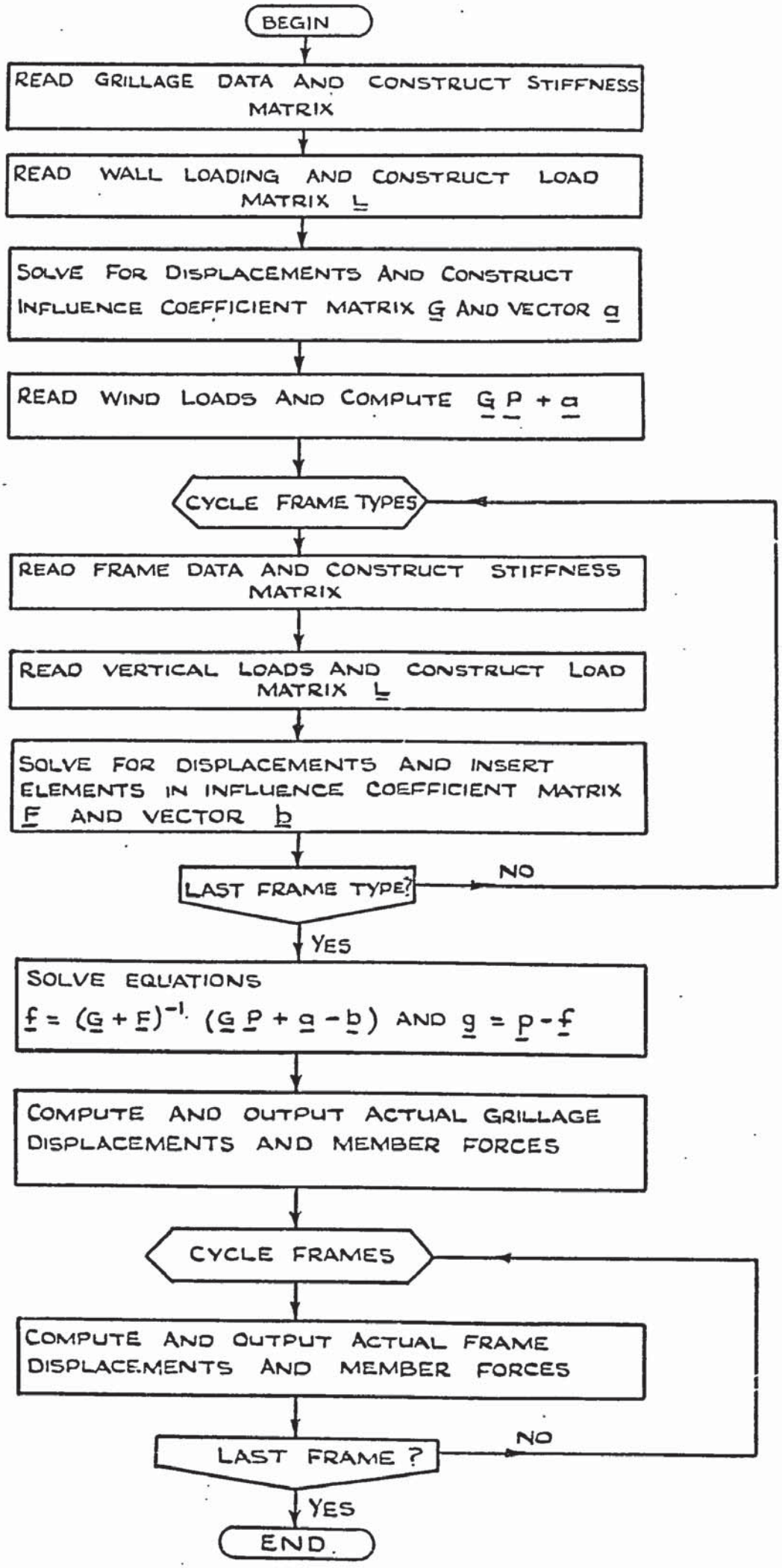

Fig. 6.1 Flow diagram for method of influence coefficients

(a) Line diagram

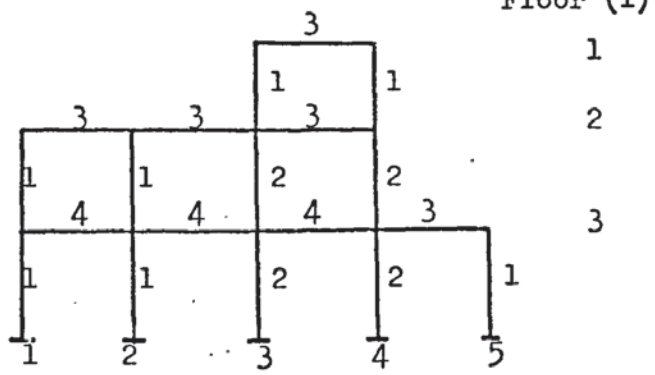

(b) General data

Young's modulus
No. of frames of this type
Skew symmetry code

(c) Member properties

	AREA	INERTIA	LENGTH
Type 1			
Type 2			
Type 3			
Type 4			

(d) Position of first and last column

	FIRSTCOL (I)	LASTCOL (I)
Floor 1	3	4
Floor 2	1	4
Floor 3	1	5

(e) Arrangement of columns

	COLUMN TYPES
Floor 1	1 1
Floor 2	1 1 2 2
Floor 3	1 1 2 2 1

(f) Arrangement of beams

	BEAM TYPES
Floor 1	3
Floor 2	3 3 3
Floor 3	4 4 4 3

Fig. 6.2 Data format for a frame

The configuration of the frame is defined by using the type numbers to indicate the positions of the members in the frame. Two tables of type numbers are used, one for columns and one for beams. These tables are shown in sections (e) and (f) of Fig. 6.2, where space characters have been used to make the tables resemble the line diagram of the frame. Checking of the data against the line diagram is thus rendered extremely rapid and simple. The introduction of arbitrary space and newline characters into the data is made possible by storing the tables as one dimensional arrays, indicating the positions of the first and last columns in each row by two arrays FIRSTCOL and LASTCOL respectively as shown in Fig. 6.2(d). The data described above are sufficient to define the shape of most regular building frames composed of rectangular panels.

In interpreting the data for the construction of the stiffness matrix, it is recognised that only seven configurations of the members at a joint are possible as shown in Fig. 6.3(a), each of which contributes a unique pattern of elements to the stiffness matrix. For example, the configuration of four members contributes the pattern shown in Fig. 6.3(b), the subscripts denoting the type numbers of the members. The pattern is derived directly from the matrices of equation (2.17), assuming positive directions of the P axes as shown. Elements above the leading diagonal and before the first non-zero element in each row are excluded since they are not required by Jenning's compact elimination subroutine. Patterns for the other configurations are all subsets of this basic pattern. The stiffness matrix is constructed by examining each joint in turn, starting at the top left hand corner of the frame, determining the member configuration at the joint and inserting the appropriate pattern of elements into the matrix. This procedure eliminates the need either for scanning through lists of members to test for incidence on the current joint, or for the

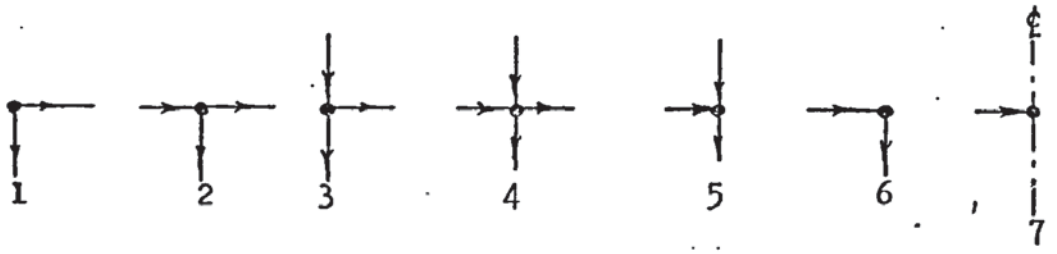

(a) Member configurations

JOINT r			JOINT s - 1			JOINT s		
$-b_2$	0	$-d_2$	$-a_1$	0	0	$a_1+b_2+a_3+b_4$		
0	$-a_2$	0	0	$-b_1$	d_1	0	$b_1+a_2+b_3+a_4$	
d_2	0	f_2	0	$-d_1$	f_1	$-d_2+d_4$	d_1-d_3	$e_1+e_2+e_3+e_4$

(b) Stiffness coefficients for configuration No. 4

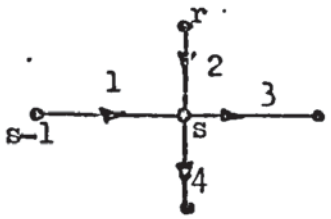

Fig. 6.3 Patterns of stiffness coefficients.

		MEMBER CONFIGURATIONS						
		1	2	3	4	5	6	7
CONDITIONS	J = FIRSTCOL (I)	Y	N	Y	N	N	N	N
	J = LASTCOL (I)	N	N	N	N	Y	Y	Y
	J ≥ FIRSTCOL (I-1)	N	N	Y	Y	Y	Y	Y
	J ≤ LASTCOL (I-1)	Y	N	Y	Y	Y	N	N
	SKEW SYMMETRY EXISTS	E	E	E	E	N	N	Y
FORM COEFFICIENT PATTERN NO.		1	2	3	4	5	6	7

Table 6.1 Logic for selection of member configurations

multiple addressing of locations in the stiffness matrix which can result when the matrix is constructed member by member.

Where a number of logical combinations of data are possible, each leading to a unique set of actions, decision tables[43,44] form a convenient means of expressing all the possible conditions and corresponding actions as a complete picture. By examining the tables, ambiguities and omissions in the logic can be detected more easily than from a flow diagram. The tables also facilitate the construction of flow diagrams.[45]

Defining I and J as the floor and column numbers respectively as shown in Fig. 6.2(a), the rules for determining the member configuration at any joint IJ in a regular frame are set out in Table 6.1 in the form of a decision table. The possible configurations are shown at the heads of the columns of the table. Each column or rule contains a list of the conditions, which may be considered in any order, necessary for the isolation of a particular configuration. They symbols Y(YES) and N(NO) refer to the results of the tests shown on the left hand side of the table. The symbol E(EITHER) indicates that the result of a test is immaterial and that either YES or NO will satisfy the conditions. It can be seen from the table that all the configurations can be isolated merely by testing appropriate elements of the arrays FIRSTCOL and LASTCOL and checking the skew symmetry code.

The test for ambiguity consists of checking whether any of the columns are identical (interpreting E as either YES or NO) and at the same time lead to different sets of actions. On this basis Table 6.1 is clearly not ambiguous. A flow diagram derived from the table is given in Fig. 6.4. The routes leading to the selection of patterns of stiffness coefficients, in the inner loop of the diagram, may be compared with the columns of Table 6.1.

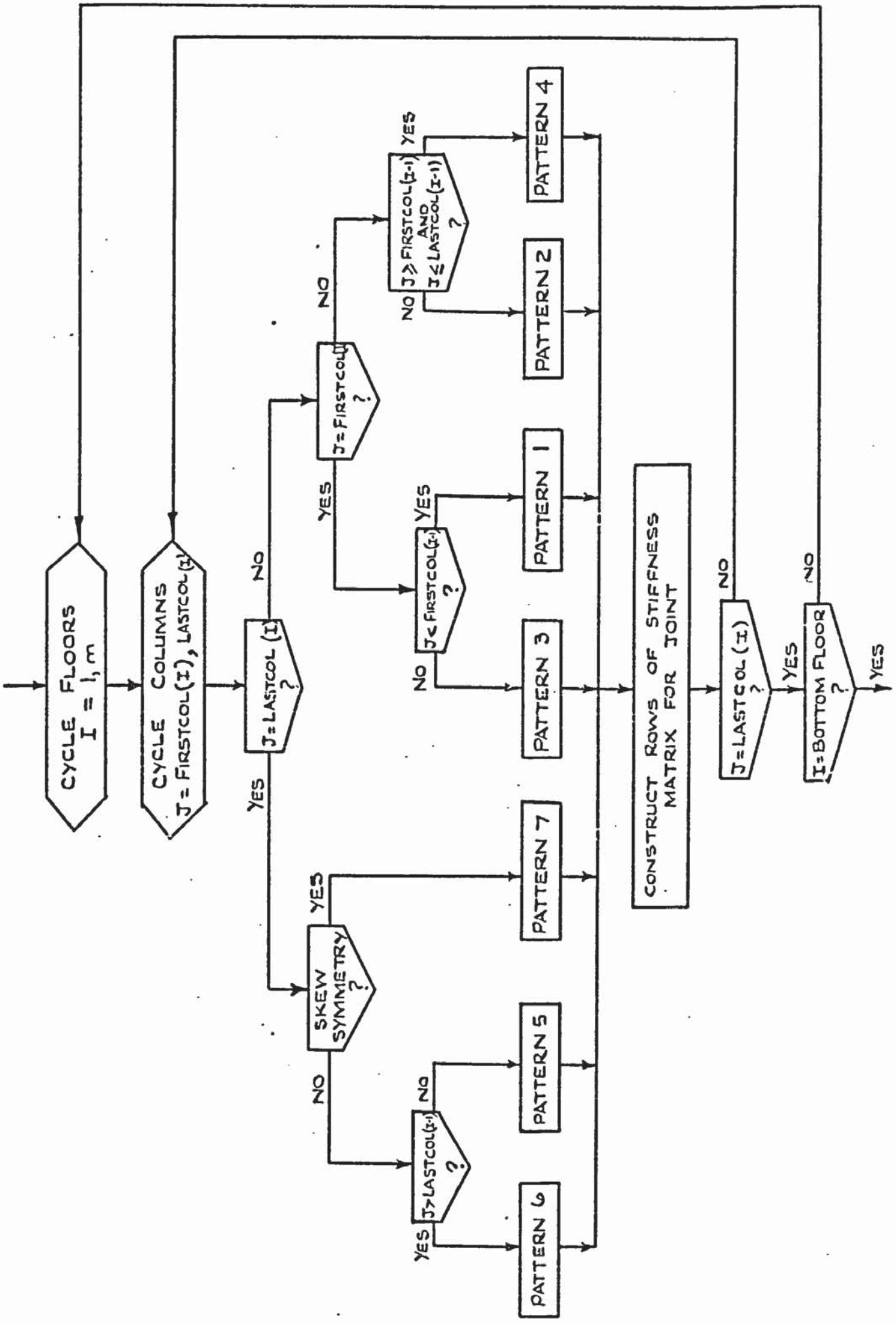

Fig. 6.4. Selection of joint configurations

The size of the structure that can be analysed by the method of influence coefficients is limited by the fact that the program was designed to operate without the use of backing store. The storage requirements are chiefly governed by the influence coefficient matrix for the grillage and the load matrix used in deriving the influence coefficients. Both these matrices are required to be in store at the same time. The load matrix is extremely sparse but must be stored in full matrix form because it is subsequently overwritten by the displacement matrix which is not sparse. As an example, the main storage requirements, ignoring symmetry, for Goldberg's 10 storey structure are given in Table 6.2. Doubling the number of storeys merely doubles the sizes of the compact stiffness matrices which are in any event relatively small. The sizes of the load and influence coefficient matrices however are increased by a factor of 4.

6.3 The restrained grillage method

In this program the regularity of the overall structure is again exploited to simplify the preparation and checking of data. In order to obtain a more general analysis of the frames however, it has been necessary to revert to a more conventional and less economical format for the data. The Fortran program consists of a short master segment calling a number of subroutines, the functions of which are illustrated by the flow diagram, Fig. 6.5, using the notation of Chapter 5.

The program is designed so that the main storage arrays are stored on disc files using standard Fortran input-output procedures both for direct access and serial transfers. The construction of the arrays and the subsequent operations on them take place in small buffer arrays in the core store. Transference of data between subroutines, except in the case of relatively small arrays and single variables, is by means of the

MATRIX	NUMBER OF LOCATIONS
Grillage Load Matrix	19000
Influence Coefficient Matrix.	4900
Grillage Stiffness Matrix.	2500
Frame Load Matrix	1300
Frame Stiffness Matrix	1200

Table 6.2 Storage requirements for Goldberg's 10 storey structure.

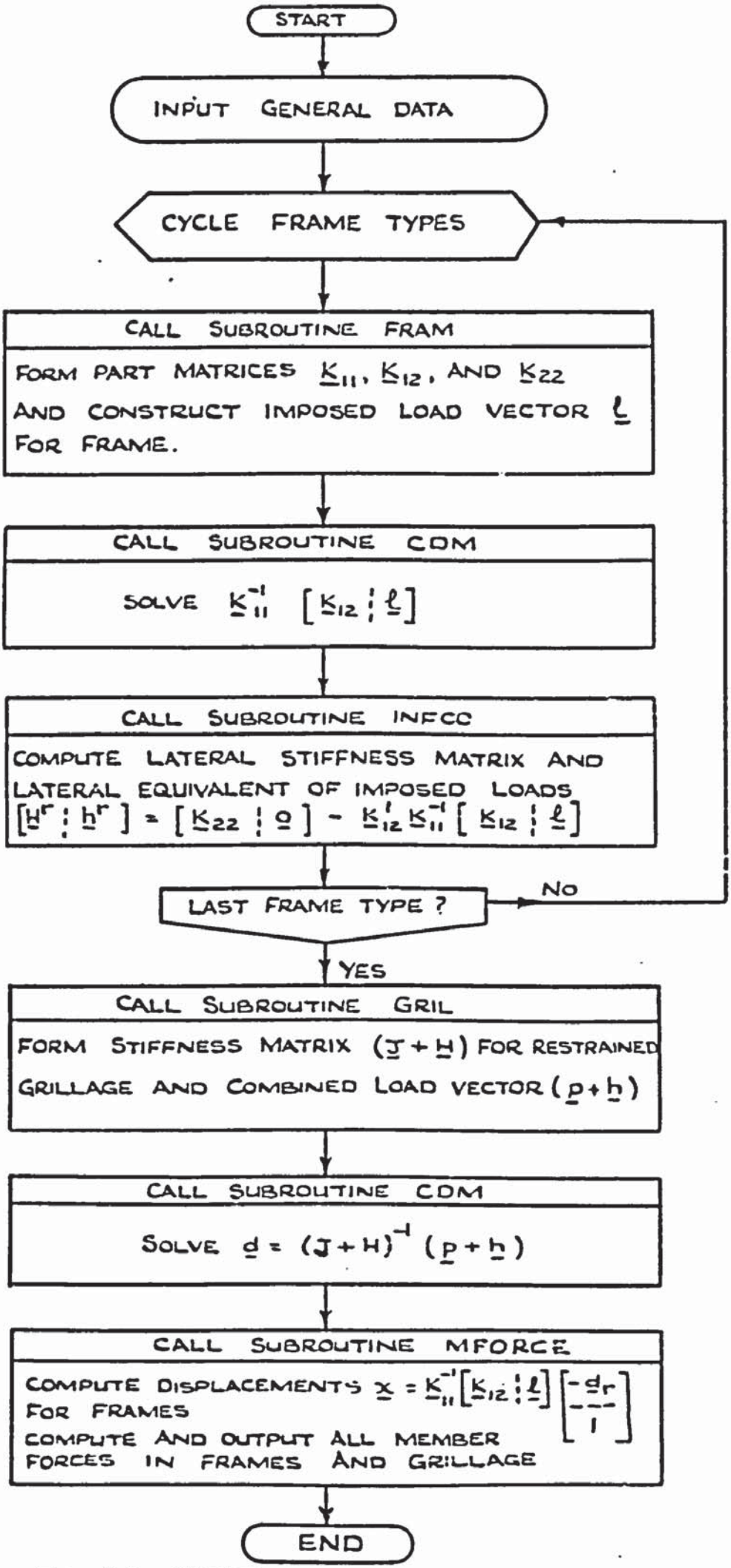

Fig. 6.5 Master program

disc files as shown diagrammatically in Fig. 6.6.

Direct access files 1 and 3 are required explicitly by the subroutine CDM, which uses the compact elimination technique described in Chapter 3 for the solution of the equations generated in the subroutines FRAM and GRIL. On entry to CDM, file 1 contains the right hand side columns of the equations, which are overwritten by the solution matrix on exit from the subroutine. File 3 contains the coefficient matrix. Direct access file 4 is used to preserve data that would otherwise be overwritten by CDM.

6.3.1 Analysis of the frames

In subroutine FRAM, the matrix parts $\underline{K}_{11}$, $\underline{K}_{12}$ and $\underline{K}_{22}$ are constructed, together with the imposed load vector $\underline{\ell}$, for each frame type. The format of the input data is conventional and is similar to that used by Majid and Williamson[9] for plane frames with gusset plates, except that an additional column is required in the joint data in order to specify the floor level containing each joint. This additional information defines the joints that are assumed to have a common horizontal displacement and hence indicates the columns of $\underline{K}_{12}$ and $\underline{K}_{22}$ to which the joints contribute elements. Joints which have no common displacement, for example at the bases of the columns or between floor levels, are denoted by a zero in this column.

Storage is conserved by grouping of the data. Groups are arranged so that joints in a typical group I may only be connected to joints in the same group or to joints in groups I-1 or I+1. Similarly, members in group I may only connect joints in group I to other joints in the same group or to joints in group I-1. Consequently, the rows of the stiffness matrix for joint group I can be constructed from the data of joint groups I-1, I and I+1, and member groups I and I+1. Data for these groups are

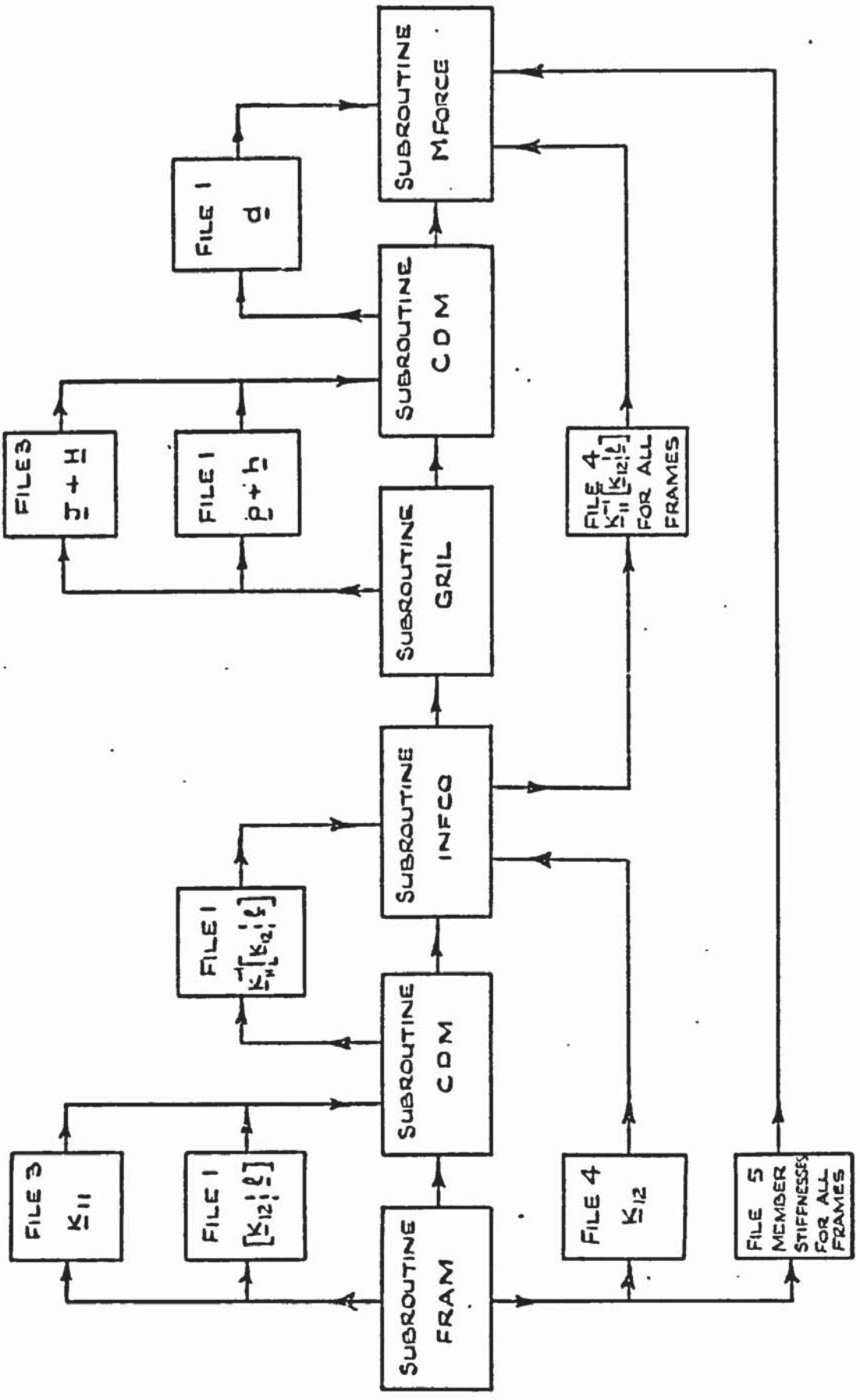

Fig. 6.6 Disc file organisation

contained in small buffer arrays operating as stacks in which items of data for new groups are added at the bottom, pushing up all the elements in the stacks so that the items for previously processed groups are lost. Items of joint and member data, which must be retained for use later in the program, are written to the serial disc file 5 as shown in Fig. 6.6. The operation of the stacks is illustrated for a system of 4 groups in Fig. 6.7. Movement of the elements in the stacks and also within the subroutine CDM is by means of the ICL subroutine FMOVE, which is very much faster than a Fortran DO loop.

The partitioned stiffness matrix is constructed directly by applying equation (2.15) to each of the parts, resulting in the formation of 16 sub-parts as shown in Fig. 6.8(a). For convenience these sub-parts are classified as leading diagonal when the second pair of subscripts is ii or jj and as off-diagonal when the subscripts are ij or ji. Fig. 6.8(b) gives the actual coefficients obtained from equation (2.15) and shows that when symmetry is taken into account, the number of sub-parts can be reduced to 12. The displacements x_i, y_i, θ_i and x_j, y_j, θ_j denote the degrees of freedom at ends 1 and 2 respectively of the member.

The matrix parts $\underline{K}_{11}$ and $\underline{K}_{12}$ are stored in fixed length blocks on disc and are constructed a block at a time in small buffer arrays in the core store. $\underline{K}_{22}$, which is relatively small, is constructed in full matrix form in the core.

Two alternative methods of construction were considered, namely by member or by joint. The former approach yields a faster running program but requires buffers large enough to accomodate the elements of $\underline{K}_{11}$ and $\underline{K}_{12}$ contributed by two complete joint groups. The method was therefore rejected in favour of the joint-by-joint approach, which, although slower, has the advantage that the buffers are only required to contain the elements contributed by a single joint. Furthermore, the operation of searching for

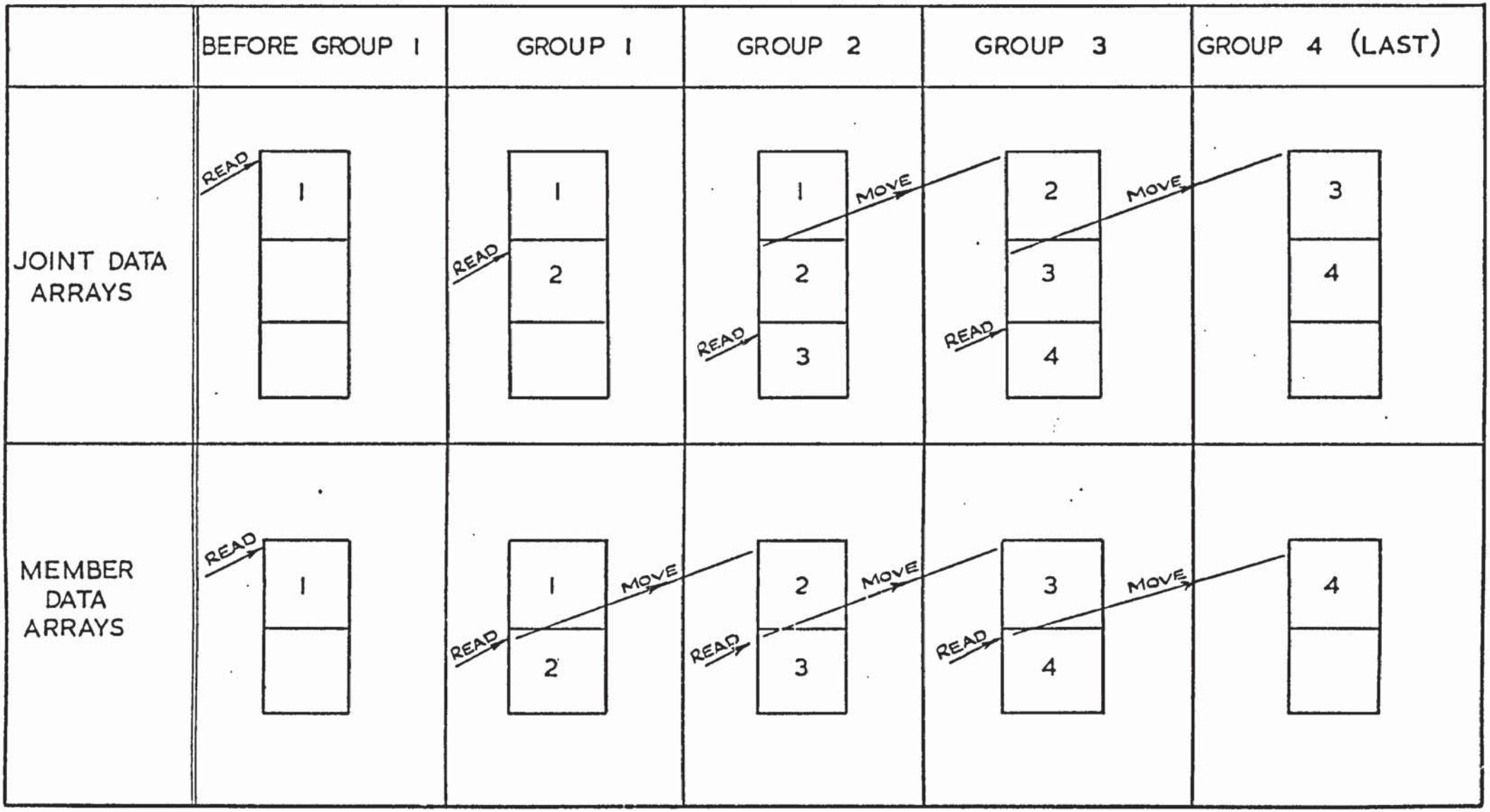

Fig. 6.7 Sequence of operation for a system of 4 groups

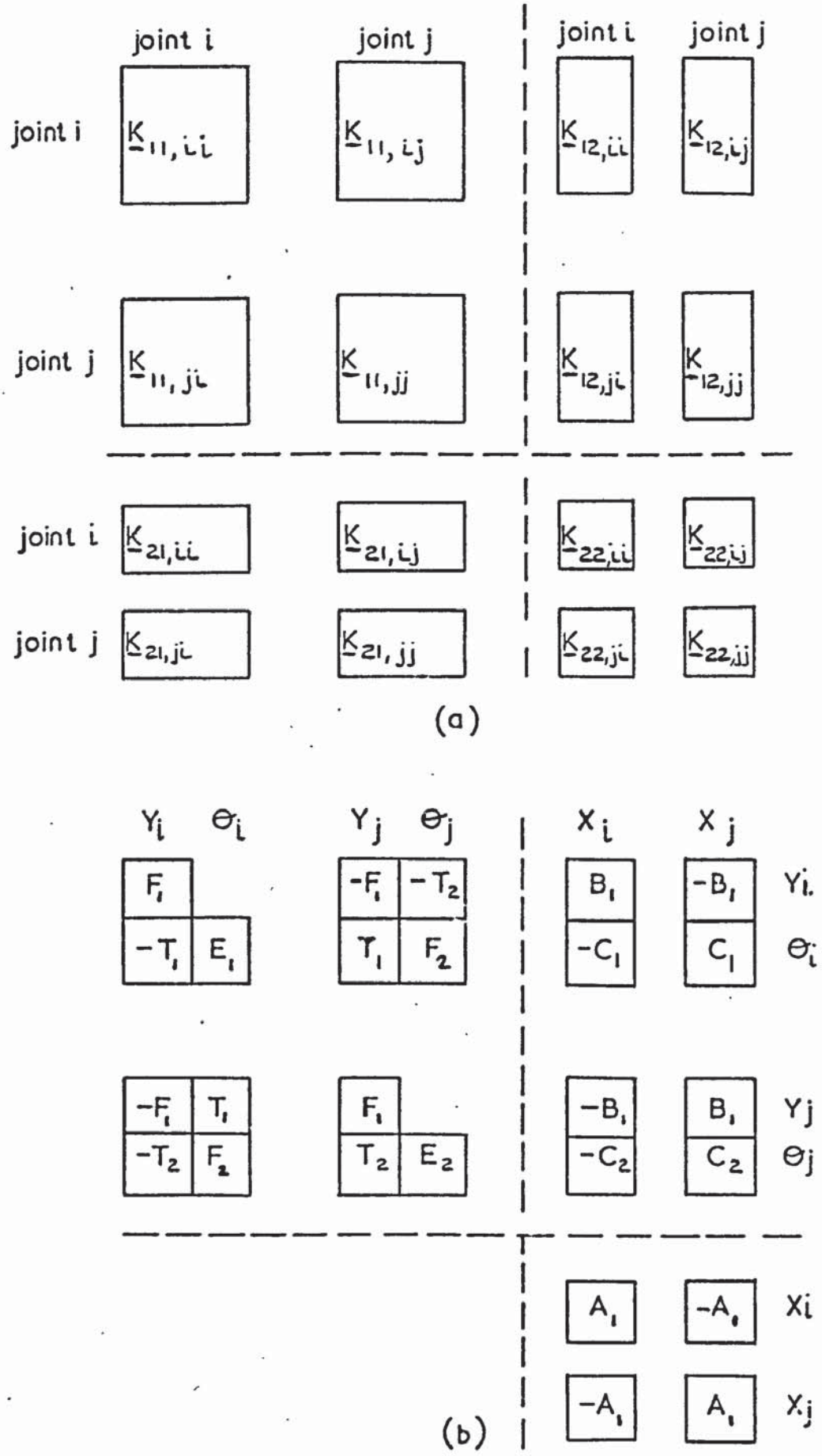

Fig. 6.8 Contributions of a member to the partitioned stiffness matrix.

members incident on a particular joint, which causes this method to be slower, is limited by the grouping of data to the members of two groups. The additional running time associated with the joint-by-joint approach does not therefore constitute a serious disadvantage in this program and can be minimised by making the member and joint groups as small as possible.

Subroutine FRAM consists of three nested loops as shown in Fig. 6.9. In the outer loop, joint and member data for the group are input. At this stage also the stiffnesses of the members, their direction cosines, the degrees of freedom of incident joints and any other data required later for the calculation of member forces are written to disc file 5. The stiffness coefficients contributed by the members to the stiffness matrix are calculated and stored temporarily in the data buffers for the member group. In the next loop the number of elements contributed to $\underline{K}_{11}$ and $\underline{K}_{12}$ by each joint is calculated and the current state of the buffers is checked, writing their contents to disc if there is insufficient space for the current joint. The imposed load vector $\underline{\ell}$ is also constructed at this stage. The inner loop searches the two member groups in core for members incident on the current joint, placing the stiffness coefficients contributed by these members in the appropriate parts of the stiffness matrix. In order to avoid repeated calculation of addresses, the contributions of all incident members to the leading diagonal elements are summed prior to their insertion into the matrix.

Before stiffness coefficients can be placed in the matrices it is necessary to institute a series of tests in order to determine whether or or not a particular group of elements exists or is required to be stored. For example, since only the lower triangle of $\underline{K}_{11}$ is stored, off-diagonal elements are not stored when the number of the current joint is lower than the number of the joint at the other end of the member; leading diagonal elements do not exist in $\underline{K}_{12}$ when there is no common displacement associated with the current joint, and so on. The complete set of

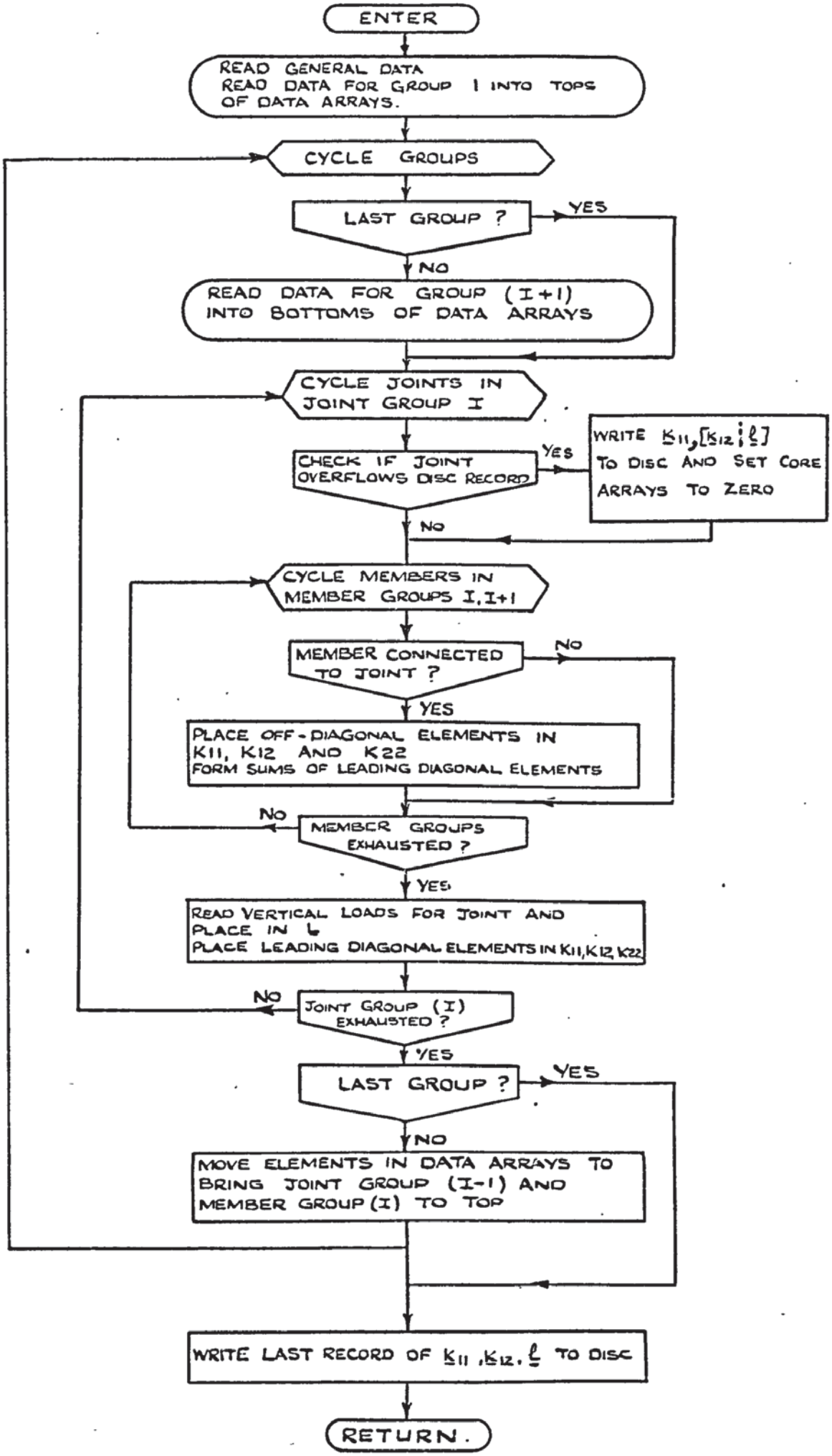

Fig. 6.9 Subroutine FRAM

conditions for the placement of elements is stated as a decision table in Table 6.3. The table is seen to be unambiguous and, interpreting E as either YES or NO, it can be observed that there are 32 independent rules. As this is the maximum number of rules that can be obtained from 5 conditions, it can also be concluded that no logical combinations of the conditions have been overlooked. The flow diagram resulting from the table is shown in Fig. 6.10.

It will be shown later that programming is simplified by the use of common subroutines for the selection and placing of elements in the stiffness matrices both of the frames and the grillage.

It was demonstrated in Chapter 3 that in order to solve a set of equations in the compact serial form required by the subroutine CDM, an auxiliary sequence is required giving the address of the leading diagonal element in each row of the coefficient matrix. This sequence is equally necessary in the construction of the matrix so that the addresses can be calculated for the serial form of the matrix corresponding to locations in the full matrix. The formation of this sequence, which essentially entails the calculation of the band-width of each row of the lower triangle of the stiffness matrix, is facilitated by forming two further sequences LJ and NC. In the first of these arrays, a typical element LJ(K) is the lowest number of any joint connected to joint K. The second array takes into account the number of degrees of freedom allocated to the joints. A typical element NC(K) is the total number of columns in the matrix up to but not including joint K. The purpose of these two arrays is illustrated in Fig. 6.11 which shows the rows of the stiffness matrix correspnding to joint 6 in a frame with skew symmetry. All joints are assumed to have three degrees of freedom except those on the centre line which have two. Elements contributed by the members are indicated by shading. From the figure it can be observed that LJ(6) = 2, NC(6) = 14 and NC(2) = 3. The band-width of the first row is thus NC(6) - NC(2) + 1 and is

	RULE	1	2	3	4	5	6	7	8	9	10	11	12	13	14
CONDITIONS	NFK = 0	Y	Y	Y	Y	N	N	N	N	N	N	N	N	N	N
	IC = 0	Y	N	N	N	Y	Y	Y	Y	N	N	N	N	N	N
	JC = 0	E	Y	N	N	Y	Y	N	N	Y	Y	N	N	N	N
	NDS = 0	E	E	E	E	Y	N	Y	N	Y	N	Y	Y	N	N
	IC < JC	E	E	Y	N	E	E	E	E	E	E	Y	N	Y	N
ACTIONS	Place leading diagonal elements K11					x	x	x	x	x	x	x	x	x	x
	Place leading diagonal elements K12									x	x	x	x	x	x
	Place leading diagonal elements K22		x	x	x					x	x	x	x	x	x
	Place off-diagonal elements K11						x		x		x			x	x
	Place off-diagonal elements K12							x	x			x	x	x	x
	Place off-diagonal elements K22				x								x		x
	Goto next member		x	x	x	x	x	x	x	x	x	x	x	x	x
	Goto next joint	x													

NFK – Number of degrees of freedom of the current joint.

IC – Storey containing the current joint. No common displacement if IC = 0.

JC – Storey containing the joint at the other end of the member. No common displacement if JC = 0.

NDS – A flag which is set to zero when the current joint has a smaller number than the joint at the other end of the member.

Table 6.3 Decision table for the placement of stiffness coefficients

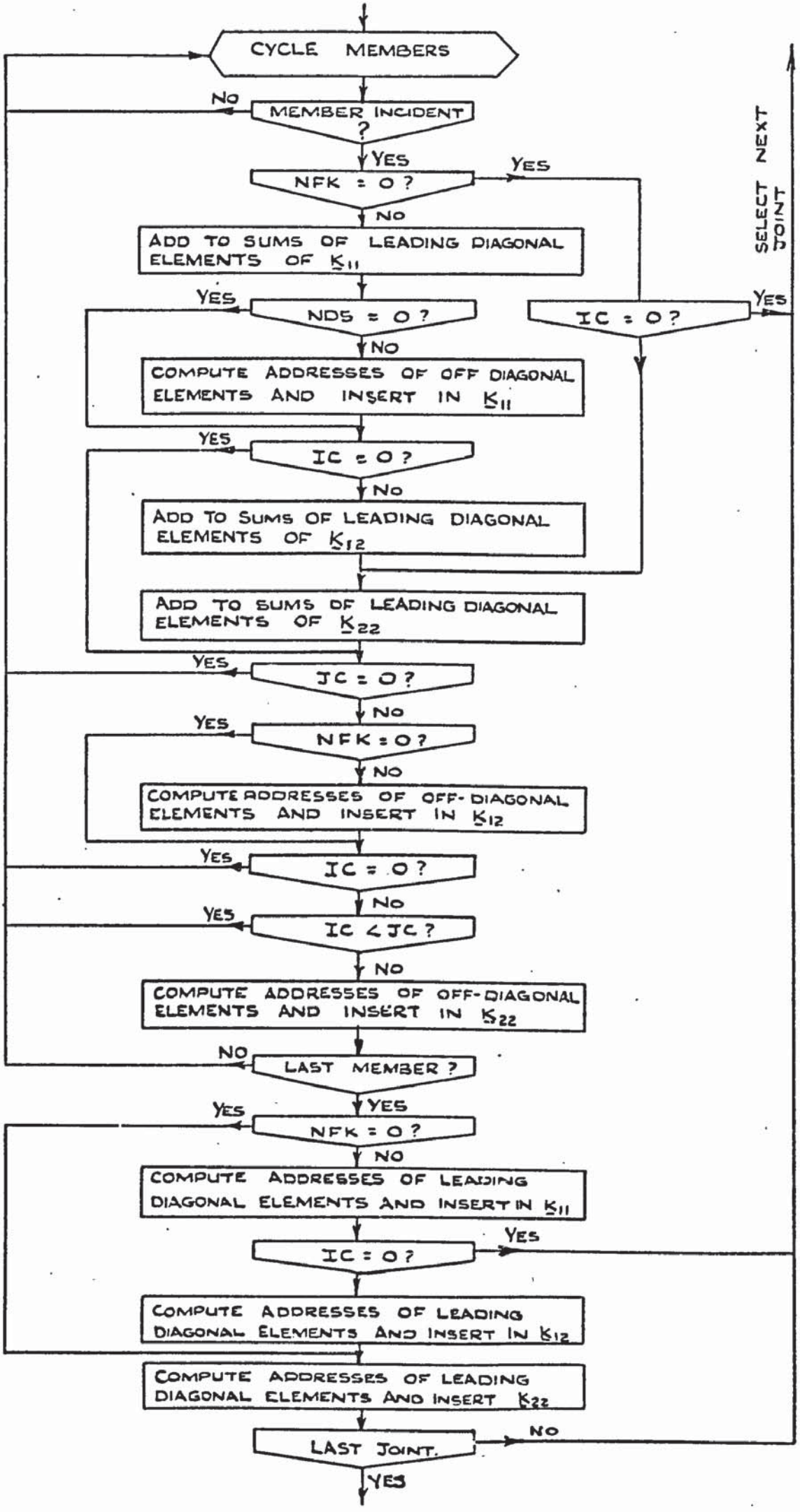

Fig 6.10 Construction of stiffness matrix

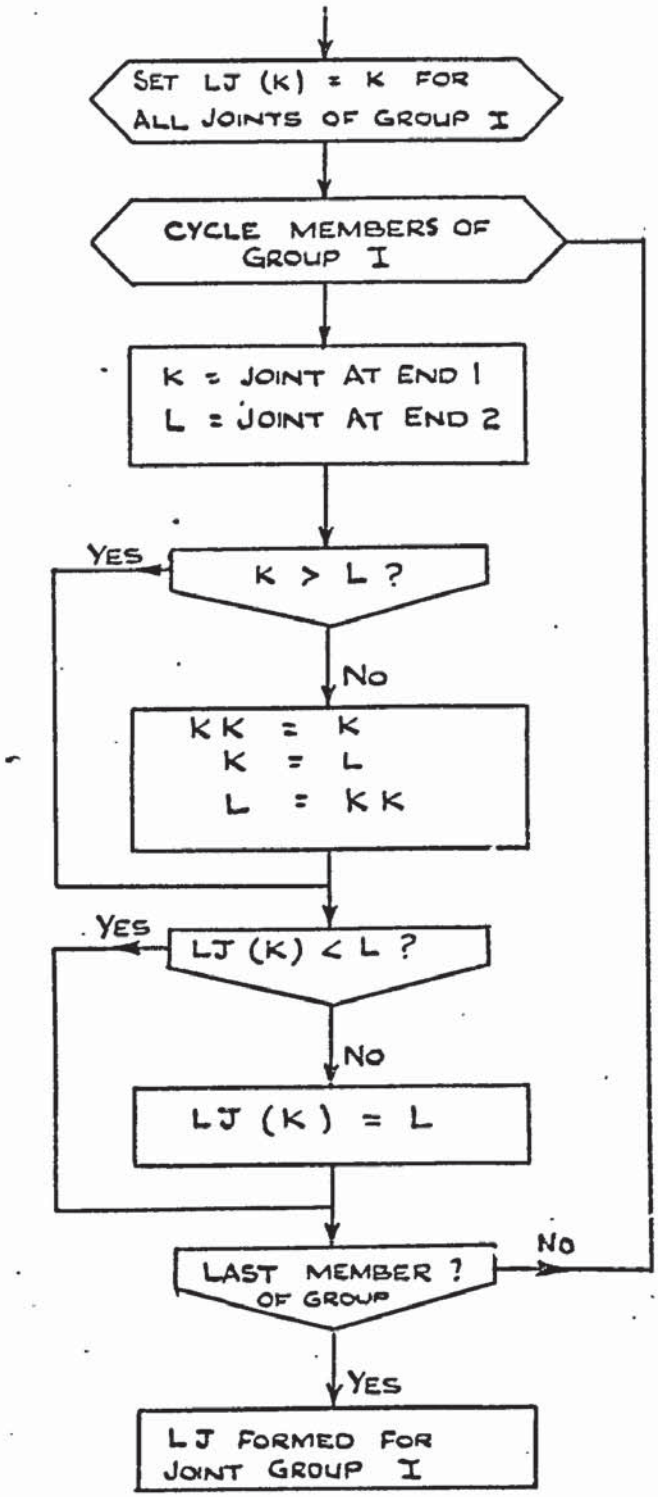

Fig. 6.12. Flow diagram for formation of array LJ

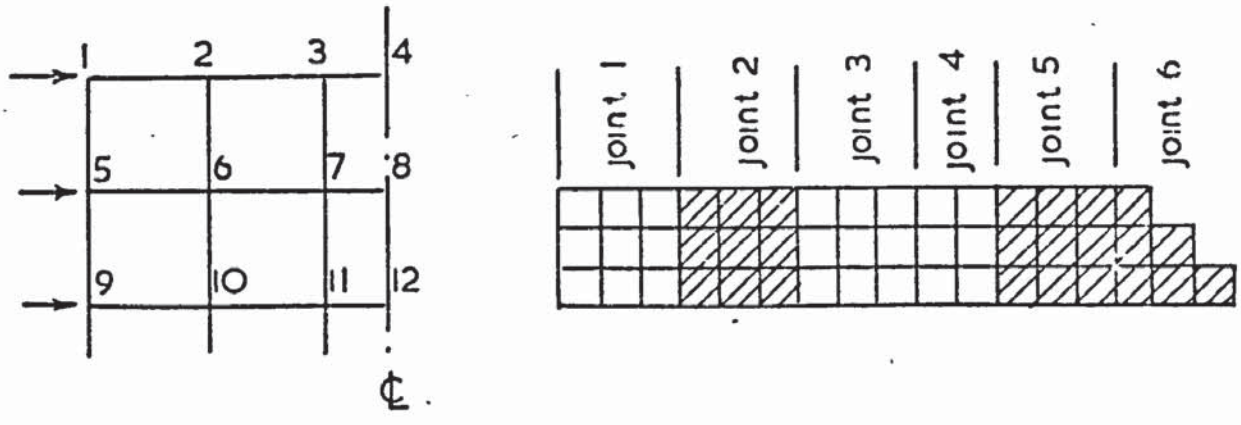

Fig 6.11 Rows of stiffness matrix for joint 6

progressively increased by 1 for each of the other two rows.

The elements of NC are determined from the cumulative summation of the degrees of freedom of each joint as the data for the joints are input. Array LJ, on the other hand, can most efficiently be obtained from the member data alone by considering the numbers of the joints at each end of the members. Thus the elements of LJ for the joints of group I may be obtained by considering the members of group I. Members of group I+1, although possibly connected to joints in group I, are automatically eliminated because the joints at their other ends are in the higher numbered group I+1. This section of the program is described by means of the flow diagram in Fig. 6.12.

The lateral stiffness matrix $\underline{H}^r$ of each frame type and the lateral equivalents $\underline{h}^r$ of the imposed loads are computed by the subroutine INFCO using equation (5.27) as shown in Fig. 6.5. This subroutine, which is shown as a flow diagram in Fig. 6.13, consists essentially of two nested loops in which the right hand side of equation (5.27) is evaluated. In the diagram the identifier K12 refers to the buffer array previously used in subroutine FRAM for the construction of the compound matrix $[\underline{K}_{12} \mid \underline{\ell}\,]$. Similarly, K22 identifies a similar buffer used in constructing the compound matrix $[\underline{K}_{22} \mid \underline{0}]$. The evaluation of $\underline{K}_{12}' \underline{K}_{11}^{-1} [\underline{K}_{12} \mid \underline{\ell}\,]$ in equation (5.27) is carried out block-by-block, storing successive columns of the solution matrix $\underline{K}_{11}^{-1} [\underline{K}_{12} \mid \underline{\ell}\,]$ temporarily in the last column of K12, while the unchanged blocks of $\underline{K}_{12}$ are stored in the remaining columns. On exit from the subroutine the array K22 contains the compound matrix $[\underline{H}^r \mid \underline{h}^r]$ for the frame. The lower triangle of $\underline{H}^r$, which is symmetrical, and the vector $\underline{h}^r$ are stored serially in core for each frame type or for frames subject to different imposed loads.

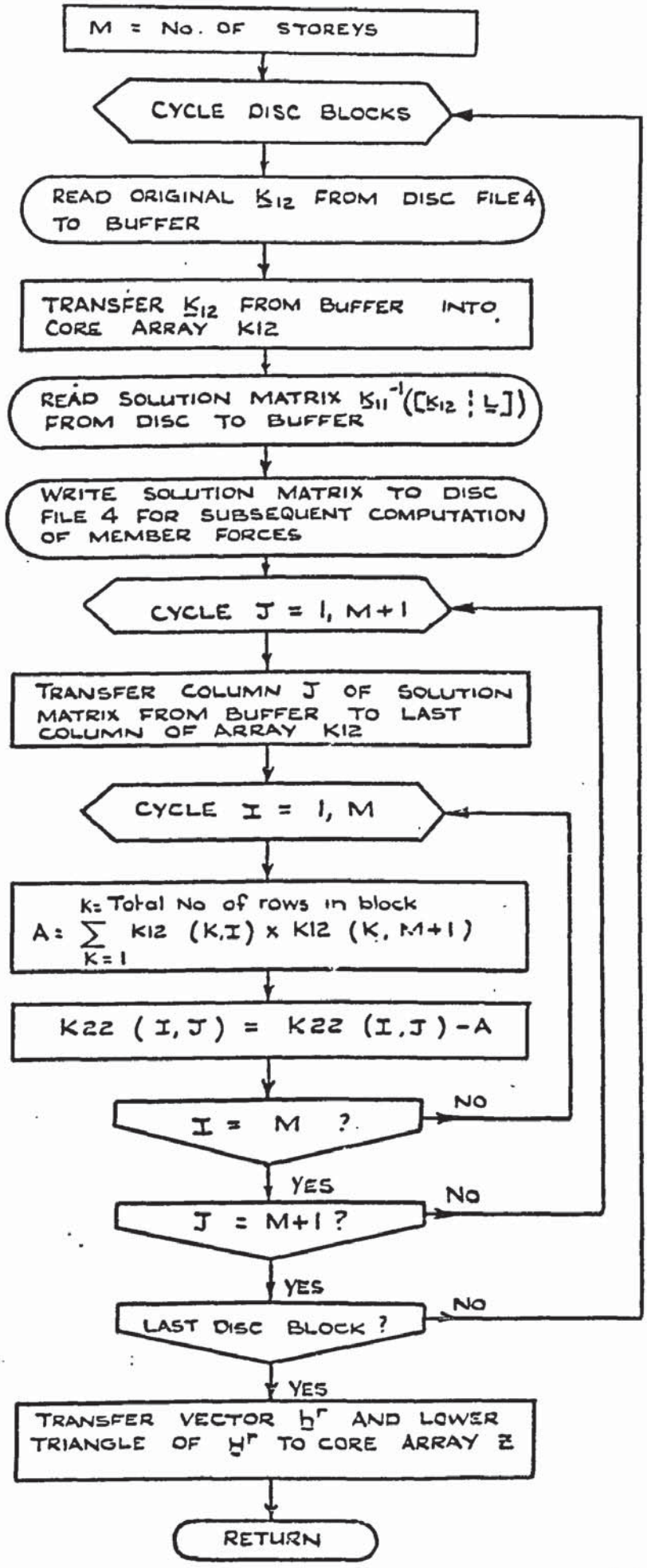

Fig 6.13. Subroutine INFCO

6.3.2 Analysis of the restrained grillage

The construction of the load-displacement equations for the restrained grillage is carried out by calling the subroutine GRIL as shown in Fig. 6.5. As in the method of influence coefficients, the regularity of the structure is used to simplify and reduce the volume of data. In this program however, the degrees of freedom of each vertical line of joints can be varied and a wider variety in the arrangement of the structural members is made possible by providing for the arbitrary omission of complete panels from the walls or floor slabs. A flow diagram of the subroutine is given in Fig. 6.14.

The procedures for constructing the stiffness matrix of the grillage and of the part matrix $\underline{K}_{11}$ in the analysis of the frames are closely similar. In the case of the grillage however the configuration of the members at each joint is inferred directly from the data without the necessity of searching through the member data for incident members. Once the incident members for a particular joint have been determined, the procedures for the selection and placing of the stiffness coefficients are the same and the same subroutines can be used. For example, the sums of the leading diagonal elements are formed by calling the subroutine LD(I,J,K,S1,S2,S3,S4,S5,S6,P1,P2,P3,P4,P5,P6) for each incident member. The input parameters I, J and K denote the degrees of freedom of the joint in the order that they occur in the displacement vector and are assigned the value of 1 if a degree of freedom exists. The output parameters S1 through S6 are the sums of the elements and are set to zero before each joint is processed. The values of the stiffness coefficients assigned to the input parameters P1 through P6 are set out in Table 6.4. In the analysis of the frames the same parameters may be used in the construction of all the part matrices $\underline{K}_{11}$, $\underline{K}_{12}$ and $\underline{K}_{22}$. The same parameters may be used also irrespective of the direction of the

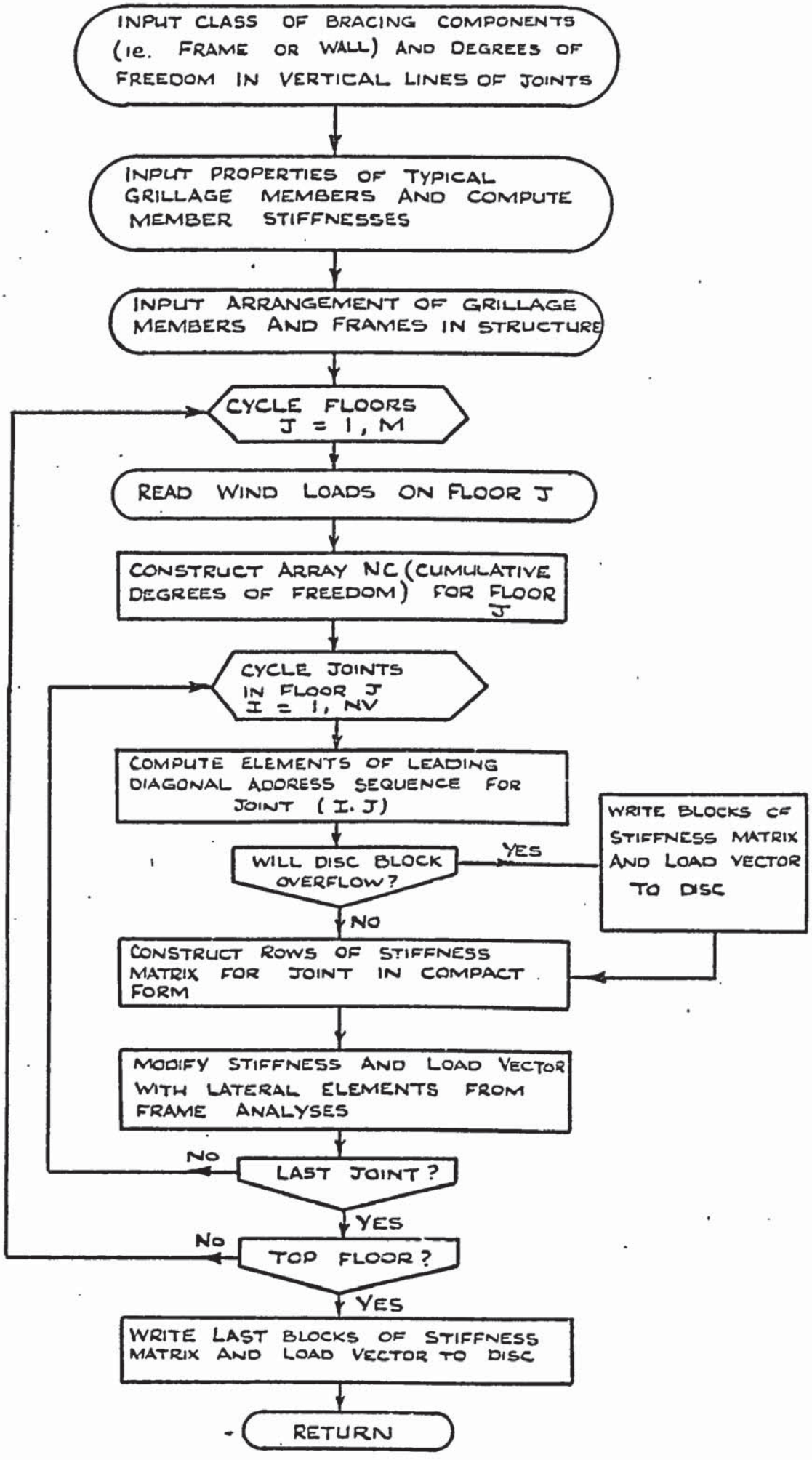

Fig. 6.14 Subroutine GRIL

P axis of the members if an exchange of identifiers for the stiffness coefficients takes place earlier in the program. For the grillage, the directions and orientations of the members are pre-determined. It is therefore convenient to use the matrices of equations (2.10) to obtain separate sets of parameters as shown in Table 6.4. A flow diagram of the subroutine is given in Fig. 6.15, where the relative positions of the leading diagonal elements are shown in the inset diagram.

In placing the off-diagonal elements it is necessary to consider the degrees of freedom of the joints at both ends of the members. Each degree of freedom of the current joint corresponds to a row in the stiffness matrix while, for a particular member, each degree of freedom of the remote joint forms a column in the pattern of off-diagonal elements contributed by the member. A typical example is shown in Fig. 6.16(a) where the current joint K has three degrees of freedom, while the remote joint J has two. For each incident member the start address in the compact sequence is calculated for each row of the pattern of off-diagonal elements. The selection and placing of the elements in the row is then made by calling the subroutine ROW (P,Q,R) where P, Q and R are input parameters to which the appropriate stiffness coefficients are assigned by the calling program. As joints in the grillage are always numbered consecutively in rows starting from the bottom left hand joint, only the members to the left and below the joint contribute off-diagonal elements to the stiffness matrix. A flow diagram of the subroutine is given in Fig. 6.16(b). Part (c) of the figure shows a simplified segment of the calling program relating to the member to the left of the joint. A similar sequence follows for the member below the joint. It is tacitly assumed in the calling program that all the grillage joints have freedom in the Z direction. The values of the stiffness coefficients, which are tabulated in Table 6.5 are obtained directly from equations (2.10) for the grillage and from equation (2.15) for the frame. In the case of the

		P1	P2	P3	P4	P5	P6
FRAME JOINT (Degrees of freedom in directions X, Y, θ)		A_1	B_1	F_1	$-C_1$	$-T_1$	E_1
GRILLAGE JOINT (Degrees of freedom in directions Z, θ^x, θ^y)	Left member	b	o	q	-d	o	e
	Right member	b	o	q	d	o	e
	Lower member	b	-d	e	o	o	q
	Upper member	b	d	e	o	o	q

Table 6.4 Leading diagonal stiffness coefficients

			REMOTE JOINT J		
LEADING DIAGONAL JOINT K			P	Q	R
		Row 1 (X)	$-A_1$	$-B_1$	$-C_2$
		Row 2 (Y)	$-B_1$	$-F_1$	$-T_2$
		Row 3 (θ)	C_1	T_1	F_2
	Left Member	Row 1 (Z)	-b	o	-d
		Row 2 (θ^x)	o	-q	o
		Row 3 (θ^y)	d	o	f
	Lower Member	Row 1 (Z)	-b	-d	o
		Row 2 (θ^x)	d	f	o
		Row 3 (θ^y)	o	o	q

Table 6.5 Off-diagonal stiffness coefficients

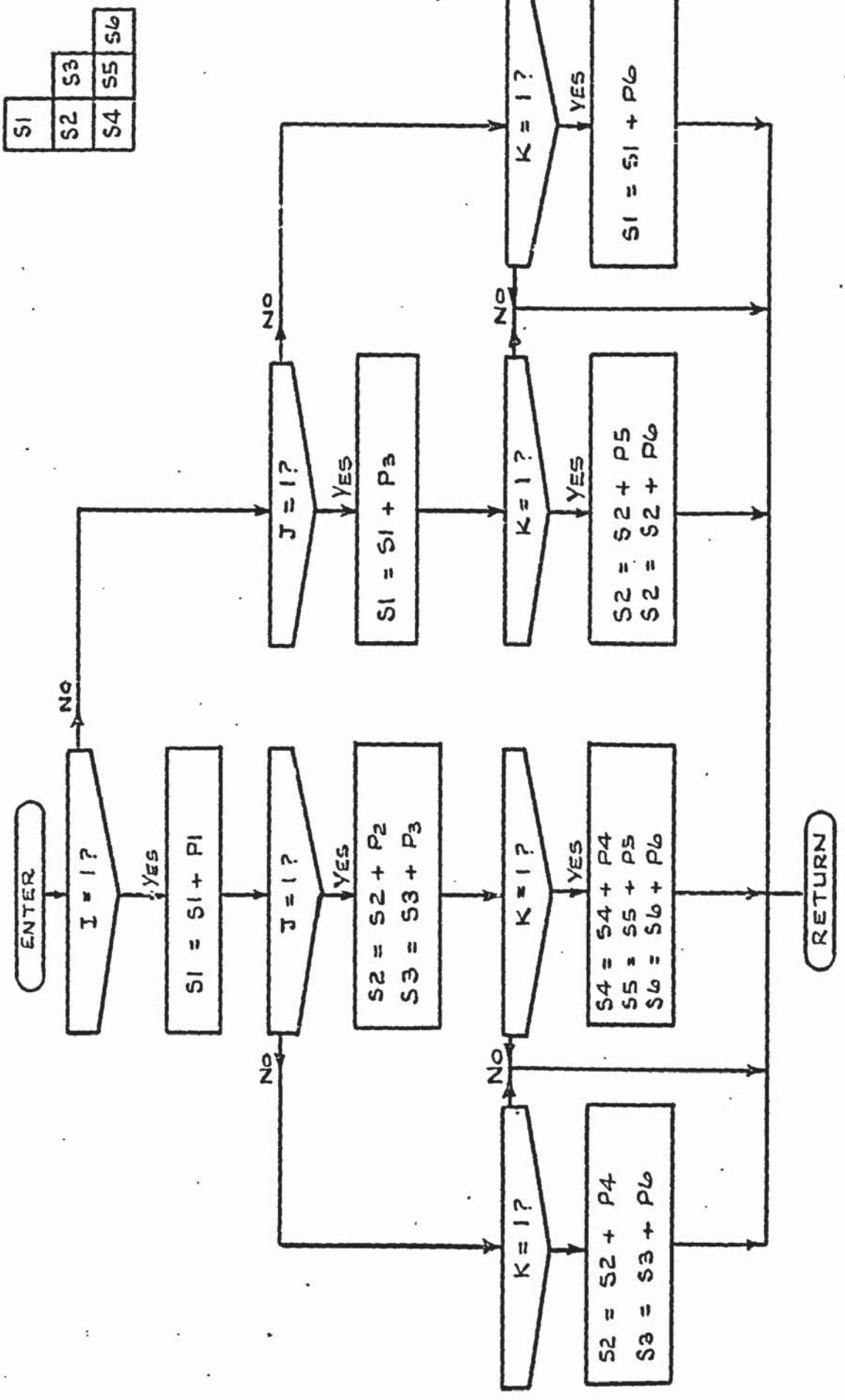

Fig 6.15. Subroutine LD

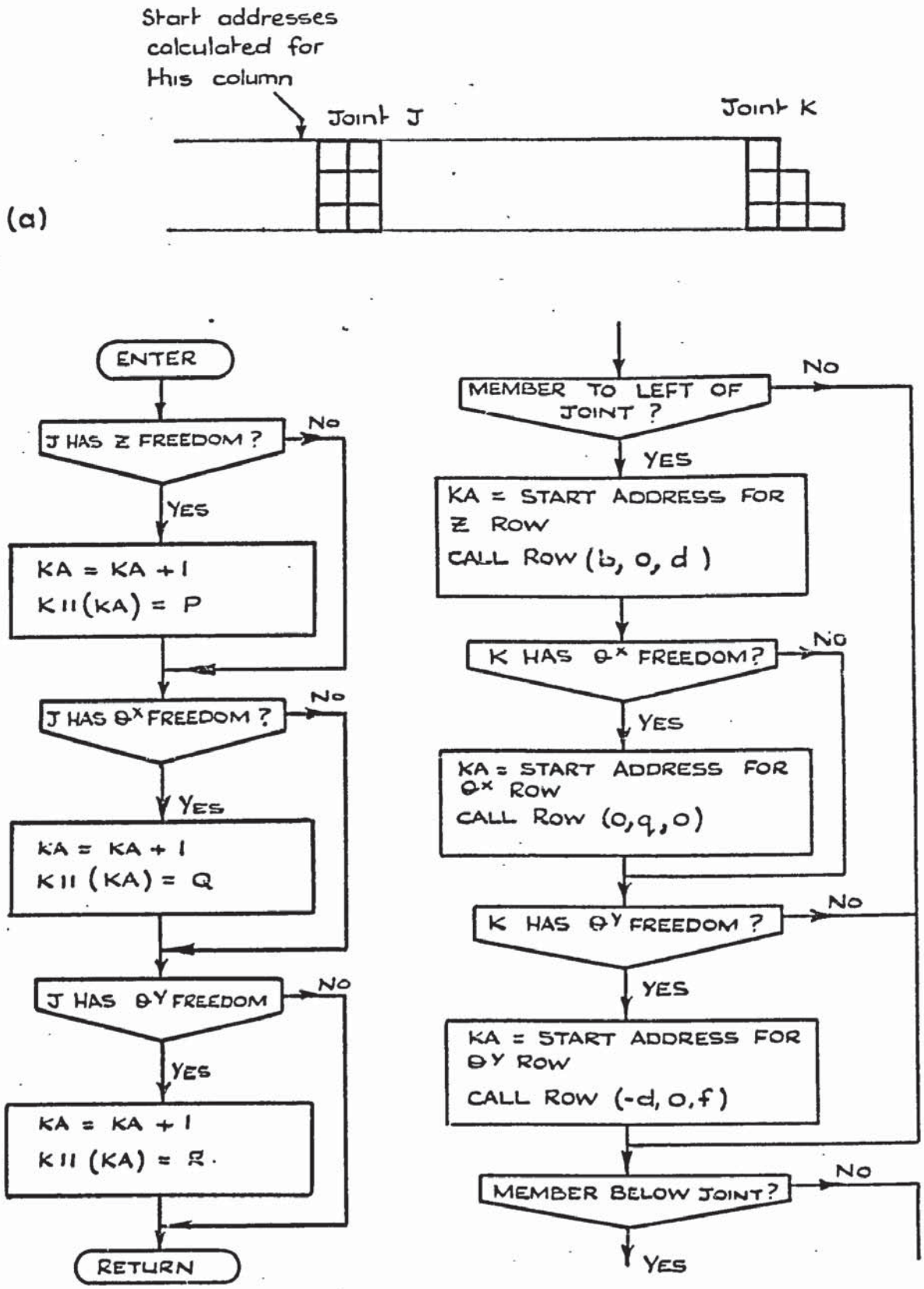

Fig. 6.16 Computation of off - diagonal elements

frame the calling program is very similar and as in the case of the leading diagonal elements, the same set of parameters may be used irrespective of the direction of the P axes of the members, by making an exchange of identifiers earlier in the program.

It may be observed that these subroutines require a complete set of stiffness coefficients to be calculated for each member, although only those appropriate to the degrees of freedom at the ends of the member are used. It is unlikely however that any significant loss of efficiency results from this practice, having regard to the simplification of the logic resulting from the use of the subroutines.

6.3.3. Calculation of member forces

The program concludes by calling the subroutine MFORCE in which the forces in all the members of the complete structure are computed and output. In this subroutine, which is illustrated by the flow diagram in Fig. 6.17, the in-plane forces in the wall panels and floor slabs are first determined by applying equation (2.11) to the displacement vector $\underline{d}$ obtained from the analysis of the restrained grillage.

For the frames, the vertical and rotational displacements are first calculated from equation (5.31) using the lateral displacements $\underline{d}_r$, extracted from vector $\underline{d}$. The right hand side of equation (5.31) is progressively evaluated for successive blocks of the solution matrix $\underline{K}_{11}^{-1}\ [\underline{K}_{12} \mid \underline{I}]$ which was retained on disc file 4. Member forces are then determined by the application of equation (2.16) to each member in turn, using the member stiffnesses and other relevant data stored on the serial disc file 5.

6.3.4. The Scope of the program

The size of a structure that can be analysed by the program, assuming

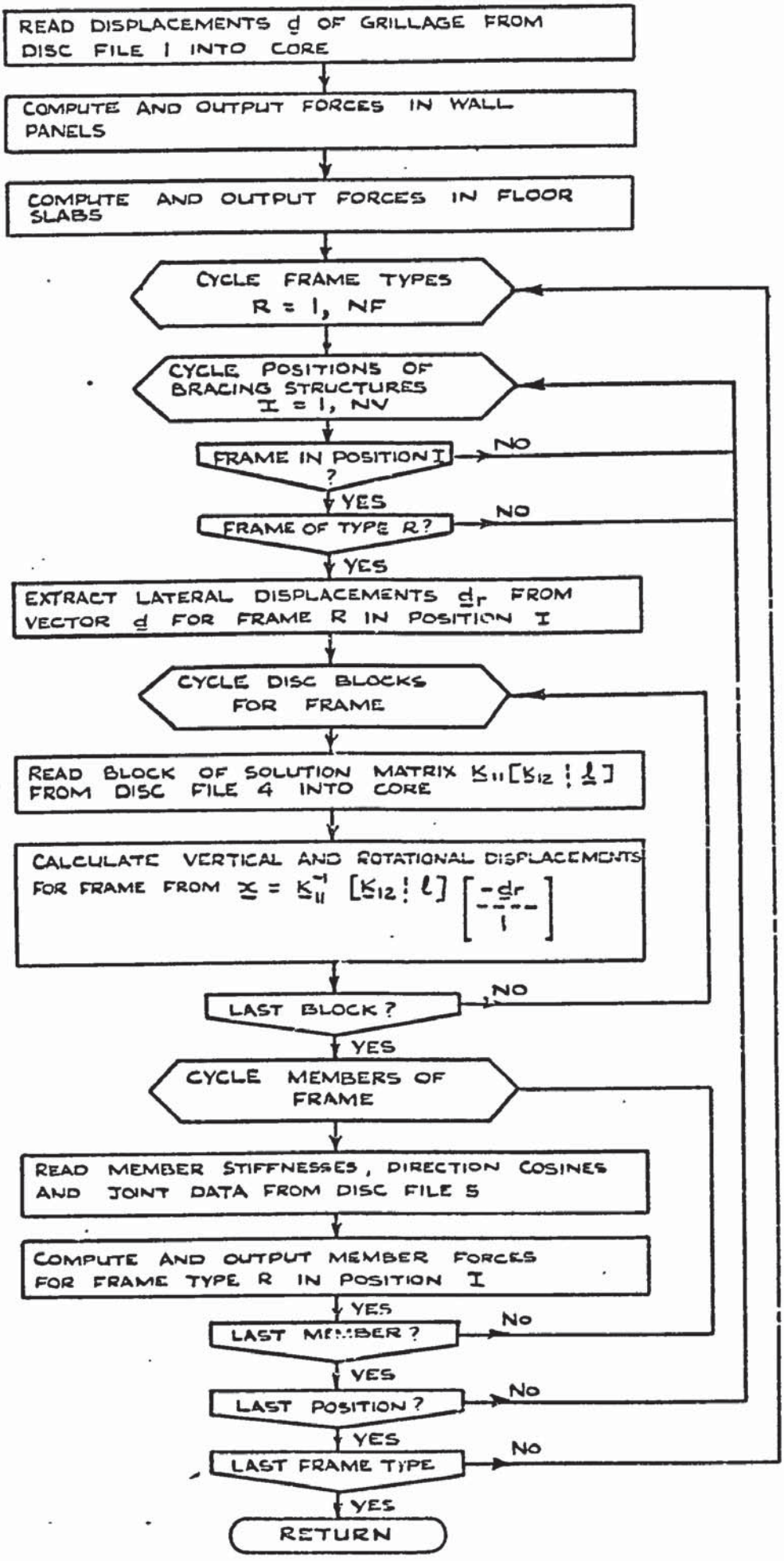

Fig. 6.17. Subroutine MFORCE

that sufficient core and backing store are available, is governed by the number of elements in the stiffness matrix corresponding to a single joint either of a frame or the grillage. Usually the grillage is the more critical. The maximum is 510 elements, which is the capacity of the largest single block of store that can be written to disc using ICL subroutines. This quantity could be increased by modifying the subroutine CDM to enable the working core arrays to be stored in multiple blocks on the disc.

As an example, the array storage requirements for a 50 storey, 5 bay symmetrical structure containing 3 different types of frame, each with 600 degrees of freedom, is shown in Table 6.6. The units of the table are real number equivalents, where one real number occupies two, 24 bit words in core and is equivalent to two integers. The largest area of core, namely that required for the formation and storage of the lateral stiffness coefficients for the frames, is significantly influenced by the height of the structure, since the part matrix $\underline{K}_{22}$ has an order equal to the square of the number of storeys, and also by the number of different types of frame in the complete structure.

Buffers required by the system for direct access disc files.	2048
Buffer arrays used as working space for the formation of the load-displacement equations.	3072
Data arrays.	1260
Formation of $\underline{K}_{22}$ and storage of the lateral stiffness coefficients for the frames.	7000

Table 6.6 Array storage for a 50 storey structure

CHAPTER 7

EXPERIMENTAL VERIFICATION

7.1 Introduction

Verification of the method of influence coefficients has already been provided for a 10 storey structure by comparison of the results with those of Goldberg in Chapter 4. The results from the restrained grillage approach for this structure were almost identical with those obtained by the method of influence coefficients. Further verification by experiment was undertaken however, in order to provide a background of experimental results with which the results of analyses by the proposed methods, and also by a finite element method, could be compared. For this experiment a small, two storey symmetrical model was chosen, firstly to avoid difficulties with storage in the finite element analysis, and secondly so that all the relevant matrices for the proposed methods could be constructed by hand, thus providing an aid in the development of the computer programs.

The model was constructed with walls and floor slabs made from Perspex and with three intermediate frames in mild steel. A general view is given in Plate 7.1 showing the model mounted on its side with the wind loads simulated by concentrated vertical loads at the junctions of the floors with the walls and frames. Details of the construction are given in Figs. 7.1 and 7.2.

Particular care was taken in the design of the foundations to ensure rigidity and to avoid differential movement of the footings of the walls and the frames. For the frames, the bases of the columns were clamped between angle brackets as shown in Fig. 7.1. These brackets were provided with a slot machined to fit accurately and tightly round the column when clamped by two $\frac{3}{8}$ in. diameter bolts. The base flanges of the brackets contained slotted holes so that their correct location on the base plates could be ensured without inducing stresses in the frames. Similar brackets were used for clamping the bases of the walls. Differential rotation of

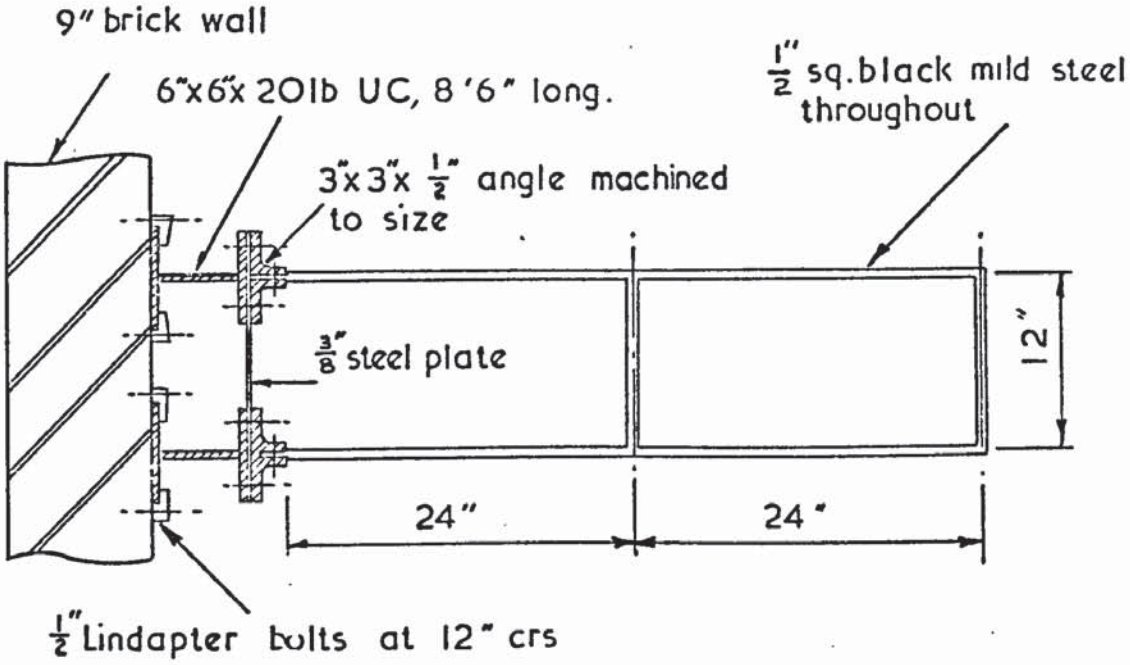

general elevation

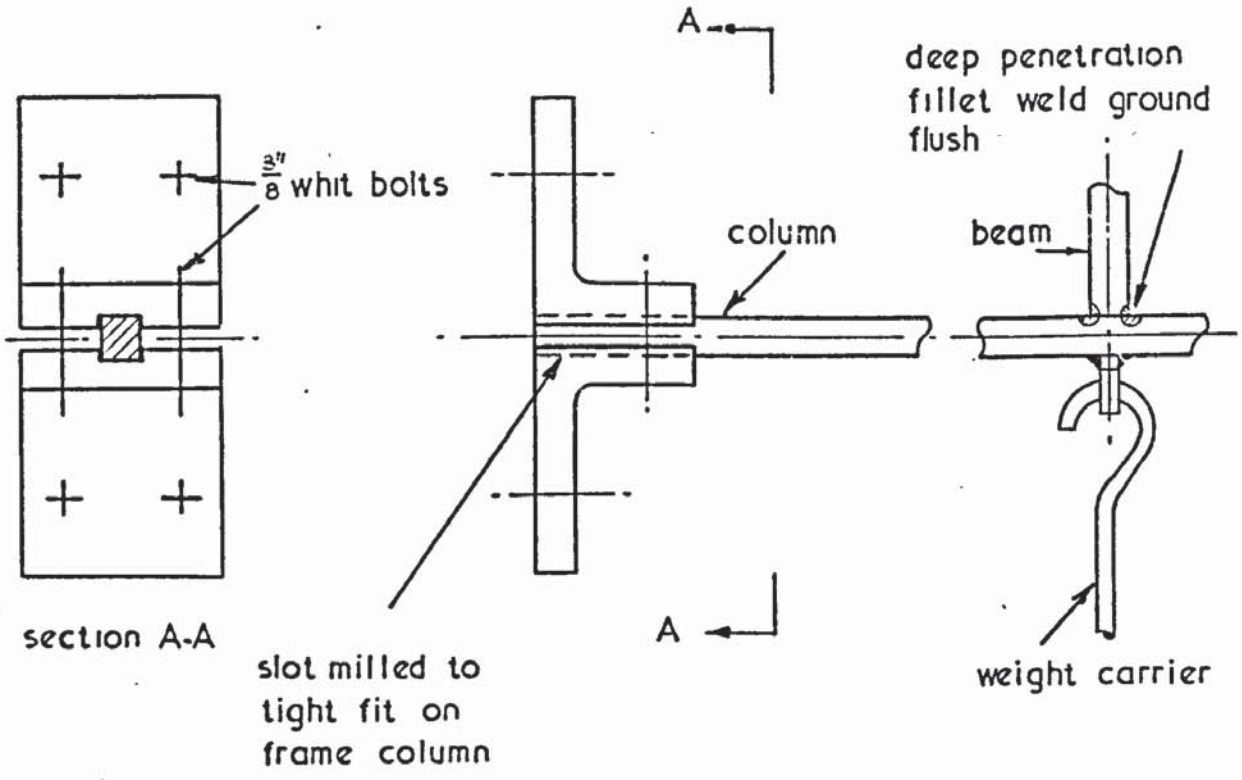

column details

Fig 7. 1 Details of steel frame

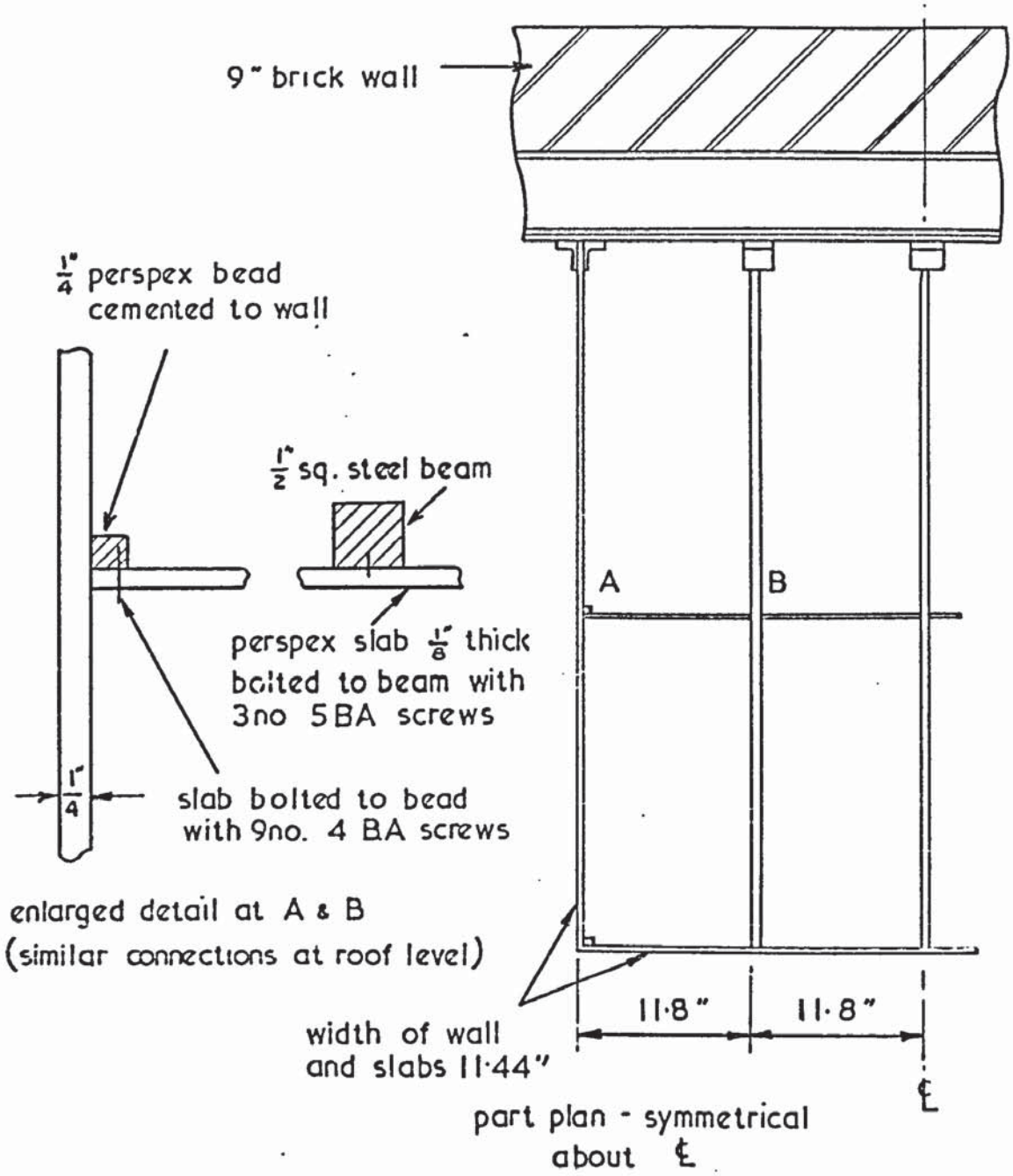

Fig.7.2 Details of junctions

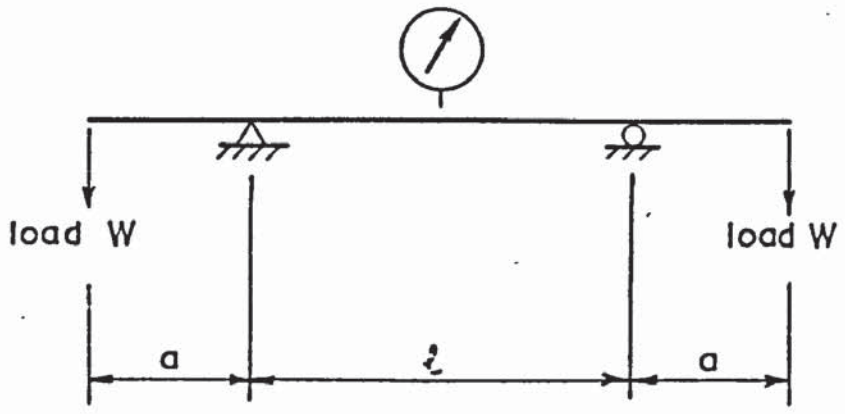

Fig. 7.3 Beam apparatus for determination of Young's modulus

the footings was prevented by bolting them to a rigid base foundation consisting of two universal columns, bridged by a mild steel plate $\frac{3}{8}$ in. thick, the whole bolted to a 9 in. brick wall by "Lindapter" bolts at 12 in. centres.

Local stiffening of the beams and columns at their joints by surplus weld metal was avoided by using deep penetration fillet welds which were ground flush afterwards. The junctions of the floor slabs with the frames were made with three screws only in order to provide compatibility of lateral displacements at the junctions without introducing composite action between the Perspex slabs and the steel beams. At the junctions between the slabs and the walls on the other hand, the screws were more closely spaced so that horizontal compatibility would be achieved and the rotations of the walls would be fully transmitted to the slabs. Screws were used so that the Perspex plates could be assembled after the preliminary testing of the bare frames, without disturbing the base connections of the frames.

The results of primary interest, which were required from the experiment, were the deflections at the junctions and the distribution of lateral forces to the frames. The deflections were measured directly by means of dial gauges mounted on a slotted angle frame as shown in Plate 1. The loading of the frames could not be determined directly. However, since the combination of strains in the upper and lower storeys is unique for a given combination of loads, the strains in the columns were used as a basis for comparison. Strains were measured initially by electrical resistance foil gauges, using a Peekel electronic strain indicator, type B103U, with a single dummy gauge for temperature compensation. Subsequently however, confirmation of some of the results by means of Huggenberger mechanical gauges was found to be necessary.

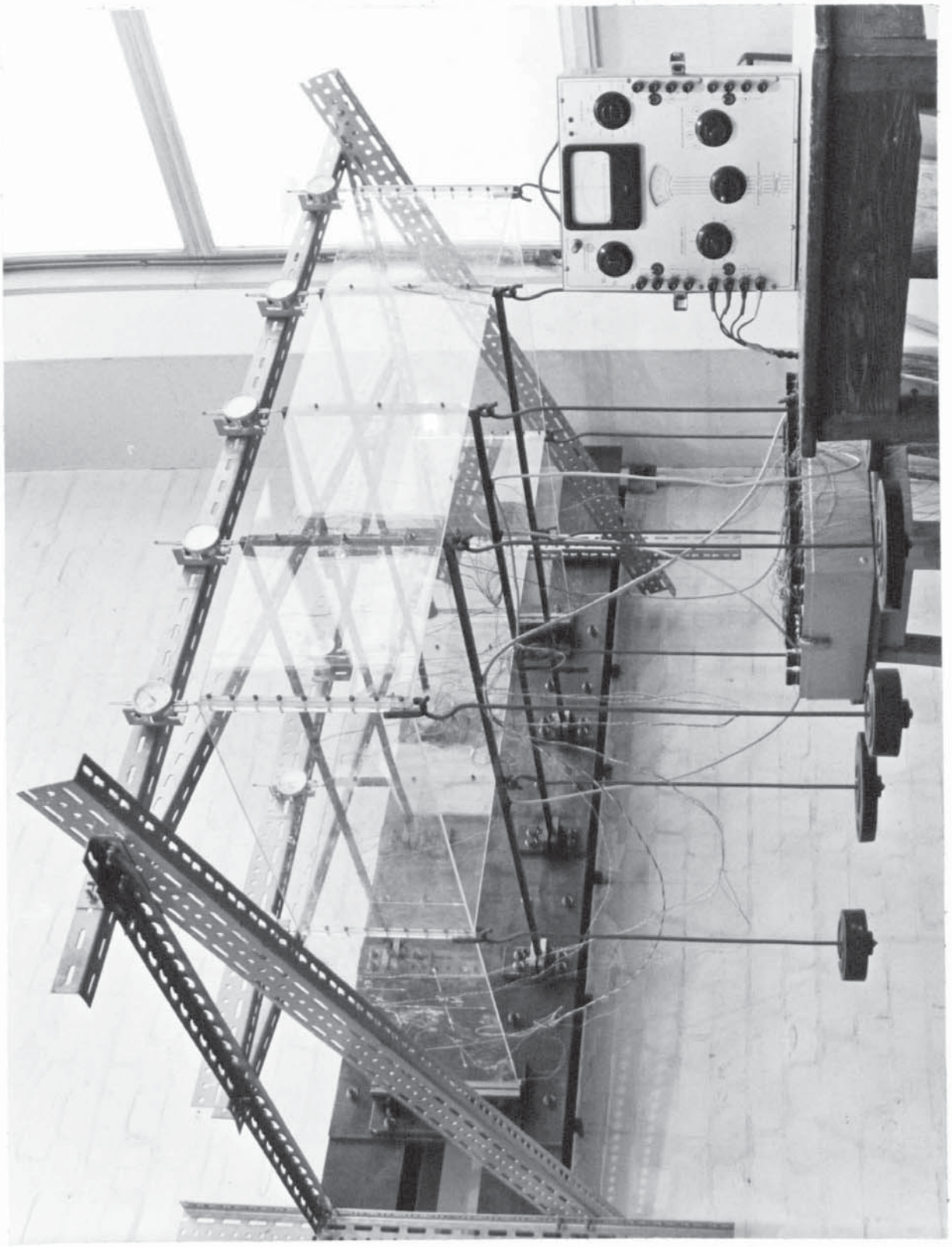

Plate 7.1 General view of experimental model.

7.2 Preliminary testing

Before a computer analysis of the model could be undertaken it was necessary to determine Young's modulus for the materials. Tests were carried out using the simple beam apparatus shown diagrammatically in Fig. 7.3. Care was taken in the case of the very flexible Perspex specimens to avoid friction at the supports. It was also found that results were affected by the varying force exerted by the dial gauge return spring which was therefore removed.

In all the tests loads were applied simultaneously to the ends of the beam in equal increments, taking readings of deflection during loading and unloading. Since Perspex is susceptible to creep, the loads and spans were chosen to give strains of approximately the same order as those occurring in the model, and the duration of the tests was made equal to the time required for a complete loading cycle on the model, namely 2 hours. Detailed results of these tests are given in Table 7.1 for Perspex and in Table 7.2 for steel. The corresponding load-deflection graphs are plotted in Figs. 7.4 and 7.5 respectively.

Using simple beam theory and considering the circular bending of the central span of the beam, it can be shown that Young's modulus is given by

$$E = \frac{1.5\, a \ell^2}{bt^3} \times \frac{w}{\delta}$$

where a and ℓ are the lengths of the cantilever and central spans of the beam as shown in Fig. 7.3; b and t are the breadth and depth of the section respectively, and w/δ is the slope of the load-deflection graph. Values of Young's modulus calculated from the graphs, using the above expression, are given in the tables for each specimen. The linearity of the load-deflection graphs for Perspex indicates that creep deflections did not have a significant effect.

Material	Load (lb)	Deflection (.001 in)		Zeroed Average	Test Data and Results
		Load	Unload		
Perspex from left hand wall	0.0 0.1 0.2 0.3 0.4 0.5 0.6	43 53 62 72 81 91 101	46 55 65 74 84 92	0.0 9.5 19.0 28.5 38.0 47.0 56.5	ℓ = 13in a = 4in b = 1.44in (average) t = 0.258in (average) slope W/δ = 10.55 E = 433,000 lb/in^2
Perspex from right hand wall	0.0 0.1 0.2 0.3 0.4 0.5 0.6	232 234 257 270 283 295 309	233 247 260 273 284 297	0.0 13.0 26.0 39.0 51.0 63.5 76.5	ℓ = 13in a = 4in b = 1.25 (average) t = 0.246 (average) slope W/δ = 7.93$_2$ E = 432,000 lb/in^2
Perspex from upper floor slab	0.0 0.1 0.2 0.3 0.4 0.5 0.6	262 296 340 373 410 447 482	269 307 346 384 417 453	0.0 36.0 77.5 113.0 148.5 184.5 216.5	ℓ = 13in a = 1.5in b = 1.38 (average) t = 0.120 (average) slope W/δ = 2.78$_2$ E = 433,000 lb/in^2
Perspex from lower floor slab	0.0 0.1 0.2 0.3 0.4 0.5 0.6	221 257 303 339 377 417 459	233 272 313 353 392 427	0.0 38.0 81.5 119.5 158.5 195.5 232.0	ℓ = 13in a = 1.5in b = 1.25in (average) t = 0.121in (average) slope = W/δ = 2.60 E = 446,000 lb/in^2
Average value of Young's modulus					436,000 lb/in^2

Table 7.1 Tests for Young's modulus of Perspex

Material	Load (lb)	Average Deflection (.001in)	Test Data and Results
Steel from frame 1	0.0 2.0 4.0 6.0 8.0 10.0 12.0	0.0 12.0 26.0 38.5 51.0 64.0 77.0	ℓ = 29.98in a = 9.0in b = 0.506in (average) t = 0.504in (average) slope W/δ = 152.5 E = 28,611,000 lb/in^2
Steel from frame 2	0.0 2.0 4.0 6.0 8.0 10.0 12.0	0.0 12.5 25.5 38.5 51.0 64.0 77.0	ℓ = 29.98in a = 9.0in b = 0.5045in (average) t = 0.506in (average) slope W/δ = 152.5 E = 28,357,000 lb/in^2
Steel from frame 3	0.0 2.0 4.0 6.0 8.0 10.0 12.0	0.0 12.5 26.0 38.5 51.0 64.0 77.0	ℓ = 29.98in a = 9.0in b = 0.506in (average) t = 0.504in (average) slope W/δ = 152.5 E = 28,611,000 lb/in^2
Average Young's modulus			28,526,000 lb/in^2

Table 7.2 Tests for Young's modulus of steel

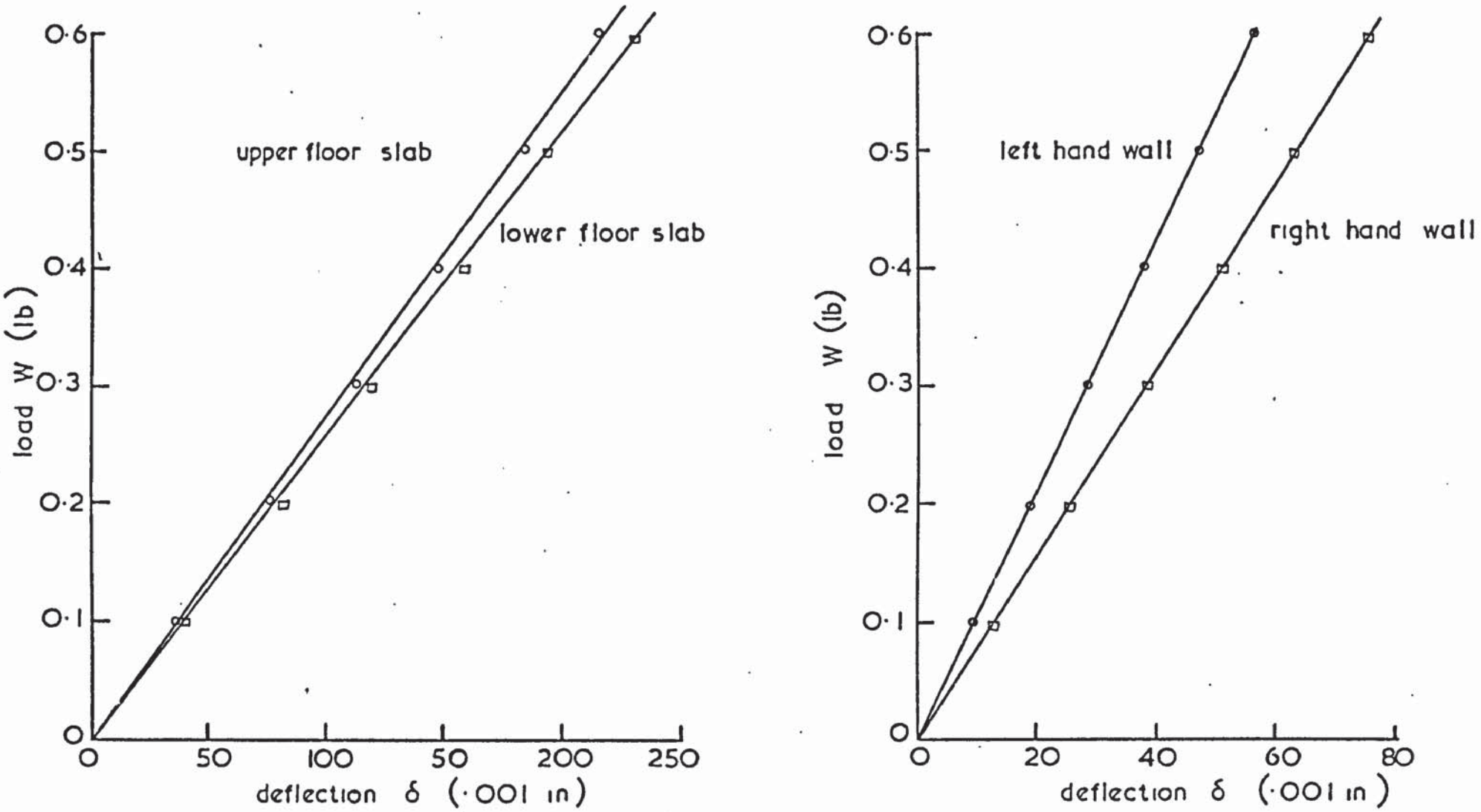

Fig 7.4 Tests for Young's modulus of perspex

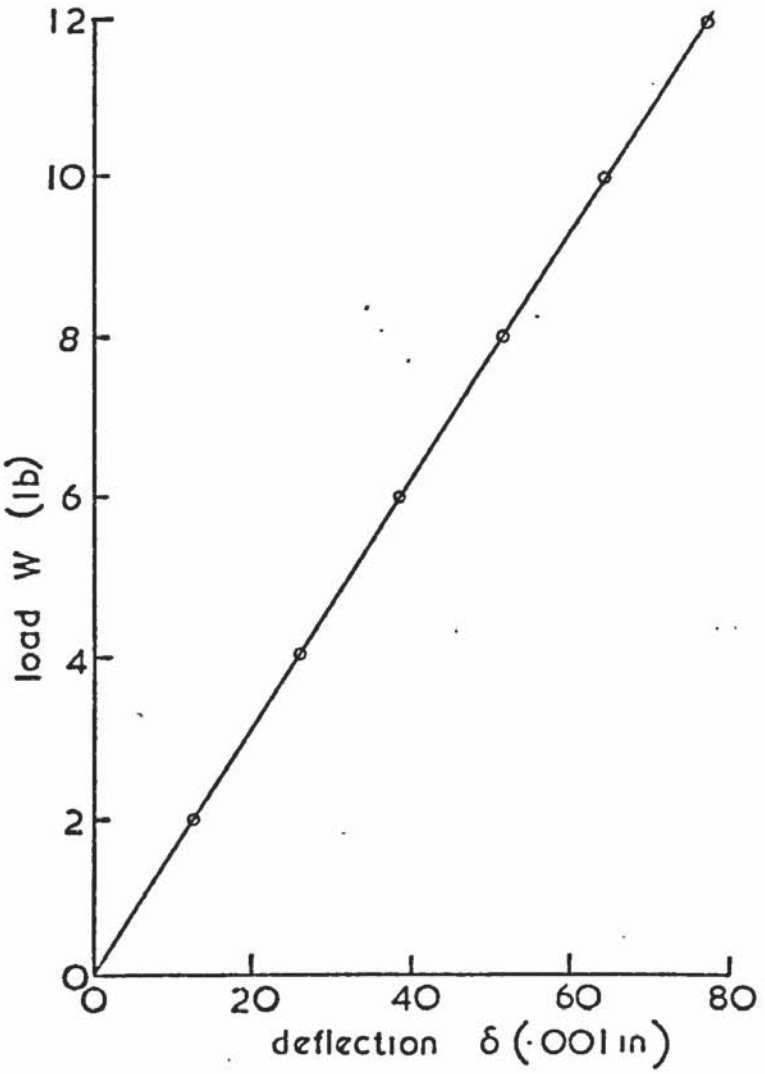

Fig. 7.5 Test for Young's modulus of members of steel frames

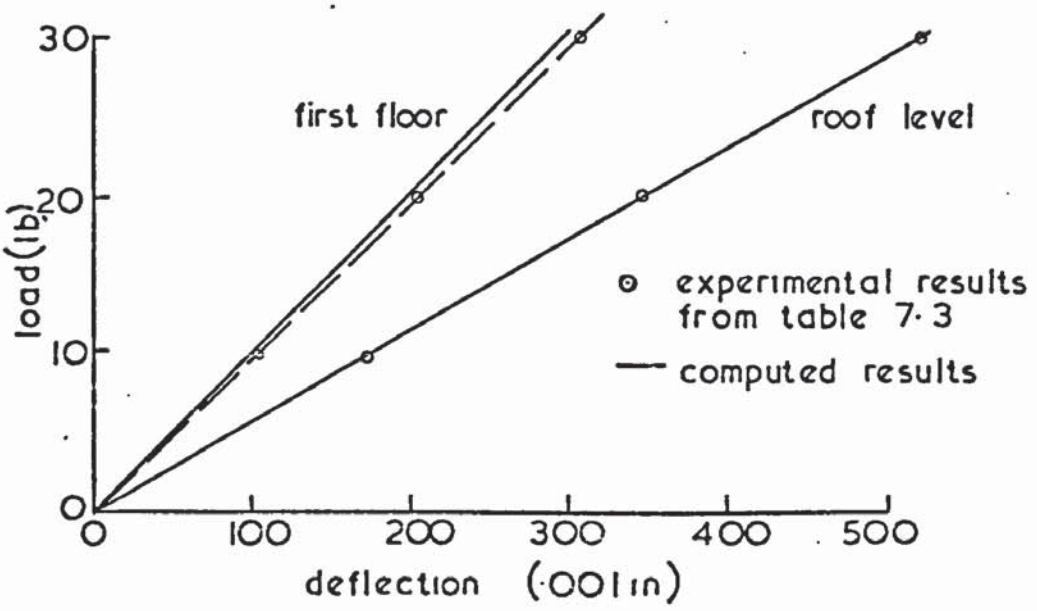

Fig 7.6. Average load deflection graphs for bare frames

Load	ROOF LEVEL				FIRST FLOOR			
	Frame 1	Frame 2	Frame 3	Average	Frame 1	Frame 2	Frame 3	Average
0	0	0	0	0	0	0	0	0
10	174	173	172	173	103	103	102	103
20	348	347	345	347	206	206	204	205
30	525	522	519	522	310	310	307	308
20	351	349	347		207	208	205	
10	176	176	173		105	105	103	
0	2	2	1		2	2	1	

Table 7.3 Deflections of bare frames (.001 in)

The values obtained for Young's modulus, both of Perspex and steel, were within 3% of the mean, justifying the assumption of average values in the computer analysis. The modulus of rigidity of Perspex was calculated, using the manufacturer's quoted value of 0.35 for Poisson's ratio.

Further preliminary tests were carried out on the bare frames in order to establish that they were identical and that the deflections and strains were in agreement with the computed results. During these tests the three frames were loaded simultaneously in their final mountings in order to ensure that no differential displacements occurred as a result of small elastic rotations of the footings. Confirmation of the strains recorded by the electrical gauges was obtained by repeated tests with six Huggenberger mechanical strain gauges attached to each frame in turn.

The deflections for the three frames are recorded in Table 7.3 which shows that the deflections at each floor level agreed within 1% of the average. The average deflections are plotted against load in Fig. 7.6, where the computed values are shown to agree closely with the experimental results.

Load-strain graphs are given for the electrical strain gauges in Fig. 7.7, where the figures in brackets denote the positions of the gauges as shown in Fig. 7.8(a). Similar graphs for the Huggenberger gauges are plotted for each frame in Fig. 7.9, where the positions indicated for the gauges in this case refer to Fig. 7.8(b).

The strains, obtained from these graphs are compared in Fig. 7.10 with the computed results for each frame at the loads shown. The computed results, including axial strains, are the same for all the frames and are indicated in micro-strains by the printed figures at the ends of the columns in frame 2. It is noticed that the Huggenberger gauges gave more consistent results throught and that with the exception of some of the

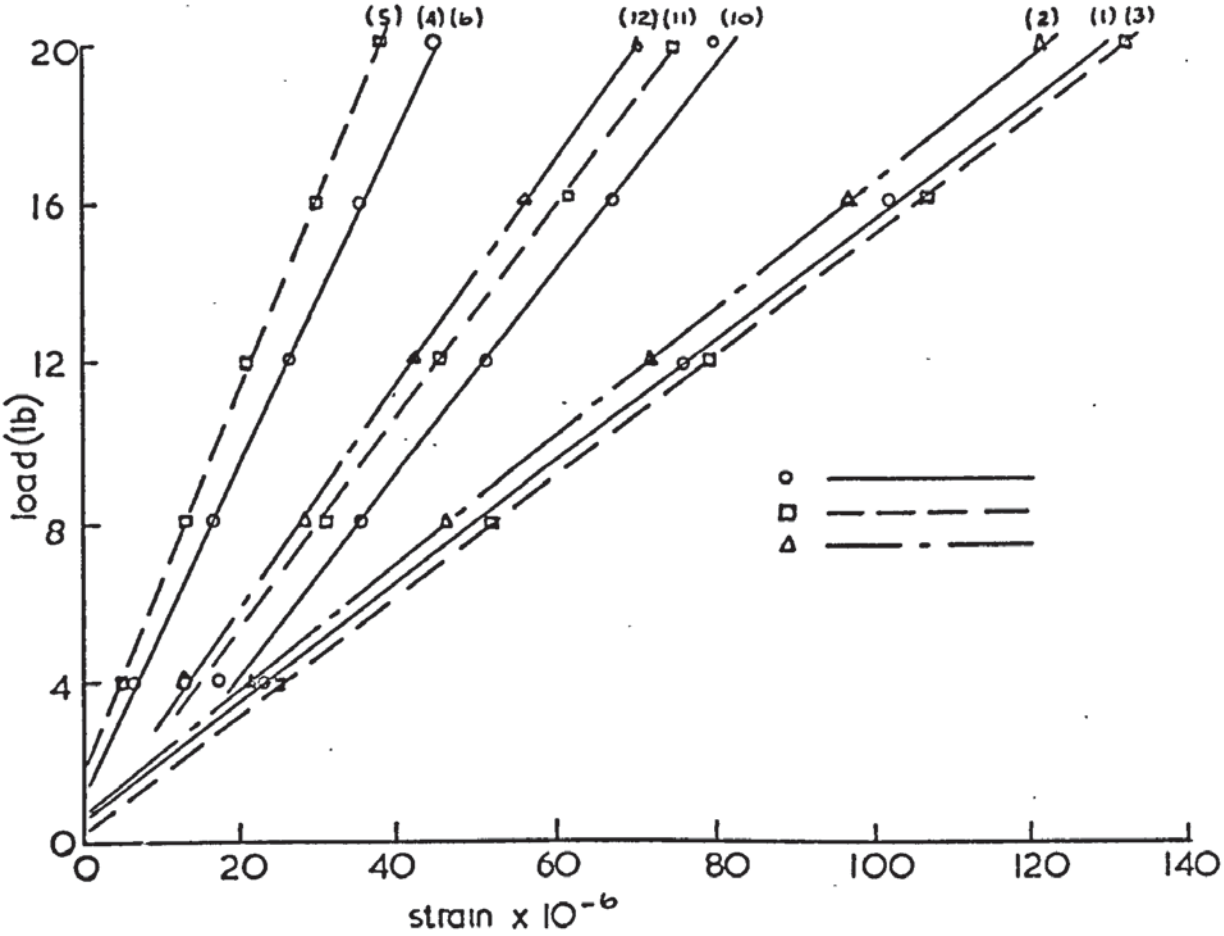

(a) storey no. 2

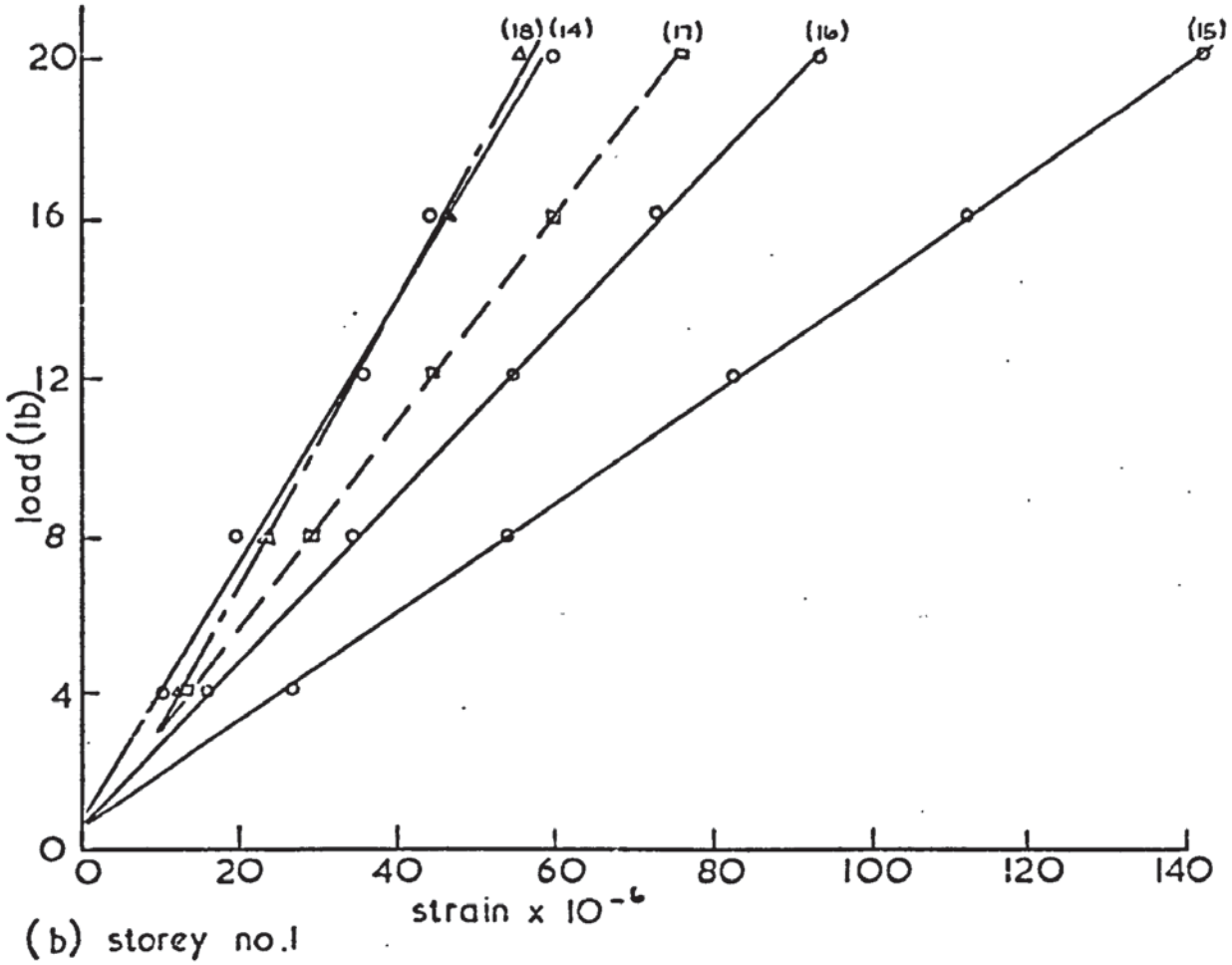

(b) storey no. 1

Fig. 7.7 Load strain graphs for bare frames (electrical gauges)

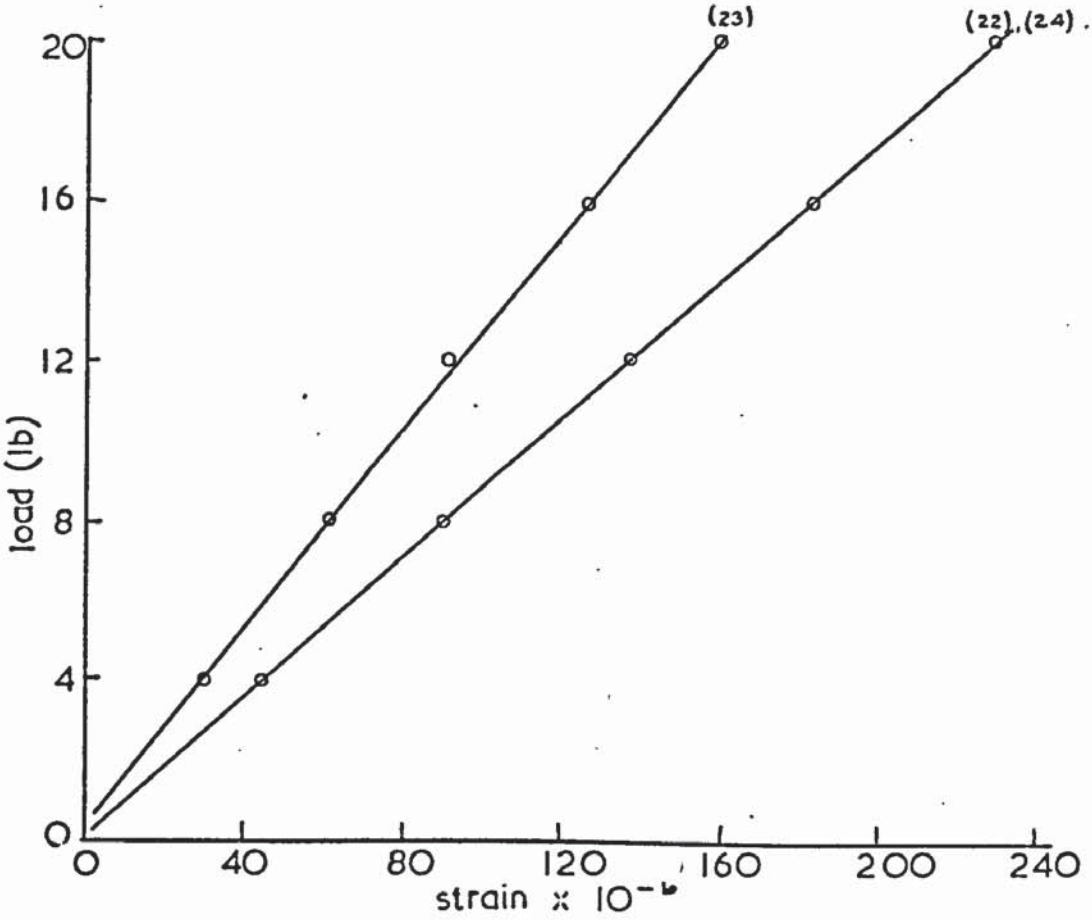

(c) storey no1 - additional electrical gauges

Fig. 7.7. (continued)

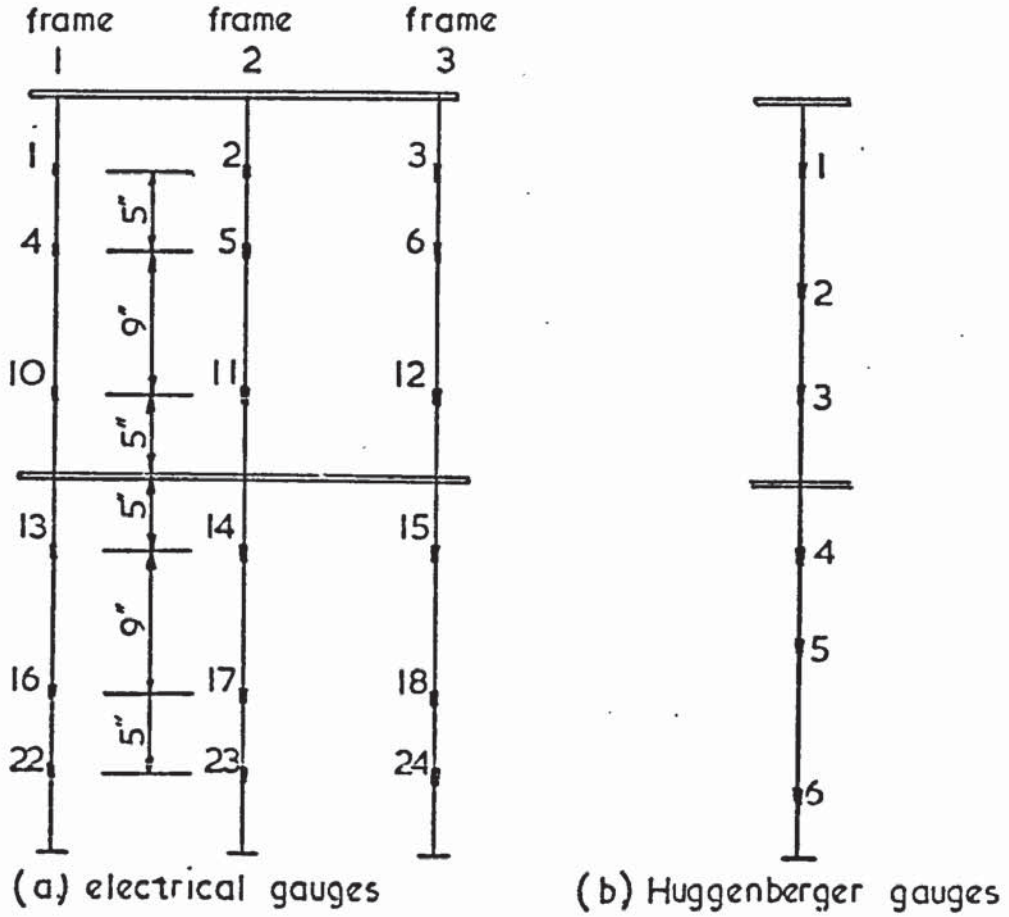

(a) electrical gauges

(b) Huggenberger gauges

Fig. 7.8 Position of gauges

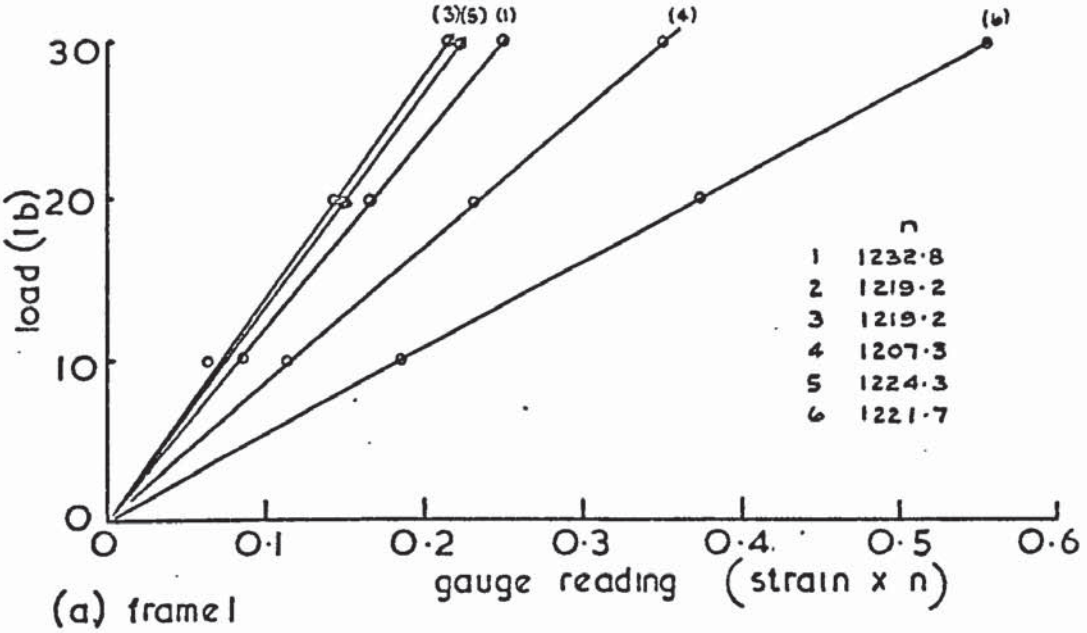

(a) frame 1

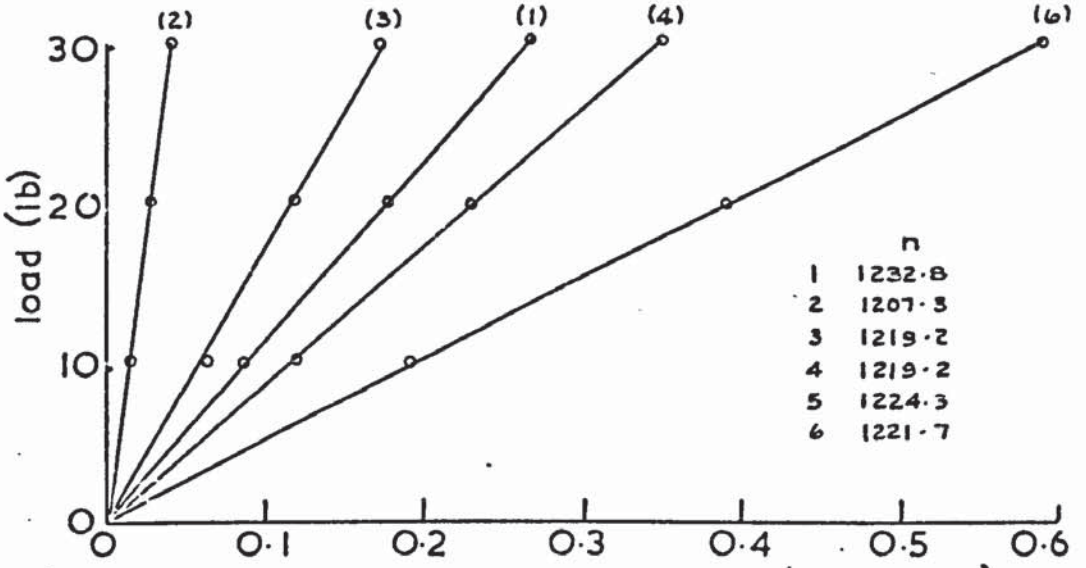

(b) frame 2

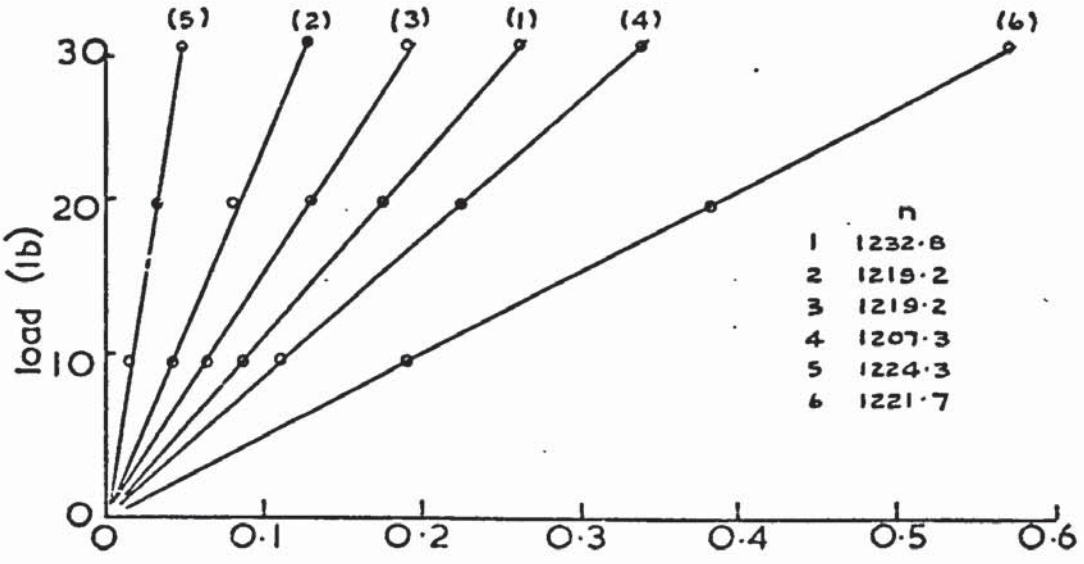

(c) frame 3

Fig 7.9 Load – strain graphs for bare frames (Huggenberger gauges)

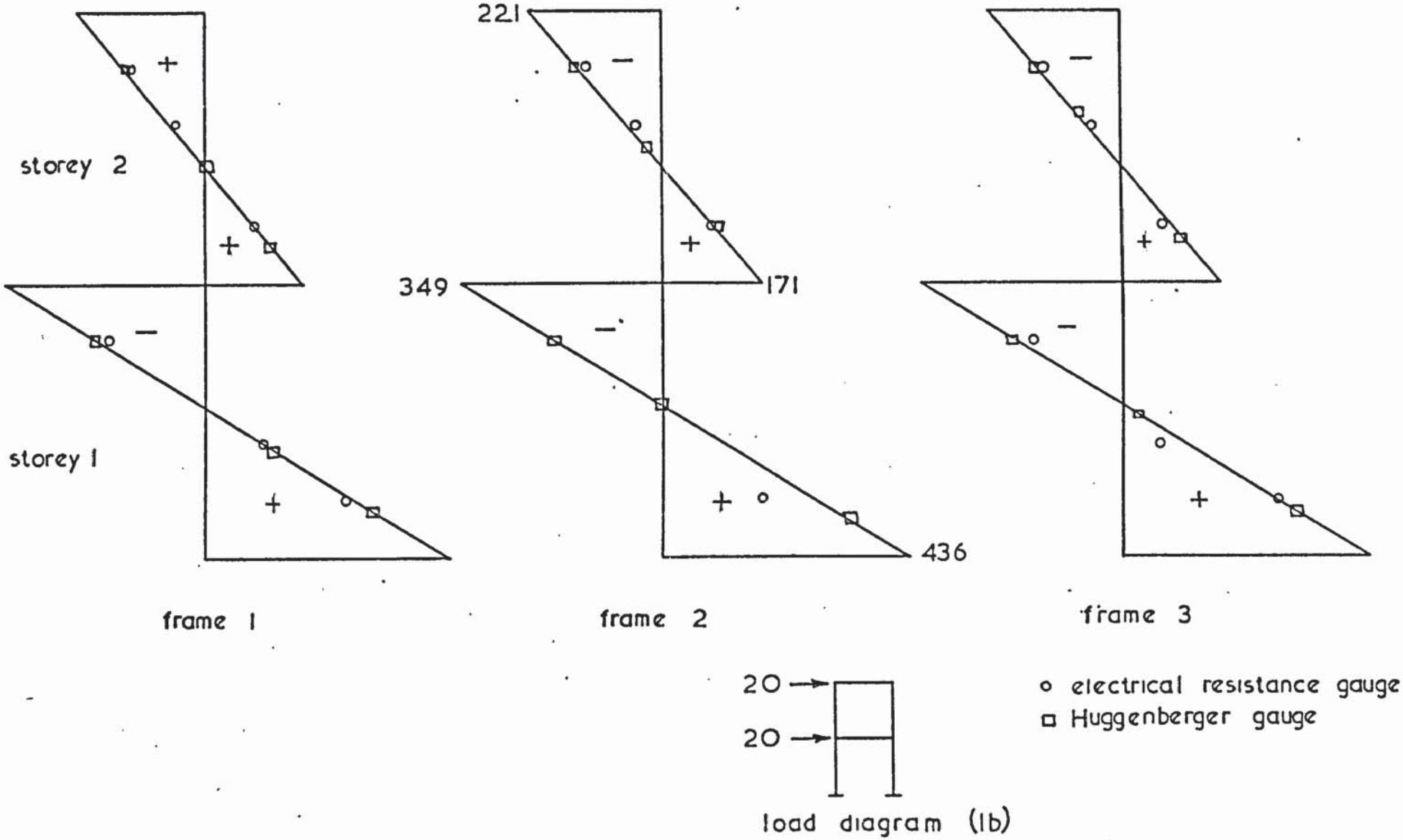

Fig. 7.10 Strains in columns of bare frames

electrical gauge readings, extremely close agreement exists between the experimental and computed results. In the subsequent test on the assembled model, the most unreliable of the electrical gauges were replaced by Huggenberger gauges.

The importance of providing a rigid base for the model was demonstrated in an earlier test on the bare frames. For this test the mounting beams shown in Fig. 7.1 were fixed to rigid supports at their ends only and not to a solid brick wall as illustrated. It was found that considerable variation from the computed results occurred, especially in the central frame.

7.3 Test on the assembled model

A test was carried out on the assembled model with maximum loads on the junctions of 20 lb. at the frames and 10 lb. at the walls. Detailed load-deflection and load-strain graphs for this test are given in Figs. 7.11 through 7.13. The strains at full load, obtained from these graphs, and the results obtained by the proposed computer methods of analysis are compared in Fig. 7.14, where the computed strains are again given in micro-strains at the ends of the columns. For the two outer frames, where the strains are recorded in the same positions, the average result is given. Both results are given when the gauges are in different positions, for example when one of the electrical gauges has been replaced by a Huggenberger gauge. It can be seen from the diagram that experimental and computed results are in good agreement. During the test slight buckling of the wall panels in the lower storey was noticed at the maximum load. Non-linearity in the graphs, was not apparent however.

The model was also analysed by a computer program[9], written for the analysis of general structures consisting of plates and prismatic

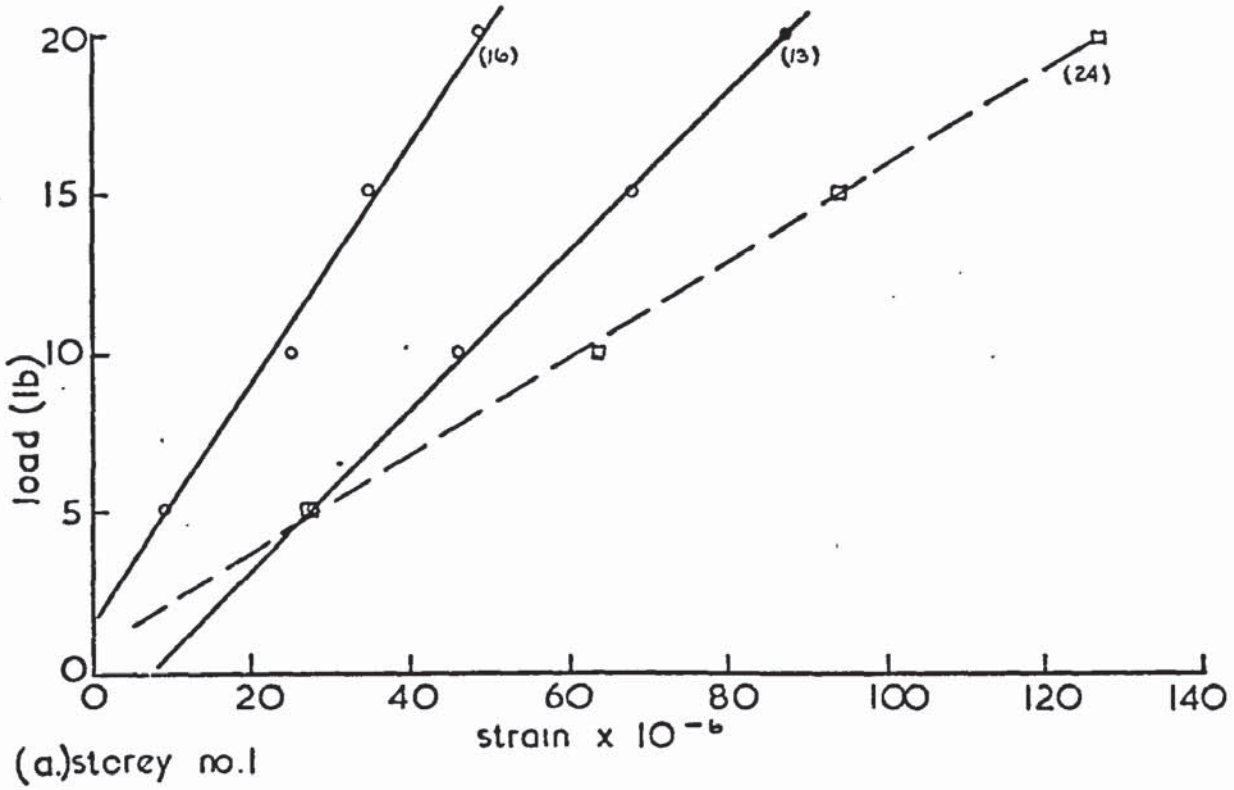

(a.)storey no.1

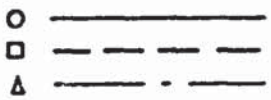

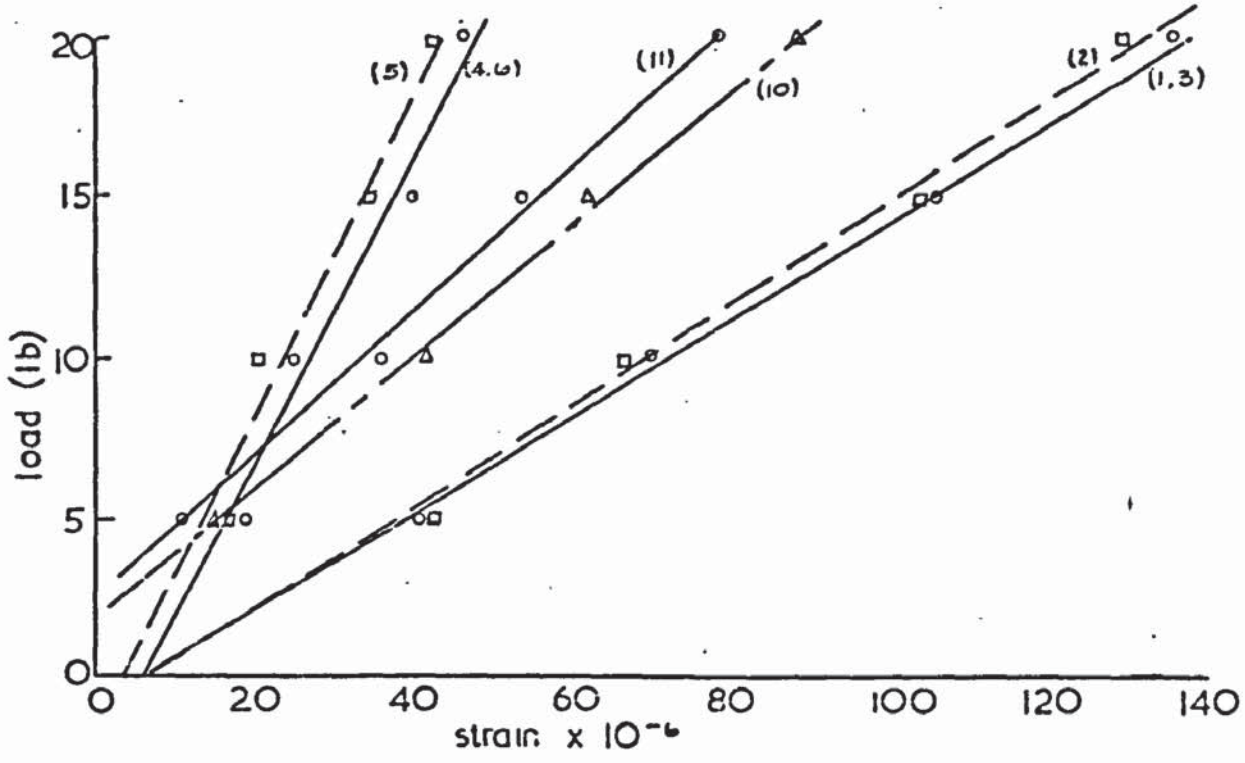

(b.) storey. no. 2

Fig. 7.11. Load - strain graphs for model (electrical gauges)

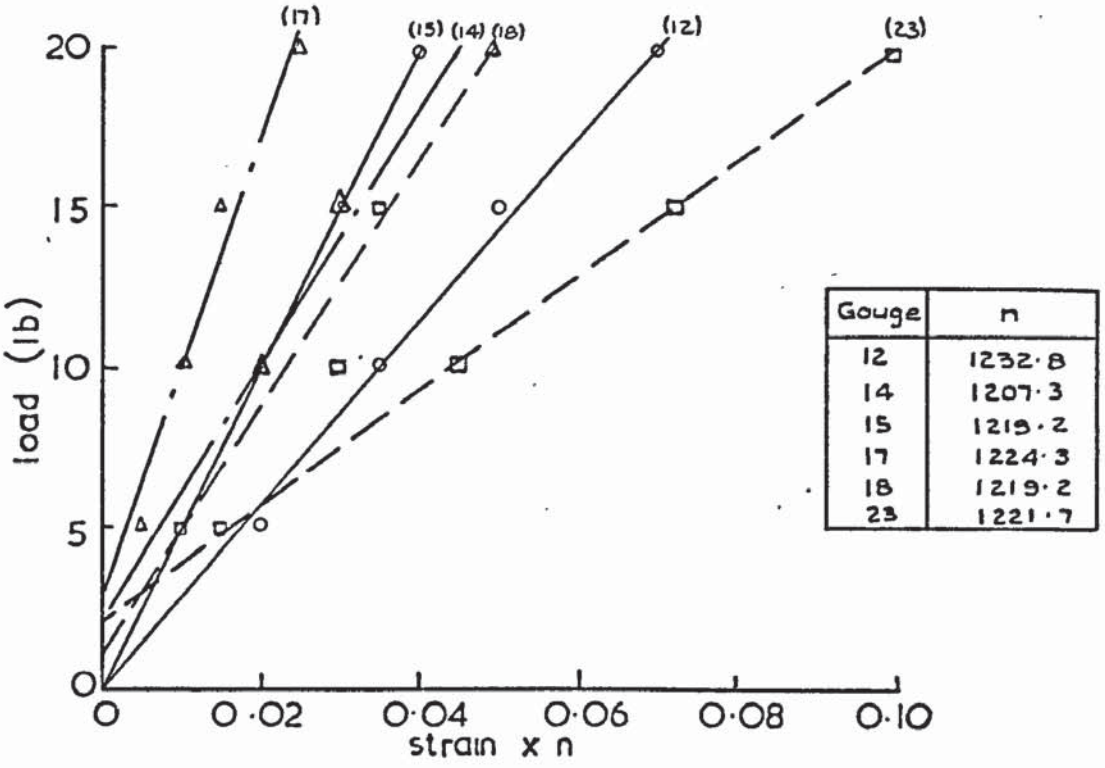

Fig. 7.12 Load - strain graphs for Huggenberger gauges on model

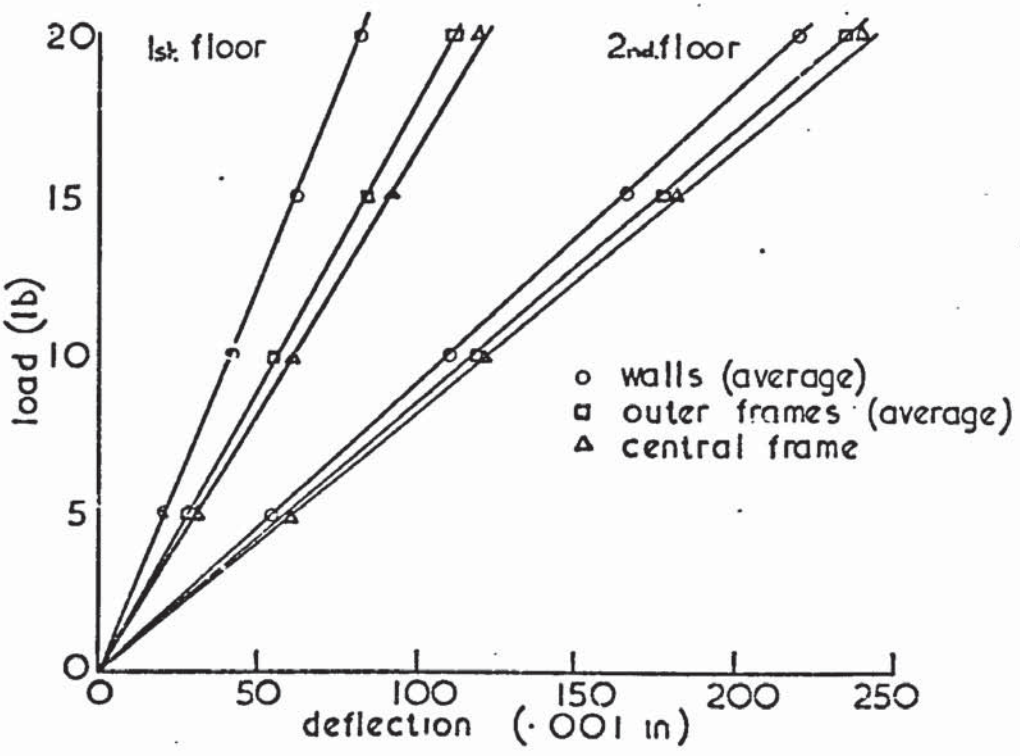

Fig. 7.13 Load deflection graphs for model

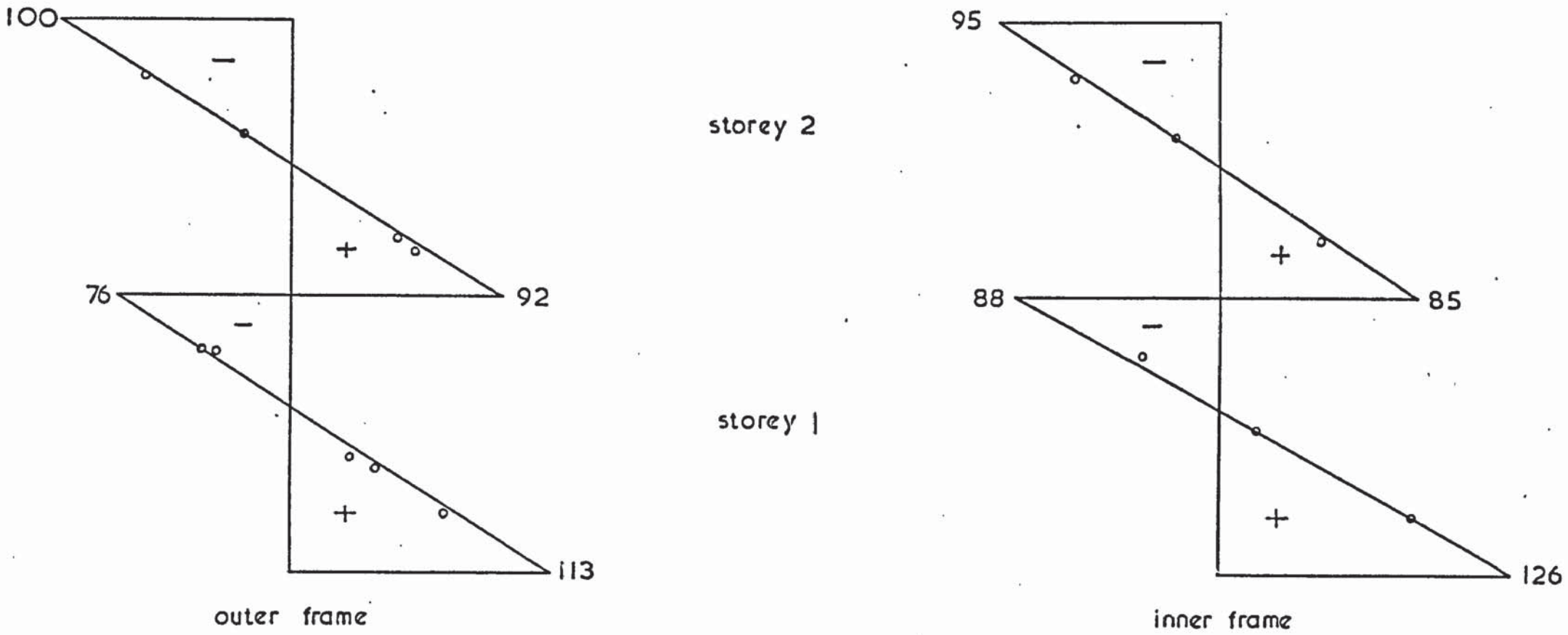

Fig. 7.14. Strains in columns of model frames

members. The panels of the walls and floor slabs were considered as thin plates under the action of both in-plane and out-of-plane forces. For this purpose they were each subdivided into 16 rectangular finite elements. The deflections obtained by this analysis are compared with those computed by the proposed methods and by experiment in Table 7.4. This shows that all the deflections are in good agreement and that the proposed methods give slightly better agreement with the experiment. The strains obtained by the finite element approach were also slightly less than those obtained by the proposed method but agreement in this case was within 2%.

The advantages of the method of influence coefficients over the finite element approach, with regard to data preparation and computer running time, can be demonstrated for this structure. In the finite element analysis two axes of symmetry were used, enabling the analysis to be carried out on a quarter of the structure, while in the method of influence coefficients symmetry was not considered. Nevertheless a comparison of the volume of data and the computer running time for the two analyses shows that, on the Chilton Atlas computer, the method of influence coefficients required a running time of 0.25 minutes and 210 characters of data, compared with 2.82 minutes and 1885 characters of data for the finite element method.

Floor	Position	DEFLECTIONS (.001 in)		
		Experiment	Proposed methods	Finite element
1	Wall	40.0	39.9	38.3
	Outer Frame	55.5	52.9	51.4
	Central Frame	60.0	58.1	56.6
2	Wall	110.0	109.7	106.0
	Outer Frame	118.0	116.0	113.2
	Central Frame	120.0	119.1	116.1

Table 7.4. Deflections of model

CHAPTER 8

AN INVESTIGATION INTO THE BEHAVIOUR OF COMPLETE STRUCTURES

8.1 Introduction

The only method in which the effects of in-plane bending in the floors of a large structure are reported, is that due to Goldberg who showed that the distribution of the lateral shear forces carried by the frames in two symmetrical structures was influenced in part by these effects. Goldberg's conclusions however are mainly concerned with the relative importance of shear and flexural deformations in the walls and slabs, and no comparative results are quoted in which the slabs are considered to act as rigid diaphragms.

Using the computer programs described in Chapter 6, an investigation was carried out to examine more fully the effects of in-plane bending of the floor slabs on the deflections and member forces in the components of three complete structures. In each analysis the significance of including the axial deformations of the columns of the frames was also studied.

The investigation was extended to consider the effects of the sidesways produced by eccentrically imposed vertical loads on the distribution of lateral forces. The effects of local irregularities, such as a discontinuity in a floor slab, were also examined.

Goldberg's two structures were selected as the basis for these investigations. The 10 storey structure has already been described in Chapter 4 (Fig. 4.6). The 20 storey structure, which is very similar in general arrangement, is shown in Fig. 8.1. Again the cross sectional areas of the columns, which were not specified by Goldberg, have been taken from the nearest equivalent British sections.

The walls and floors of the building are of reinforced concrete for which Young's modulus is 3×10^6 lb/in^2 and Poisson's ratio is 0.1. Wind

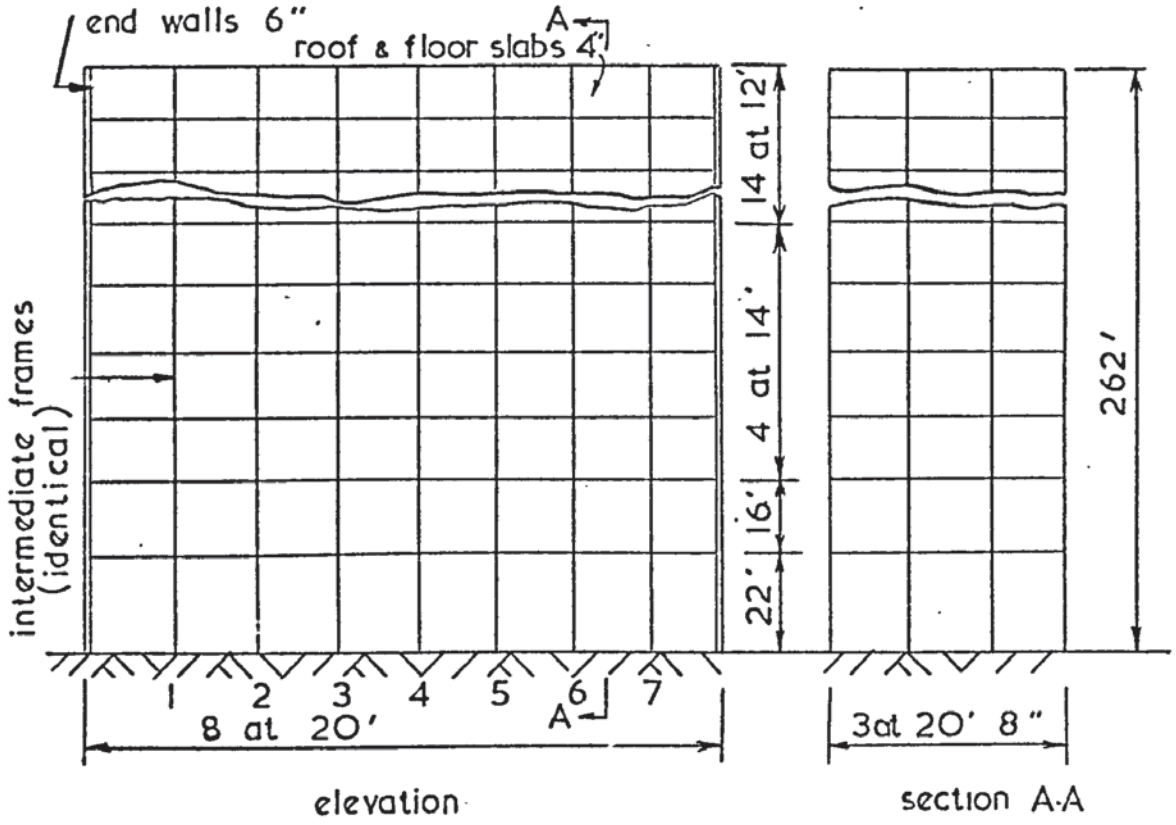

Storey	Beams I (in^4)	Outer Columns		Inner Columns	
		I (in^4)	A (in^2)	I (in^4)	I (in^2)
20	2025	1981	56	1896	56
19	2025	1981	56	1896	56
18	2025	1981	56	1896	56
17	2025	1981	56	1896	56
16	2025	2055	57	2106	57
15	2025	2055	57	2106	57
14	2025	2634	67	2684	67
13	2025	2634	67	2684	67
12	2025	2707	67	2866	67
11	2025	2707	67	2866	67
10	2025	3036	77	3758	77
9	2025	3036	77	3758	77
8	2025	4132	92	4325	92
7	3387	4132	92	4325	92
6	3717	4926	109	5106	109
5	5161	4926	109	5106	109
4	5321	5946	125	5946	125
3	5641	5946	125	5946	125
2	5862	6816	125	6816	125
1	8058	6816	125	6816	125

TABLE OF SECTION PROPERTIES

Fig. 8.1 Goldberg's 20 storey structure

loads are equivalent to a uniform pressure of 15 lb/ft^2. For comparison of the sectional properties of the two frames, the second moments of area of the members are plotted horizontally to scale in Fig. 8.2. From these diagrams it is seen that the beams of the 10 storey structure are of uniform section, while the columns are tapered, changing in section at each storey. In the 20 storey frames the column sections change at approximately every two storeys, while the sections of the beams, which are uniform for the top 14 storeys, are increased irregularly below this level. Notably the stiffness of the 10 storey frames is less than that of the top 10 storeys of the 20 storey frames.

The behaviour of a hypothetical 10 storey reinforced concrete building structure was also studied. This structure, which is shown in Fig. 8.3, was chosen as an extreme case with the walls and frames arranged asymmetrically in plan, and the columns of the frames also arranged asymmetrically. Young's modulus and Poisson's ratio for the concrete were taken to be 28 x 10^6 kN/m^2 and 0.15 respectively. Wind loads equivalent to a uniform pressure of 1 kN/m^2 were assumed to act on the long face of the building in the direction shown. These loads are tabulated in Appendix 1, together with the loads acting on the 20 storey structure of Goldberg. The derivation of the loads is also given in the appendix.

8.2 The effects of bending of the floor slabs in their own plane

In this part of the investigation the three structures were analysed under the action of a uniformly distributed wind load. The effect of treating the floor slabs as rigid diaphragms was obtained by increasing the thickness of the slabs by a factor of 1000. The effects of increasing the overall length of the structure, were also examined in the case of Goldberg's 10 storey structure.

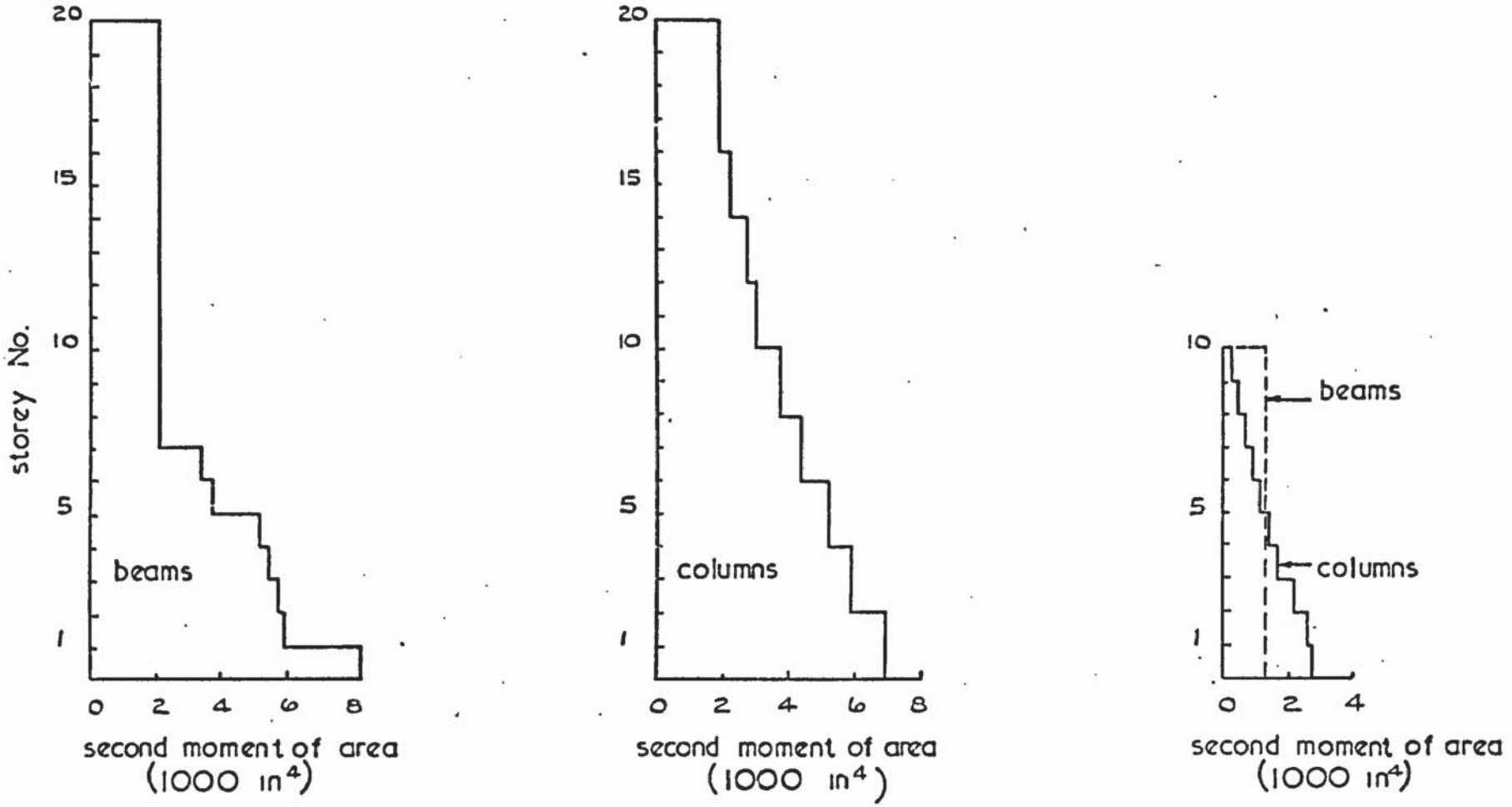

(a) 20 storey structure

(b) 10 storey structure

Fig 8.2 Section properties of Goldberg's frames

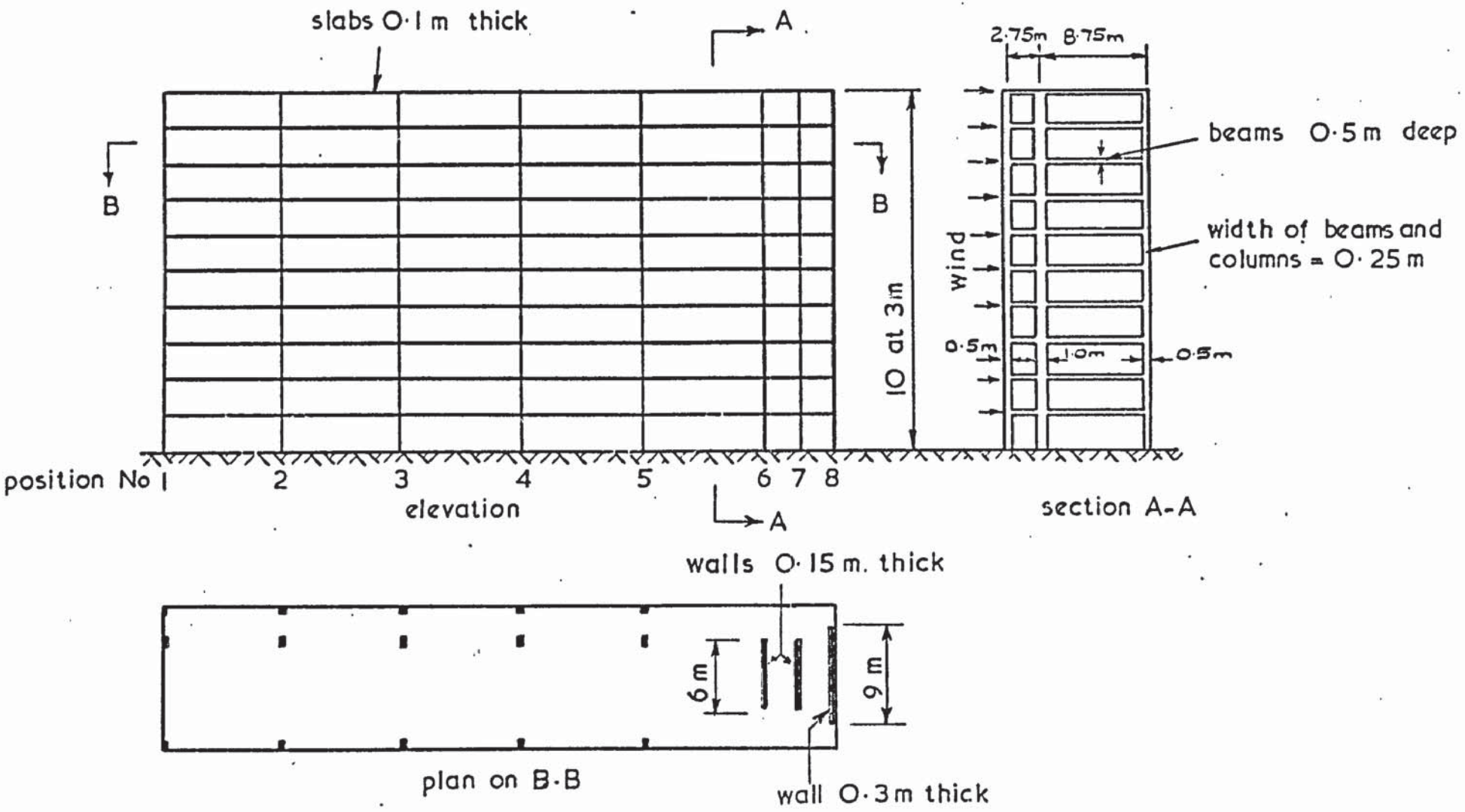

Fig. 8.3 10 storey asymmetrical structure

8.2.1 Goldberg's structures

Diagrams showing the lateral shear forces in the walls and frames of Goldberg's 10 and 20 storey structures are given in Figs. 8.4 and 8.5 respectively. In these structures, which are symmetrical and contain identical frames, the loads carried by the frames at any particular floor level would be equal if the floor slabs behaved as rigid diaphragms. The difference between the lateral shear forces in the central and outer frames can therefore be used as an indicator of the effect of in-plane bending of the floor slabs. These forces are shown by graphs A and B respectively in the figures. The effect of treating the slabs as rigid diaphragms is indicated by graph C.

It is of interest firstly to compare the shapes of the shear force diagrams for the two structures. In the 20 storey structure the shear force in the frames is approximately uniform throughout their height. This is the condition produced by a single concentrated lateral force applied at the top of the frame, as assumed by Rosman[19] in his approximate method of analysis, leading to a negative shear force at the top of the walls. In the uniformly tapered frames of the 10 storey structure however, the shear force at the top of the frames is small and no negative shear occurs in the walls. Also in contrast with the 20 storey structure, there is a sudden large increase in shear force in the bottom storey.

In both structures the bending of the floor slabs causes an increase in shear at the base of the central frame, and a reduction in shear at the top. At intermediate storey levels, small, irregular variations in shear occur between the central and outer frames of the 20 storey structure, but in the 10 storey structure the effect is negligible.

The diagrams show that the effect of rigid diaphragm action in the slabs is to produce errors which are in the same sense for all the frames

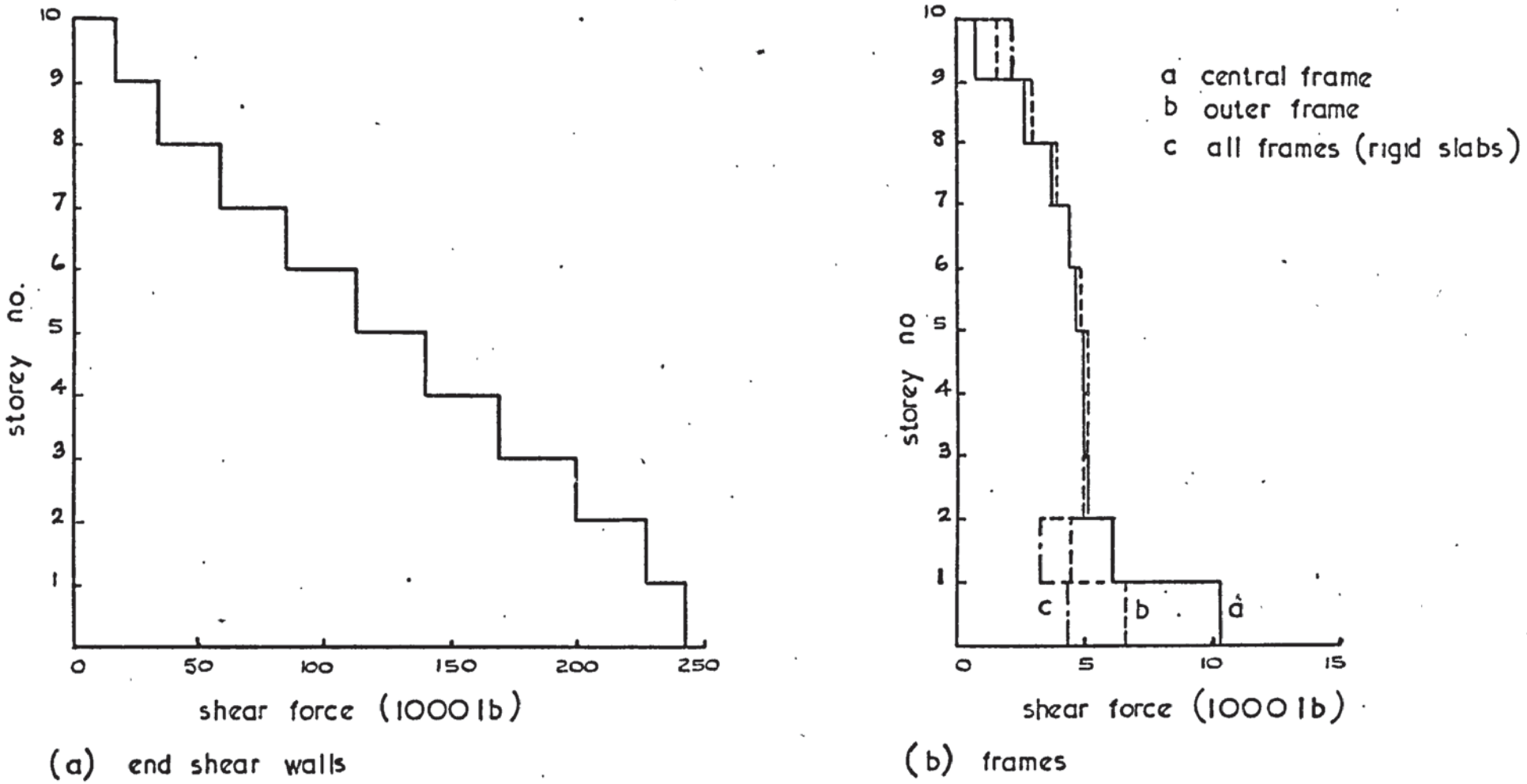

Fig. 8.4 Effect of slab bending on shear froce distribution in Goldberg's 10 storey structure

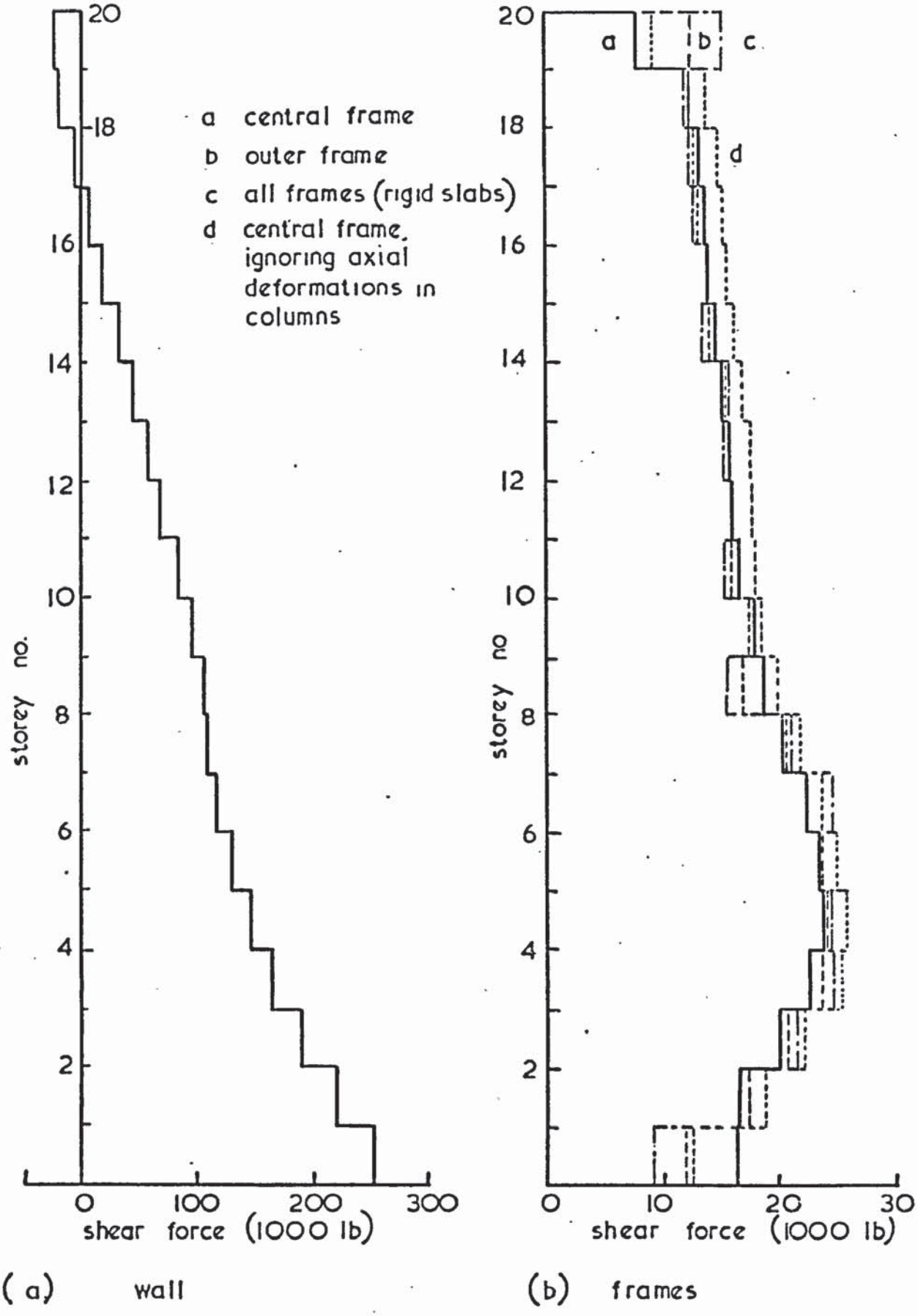

Fig 8.5. Distribution of shear force in Goldberg's 20 storey structure

at any particular level. This result is unexpected, since it would have been reasonable to assume that the shear forces obtained for rigid slabs would lie between those for the central and outer frames. For the central frame in particular, the differences between the results obtained by assuming slab bending on the one hand, and rigid diaphragm action on the other, are therefore greater than might have been expected from intuitive reasoning.

The shear force diagrams for the walls show that in both structures the majority of the wind load is carried by the walls. In the 10 storey structure the walls carry approximately 7 times the total load carried by all the frames, while in the larger structure the factor is approximately 5.

From the point of view of the designer, more useful data for comparison are the bending moments and axial forces in the individual members of the frames. On examination of the bending moments at a number of points in the frames, it was found that similar patterns evolved. In the remainder of this thesis the bending moments at the lower ends of the inner columns are used as indicators of the general trend. It may be assumed therefore that any subsequent, unspecified reference to bending moments relates to these points.

Bending moments in Goldberg's 10 storey frames are shown by graphs A, B and C on the left hand side of Fig. 8.6, from which it is evident that the differences due to bending of the slabs are again significant only at the bases of the frames. When the slabs are treated as rigid diaphragms, the general effect on the bending moments is similar to that on the shear forces. At the base of the central frame for example, the bending moment is less than half the value obtained when the bending of the slabs is taken into account.

Similar results were obtained for the 20 storey structure and these are plotted in Fig. 8.7. Here the increase in stiffness of the lower part of the frame is reflected in the graph of bending moments. It is also noticed

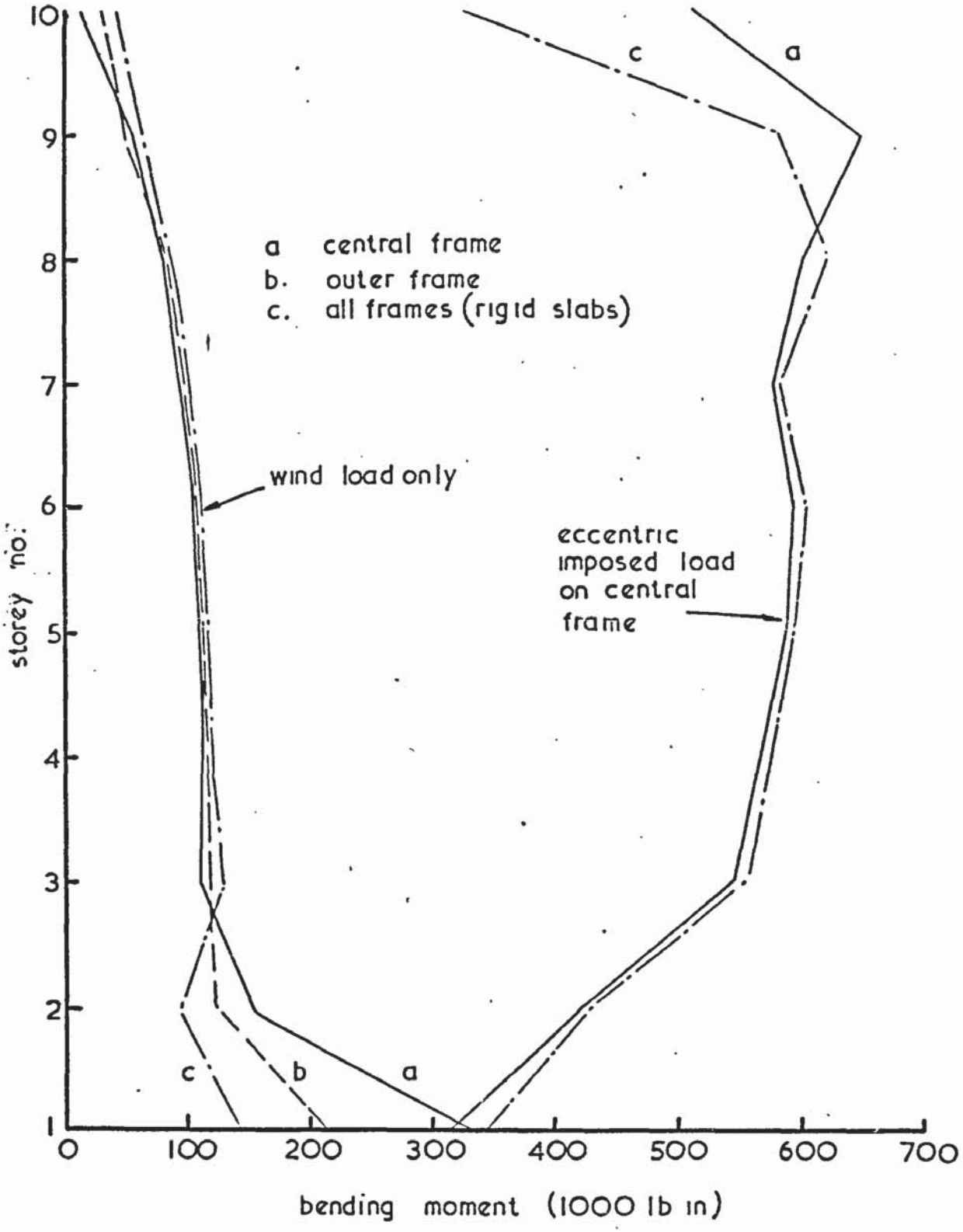

Fig 8.6. Bending moments in inner columns of Goldbergs 10 storey frames

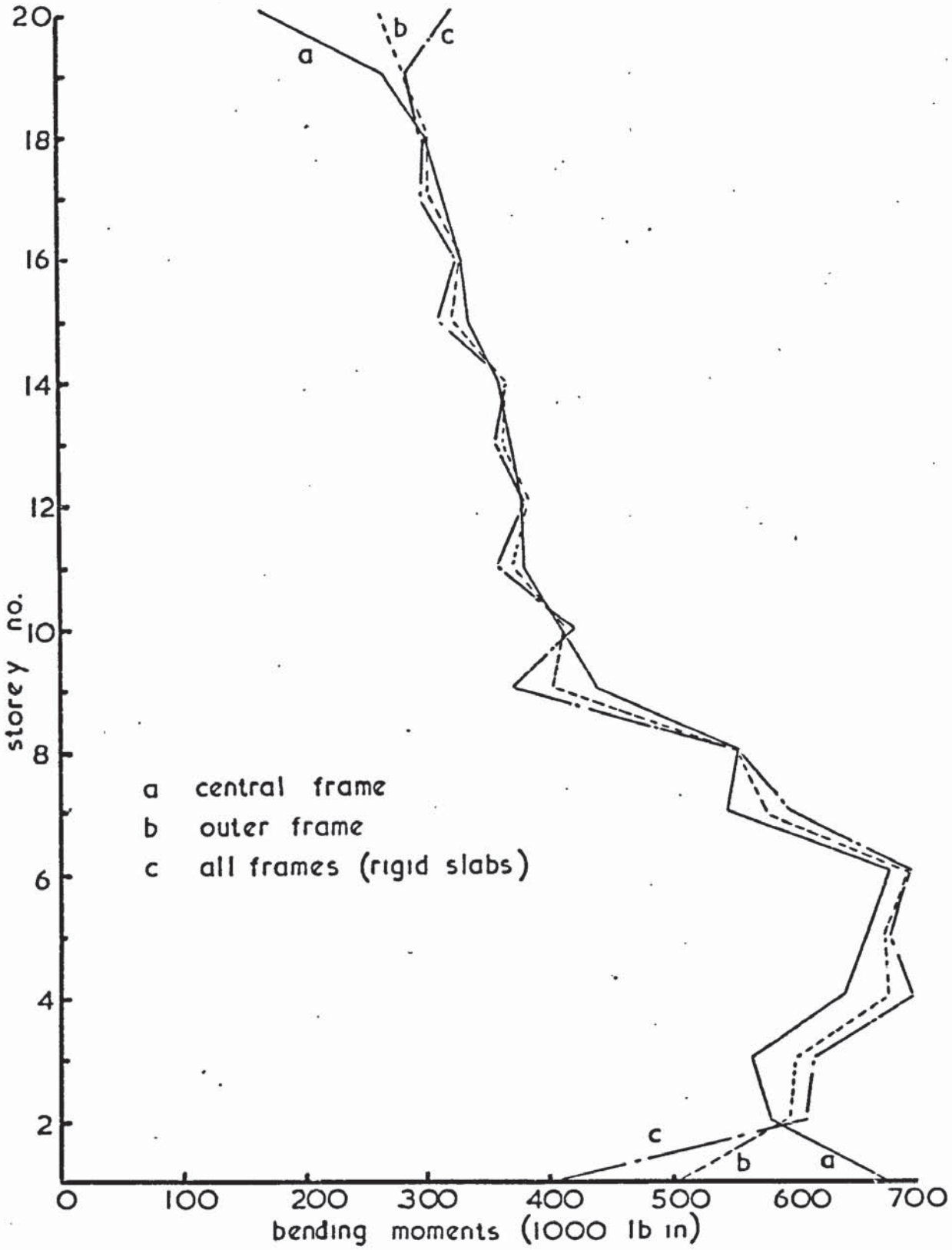

Fig. 8.7 Bending moments in central columns of Goldberg's 20 storey frames

that in the intermediate storeys of this structure, the assumption of rigid floor slabs leads to errors of up to 15% in either sense. These errors occur in the regions where the sectional properties of the members change. At the tops of the frames, the bending moments are over-estimated by amounts varying from 90% in the central frame to 23% in the outer frame.

8.2.2. The effect of variations in wall stiffness

Using Goldberg's 10 storey structure, subject to the same wind loads, the effect of changes in the relative stiffness of the walls and frames was examined by varying the thickness of the walls from 1 in. to 15 in. Fig. 8.8(a) shows the deflections at the top of the structure in the central frame (graph A) and in the outer frame (graph B) for different values of wall thickness. Curves of similar shape were obtained for the bending moments in the frames. Fig. 8.8(b) shows, for example, the bending moments in the top and bottom storeys of the central and outer frames (Graphs A and B). The effect of rigid diaphragm action in the floor slabs is shown by graph C.

The increasing difference in the deflections of the central and outer frames indicates that the bending of the slabs increases as the stiffness of the walls is increased. This is due to the increased loading of the floor slabs as a greater portion of the wind load is carried by the walls. The increase in bending of the slabs probably accounts also for the fact that the difference between the three graphs of bending moment remains approximately constant, in spite of the reduced loading of the frames.

The shape of the curves of bending moment shows that as the stiffness of the walls is increased, they become progressively less effective in reducing the loading of the frames. This suggests that for a given arrangement of walls and frames an optimum value of their relative stiffness could be found.

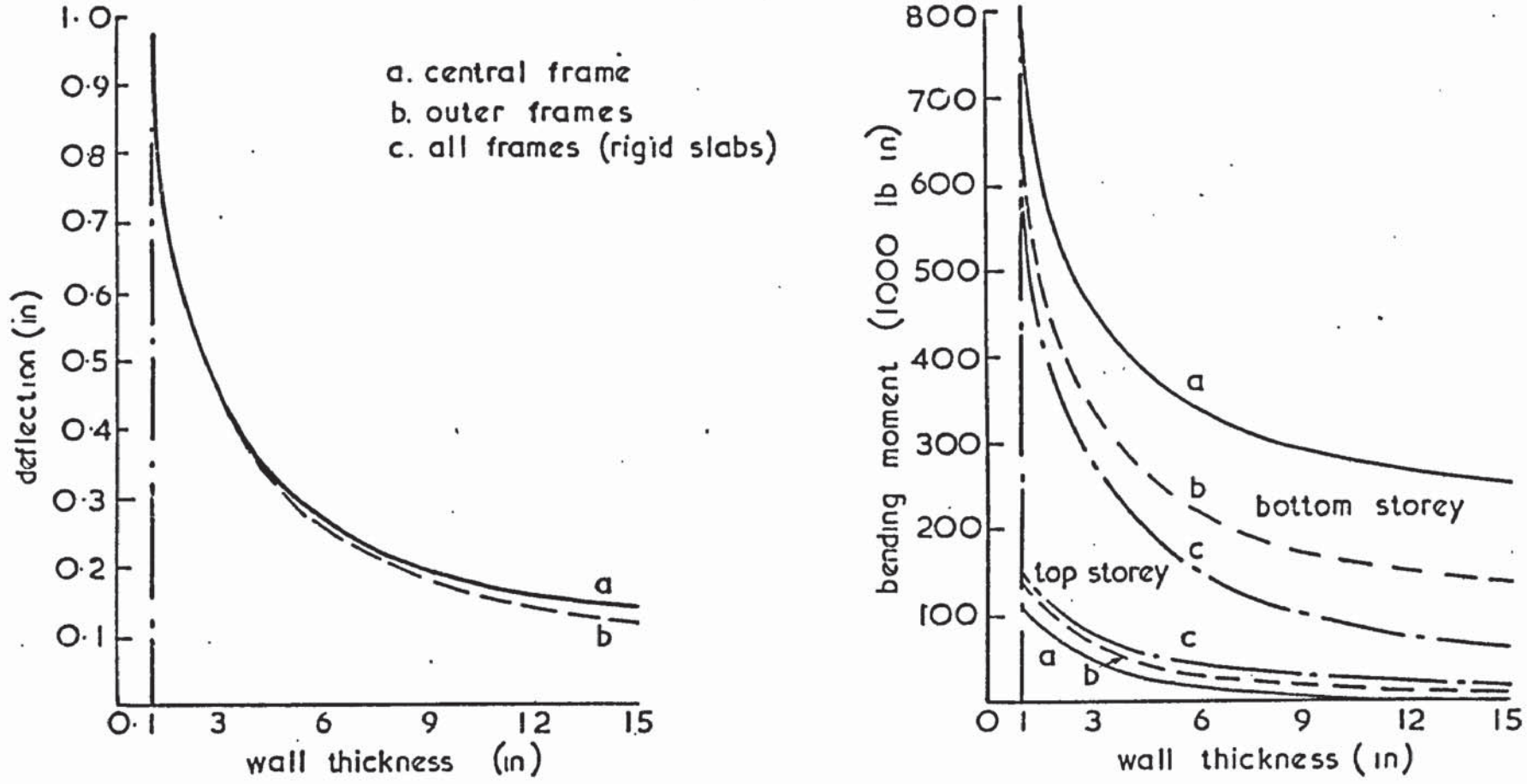

(a) deflection at top of structure

(b) bending moment at lower end of central columns

Fig. 8.8 Effect of variations in wall stiffness

8.2.3 The effect of variations in the number of intermediate frames

Using the same structure a further investigation was carried out in which the proportions of the load carried by the grillage and the frames was varied by changing the overall length of the structure and the number of intermediate frames. The distances between the frames, and hence the wind loads at the junctions were kept at their original values. Fig. 8.9(a) shows the variation in deflection at roof level for the central frame and the end walls. As the number of intermediate frames is increased, the deflections of the structure increase generally and the effects of bending of the floor slabs become more significant as shown by the divergence of graphs A and D. The deflections of the end walls are seen to be almost coincident with the deflections obtained when rigid floor slabs are assumed.

The effects of bending of the floor slabs are also shown in Fig. 8.9(b) where the bending moments in the frames are plotted against the number of intermediate frames. As this is increased, the loading increases, as shown by the general slope of the graphs. The effects of slab bending become more significant as the central frame becomes more remote from the end walls, and is most marked at the bottom and top of this frame. In the bottom storey the effect is significant even when there are only 3 intermediate frames. On the other hand, it is negligible in the intermediate storeys, as shown by storey number 4 in the figure, even when the number of frames is increased to 9.

8.2.4 The asymmetrical structure

For the asymmetrical structure the deflections and rotations of the floor slabs are given in Fig. 8.10 where it is seen that the greatest deflections occur at the unsupported frame in position 1. Treatment of the slabs as rigid diaphragms was found to make practically no difference at all to the deflections in this structure.

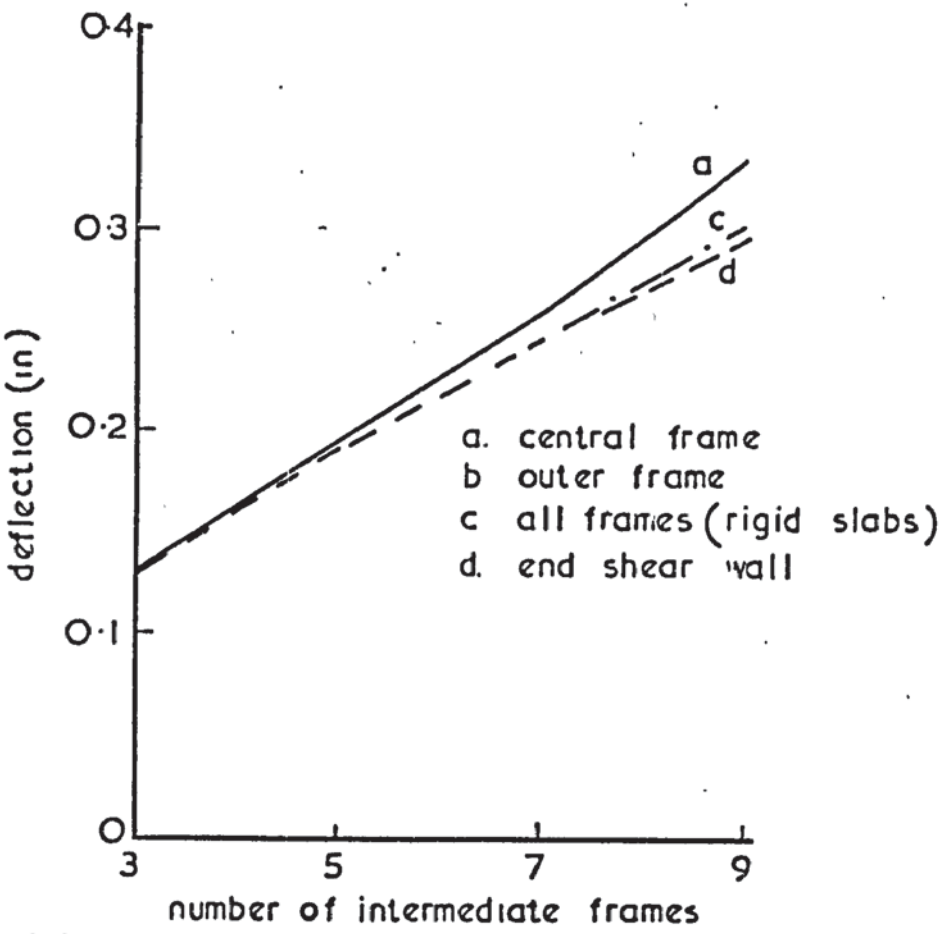

(a) Deflection at top of structure

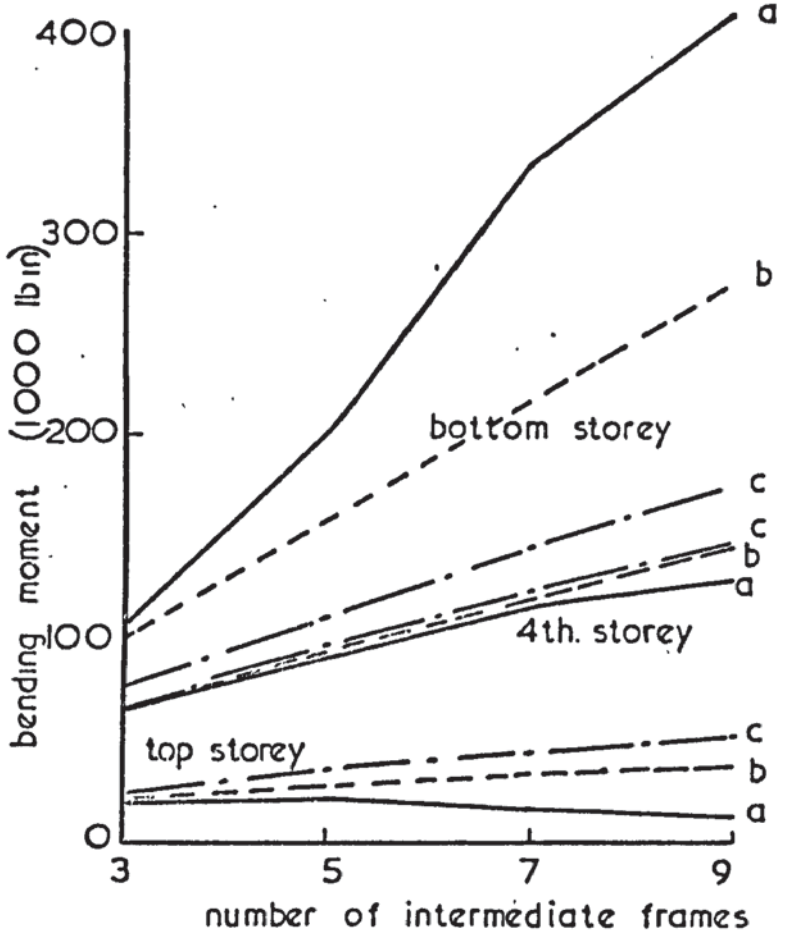

(b) bending moment in central columns

Fig 8.9 Variations in deflection and bending moment with number of intermediate frames

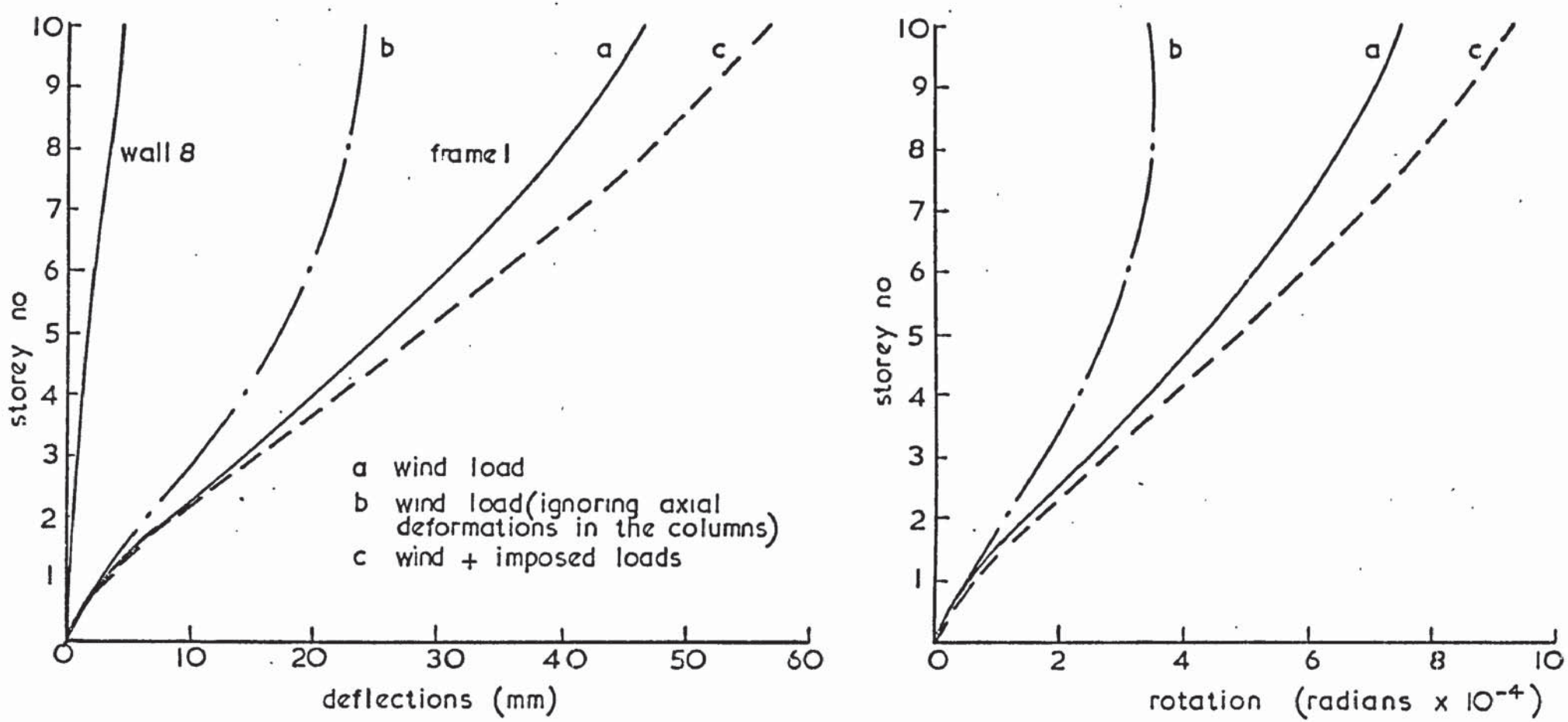

(a) deflection at each end of the structure

(b) rotation at floor slabs

Fig 8.10 Deflections and rotations of floor slabs in an asymmetrical structure

The distributions of shear forces in typical walls and frames are plotted in Fig. 8.11, from which a comparison of graphs A and B shows that the effect of treating the slabs as rigid diaphragms is negligible in the frames and of only slightly greater significance in the walls. From Fig. 8.12(a) it is seen that the shear forces in the frames have an approximately linear relationship to one another. It is also noticed that the total loads carried by the frames and the walls are of the same order. The frame in position 1 actually carries a total load in excess of the total wind load acting on the structure at this position, indicating that a negative load acts on the slabs. The portion of the wind load acting at the other frame junctions is also small in comparison with Goldberg's structure, which probably accounts for the relative insignificance of the effects of slab bending in this structure.

8.3 The effects of torsion in the walls and slabs

In an asymmetrical structure the rotation of the floor slabs induces torsion in the walls. Also, since the deflected shape of the bracing components varies from one end of the structure to the other, torsion of the floor slabs about their longitudinal axes takes place. In the 10 storey asymmetrical structure, which is an extreme case, the torques in the walls were found to be insignificant, amounting to a maximum of 1/10,000 of the bending moment or the base of the walls, thus confirming the findings of previous workers[11,23]. Torques in the slabs between the walls were of the same order.

Torsion can also be induced in the walls and slabs of a symmetrical structure if the floor slabs bend appreciably in their own plane. In Goldberg's structures the torques in the walls were found to be insignificant, producing a maximum torsional shear stress of only 2 lb/in^2.

Since torsional equilibrium at the frame junctions is not considered in the methods of analysis described in this thesis, torsion can only be

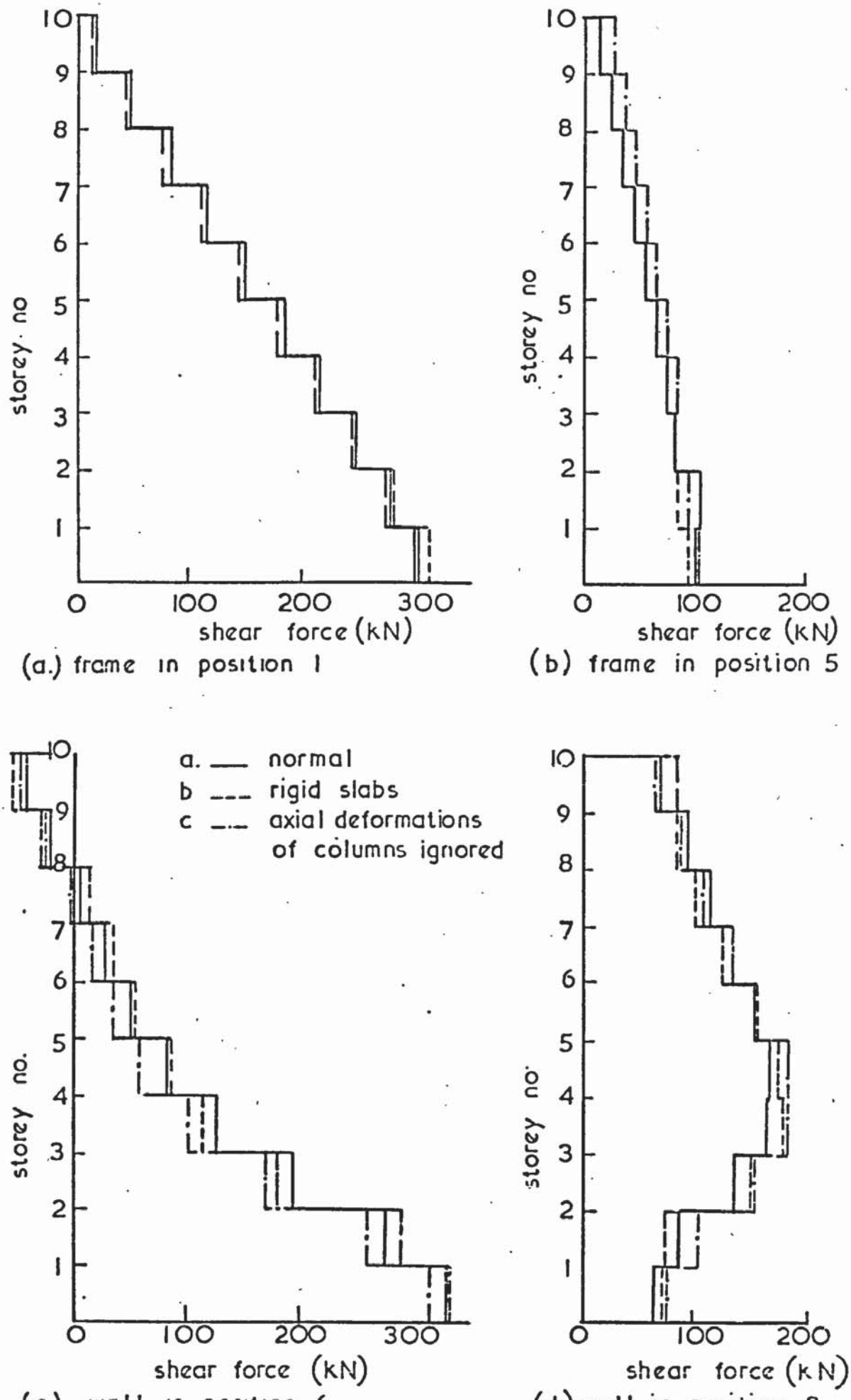

Fig. 8.11. Effect of axial deformations and slab bending on the distribution of shear force in an asymmetrical structure.

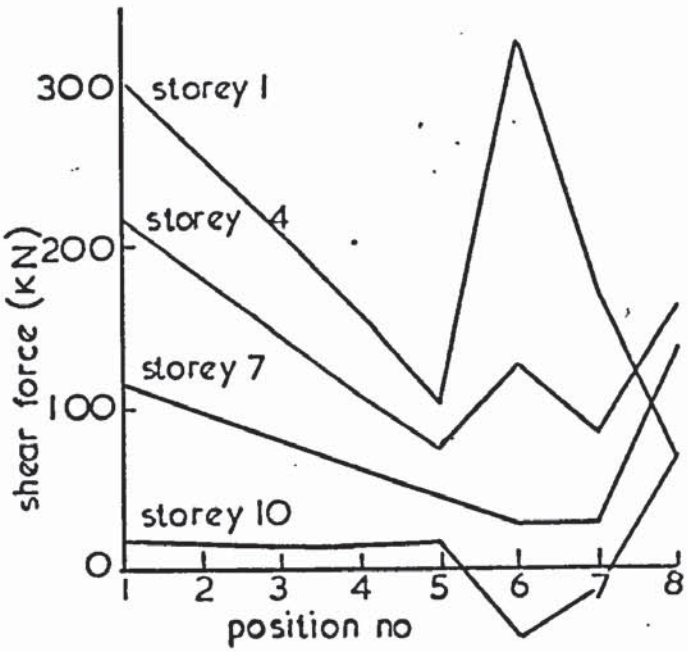

(a.) distribution of shear force across the structure (wind load only)

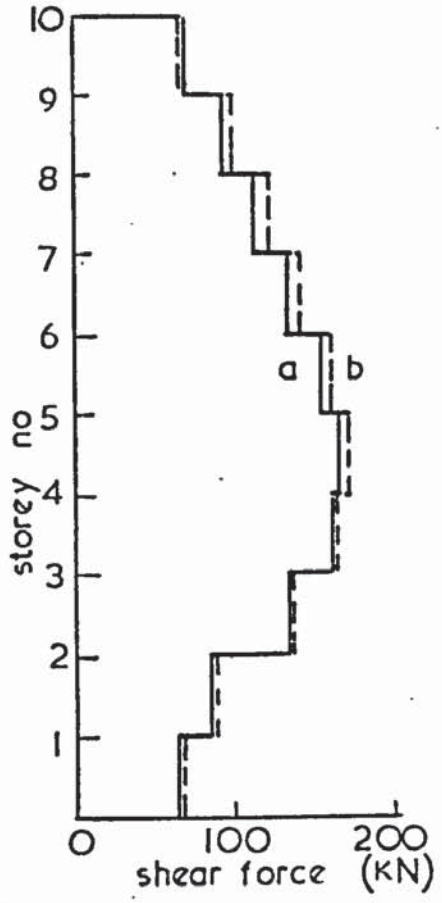

(d.) wall in position 8

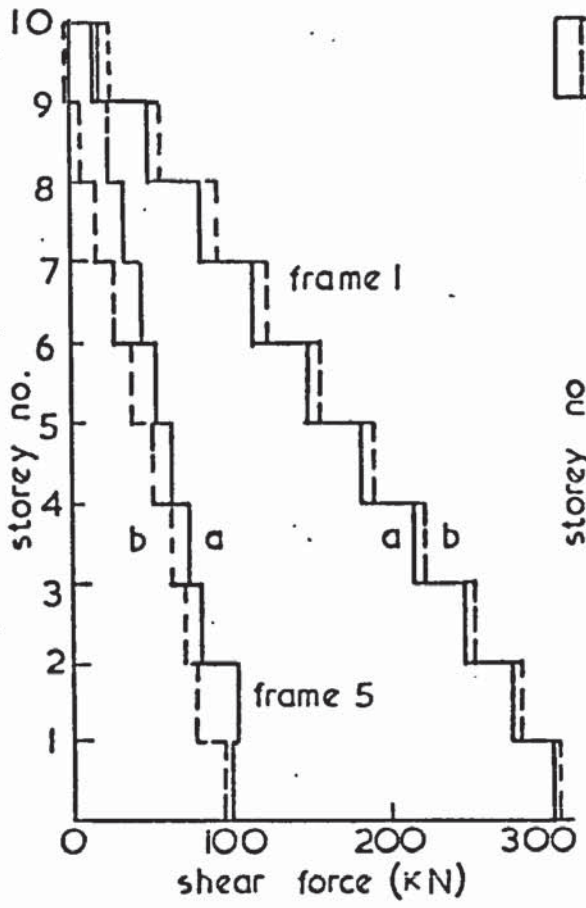

(b) frames in positions 1 & 5

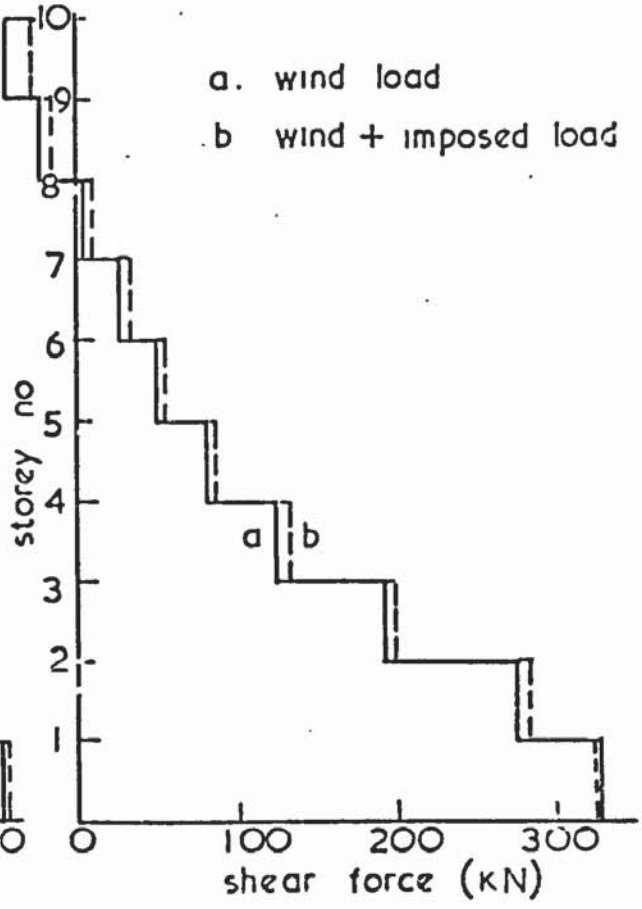

(c) wall in position 6

a. wind load
b wind + imposed load

Fig. 8.12. Distribution of shear force in an asymmetrical structure subject to wind and imposed vertical loading

induced in a slab spanning between a wall and a frame by setting the torsional rotation of the slab to zero at the frame junction. This condition, which is probably more severe than that existing in practice was tested in Goldberg's 10 storey structure for the slabs connected to the end walls. Here it was found that the maximum torque in the slabs was only 1/100,000 of the bending moment at the base of the walls. It is evident therefore that, even allowing for a possible increase in torsional stiffness resulting from the warping restraint of the wall-slab junctions, it is most unlikely that the cummulative effect of the torques in the slabs, on the bending moment at the base of the walls, could ever be significant in this type of structure.

8.4 The effects of axial deformations

The effects of neglecting axial deformation in the columns of frames have already been discussed in Chapter 1, with reference to the published literature. In this chapter the effects are examined for each of the three structures analysed. Two approaches were adopted in the analyses. Firstly the cross sectional areas of the columns were increased by a factor of 1,000, and secondly the vertical displacements of all the joints in the frames were set to zero. The first method, which has been found to lead to ill-conditioned load-displacement equations[10], was included to test the sensitivity of the elimination subroutine CDM. No evidence of ill-conditioning was revealed however in these analyses.

Axial deformations in Goldberg's 10 storey frames have been shown in Chapter 4 to have negligible effect either on the deflections or on the distribution of shear forces. For the 20 storey structure the deflections at roof level are given in table 8.1, from which it is evident that here also the effect of axial deformations is negligible, although of greater significance than the assumption of rigid diaphragms.

	DEFLECTION (in)				
	Wall	Frame 1	Frame 2	Frame 3	Frame 4
Axial deformations included	1.09	1.09	1.08	1.08	1.08
Axial deformations excluded	1.00	0.99	0.98	0.98	0.98
Rigid slabs	1.08	1.08	1.08	1.08	1.08

Table 8.1 Deflections at top of Goldberg's 20 storey structure

On the other hand, a comparison of graphs A and D in Fig. 8.5 shows that the shear forces in the frames are over-estimated by approximately 10% in all storeys by suppressing the axial deformations in the columns. This figure may be compared with Goldberg's prediction of 8%.

It was found that in general, the effects on the forces in individual members proved to be more significant than was apparent from a consideration of the shear force diagrams for the frames. For example, the axial forces in the outer columns may be seen from Fig. 8.13 to be over-estimated by amounts varying from 20% at the base of the frames to zero at the top. In the inner columns, the axial forces are under-estimated by a proportionally greater amount, although in this case the absolute values of the forces are small. Fig. 8.14 shows that the bending moments at the ends of the beams are over-estimated by approximately 20% in the outer bays and under-estimated by 10% in the inner bay. These errors are approximately constant throughout the height of the frame.

A different pattern of results was obtained for the asymmetrical structure, where it was found that the deflection at the top of the frame

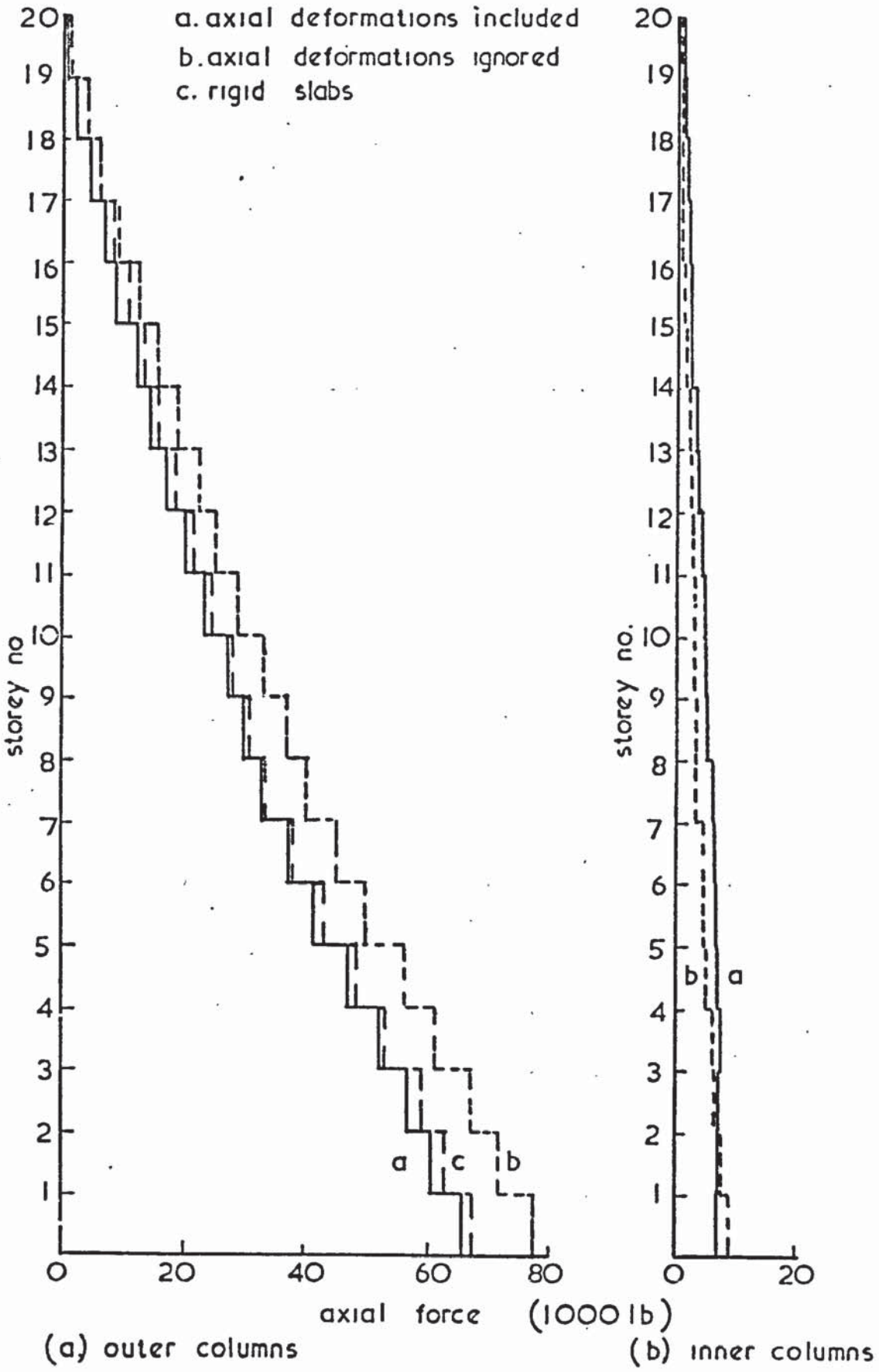

Fig. 8.13. Axial forces in columns of Goldberg's 20 storey frames.

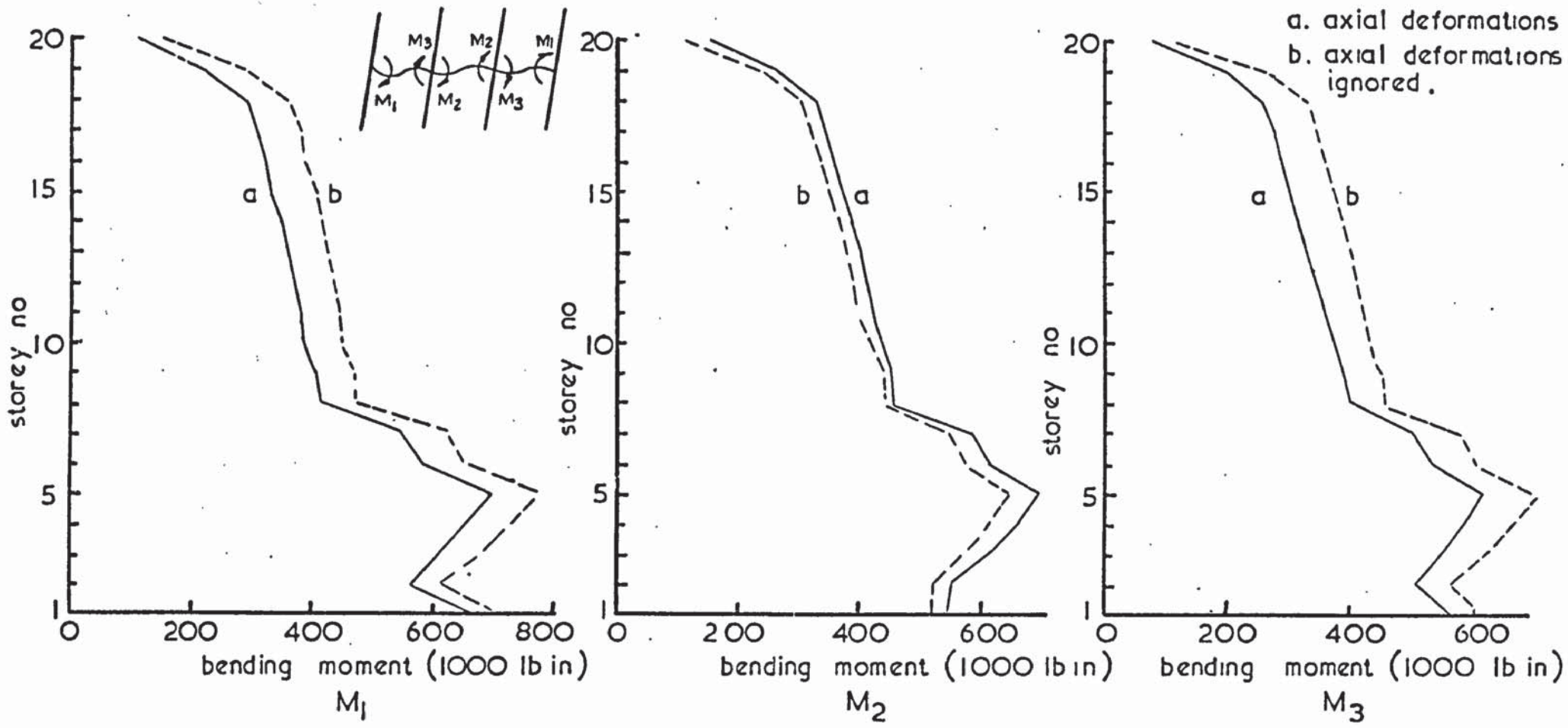

Fig. 8.14 Bending moments in beams of Goldberg's 20 storey frames

in position 1 was under-estimated by approximately 50% when axial deformations were suppressed. This result is shown by graph B in Fig. 8.10, where the effect on the rotations of the floor slabs is also indicated. The deflections of the wall in position 8 were unchanged.

The effect on the shear forces in this structure is shown by graph C of Fig. 8.11, indicating maximum errors of 10% only in the frames and 20% in the walls. The effect on individual member forces however was again greater, resulting in gross errors of up to 66% in the axial forces at the bases of the columns, as shown in Fig. 8.15 for the frame in position 1.

The values obtained for the bending moments in the beams, which are given for frame 1 in Fig. 8.16, are also seen to be subject to large errors, especially at the tops of the frames. The bending moments at the lower ends of the columns are plotted in Fig. 8.17, indicating that the errors produced here are generally less than in the beams.

The results obtained from the suppression of axial deformations in the columns of these three structures show that the relationship between the errors produced in deflection, in the lateral shear forces carried by the frames, and in the member forces, varies from structure to structure. In order to form an assessment of the effect of ignoring axial deformations therefore, it is not sufficient to adopt a single criterion such as shear force. The results also indicate that the height-to-width ratio of a frame, which has been suggested as a guide to the scale of errors likely to result[4], has less significance than other parameters such as the degree of asymmetry and the stiffness of the beams and columns.

8.5 The effects of imposed loads

In Chapters 4 and 5 it was shown that the lateral forces carrried by the frames are modified when imposed vertical loads are applied

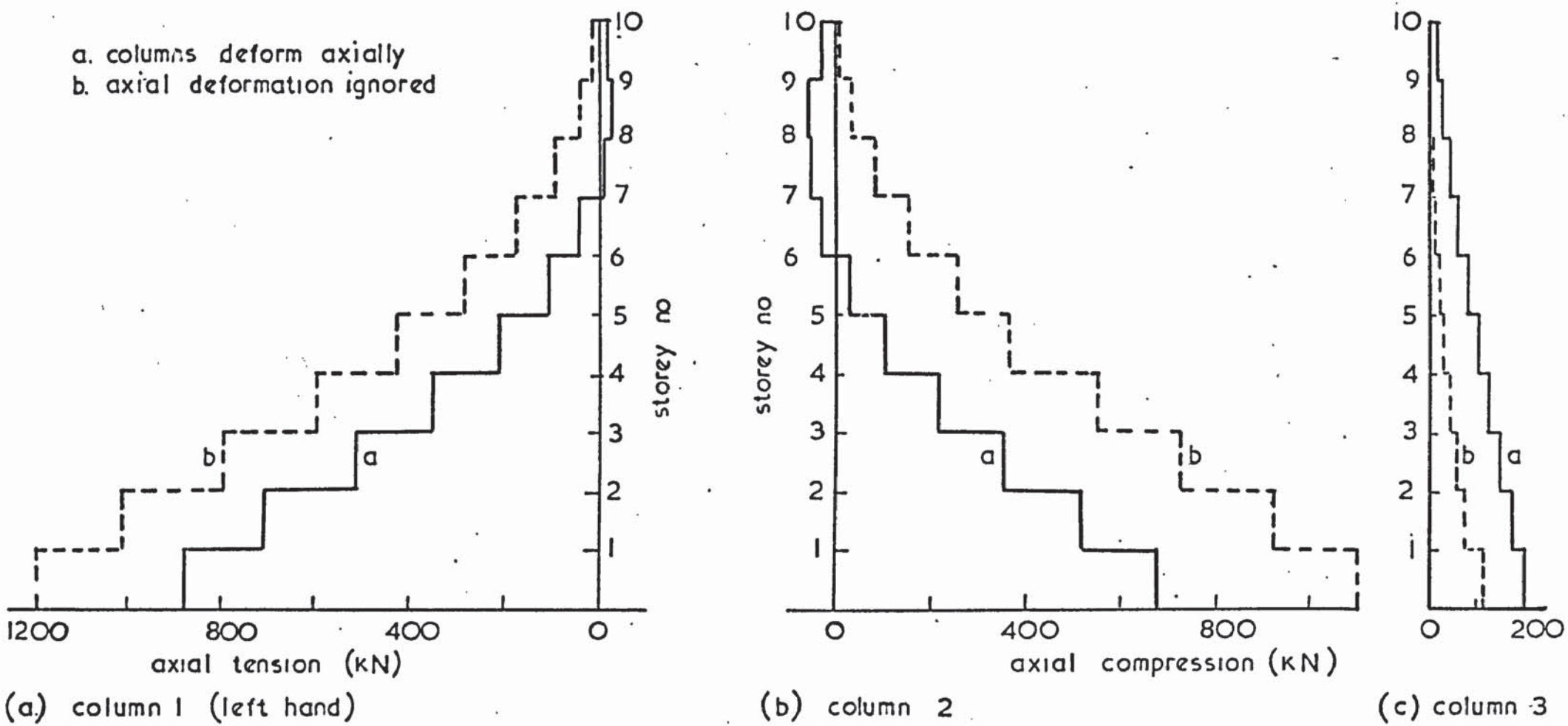

Fig. 8.15 Effect of axial deformation on axial forces in columns of asymmetrical frame

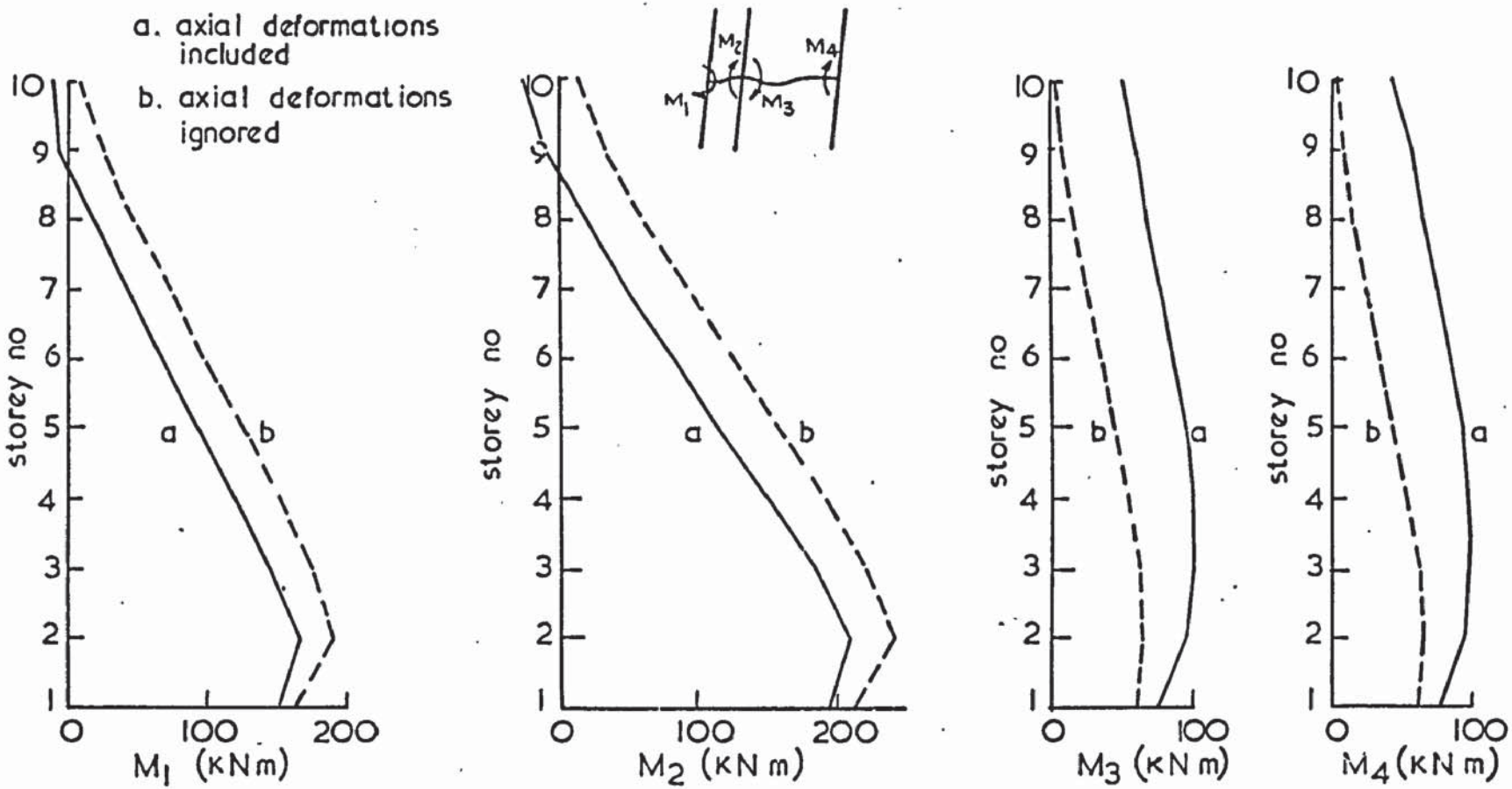

Fig. 8.16 Bending moments in beams of frame 1 in an asymmetrical structure

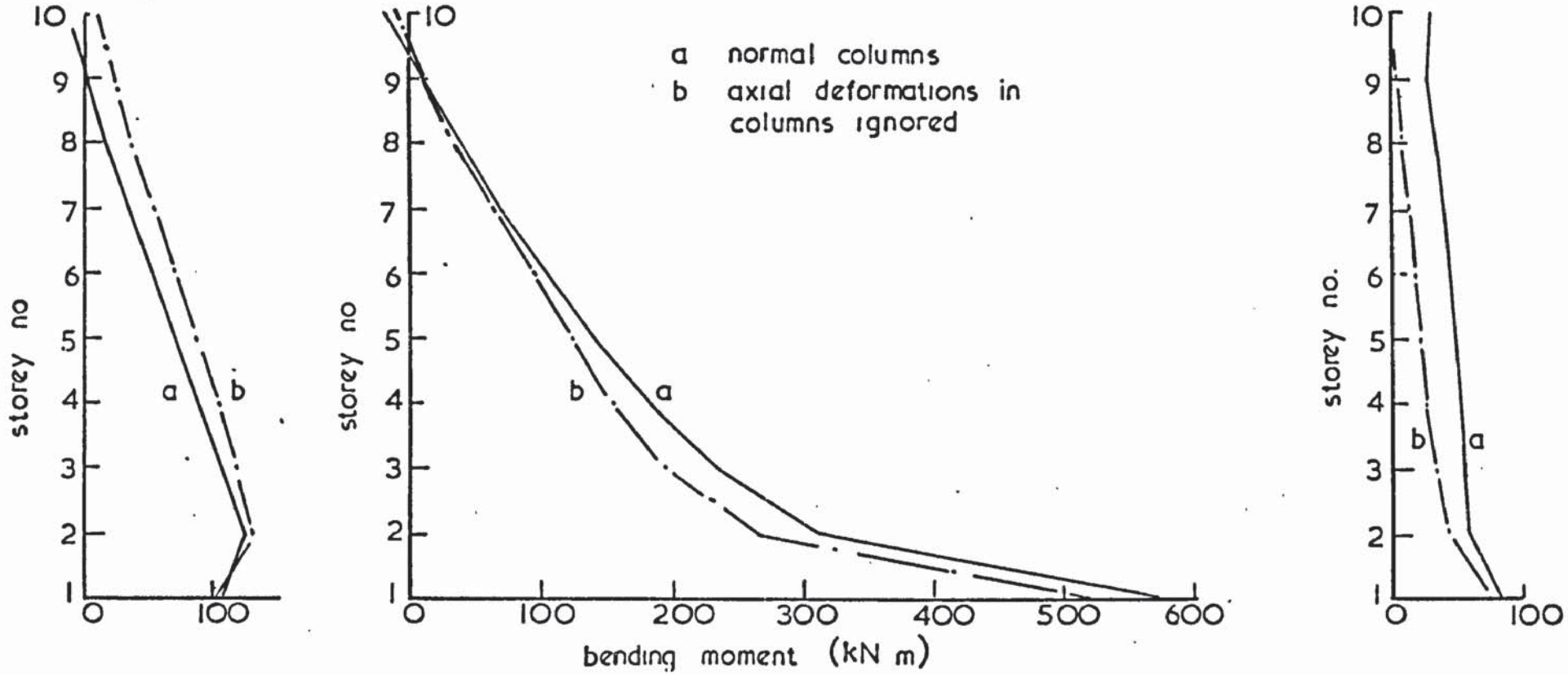

(a) column 1 (left hand) (b) column 2 (c) column 3

Fig. 8.17. Bending moments in columns of frame 1 of asymmetrical structure.

eccentrically to the frame. This effect was investigated using the two 10 storey structures as examples. In Goldberg's structure the windward bays of the frames were subjected to vertical loads equivalent to 100 lb/ft^2 acting on the slabs. This loading tends to cause sidesways opposing the action of the wind, thus reducing the deflections of the structure generally and increasing the proportion of the total wind load carried by the frames.

In the first instance the imposed load was applied to all the frames, resulting in a reduction of approximately 4% in the deflections at the top of the structure. The effect on the shear forces is given by graph C in Fig. 8.18, which shows that between the second and eighth storeys, the shear force carried by all the frames is increased by approximately 50%. When the eccentric vertical loading on the walls is taken into account however, the increase in shear force is only 10%, as shown by graph D. The effect of the first loadcase could be regarded as the converse of the differential sidesway produced by a small elastic rotation of the foundations at the base of the walls, which was shown by Rosman[19] also to cause considerable modification of the distribution of shear forces in the structure.

For the purpose of determining realistic values of imposed loads on the asymmetrical structure, it was assumed that the slabs were supported by lateral and longitudinal beams spanning between the columns of the frames. The slabs were assumed to carry distributed loads of $3kN/m^2$ and $2kN/m^2$ as shown in Appendix 1. This loading, which was reduced in the upper storeys in accordance with CP3, Chapter 5, is lighter than that assumed for Goldberg's structure and more in accordance with that likely to be experienced in practice. The derivation of the loads on the joints of the frames is given in the appendix.

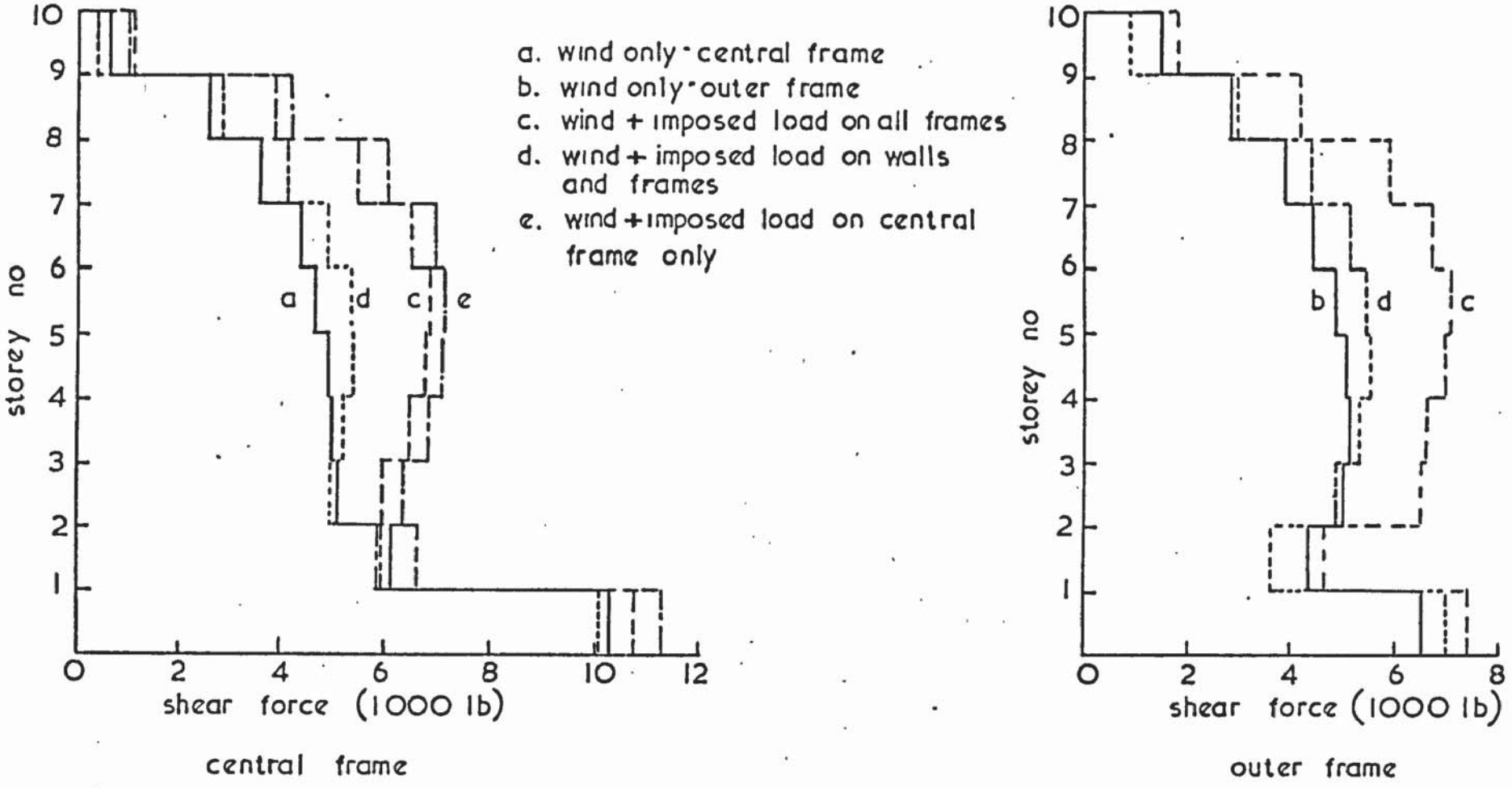

Fig. 8.18 Effect of eccentric imposed loading on distribution of shear force in Goldberg's 10 storey structure

The effects on the deflections and rotations of the slabs are shown by graphs C in Fig. 8.10, and the corresponding shear forces by graphs B in Fig. 8.12. It is interesting to observe that in this structure, since the sidesways due to the imposed loads were in the direction of the wind, the loads carried by most of the frames were reduced. The additional rotation of the floor slabs was sufficient however, to cause the load carried by the frame in position 1 to be increased. It was also noticed that, in contrast with Goldberg's structures, the proportional changes in deflection were greater than in the shear forces.

For the asymmetrical structure the effect of suppressing axial deformations was also examined, while the frames were subject to the imposed loading. It was found that in this case the changes in deflection and shear force were almost totally suppressed.

8.6 The effects of local irregularities

Two examples of local irregularities are considered in this section, using Goldberg's 10 storey structure. In the first instance, in addition to the wind load, the central frame alone was subjected to the eccentric vertical loads described in the previous section. As a result, the shear forces carried by this frame were increased, as shown by graph E in Fig. 8.18, to a greater extent than when all the frames were so loaded. The effect on the other frames however was found to be negligible.

The bending moments, which include both the vertical and lateral effects of the imposed loading, are shown for the central frame by the graphs on the right hand side of Fig. 8.6. In the other frames the bending moments are virtually unchanged and lie between graphs A and B on the left of the figure. When the slabs are treated as rigid diaphragms (graph C), it is noticed that the bending moments in the central frame are under-estimated by approximately 40% in the top storey and 11% in the

ninth storey. In all other storeys the errors are negligible and of opposite sign. These results are almost the reverse of those obtained from wind loads alone.

The loading of a single frame in the manner described is probably unlikely to occur in practice. A similar effect would result however from a uniformly distributed load over the whole of the floor slabs if, for example, alternate frames were constructed with an unsymmetrical arrangement of columns.

The manner in which the bending moments in the columns of a frame are affected by discontinuities in the section properties, has been described in section 8.2.1. The effect of a local discontinuity in the grillage due to a sudden reduction in the effective width of a floor slab will now be discussed. A practical example of this type of discontinuity occurs when a large opening is provided for visual communication between floors - an architectural feature of some modern buildings.

For this investigation, the width of the floor slab was reduced alternately on the first, fourth and tenth floors, on either side of the central frame as shown in Fig. 8.19.

The effects on the central frame, when the structure was subjected to wind loads only, are shown by the bending moments in Fig. 8.20. From the figure it is apparent that when the reduction occurs in the first floor, the bending moment is increased by approximately 30% at the base of the frame. It is reduced in the same proportion just above the first floor level. The effect decreases to negligible proportions in other storeys, dying out completely above the fourth floor. With the reduced slab in the fourth floor the oscillation of the bending moment is greater, amounting to 100% of the normal value. A large increase, but with no oscillation also occurs when the reduction is made in the roof slab.

The effect on the frames on either side of the central frame is symmetrical and is shown for the left hand side of the structure in

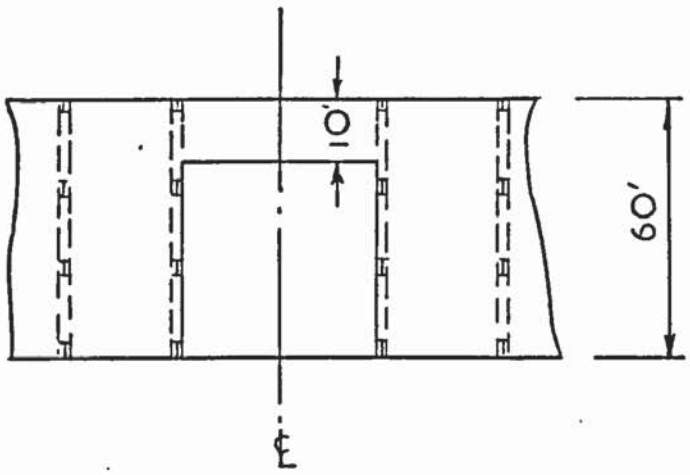

Fig. 8.19 Floor plan showing reduced width of slab

Fig. 8.21. At each of the three floor levels shown in the figure, only the changes due to the discontinuity in that particular floor are apparent, owing to the rapid damping. It is noticed that in each case the effect is greatest in the three middle frames, but persists to a lesser degree in all the frames, especially when the reduction occurs in the roof slab.

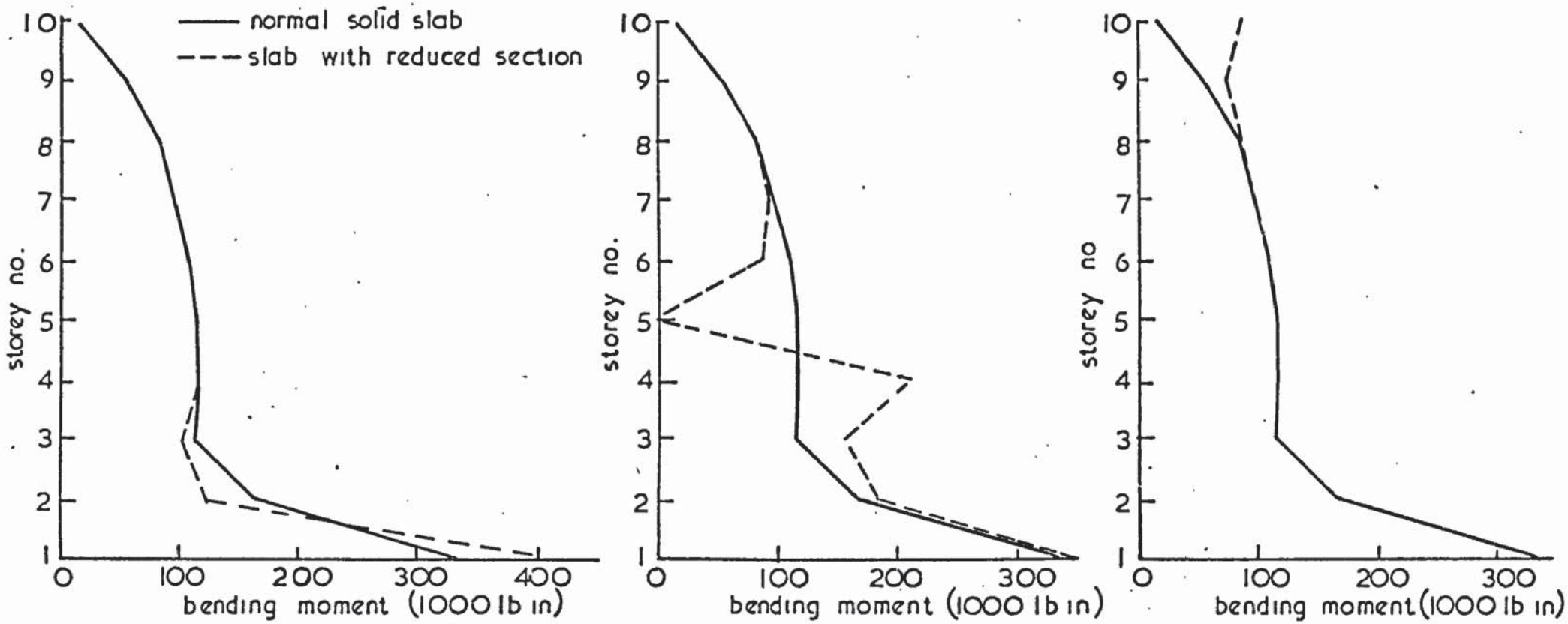

slab reduced on first floor

slab reduced on fourth floor

slab reduced on tenth floor

Fig. 8.20 Effect of reductions in slab width on column bending moments in central frame

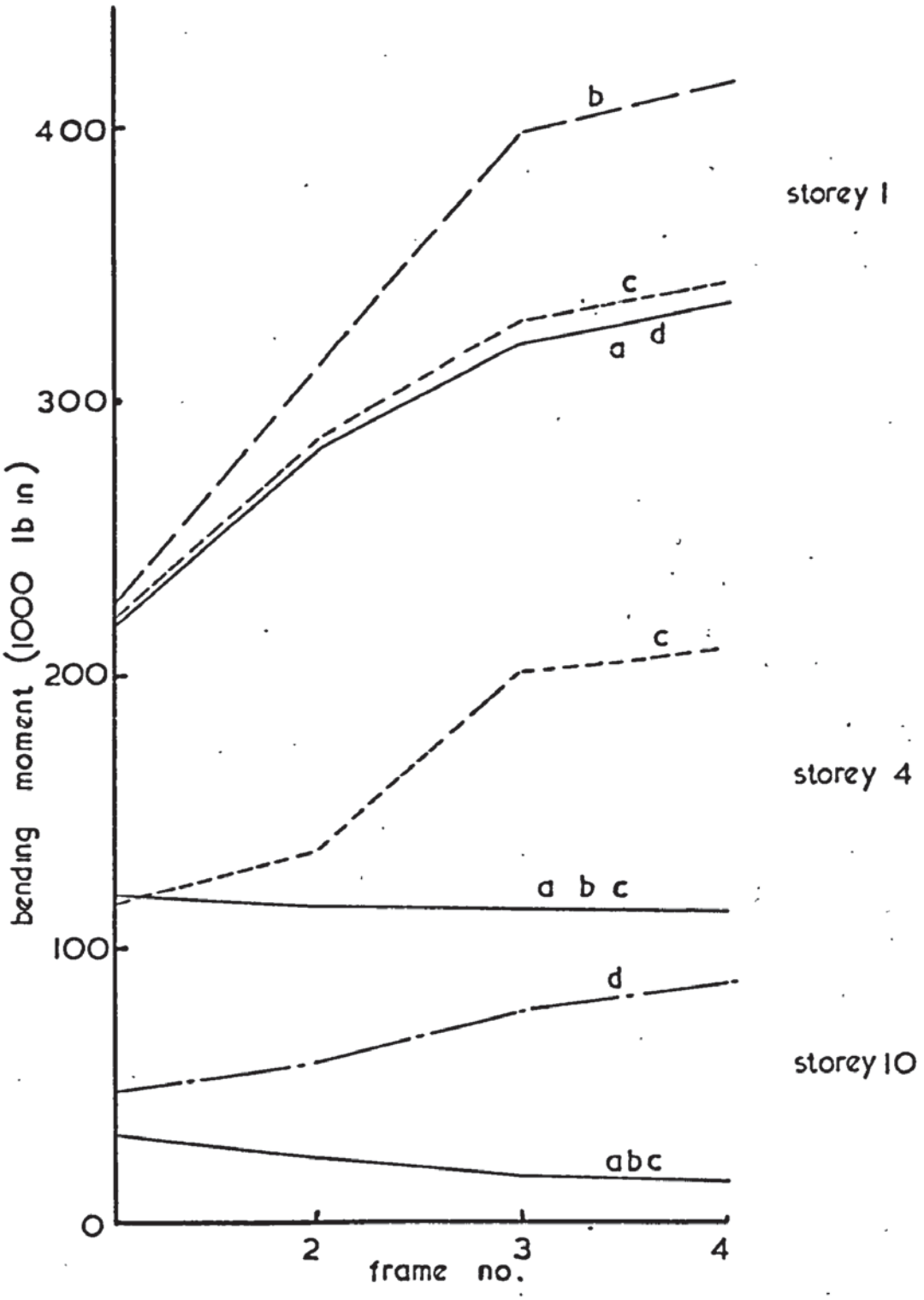

a. normal solid floors
b. reduced slab in floor 1
c reduced slab in floor 4
d reduced slab in floor 10

Fig. 8.21 Effect of local reductions in slab width

CHAPTER 9

CONCLUSIONS AND SUGGESTIONS FOR FURTHER RESEARCH

9.1 The methods of analysis

Computer programs have been written for two proposed methods of analysis of the class of structures consisting of arbitrary parallel systems of shear walls and plane frames, interconnected by continuous floor slabs. The effects of static wind loading together with eccentrically imposed vertical loading were considered. Bending of the floor slabs in their own planes was taken into account by considering all the plate components of the structure as the members of a plane grillage of deep beams. The torsion of the walls and, to a limited extent, the torsion of the slabs were also included.

Division of the structure into a number of plane components allowed separate analyses of these components to be carried out, thus reducing the number of equations that were required to be solved at any stage of the analysis. Furthermore, the necessity for repeated analyses of identical frames was avoided, reducing computation time and simplifying the preparation and checking of data. Additional simplifications were made, wherever possible, by taking advantage of the regularity of the shape of the structure and the recurrence of identical wall and floor panels. The measure of these savings, for the method of influence coefficients, was demonstrated by comparison with a general finite element analysis of the two storey model described in Chapter 7.

The method of influence coefficients, which is basically a matrix force approach, concludes with the solution of a set of compatibility equations, from which the lateral forces acting on the frames at the frame junctions are determined. In some cases difficulty was experienced in solving these equations, which, although relatively small in number,

were not sparse and tended to be ill-conditioned.

The second, or restrained grillage, approach uses the matrix displacement technique throughout, concluding with the analysis of a grillage, in which the action of the frames is replaced by a system of lateral restraints. By means of the wide column frame analogy it was possible to extend the range of structures that could be analysed, without increasing computation time, and with a relatively small increase in the volume of data required. Computer programming, however, was complicated by the partitioning of the stiffness matrices of the frames together with the compact method of storage, by the allocation of variable degrees of freedom to the joints of the frames and the grillage, and by the use of backing storage facilities. On the other hand, all the equations were sparse and could be solved by the modified version of Jennings' compact elimination technique. No evidence of ill-conditioning was detected. The use of direct access disc files, for the storage of all large arrays, enabled fairly large structures to be analysed by a computer with only a moderate core store.

Since the basic assumptions for the two proposed methods were the same, the results obtained from their use, in the analysis of any particular structure, were almost identical. The accuracy of these results was verified by comparison with previous results by Goldberg. Further verification was provided by comparison with the results of an experiment on a two storey model structure, for which a general finite element analysis was also carried out. In this case it was found that the proposed methods gave a slightly better measure of agreement with the experiment.

9.2 The behaviour of complete structures

A number of conclusions can be drawn from the results of the investigations described in Chapter 8. The degree of bending which takes

place in the plane of the floor slabs depends upon both the size and the distribution of the loads carried by the slabs. The most severe effects are likely to occur in symmetrical structures of the type analysed by Goldberg, where the slabs are supported by walls at their ends. At the intermediate frame junctions the proportion of the wind load carried by the slabs is increased when the stiffness of the walls relative to that of the frames is increased. Paradoxically therefore, the errors in the member forces for the frames, which result from the assumption of rigid diaphragm action of the slabs, could be most serious when the proportion of the total wind load carried by the frames is least. The total lateral load carried by the floor slabs, and hence the effect of in-plane bending, is also increased when the overall length of the slabs between the supporting walls is increased.

The assumption of rigid diaphragm action does not have an averaging effect on the distribution of the lateral shear forces carried by the frames, as might have been expected. Instead, it tends to produce errors which are in the same sense for all the frames, the most serious errors occurring in the frames most remote from the supporting walls. The forces in the members of the frames, were found to be significantly in error in the bottom storeys of the frames. Here the forces were under-estimated by assuming rigid floor slabs. Errors of over-estimation occurred at the tops of the frames. At all other levels the effect was negligible except in the vicinity of sudden changes in the section properties of the frames.

The neglect of axial deformations in the columns of the frames leads to over-estimation of their lateral stiffness, and hence of the lateral shear forces carried by them at all storey levels. The lateral shear force, which is the sum of the shears in the individual columns at a particular level, is not in itself however, a good indicator of the

effects of neglecting axial deformations. In the structures analysed it was found that larger errors, together with errors of under-estimation, occurred in the bending moments and axial forces in individual members. The most serious of these errors occurred in the bending moments at the ends of the shorter beams in the asymmetrical structure.

It has been shown that when vertical loads are applied to a wall or a frame in a manner which tends to cause sidesway, the restraints provided by the floor slabs give rise to lateral shear forces at the junctions. This effect is likely to be most sifnificant when the greatest restraint is provided and will not necessarily be associated with large changes in the deflections of the structure as a whole.

It was shown in Chapter 8, for example, that in a symmetrical structure, braced by relatively stiff end walls, significant changes in the lateral forces carried by the frames resulted when eccentrically imposed loads were applied to the frames, but not to the walls. The changes in deflection however were small. Similarly, when eccentric loading was applied to a single frame, the loads carried by that frame were significantly affected, but the effect on adjacent frames was neglibible.

Conversely, in an asymmetrical structure where the rotation of the floor slabs was only partly restrained by the walls, large changes in deflection occurred as a result of eccentric vertical loads on the frames. The effect on the distribution of lateral forces, on the other hand, was small.

It was found that the lateral effects of vertical loading were almost entirely dependant on the development of axial deformations in the columns and would therefore be overlooked if these deformations were supressed in the analysis.

Consideration of the floor slabs as deep beams enables the effects of variations in the section properties of the slabs to be investigated. The effect of a sudden reduction in the width of a floor slab of a symmetrical structure was studied at three different levels. It was shown that the member forces in the frames adjacent to the discontinuity were significantly affected. The effects on the other frames in the structure were smaller, but not negligible. In the vertical direction however, rapid damping occurred.

In conclusion it may be stated that the methods of analysis described in this thesis take account of two effects, which are not included in the majority of published methods, namely the effects of in-plane bending of the floor slabs and of eccentric vertical loading on the frames. It has been shown that the inclusion of these effects can be achieved without undue additional expense, either in data preparation, or in computer time and storage. The results of the analyses carried out suggest that for some structures the results of neglecting these effects could not be predicted and may involve serious errors in the computation of deflections, or of member forces in the frames.

9.3 Suggestions for further research

The chief limitation of the above methods of analysis is the restriction to the class of structures containing only parallel walls and frames, implying that the deflections of all the bracing components are in parallel planes. The analysis of L shaped structures in which torsion produces perpendicular displacements of the two arms of the L, or of structures in which the bracing components are not parallel, is therefore precluded. The restrained grillage approach could be extended however, to include a wider range of structures, by replacing the grillage by a space frame. The simplified conditions of equilibrium and compatibility at the frame junctions could be retained, together with the advantages.

gained by analysing the frames separately. In this space frame a maximum of 5 degrees of freedom would be required at the wall junctions, but at the junctions with plane frames, since the torsion of the floor slabs has been shown to be unimportant, the degrees of freedom could be reduced to two translations and a rotation in the planes of the floors. The total number of degrees of freedom, and consequently the storage requirements and running time for the space structure, would not therefore be very much greater than that for the grillage.

The importance of the effects of axial deformations in the columns of frames or perforated shear walls has been pointed out both in this thesis and in the published literature. In general, discussion has taken the form of comments on the results of particular analyses rather than a statement of principles. In the report by ACI committee No. 442 [4], which was intended as a reference work for practising designers, it was stated that 'while no definite rules can be given, the effects of column axial deformation will generally be important if the height to width ratio exceeds about three'.

The results obtained for the structures analysed in this thesis show that the height-to-width ratio is not necessarily the most important parameter to be considered when deciding whether or not to include axial deformations. A systematic investigation therefore, into the influence of axial deformations in regular multi-storey frames, appears to be desirable.

In this thesis, as in most published methods of analysis of complete structures, it is assumed that the bases of the walls and frames are rigid. It has been shown however[19], that the distribution of lateral forces is extremely sensitive to small elastic rotations at the base of a wall. In contrast, work has been carried out, for example by Sommer[46] and Heil[47], which shows that more accurate values for the contact pressures under a

flexible strip footing can be obtained if the stiffness of the superstructure is considered. The work of this thesis indicates that the distribution of lateral shears is likely to be significantly affected by small differential settlements of the footings of the frames. Such settlements could be included in the restrained grillage analysis by extending the lateral stiffness matrices, derived in Chapter 5, to include rows and columns corresponding to vertical displacements at the column bases. An influence coefficient approach, similar to that of Sommer and Heil, but in three dimensions, would be required to determine the relationship between contact pressures and vertical displacements in the soil.

One extension of the present work has already been mentioned in Chapter 4, namely the work of Majid and Onen, relating to the elastic-plastic behaviour of the frames incorporated in a complete structure. This work is based on the analysis by influence coefficients described in this thesis. A similar project, in which buckling and shear failures of the walls and slabs are also to be considered, has now been started. It is expected that the restrained grillage approach, described in Chapter 5 of this thesis, will be used as the basis for this investigation.

REFERENCES

1. Coull A. and Stafford Smith B. (Eds.) "Tall Buildings". Proc. Symp. on tall buildings, Univ. Southampton, 1966. Pergamon, London, 1967.

2. Coull A. and Stafford Smith B. "Analysis of shear wall structures". Ref. 1, 139-155.

3. Coull A. and Stafford Smith B. "Structural analysis of tall concrete buildings." Proc. Instn. Civ. Engrs, 1973, Pt.2, Vol.55, March, 151-166.

4. Fintel M. et al. "Response of buildings to lateral forces." J. Am. Concr. Inst., 1971, Vol. 68, Feb., 81-106.

5. Khan F. R. "Recent structural systems in steel for high-rise buildings." Proc. Conf. "Steel in Architecture," Association of Societies of Art and Design, London, Nov., 1969, B.C.S.A. Ltd., 1970.

6. Clough R. W., King I. P. and Wilson E.L. "Structural analysis of multi-storey buildings." J. Struct. Div. Am. Soc. Civ. Engrs, 1964, Vol.90, ST3, June, 16-34.

7. Macleod I. A. "Lateral stiffness of shear walls with openings." Ref. 1, 223-244.

8. Macleod I. A. "New rectangular finite element for shear wall analysis." J. Struct. Div. Am. Soc. Civ. Engrs., 1969, Vol.95, ST3, March, 399-409.

9. Majid K. I. and Williamson M. "Linear analysis of complete structures by computers." Proc. Instn. Civ. Engrs., 1967, Vol.38, Oct., 247-266.

10. Rosman R. "Approximate analysis of shear walls subject to lateral loads." Proc. Am. Conc. Inst., 1964, Vol.61, 717-732.

11. Coull A., Puri R. D. and Tottenham H. "Numerical analysis of coupled shear walls." Proc. Instn. Civ. Engrs., 1973, Pt.2, Vol.55, March, 109-128.

12. Timoshenko S. P. "Strength of materials Part 1." Second edition, D. Van Nostrand Co. Inc., New York, 1940, 170-171.

13. Cowper G. R. "The shear coefficient in Timoshenko's beam theory." J. Appl. Mechs. Trans. A.S.M.E., 1966, Vol.33, June, 335-340.

14. Khan F. R. and Sbarounis J. A. "Interaction of shear walls and frames." J. Struct. Div. Am. Soc. Civ. Engrs., 1964, Vol. 90, ST3, June, 285-312.

15. O'Donnell W. J. "The additional deflection of a cantilever due to the elasticity of the support." J. Applied Mech., Trans. A.S.M.E., 1960, Vol.27, 461-464.

16. Michael D. "The effect of local wall deformations on the elastic interaction of cross walls coupled by beams." Ref. 1, 253-270.

17. Choudhury J. R. "Analysis of plane and spatial systems of interconnected shear walls." Ph.D. Thesis, Univ. Southampton, 1968.

18. The Steel Designer's Manual, Crosby Lockwood, London, 1955, 588-593.

19. Rosman R. "Laterally loaded systems consisting of walls and frames." Ref. 1, 273-289.

20. Heidebrecht A.C. and Stafford Smith B. "Approximate analysis of tall-frame structures." J. Am. Soc. Civ. Engrs., 1973, Vol.99, ST2, 199-221.

21. Stafford Smith B. "Modified beam method for analysing symmetrical interconnected shear walls." Proc. Am. Conc. Inst., Vol. 67, Dec., 1970, 977-980.

22. Gluck J. "Lateral load analysis of multistorey structures comprising shear walls with sudden changes in stiffness." Proc. Am. Conc. Inst., Vol.66, Sept., 1969, 729-736.

23. Weaver W. and Nelson M. F. "Three dimensional analysis of tier buildings." J. Struct. Div. Am. Soc. Civ. Engrs., 1966, Vol.92, ST6, 385-404.

24. Webster J. A. "The static and dynamic analysis of orthogonal structures composed of shear walls and frames." Ref. 1, 377-399.

25. Coull A. and Irwin A. W. "Analysis of load distribution in multi-storey shear wall structures." Structural Eng., 1970, Vol.48, August, 301-306.

26. Gluck J. "Lateral load analysis of irregular shear wall multi-storey structures." Proc. Am. Conc. Inst., 1970, Vol.67, July, 548-553.

27. Winokur A. and Gluck J. "Lateral loads in asymmetric multistorey structures." J. Struct. Div. Am. Soc. Civ. Engrs., 1968, Vol.94, ST3, 645-656.

28. Stomato M. C. and Stafford Smith B. "An approximate method for the three dimensional analysis of tall buildings." Proc. Instn. Civ. Engrs., 1969, Vol.43, 361-379.

29. Heidebrecht A. C. and Swift R. D. "Analysis of asymmetrical coupled shear walls." J. Struct. Div. Am. Soc. Civ. Engrs., 1971, Vol. 97, ST5, 1407-1422.

30. Rosman R. "Analysis of spatial concrete shear wall systems." Proc. Instn. Civ. Engrs., 1970, Sup (vi), Paper No. 7266S, 131-152.

31. Gluck J. "Lateral load analysis of asymmetric multi-storey structures." J. Struct. Div. Am. Soc. Civ. Engrs., 1970, Vol.69, ST2, 317-333.

32. Barnard P. R. and Schwaighofer J., "The interaction of shear walls connected solely through slabs." Ref. 1, 157-180.

33. Quadeer A. and Stafford Smith B. "The bending stiffness of slabs connecting shear walls." Proc. Am. Conc. Inst., 1969, Vol.66, June, 464-477.

34. Goldberg J. E. "Analysis of multi-storey buildings considering shear wall and floor deformations." Ref. 1, 349-373.

35. Bray, K. H. M. "Computer analysis of large civil engineering structures." Ph.D. Thesis, Univ. Aston in Birmingham, 1973.

36. Jennings A. "A compact storage scheme for the solution of symmetric linear simultaneous equations." Computer Journal, 1966, Vol.9, No.3, November.

37. Jennings A. and Tuff A. D. "A direct method for the solution of large sparse symmetric simultaneous equations." I.M.A. Conf. on large sparse sets of linear equations, Academic Press, 1970.

38. Majid K. I. and Anderson D. "The computer analysis of large multi-storey structures." The Structural Engineer, 1968, Vol.46, Nov, 357-365.

39. Anderson D. "Investigation into the design of plane structural frames." Ph.D. Thesis, Univ. Manchester, 1969.

40. Majid K. I. and Croxton P. C. L. "Wind analysis of complete structures by influence coefficients." Proc. Instn. Civ. Engrs., 1970, Vol.47, Oct., 169-184.

41. Majid K. I. and Onen Y. H. "The elasto-plastic failure load analysis of complete building structures." Proc. Instn. Civ. Engrs., 1973, Pt.2, Vol.55, Sept., 619-634.

42. Onen Y. H., "Elastic-plastic analysis of complete building structures." Ph.D. Thesis, Univ. Aston in Birmingham, 1973.

43. Pollack S. L. "Analysis of the decision rules in decision tables." RAND Corporation Memo RM-3669-PR, May 1963.

44. I.B.M. Corp. "Decision tables - a systems analysis and documentation technique." I.B.M. Corp., Form No. F20-8102.

45. Fenves S. J. "Computer methods in Civil Engineering." Prentice-Hall International, 1967.

46. Sommer H. "A method for the calculation of settlements, contact pressures, and bending moments in a foundation, including the influence of the flexural rigidity of the superstructure." Proc. 6th Int. Conf. Soil Mech., Montreal, 1965, Vol.2, 197-201.

47. Heil H. "Studies on the structural rigidity of reinforced concrete building frames on clay." Proc. 7th Int. Conf. Soil Mech. Fdn. Eng., Vol.2, 1969, 115-122.

APPENDIX 1

DETERMINATION OF LOADING

A1.1 Wind loads

The wind pressure on the structures was assumed to be uniformly distributed over the face of the structure in each of the cases analysed, except in Goldberg's 10 storey structure, when the concentrated loads quoted by Goldberg were used, giving a slightly reduced wind pressure on the bottom two storeys. In the other two structures it was assumed that, from an area enclosed by 4 joints, the wind force was apportioned equally to each of the joints. The method is illustrated, for the joints at the top left hand corner of Goldberg's 20 storey structure, in Fig. A1.1. In this example the load apportioned to joint A was 15 x 12 x 20 = 3600 lb. Similarly the load carried by joint B was 1800 lb and by joint C was 900 lb. Applying the above method to the whole structure and assuming that only the left hand half of the symmetrical structure was to be analysed, the wind loads given in Table A1.1 were obtained.

Using the same approach, the wind loads given in Table A1.2 were obtained for the 10 storey asymmetrical structure.

A1.2 Imposed loads

For the purpose of the investigations carried out on Goldberg's 10 storey structure, the imposed loading was assumed to be equivalent to 100 lb/ft^2 on the floor slabs, supported by the beams of the frames and the end walls in one bay only as shown in Fig. A1.2a. The resulting moments and shears acting on the joints are shown in Fig. A1.2b. The overturning moments on the walls were determined from the formula derived in Chapter 4, section 4.5, assuming half the loads acting on the frames. This loading is shown diagrammatically in Fig. A1.2c.

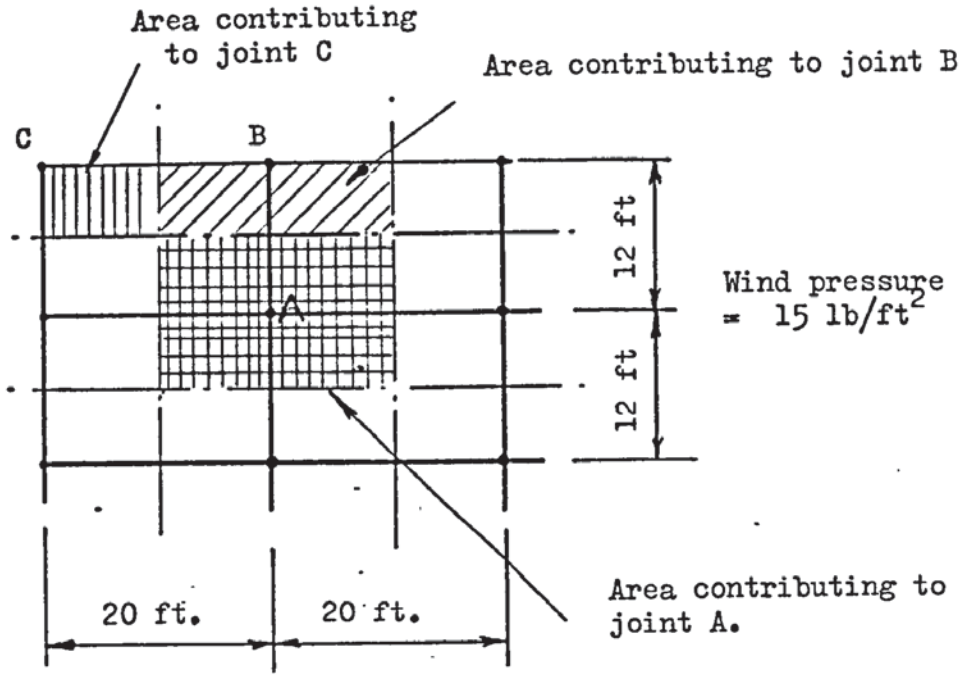

Fig. A1.1 Method of apportioning wind pressure to joints

Storey	End Wall	Frames 1 to 3	Frame 4
20	900	1800	900
19 • • • • • 7	1800	3500	1800
6	1950	3900	1950
5 4 3	2100	4200	2100
2	2250	4500	2250
1	2850	5700	2850

Table A1.1 Wind loads in pounds on Goldberg's 20 storey building

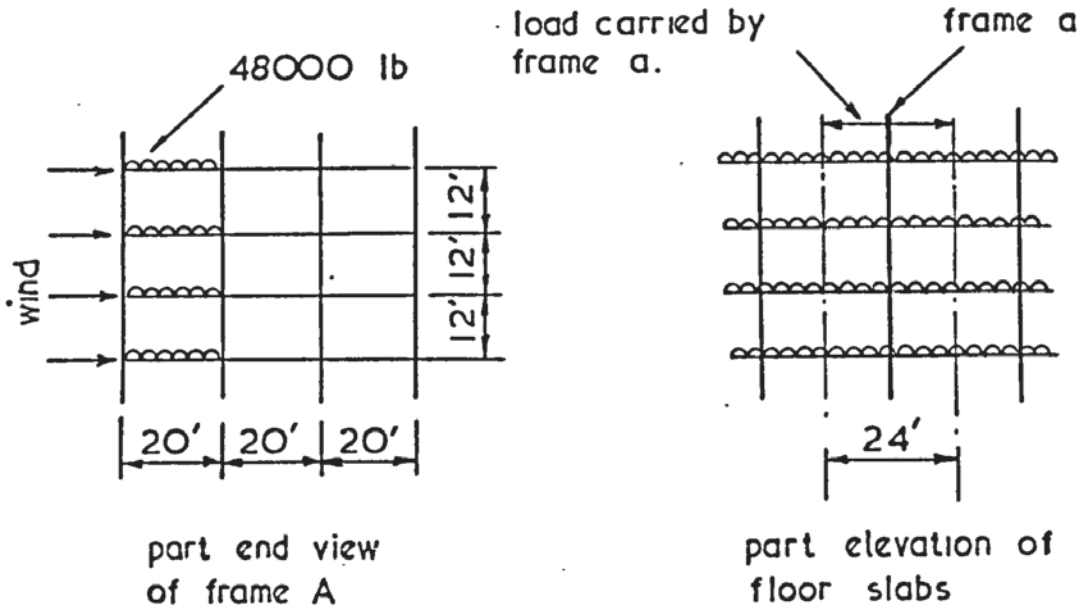

(a) loading of floor slabs

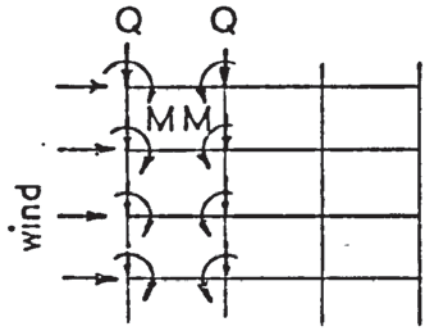

Q = 24,000 lb
M = 960,000 lb in

(b) loading of joint

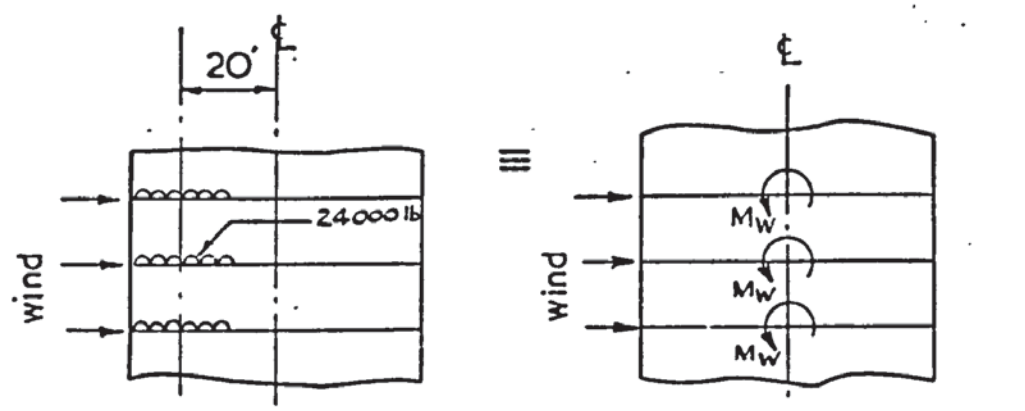

M_w = 5,760,000 lb.in

(c.) loading and equivalent moments on end walls

Fig. A I.2 Imposed loads on Goldberg's 10 storey structure

Imposed loading on the floors of the asymmetrical structure was apportioned to the beams of the frames and to the longitudinal beams, in accordance with CP110 Part 1, 1972, as shown in Fig. A1.3a. The loads from the shaded areas marked A were used for the calculation of shears and end moments in the beams of the frames. The areas marked B and C contributed loads to the longitudinal beams. The end shears of these beams were transferred to the joints of the frame, but their end moments, which do not affect the sidesways in the planes of the frames, were ignored. The resulting shears and moments on the joints of a typical frame are shown in Fig. A1.3b.

	POSITION				
Storey	1	2 - 5	6	7	8
10	7.50	15.00	9.75	4.50	2.25
9 1	15.00	30.00	19.5	9.0	4.5

Table A1.2 Wind loads in kN on the 10 storey asymmetrical structure

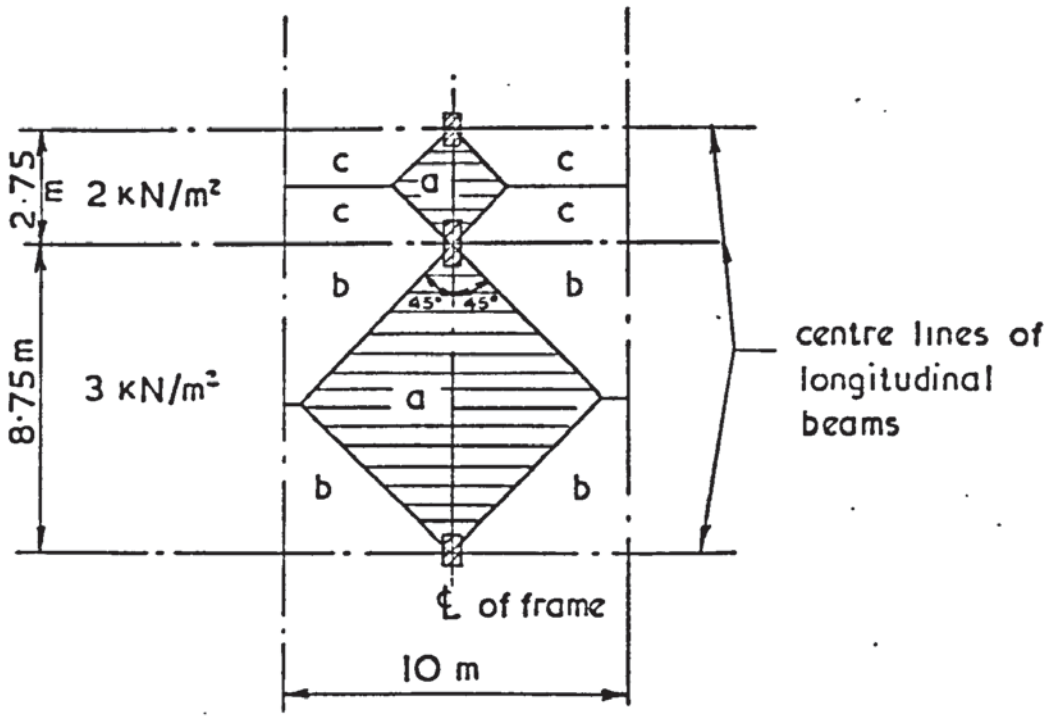

(a) loading on beams of frame and on lonitudinal beams

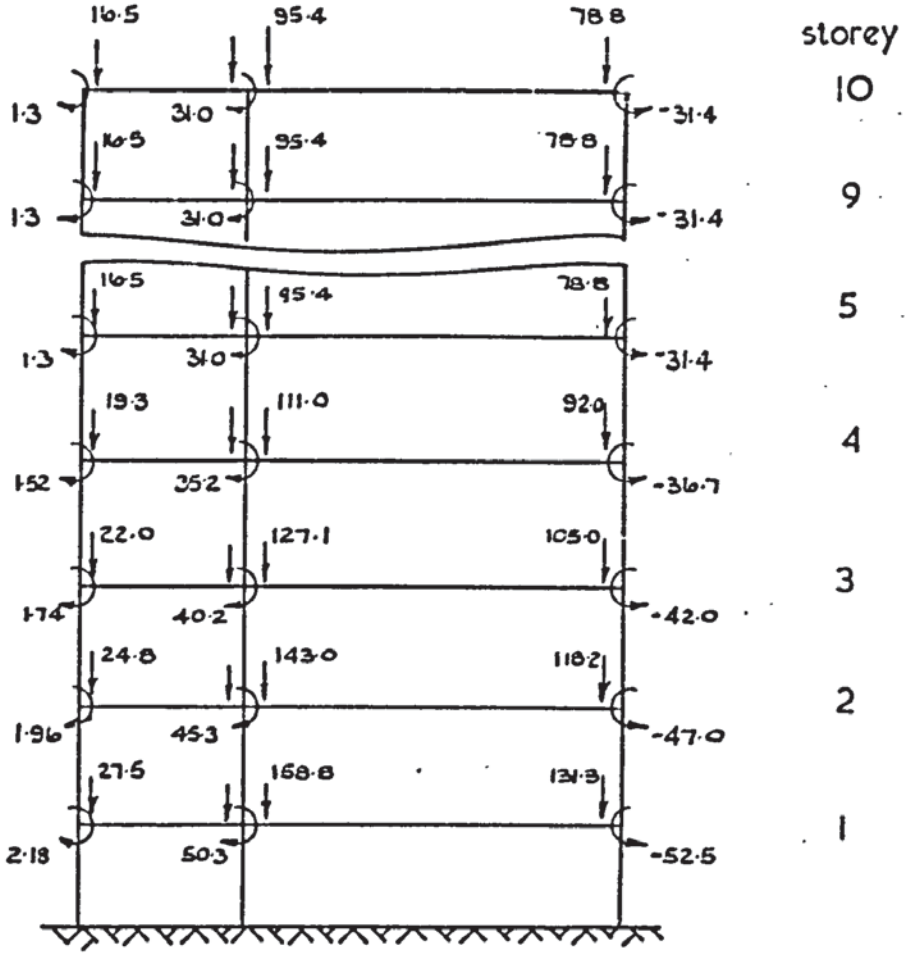

(b) loading of joints (kN and kN. m)

Fig. A.1 3 Imposed loads on asymmetrical structure